Identifying Host-Pathogen Interactions Which Cause Severe Malaria

Athina Georgiadou

Section of Paediatrics, Division of Infectious Diseases, Department of Medicine

Imperial College London

Submitted for the degree of Doctor of Philosophy
January 2019

"Imagination is more important than knowledge. Knowledge is limited. Imagination encircles the world."

Albert Einstein

To my parents,

Abstract

Infectious diseases pathogenesis is dependent on the interactions between the host and the pathogen. Being able to simultaneously assess the transcriptomes of both host and pathogen as we have shown here, using dual RNA sequencing of whole blood from *Plasmodium falciparum* malaria patients, can reveal these crucial interactions. Using Gambian children samples we tried to unravel the mechanisms leading to severe malaria. The main finding was the clear involvement of neutrophil related genes in severe malaria while host gene expression was mainly dependent on pathogen load. Identifying that parasite load imposes a huge effect on host gene expression while being a key determinant of severe disease, we aimed to develop a new method to identify the host mechanisms which constrain parasite growth. Using a mathematical model and RNA sequencing to discover genes positively associated with parasite growth inhibition, we identified Cathepsin G and matrix metallopeptidase 9 (MMP9). Using *in vitro* validation, I showed that both Cathepsin G and MMP9 decrease parasite growth. They do that using different mechanisms, cathepsin G cleaves red cell surface receptors crucial for the parasite invasion while MMP9 acts directly on the parasite. Our findings underline the importance of accounting for the interaction between host and pathogen when seeking to identify correlates of protection, and reveal novel mechanisms controlling parasite growth in humans. Finally, I used five different parasite strains *P. berghei ANKA*, *P. berghei NK65*, *P. yoelii 17XL*, *P. yoelii 17XNL*, and *P. chabaudi AS* to infect C57BL/6 mice and compare the transcriptome of these different malaria models with our human RNA dataset. This experiment revealed a new malarial hyperlactataemia model (*P. yoelii 17XL*). The mouse hyperlactataemia model also showed the greatest similarity of all the mouse models to the human hyperlactataemia phenotype at a transcriptional level.

Acknowledgements

First and foremost, I would like to thank my main supervisor Dr Aubrey Cunnington, for giving me the opportunity to work on such an amazing project and for his constant support, trust and encouragement over these three years. I so am grateful for his support and patience, for sharing with me his in-depth knowledge in the field and for trusting me with every experiment I wanted to do. His enthusiasm and passion about research, has been invaluable for keeping me going. I should also thank my second supervisor Professor Michael Levin, who has been very motivating and supportive throughout my project, always excited to hear about new findings. I feel the need to thank deeply both my supervisors for helping me to grow as a scientist, for offering me opportunities to work in other labs and meet valuable collaborators, trusting me to present our work in conferences and meetings.

I would also like to thank all the amazing people I have been lucky enough to meet in the Department of Paediatrics, Meg, Fadil, Evan, Roberto, Emma, Lorenza, Ivana, and Rahmeen.

I should also thank Dr Hyun Jae Lee from University of Queensland for the helpful discussions and his patience to explain his bioinformatic analyses through many emails and long Skype sessions. Also, thank you to Pablo Soro Barrio who recently joined our team for his bioinformatic contribution.

A massive thank you goes to Eloise Walker at London School of Hygiene & Tropical Medicine, who taught me everything I know about malaria parasite culture. Thank you for being always there for any scientific question I had, all the support and genuine interest. Thank you to all the lab members of Professor David Baker group at LSHTM, for having me in the lab all this time, for the interesting scientific discussions and the support. Thank you to our collaborator Professor David Conway for hosting me in his lab at LSHTM and everyone in his group.

Thank you to everyone at the CBS facility of St. Mary's for their amazing support and help with everything I needed. Also, big thanks to Dr Guo Yanping from St. Mary's NHLI FACS core facility for training me, as well as her true interest on my project, always happy to help and excited to hear any new results. Thank you to the South Kensington FILM facilities and specifically to Dr David Gaboriau for his help with the microscopes and all the scientific advice. I should also give a big thank you to our collaborator Dr Chris Moxon, a bright paediatrician and passionate

malaria researcher through who I gained access to valuable human ocular tissue samples from Malawian children. Also, thank you to Professor Simon Harding guardian of these samples who hosted me in his lab and everyone else at the Institute of Ageing and Chronic Disease of Liverpool University, who made me feel so welcome.

Big thank you goes to my amazing friends from Greece, London and Birmingham for being by my side. Especially to Sergia, Elena, Katerina and Evi in Greece, thank you for being next to me even when you are miles away and for all the great time we always have whenever I am back home. My friends in Birmingham with most of which we went through our Masters together, Nansy, Pantelis, Socratia, Giannis, Vicky, Grigoris and Nikos. Huge thank you to my friends from Imperial who were next to me during this PhD, Sara, Stephanie and Myrsini thank you for being next to me, for believing so much in me, for taking care of me and for all the amazing time we have had together in conferences and nights out.

A massive thank you goes to my family. To my parents for their endless support with everything I have ever wanted to do, for believing in me more than anyone, for raising me with so much love and care. Thank you, dad, for making me believe that I can achieve anything I want if I try. Thank you, mum, for always taking care of me even when you are far away.

Finally, I need to thank the person who was next to me more than anyone, my partner and best friend Spyros, for the love and support through everything, thank you for taking care of me.

London 2019

Table of Contents

Abstract 7
Acknowledgements 9
Declaration of Originality 19
Copyright Declaration 21
Publications 23
Abbreviations 25
Chapter 1: Introduction 29
1.1 Malaria 29
1.2 Parasite life cycle 30
1.3 Selected aspects of *Plasmodium falciparum* biology 32
1.3.1 Gene expression 32
1.3.2 Erythrocyte invasion 33
1.4 Clinical features of malaria 38
1.5 Different severe malaria syndromes - Independent predictors of death 39
1.6 Approaches to studying severe malaria 41
1.7 Immune response and naturally acquired immunity 42
1.8 Pathogenesis of severe malaria 44
1.8.1 Sequestration and microvascular obstruction 44
1.8.2 Endothelial activation and inflammation 46
1.8.3 Pathogen load 50
1.8.4 Lactate 50
1.9 Treatment and protection from severe malaria 51
1.10 New discovery approaches 52
1.11 Transcriptomic approaches to understanding malaria 53
1.12 Key points: 54
1.13 Objectives of the thesis 55
Chapter 2: Methods 57
2.1 Ethics 57
2.1.1 Human subjects 57
2.1.2 Mice 58
2.2 Mouse Infections 58

2.2.1 Protocols used for monitoring 58
2.3 RNA isolation 59
2.3.1 Quantification and purity of RNA 59
2.3.2 Integrity of RNA 59
2.4 Dual-RNA sequencing 60
2.4.1 Human 60
2.4.2 Mice 61
2.5 Gene annotations 61
2.6 Differential gene expression analysis 61
2.7 Pathway analysis 62
2.8 *In vitro* parasite culture 63
2.8.1 Synchronisation 63
2.8.2 Growth assay 64
2.8.3 Invasion assay 64
2.8.4 Blood smears 65
2.9 Flow cytometry 65
2.9.1 Parasitaemia counting using flow cytometry 65
2.9.2 White blood cell proportions count with flow cytometry 65
2.9.3 Instruments and software 66
2.9.4 Gating strategy 67
2.10 Erythrocyte surface receptor expression 69
2.11 Whole blood stimulation with PMA 69
2.12 ELISA 70
2.13 Immunohistochemistry 70
2.13.1 Immunofluorescence 72
2.14 Microscopy 72
2.14.1 Imaging software 72
2.14.2 Evaluation of parasitaemia by microscopy 72
2.14.3 Haemorrhages counting in mouse brain 73
2.15 Statistics 73
Chapter 3: Uncovering pathogenesis mechanisms of severe malaria 75
3.1 Introduction 75
Host 78
3.2 Dual RNA sequencing on whole blood from Gambian Children with malaria 78
3.2.1 Subjects 78

3.3 Candidate selection 81
3.4 Identification of MMP8 as a plausible contributor to SM pathogenesis 81
3.4.1 Validation using Gambian plasma samples protein levels 83
3.4.2 Immunohistochemistry on human retinal tissue 84
3.4.3 Netosis 93
3.5 Targeting MMP8 *in vivo* 100
Parasite 102
3.6 Sodium L-lactate supplementation *in vitro* 102
3.7 RNA sequencing of lactate supplemented 3D7 parasite cultures 105
3.8 Summary 107
3.9 Conclusion 109
Chapter 4: Investigation of mechanistic correlates of protection in malaria 111
4.1 Introduction 112
4.2 Mathematical model and RNA seq combination 113
4.3 Identification of mechanistic correlates of parasite growth inhibition 114
4.4 *In vitro* experiment methods 116
4.5 Growth assays reveal that both Cathepsin G and MMP9 inhibit parasite growth 117
4.6 Invasion assays show that Cathepsin G acts on the RBC 117
4.7 PMA stimulation of healthy donor whole blood 118
4.8 The effect of cathepsin G is independent of the parasite invasion phenotype 118
4.9 Cleavage of RBCs receptors after dose response treatment with cathepsin G 120
4.10 RBC receptors get cleaved after PMA stimulation of healthy donor whole blood 122
4.11 Validation using Gambian samples 123
4.12 Summary 125
4.13 Conclusion 126
Chapter 5: Transcriptomic comparison of mouse malaria models with the human host 129
5.1 Introduction 130
5.2 Experiment design 134
5.3 Differences in pathology and severity 134
5.3.1 Parasitaemia 136
5.3.2 Scoring and severity of infection 138
5.3.3 Weight loss 140
5.3.4 Discovery of a new mouse model for hyperlactataemia 142
5.4 RNA sequencing and data analysis 143

5.4.1 Deconvolution using flow cytometry data 143
5.5 DGEA 144
5.5.1 Genes associated with high lactate 144
5.6 Comparison of the mouse with the human host 145
5.6.1 Concordance and discordance in gene expression 147
5.7 Summary 148
5.8 Conclusion 149
Chapter 6: Conclusions-Discussion 151
6.1 Work achieved in this thesis 151
6.2 Limitations 153
6.3 Future directions 154
References 157
Appendix 179
Transcriptomic studies in malaria 179
MMP8 Immunohistochemistry 187
Protocols used for animal work 188
Moderate severity limit- Parasite passage 188
Moderate severity limit 190
Severe severity limit 193
Severe severity limit- Rapid Murine Coma and Behaviour Scale 195
Parasite genes associated with high lactate 197

List of Figures

Figure 1: P. falciparum asexual life cycle stages. 31
Figure 2: RBC surface receptors important for P falciparum invasion. 36
Figure 3: Venn diagrams comparing mortality rates of children and adults associated with predictors of death in severe malaria. 40
Figure 4: Transcriptomic response of the host to malaria: Similarities and differences between human and mouse. 42
Figure 5: Bioanalyzer traces. 60
Figure 6: Gating strategy for parasitaemia counting and RBC receptor detection. 67
Figure 7: Gating strategy for defining WBC proportions in mouse blood 68
Figure 8: Deconvolution heatmaps. 80
Figure 9: Comparisons of human gene expression between severe and uncomplicated malaria. 81
Figure 10: Plasma protein concentrations in Gambian plasma samples. 83
Figure 11: MMP8 release after overnight stimulation with P. falciparum 3D7 schizont lysate from healthy donor whole blood 84
Figure 12: Histology of the whole ocular tissue showing the anatomy (a & b) and cell layers of the retina (c) 87
Figure 13: Retinopathy positive case showing extensive sequestration (arrowheads) of parasites on the retinal endothelium. Mature parasites appear as black dots due to the hemozoin pigment accumulated in their food vacuole. 87
Figure 14: Immunohistochemistry staining with MMP8 (a & b) and OLFM4 (c & d) on cerebral malaria retinopathy negative (CM ret-) or positive (CM ret+) cases. 89
Figure 15: Retinopathy positive sample stained with MMP8. 90
Figure 16: MMP8 co-localises with fibrinogen leak. 92
Figure 17: CM retinopathy positive case stained with citrulinated histone H3, Elastase and DAPI. 96
Figure 18: CM retinopathy negative and non-CM case stained with citrulinated histone H3, Elastase and DAPI. 97
Figure 19: 3D visualization of a CM ret+ capillary stained for NETosis 98
Figure 20: NETosis and UEA I staining in CM ret + versus CM ret - cases. 99
Figure 21: In vivo supplementation with MMP8 inhibitor in mice infected with P. berghei ANKA did not improve survival but delayed the neurological symptoms manifestation. 101
Figure 22: Key genes that belong in the parasite glycolysis pathway which are negatively associated with increased blood lactate. 103
Figure 23: Supplementation of in vitro parasite cultures with sodium L-lactate for 48 hours. 104
Figure 24: Supplementation of in vitro parasite cultures with sodium L-lactate for 96 hours. 105
Figure 25: Parasitaemia measurement at 48 hours after supplementation with 15mM L-lactate. 106
Figure 26: Factors affecting parasite load. 112
Figure 27: Estimating the host response and parasite load dynamics in malaria 114
Figure 28: Transcriptional correlates of parasite growth inhibition. 115

Figure 29: Cathepsin G and MMP9 growth assay (A) and invasion assay (B). 117
Figure 30: Cathepsin G and MMP9 release following healthy donor whole blood (n=8) stimulation with 1µM PMA. 118
Figure 31: Dose response for invasion inhibition using cathepsin G pre-treated erythrocytes against four parasite strains. 119
Figure 32: Dose response of cathepsin G for the assessment of erythrocyte surface receptor cleavage. 120
Figure 33: Dose response of MMP9 for the assessment erythrocyte surface receptor cleavage. 121
Figure 34: Effect of PMA stimulation of healthy donor whole blood erythrocyte surface receptor expression assessed by fluorescence intensity. 122
Figure 35: Plasma concentrations of A) Cathepsin G and B) MMP9 using Gambian samples from uncomplicated and severe malaria cases. 123
Figure 36: Percentage of erythrocyte receptor expression using erythrocytes from Gambian children 124
Figure 37: Experimental design for the infections. 134
Figure 38: Parasitaemia percentage measured by microscopy. 137
Figure 39: Severity scores. 139
Figure 40: Percentage of weight compared to baseline weight. 141
Figure 41: Lactate (mmol/L) measured at the end point for each infection. 142
Figure 42: WBC proportions measured in whole blood by flow cytometry in C57BL/6 mice. 143
Figure 43: *Predicted upstream regulators of genes positively associated with lactate concentration in human and mouse blood (edited from Ingenuity Pathway Analysis).* 144
Figure 44: Heatmap of the top human malarial hyperlactataemia phenotype (CH+HL) DE genes with a mouse otholog 145
Figure 45: Heatmap of the top human cerebral malaria phenotype (CH+CM) DE genes with a mouse ortholog 146
Figure 46: Concordant and discordant genes between human hyperlactataemia phenotype (CHHL) and mouse hyperlactataemia phenotype (Py17XL). 147
Figure 47: Comparison of MMP8 staining of the retinal vasculature among non-CM, CMret-, CMret+ (vessels without sequestration) and CMret+ (vessels with sequestered parasites). 187

List of Tables

Table 1: Criteria for defining Plasmodium falciparum severe malaria in children. 39
Table 2: Antibodies used for defining WBC proportions using FACS. 66
Table 3: *Antibodies used to assess the erythrocyte receptors surface expression.* 69
Table 4: ELISA Kits 70
Table 5: Antibodies used for IHC and IF 72
Table 6: Characteristics of subjects selected for RNA-sequencing 78
Table 7: Clinical diagnosis and classification of subjects whose ocular tissue was used for immunohistochemistry and immunofluorescence experiments. 85
Table 8: Pathways in which genes associated with lactate are involved (PlasmoDB) 102
Table 9: Commonly used malaria mouse models. 132
Table 10: Selected transcriptomic studies in malaria. 179
Table 11: Parasite genes associated with host lactate. 197

Declaration of Originality

This dissertation describes my work jointly supervised by Dr Aubrey Cunnington and Professor Michael Levin at the Department of Paediatrics at Imperial College, London. It is submitted in fulfilment of the requirements for the degree of Doctor of Philosophy. The work described here has not been submitted for any degree, diploma, or any other qualification. This dissertation is the result of my own work and the guidance of my supervisors, exceptions are described at the text below.

The RNA sequencing samples and clinical information were made available to me via my supervisor Dr Aubrey Cunnington. Bioinformatics analysis for RNA sequencing was performed by Dr Hyun Jae Lee from University of Queensland for chapter 3 and 4, and by Pablo Soro Barrio from Imperial College London for chapter 5 after initial pipeline design by Dr Hyun Jae Lee. RNA sequencing and library preparation was performed at Exeter University Sequencing Service. The mathematical model fitting and analysis for chapter 4 was performed by Dr Michael Bretscher from the Malaria Modelling Group at Imperial College.

Athina Georgiadou

London, January 2019

Copyright Declaration

The copyright of this thesis rests with the author. Unless otherwise indicated, its contents are licensed under a Creative Commons Attribution-Non Commercial 4.0 International Licence (CC BY-NC). Under this licence, you may copy and redistribute the material in any medium or format. You may also create and distribute modified versions of the work. This is on the condition that: you credit the author and do not use it, or any derivative works, for a commercial purpose. When reusing or sharing this work, ensure you make the licence terms clear to others by naming the licence and linking to the licence text. Where a work has been adapted, you should indicate that the work has been changed and describe those changes. Please seek permission from the copyright holder for uses of this work that are not included in this licence or permitted under UK Copyright Law.'

Publications

Publications' list arising from the work described in this thesis at the time of submission:

1. Lee HJ, **Georgiadou A**, Walther M, Nwakanma D, Stewart LB, Levin M, Otto TD, Conway DJ, Coin LJ, Cunnington AJ et al., 2018, Integrated pathogen load and dual transcriptome analysis of systemic host-pathogen interactions in severe malaria, SCIENCE TRANSLATIONAL MEDICINE, Vol: 10, ISSN: 1946-6234
2. **Georgiadou A***, Bretscher M*, Lee HJ*, Walther M, van Beek A, Fitriani F, Wouters D, Kuijpers T, Nwakanma D, D'Alessandro U, Riley E, Levin M, Coin L, Ghani A, Conway D, Cunnington A, et al., 2018, Estimating parasite load dynamics to reveal novel resistance mechanisms to human malaria, "Preprint", BioRxiv, doi: https://doi.org/10.1101/321463 (under review in Nature Microbiology)
3. Lee HJ*, **Georgiadou A***, Otto TD, Levin M, Coin LJ, Conway DJ, Cunnington AJ et al., 2018, Transcriptomic Studies of Malaria: a Paradigm for Investigation of Systemic Host-Pathogen Interactions, MICROBIOLOGY AND MOLECULAR BIOLOGY REVIEWS, Vol: 82, ISSN: 1092-2172

* Joint first author

Abbreviations

AMA1 apical membrane antigen 1

BSG or CD147 basigin

CD36 cluster of differentiation 36

CD55 or DAF receptor Decay accelerating factor

CH Malarial Hyperlactataemia + CM Cerebral Malaria

CitH3 Citrullinated Histone 3

CM Cerebral Malaria

CR1 or CD35 complement receptor 1

CSF cerebrospinal fluid

DBL Duffy binding-like protein

DEFA3 defensin A3

DEGs differentially expressed genes

EBL erythrocyte-binding-like protein

ECM experimental cerebral malaria

Elastase or ELANE Neutrophil Elastase

ELISA Enzyme-linked immunosorbent assay

EPCR endothelial protein C receptor

FDR False discovery rate

FNG fibrinogen

FSC-A Forward scatter area

GBP Glycophorin binding protein

GPA or GYPA glycophorin A

GPB or GYPB glycophorin B

GPC or GYPC glycophorin C

HL Malarial Hyperlactataemia

ICAM-1 intracellular adhesion molecule 1

IFN-y Interferon gamma

LCN2 Lipocalin 2

LRG1 Leucine Rich Alpha-2-Glycoprotein 1)

LTa lymphotoxin a

MA-ARDS malaria-associated acute respiratory distress syndrome

MIP Malaria in pregnancy

MMP8 matrix metallopeptidase 8

MMP9 matrix metallopeptidase 9

MSP merozoite surface protein

NLR NOD-like receptor

OLFM4 olfactomedin 4

PAMP's Pathogen-associated molecular pattern molecules

PfEMP1 *P. falciparum* erythrocyte membrane protein 1

PMA phorbol 12-myristate 13-acetate

RBCs Red Blood Cells

Rh or RBL reticulocyte-binding –like protein

RMCBS Rapid Murine Coma and Behaviour Scale

RNA seq RNA sequencing

S100A8 S100 Calcium Binding Protein A8

S100A9 S100 Calcium Binding Protein A9

Sema7a or CD108 Semaphorin 7A

SM Severe Malaria

SSC-A Side scatter area

SUB1 subtilisin 1 protease

TGF- β transforming growth factor-β

TLR Toll-like receptor

TNF Tumor necrosis factor

UM Uncomplicated Malaria

VACM-1 vascular cell adhesion molecule 1

WHO World Health Organization

Chapter 1: Introduction

1.1 Malaria

With considerable contribution to the global disease burden and ~ 219 million new cases in 2017 (~3.5 million more cases compared with the previous year), malaria is still among the most prevalent infectious diseases in the world as well as being the most significant vector borne infectious disease (1, 2). Severe malaria claims 435,000 deaths annually, according to the World Malaria Report 2018 from World Health Organization, 90% of which occur in the African Region (1). The female *Anopheles* mosquito is responsible for the transmission of the protozoan, *Plasmodium,* parasites that cause malaria infection. There are five main species of *Plasmodium* responsible for human disease: *P. falciparum, P. knowlesi, P. vivax, P. ovale*, and *P. malariae*. *Plasmodium falciparum,* is the deadliest (3) among these species, accounting for 90% of deaths from malaria (4), and is the focus of studies of human malaria in this thesis. Despite the significant progress in malaria eradication achieved over the last 15 years (WHO 2016), the limited efficacy of the currently available vaccines (5, 6) and the *Plasmodium* resistance emerging to all available anti-malaria drugs hamper the efforts (7, 8). The main victims of severe malaria are children under the age of five and pregnant women. Although, treatment with anti-malarial drugs improves the outcome in severe disease there are syndromes such as cerebral malaria (CM) in which the established pathogenesis in the host cannot be reversed. Consequently, there is a need for development of new treatments, targeting not only the parasites but the underlying pathogenesis mechanisms as well.

1.2 Parasite life cycle

During the blood meal of an infected female *Anopheles* mosquito sporozoites (parasite motile form) found in the mosquito's saliva pass from the host skin to blood vessels and then travel to the liver finding their way into hepatocytes where they massively replicate asexually (liver stage) (Figure 1). After around a week of incubation in the liver the hepatic schizonts rupture, releasing thousands of merozoites in the host's bloodstream which invade the host erythrocytes and start a repeated asexual replication cycle (9). This asexual (blood) stage is the only stage during which malaria symptoms occur. As the parasite load increases exponentially the host response gets triggered trying to constrain it, while symptoms such as muscle ache, shivering, fever, and headache may occur (9-11).

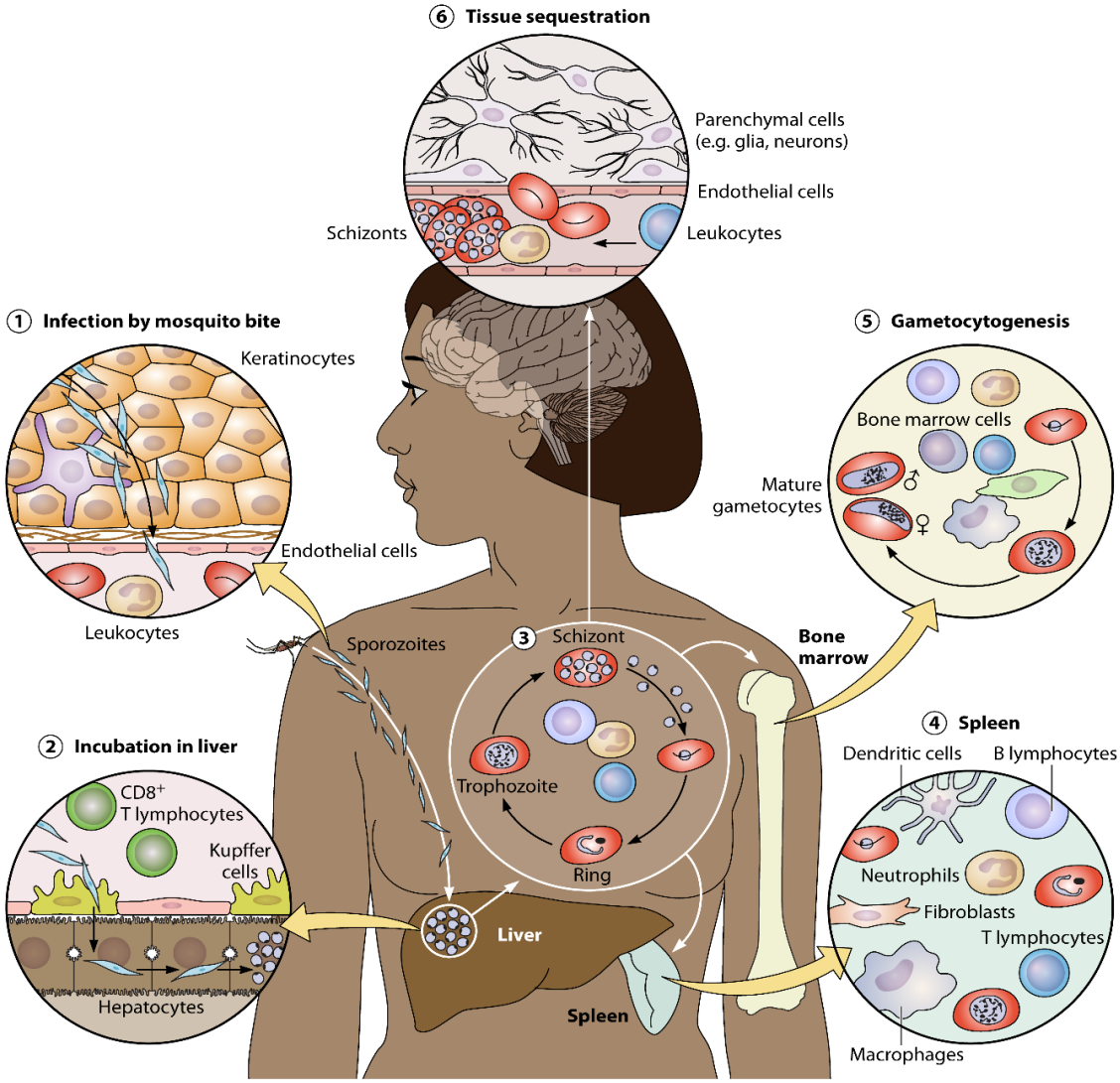

Figure 1: P. falciparum asexual life cycle stages.

1) Infection starts with a mosquito bite. Motile sporozoites injected into the host dermis quickly find their way to the liver. 2) Sporozoites start a massive replication inside the host hepatocytes. Immune cells patrolling the liver, as the CD8 T cells, can detect and kill the infected hepatocytes. 3) Infected hepatocytes containing mature parasites burst and the daughter merozoites rapidly enter the blood stream infecting red blood cells. This is the asexual stage of parasite replication during which the parasite undergoes repeated cycles of replication increasing the parasite load exponentially. During this stage parasitized red blood cells interact with blood leukocytes, while parasite products/toxins start triggering an inflammatory response. 4) Spleen is a major organ for the immune response to Plasmodium, important for clearing parasitized red blood cells. 5) Some of the parasites stop the asexual replication to produce gametocytes. Mature gametocytes are the stage of parasites that can be taken by another mosquito to continue transmission to a different host. 6) Sequestration of parasites in the brain and other organs along with obstruction of the microvasculature can cause severe disease. Reproduced from: "Transcriptomic Studies of Malaria: a Paradigm for Investigation of Systemic Host-Pathogen Interactions" under Creative Commons CC BY license (12).

1.3 Selected aspects of *Plasmodium falciparum* biology

Plasmodium species are single-celled eukaryotic organisms (13) which belong to the phylum *Apicomplexa*, named for the apical complex involved in host cell invasion (11). Up to date, comprehensive reviews on different aspects of malaria biology have provided great insights (3, 11, 14). Here, I will be focusing on parasite gene expression and invasion as these are the most relevant aspects of the parasite's fascinating biology to the rest of the work presented throughout my thesis.

1.3.1 Gene expression

The complex life cycle of *Plasmodium* and its progression is closely controlled by a coordinated cycle of gene expression which has been explored using RNA seq and micro-arrays (15-18). For the majority of genes through the intra-erythrocytic cycle, a striking phasic variation has been identified in expression (15, 16, 19), conserving protein production to only when each protein is needed (12). Genes important for parasite invasion are only expressed in the mature schizont stage, so that when merozoites are released upon schizont rupture, they are equipped appropriately so they can invade other red blood cells (15). Although there is an overall conserved pattern for this phasic variation, among different species of *Plasmodium*, the expression of individual genes in not as highly conserved, with the greatest variation appearing at the stage with the greatest host-cell interaction, which is during the development of early rings (19). Gametocytes, the stage responsible for transmission of the parasites, have a unique program of gene expression which is controlled by AP2G, a master regulator transcription factor (17, 18).

Comparing among different *Plasmodium* species, can give important insights into parasite biology (12). All the sequenced *Plasmodium* genomes until today have multigene families found in subtelomeric regions of their chromosomes (13, 20-25), encoding for proteins expressed on or close to the surface of the infected erythrocytes. Up to 30% of the parasite genome, depending on the species, is dedicated to multigene families (26), suggestive of their important role (12). The multigene *var* family of *P. falciparum* is one of the best known multigene families, encoding for ~60 different copies in each parasite, of *P. falciparum* erythrocyte membrane binding protein 1 variants, proteins which are antigenically diverse and expressed on the surface of infected red blood cells (RBCs) (27). Transcriptional control of the *var* family expression results in antigenic variation and immune evasion (27-31). This

multigene family is also involved in adhesion and interaction with host cell surfaces; endothelial adhesion (sequestration) and attachment to uninfected erythrocytes (rosetting), both being associated with virulence (27, 30).

Much of what we know about the biology of *P. falciparum* comes from *in vitro* studies where gene expression follows highly ordered sequences and results in reproducible parasite behaviour (12). Some evidence from *in vivo* studies suggests that there is a generally well conserved gene expression between parasites taken from humans naturally infected and *P. falciparum* laboratory adapted strains (32). Variation in parasite behaviours may have a genetic basis or occur in response to host environment as the genes that appear to be upregulated *in vivo* in comparison to the laboratory adapted strains belonged to the *rif* and *stevor* gene families encoding for proteins exported on the surface of the red blood cell (32), while in a another study the main differences were detected when comparing severe malaria subjects with the *in vitro* transcriptome (33). These findings suggest that when its environment is perturbed, the parasite alters its gene expression to adapt accordingly (12). This parasite ability to adapt into the host environment was recently shown in infected mice receiving different diets, one being normal and the other one low-energy, which revealed changes in the parasite transcriptome and the identification of the parasite molecule KIN (putative serine/threonine kinase) as sensor of host nutritional status and regulator of parasite growth (34). Taken together, all these studies suggest that most of the parasite gene expression variations may be due to the need for optimum interaction with the host red blood cells and within-host environment (12).

1.3.2 Erythrocyte invasion

1.3.2.1 Mechanical steps

The *Plasmodium* life cycle includes two hosts, the *Anopheles* mosquito and the vertebrate (intermediate) host, which in the case of *P. falciparum* is the human. *Plasmodium* merozoites are adapted uniquely in order to invade erythrocytes, a cell type to which they are restricted. Once they manage to enter the erythrocyte, they can remodel the host cell in a way that provides the required nutrients for development as well as the means to avoid the host immune response (35). Merozoites have as a single purpose, to invade red blood cells, so their design is optimised for this goal. They are polarized cells, and the apical end contains

structures and organelles, such as rhoptries and micronemes, which facilitate erythrocyte invasion upon contact (36). Micronemes contain adhesins important for erythrocyte binding, while the rhoptries get released after the initial engagement with the host cell, facilitating the process of invasion and the formation of the parasitophorous vacuole in which merozoites replicate and form their daughter cells. There is evidence suggesting, there might be different types of micronemes depending on the type of adhesins they contain, which allows a highly organized release program (37, 38). The dense granule organelles can also have different subpopulations, while exonemes are an organelle subset which releases the subtilisin 1 protease (SUB1) in the parasitophorous vacuole, proteolytically processing several parasite proteins to facilitate egress (39). Dense granules can be released during fusion with the parasite plasma membrane at different stages of the asexual cycle. The subsets and compartmentalization of these organelles can be critical in enabling release of specific ligands when needed for each step during invasion (36). The apical organelles do play an essential role during invasion, but the merozoite surface is what first interacts with the erythrocyte, triggering a series of mechanical steps which end with the entry into the host erythrocyte. These mechanical steps are rapid and were visualized for the first time with the use of video-microscopy looking at *P. knowlesi* merozoites (40), and then for *P. falciparum* (41), suggesting that kinetics and sequence of events in this process are conserved among different *Plasmodium* species. These visualizations have divided invasion in three phases: a) initial interaction and erythrocyte membrane deformation, b) apical interaction and invasion, and c) echinocytosis (rapid erythrocyte shrinkage) and recovery of the host cell. Previously, erythrocyte activity during invasion had been unknown, however, unravelling the merozoite interactions suggested that wrapping the cell membrane of the erythrocyte followed by underlying cytoskeleton reorganization could account as the erythrocyte active role during invasion (42). It has also been shown that merozoite contact has as a result the increase in the erythrocyte cytoskeleton phosphorylation (43). In addition, ligand binding on the surface of the erythrocyte leads to changes in deformability through activation of a phosphorylation cascade, which involves the kinase activity of the host TRPM7 (transient receptor potential cation channel) (44). Using flicker spectroscopy and real time deformability cytometry revealed that EBA175 parasite ligand binding to glycophorin A (GPA) which is its host receptor, increases the tension of the erythrocyte cytoskeleton while reducing the cell membrane bending

modulus, which correlates with merozoite invasion efficiency (45). These studies agree with the activation of a phosphorylation cascade when merozoite ligands interact with erythrocyte receptors, involving the host cytoskeleton and altering the membrane viscoelastic properties, a process important for parasite invasion (36).

1.3.2.2 Molecular basis (initial stage of invasion)

MSPs (merozoite surface proteins) may have a role during the initial invasion phase, which involves the first merozoite-erythrocyte interaction. A large complex forms on the surface of the merozoite involving MSP1 and other peripheral proteins, which is required for invasion. However, recent studies revealed merozoites without MSP1 can also invade, which suggests that it might not be essential for the invasion process (46). The initial tight interaction of merozoite with the erythrocyte is known to be through two major adhesin families most likely released, upon intracellular signaling, from the micronemes. These proteins are Rh or RBL (the reticulocyte-binding –like protein homolog) and DBL (Duffy binding-like) or EBL (erythrocyte-binding-like) protein. The first protein (DBL) binding Duffy antigen/chemokine receptor (DARC) (47) was identified looking at *P. knowlesi*, and orthologs have been identified for *P. falciparum* and *P.vivax*. This family in *P. falciparum* involves, EBA-175 which binds to glycophorin A (GPA) (48), EBL1 which binds to glycophorin B (GPB) (49), EBA-140 (also known as BAEBL) (binds to glycophorin C [GPC]) (50, 51) and EBA-181 (also known as JSEBL) which binds to an unknown receptor (52). The Rh or RBL family was first recognized in *P. vivax* (53) while now other *Plasmodium* species are known to have orthologs for this family (53). *P. falciparum* family includes PfRh1, PfRh2a, and PfRh2b, all of which bind to unknown receptors (54-57), PfRh4 binding to complement receptor 1 (CR1, CD35) (58), and PfRh5 which binds to basigin (BSG, CD147) (59) (Figure 2).

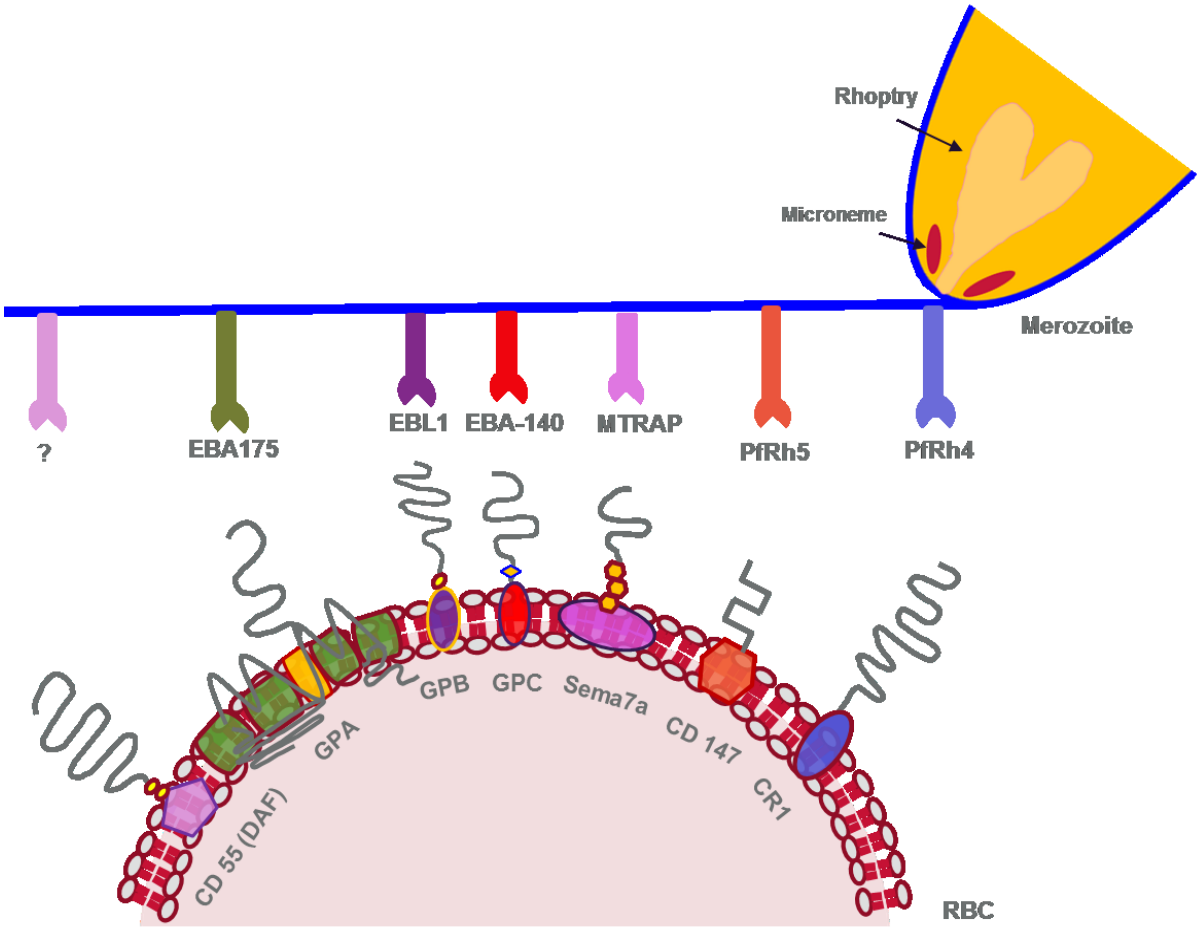

Figure 2: RBC surface receptors important for P falciparum invasion.

Schematic representation of some of the most important erythrocyte membrane receptors and the respective ligands found on the surface of the merozoite. Interaction between these RBC receptors and the merozoite ligands is crucial for the successful invasion of the parasite into the RBC.

Although, most of these merozoite proteins at an individual level might appear as non-essential, their function overall is important for invasion (60). PfRh5, which is the exception, is a much smaller protein compared to the other PfRh with no transmembrane region and in control of an essential and separate step during invasion (61, 62). Many interactions between ligands and receptors need to be characterized, since many of the PfRh/EBAs have not yet been identified. Decay accelerating factor (DAF or CD55) has been identified through a comprehensive shRNA (small hairpin RNA) knockdown screen, as receptor essential for parasite invasion (63). Identification of the parasite ligand for this erythrocyte receptor would allow an innovative focus on developing new therapeutics that could stop parasite invasion. DAF, also has a role in regulating complement on the surface of the erythrocyte, highlighting

the need for studying the parasite invasion process in an active complement environment (36).

Merozoite live imaging with the addition of specific inhibitors has revealed the distinct steps during invasion executed by different interactions between receptor-ligand including the Rh and DBL ligands (62). During the initial contact, the merozoite weakly attaches to the erythrocyte, and this leads to a stronger erythrocyte deformation due to the engagement of PfRhs/EBAs with their receptors, GPA, GPB, GPC, BSG, and CR1, and the contribution of the actinomyosin motor. The merozoites that manage to deform the surface of the erythrocyte the strongest are the ones which are more likely to invade successfully, suggesting that deformation is essential for embedding of the merozoite on the surface of the erythrocyte securely in a detachment resistant way under the condition of blood flow. Calcineurin, is parasite phosphatase complex protein, utilized by the merozoites, as it responds to Ca2+ signaling which starts at the merozoite contact with the erythrocyte, strengthening the host –pathogen adhesion as it induces stronger binding of PfRhs/EBAs with the respective erythrocyte receptors (64). It is intriguing, that calcineurin has not been associated with the first steps of attachment, but functions together with PfRh/EBAs and AMA1 (apical membrane antigen 1), suggestive of a signal transduction pathway linked to recognition of the host cell (64). Before the merozoite apical reorientation a strong deformation takes place, most probably induced through wrapping of the erythrocyte membrane (42), and the engagement of PfRh5 with basigin, its erythrocyte receptor (59). This essential step during invasion is associated with a Ca2+ flux, suggested to emanate from merozoites in the erythrocytes, from a pore formed possibly through PfRh5 engagement (61, 62).

1.3.2.3 Extracellular merozoite has evolved for protection

Some peripheral and surface proteins are not directly involved in invasion, but protect the merozoite from the immune response, and these are also naturally acquired immunity targets. After the egress from the erythrocyte, merozoites get exposed to complement. In a recent study of *P. falciparum*, a member of the 6-cys family, Pf92 was shown to actively recruit Factor H, which is one of the main negative regulators of complement activation alternative pathway (65). The merozoite inhibits activation of complement on its surface, through FH hijacking, resulting in protection from complement lysis. On the other hand, host's acquired immunity also targets MSP's, providing with an antibody repertoire that inhibit parasite

invasion. MSP1 and MSP2 human antibodies favor complement deposition on the merozoite and inhibit parasite invasion by C1q fixation (66). This complement dependent and antibody mediated inhibition seems to be an important functional mechanism that the majority of human invasion-inhibitory antibodies use to prevent parasite invasion. Together, these studies emphasize the complex interaction between the merozoite and human complement and the need to understand the immune evasion mechanisms it employs and the way invasion-inhibitory antibodies function apart from blocking the interactions between ligand-receptor (67).

1.4 Clinical features of malaria

Malaria symptoms occur only during the asexual (blood) stage, while the parasite replicates in the host red blood cells (RBCs). Every ~48 hours in human *P. falciparum* infections, parasites multiply producing ~20 merozoites per parasite (68). This synchronous burst that increases massively the parasite burden leads to the clinical disease known as malaria, with characteristic cycles of fever, chills, and sweating. The symptoms associate with the infected erythrocyte rupture and release of potential malaria toxins and pyrogens, which in turn activate peripheral blood mononuclear cells and stimulate cytokine release (69). The symptoms can include chills, fever, headache, cough, abdominal discomfort, diarrhoea, rigors, muscle ache, vomiting, anorexia, thrombocytopenia, severe anaemia, hyperlactataemia, metabolic acidosis, hypoglycaemia, respiratory distress, seizures, retinopathy, coma, and pregnancy complications such as low weight at birth due to foetal growth restriction or pre-term birth (69).

1.5 Different severe malaria syndromes - Independent predictors of death

Plasmodium falciparum infection can result in asymptomatic disease, uncomplicated malaria, or severe malaria. A few cases (~1%) of malaria infection, however, turn out to be severe causing devastating symptoms to the host, leading even to death (70) (Table 1).

Impaired consciousness	Blantyre coma score <3 in children
Acidosis	A base deficit of > 8 meq/l or plasma bicarbonate of < 15mM or venous plasma lactate > 5 mM. Severe acidosis manifests clinically as respiratory distress rapid, and deep breathing
Hypoglycaemia	Blood or plasma glucose < 2.2 mM (<40mg/dl)
Severe malarial anaemia	A haemoglobin concentration < 5g/dl or a haematocrit of < 15% in children < 12 years of age together with a parasite count > 10000/ul
Renal impairment (AKI)	Plasma or serum creatinine > 265 uM (3mg/dl) or blood urea > 20 mM
Jaundice	Plasma or serum bilirubin > 50 together with a parasite count > 100000/ul
Pulmonary oedema	Radiologically confirmed, or oxygen saturation < 92% on room air with a respiratory rate > 30/min, often with chest indrawing and crepitations on auscultation
Significant bleeding	Including recurrent or prolonged bleeding from nose gums or venipuncture sites; haematemesis or melaena
Shock	Compensated shock is defined as capillary refill > 3 s or temperature gradient on leg (mid to proximal limb), but no hypotension. Decompensation shock is defined as systolic blood pressure < 70 mm Hg in children with evidence of impaired perfusion
Hyperparasitaemia	*P. falciparum* parasitaemia > 10%

Table 1: Criteria for defining Plasmodium falciparum severe malaria in children.

Adapted from World Health Organization, Severe Malaria. Page 11, 2014.

The major syndromes that comprise severe malaria in children are severe anaemia (SA), hyperlactataemia/acidosis/respiratory distress, cerebral malaria (CM) and acute kidney injury (AKI) (71, 72). Acute respiratory distress syndrome (ARDS) and acute lung injury (ALI) is more common in adults than in children, especially in pregnant women and adults with no prior immunity, and is often due to lung pathology, caused by co-existing sepsis (bacterial) or hospital acquired pneumonia which complicate severe malaria disease (73-75). These syndromes, that can overlap or occur on their own, have different clinical manifestations, mortality rates, epidemiology, and probably differences in the underlying biological triggers (Figure 3).

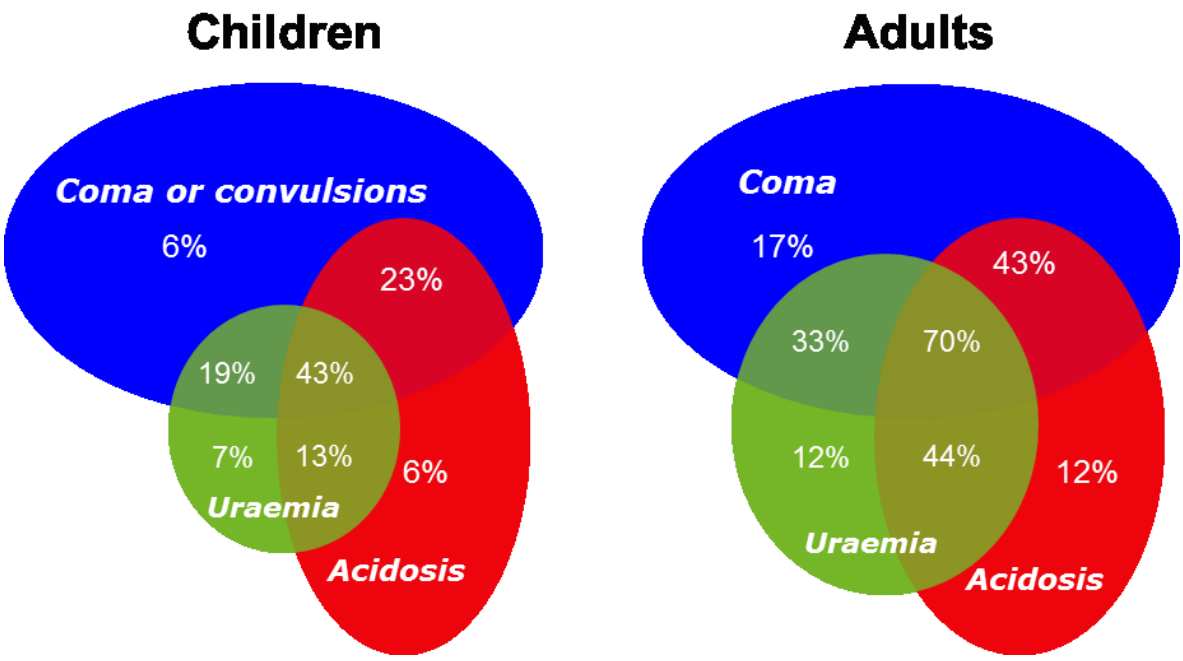

Figure 3: Venn diagrams comparing mortality rates of children and adults associated with predictors of death in severe malaria.

Surface areas denote relative prevalence in severe malaria. Uraemia is defined as blood urea nitrogen > 20 mg/dl in children and > 48 mg/dl in adults. Acidosis defined as base excess < −8 mmol/l in children and < −3 mmol/l in adults. Coma score is defined as Blantyre Coma Score < 3 in children and Glasgow Coma Score < 11 in adults. Percentages indicate mortality rates for each feature or combination of features. Adapted from World Health Organization, Severe Malaria. Page 16, 2014.

Hyperlactataemia-acidosis, coma and/or convulsions (CM), and kidney failure are the strongest independent predictors of death in children with malaria. CM and hyperlactataemia have additive effects when they coexist (3). Most of the research on malaria pathogenesis has been devoted to CM and few studies have investigated hyperlactataemia, which is an equally important syndrome. Additionally, very little research has been done to identify the factors that determine why an individual develops one syndrome rather than another (3).

Clinical manifestations between children and adults with severe malaria might be different, but recent studies revealed that kidney dysfunction, acidosis and cerebral involvement are independent predictors of death in both children and adults (76) (77). Differences in the host-parasite interactions that happen in each infected individual are probably responsible for the development of distinct SM syndromes (4). Even when antimalarial drugs are promptly administered, many children still die from severe malaria indicating how important it is to identify the underlying factors responsible for its pathogenicity and develop adjunctive treatments (71). Modern discovery approaches such as transcriptomics and proteomics have

created new opportunities for insights into the genes, proteins and pathways responsible for malaria pathogenesis (78).

1.6 Approaches to studying severe malaria

There are clear differences between human severe malaria and animal models (79-81), although there is no established way of quantifying the similarities and differences in order to understand relevance to pathogenesis (12). The mouse model of experimental cerebral malaria which has been extensively utilised in studies for human cerebral malaria pathogenesis, has been the subject of multiple debates (79). Some argue that if distinct aetiologies lead to HCM and ECM, the mechanistic insights obtained by studying ECM cannot prove useful for understanding human CM pathogenesis. One of the main differences between this mouse model and the human disease proven histologically is that while in humans multiple parasite sequestration leads to brain microvascular congestion in mice individual parasitized RBCs may occlude the brain capillaries as well along with CD8+ T-cells that also accumulate in the mouse microvasculature (80). Despite, these different presentations and the distinct mechanisms leading to parasite sequestration, there seem to be some comparable features of cerebral pathology between human and mice allowing the use of this model for studying specific features of human CM pathology (80).

The same controversy can be found in other infectious diseases, such as meningococcal disease (82), tuberculosis (83), and typhoid (84). An objective way of identifying similarities could be through a transcriptomic comparison among species (Figure 4) and across organs, looking at different timepoints, for the whole range of severity (85). Reviewing the literature, I came across few studies that allowed for comparison of the same tissue between human disease and mouse models (12). The most convenient comparison though, due to easy accessibility of the tissue, would be a whole blood transcriptomic comparison between human and mouse models, as seen already for tuberculosis (83). This way the components of a mouse model which are relevant to human disease could be identified even if there are also differences in other aspects (12) (Figure 4). Also, studies using outbred, true-wild or wild-derived mice could be quite informative as the amplified genetic variation among these mice could increase the differences seen in gene expression associated with differences in parasite load, organ dysfunction or anaemia severity, at the same time during infection, recapitulating more of the variability seen in humans.

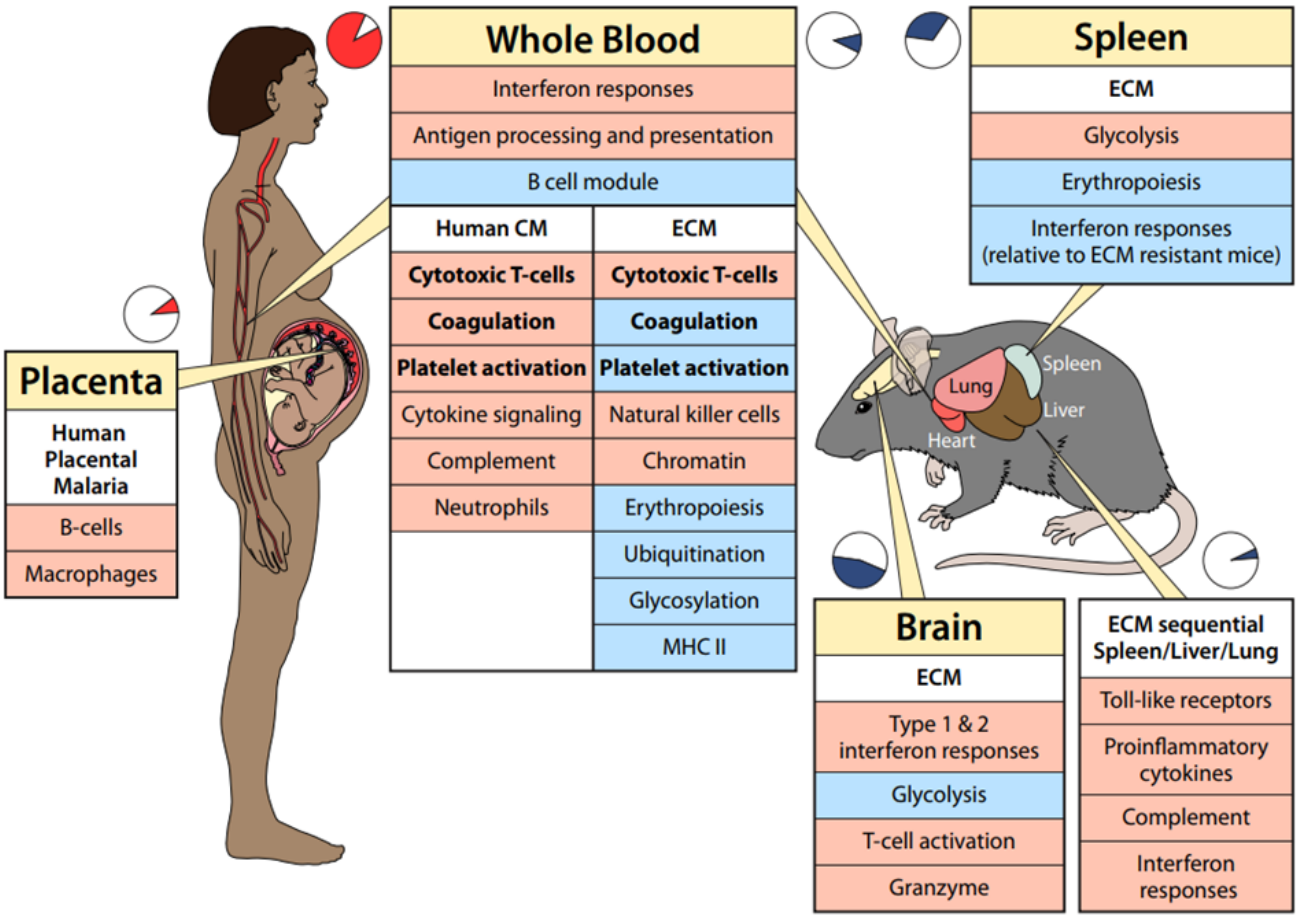

Figure 4: Transcriptomic response of the host to malaria: Similarities and differences between human and mouse.

This is a comparison of some features of host transcriptional response to malaria in mice (right) and humans (left). Pie charts indicate the frequency of studies for which this tissue has been used for each of the species. Functional groups of genes with light orange colour are the upregulated and the light blue, the downregulated. For this figure I looked at uncomplicated disease, cerebral malaria (CM) and experimental cerebral malaria (ECM).The functional groups in common between humans and mice are marked in bold (12). Reproduce from: "Transcriptomic Studies of Malaria: a Paradigm for Investigation of Systemic Host-Pathogen Interactions" under Creative Commons CC BY license.

1.7 Immune response and naturally acquired immunity

Young children under the age of 5 are at highest risk for *P. falciparum* malaria in Africa and usually the main victims of the disease. Their immune system has differences from the adult one, and these differences are probably the main contributors in the children increased

susceptibility to severe disease and the delay in immunity development. The main difference being that children have yet to develop protective immune mechanisms and antibodies after their first exposure to malaria (86). From infancy to adulthood total lymphocytes percentage as well as absolute counts of B and T cells decline. NK cells decline from infants to adults, but increase again in the elderly (87).

During acute infection, increased peripheral blood levels of pro-inflammatory chemokines and cytokines, are important for parasitaemia control however, they also contribute to the immunopathology observed during the symptomatic stage of disease. Developing clinical immunity may be dependent on the ability of the patient to control these pro-inflammatory responses, potentially through immunologic tolerance mechanisms. Although, the nature of the tolerance induced by malaria needs further investigation, many studies from both adaptive (88, 89) and innate (90) (91) (92) cell populations suggest that immunoregulatory pathways and exhaustion have a role. A recent study revealed that during acute malaria, pro-inflammatory cytokines such as IL6, IL12, IL8, GM-CSF, IL2, IL1β, IFNγ and TNF, decreased in high transmission areas, supporting the idea that malaria tolerance due to repeated exposure can be mirrored in the concentrations of plasma cytokines (93) . Interestingly, in areas of low transmission only, parasitaemia levels correlated with IL10, IL6 and TNF (93). This observation is also supported in an older study, where parasite density in European migrants and previously naïve travelers was correlated with IL10 and IL6, although no correlation was found for semi-immune adults from malaria endemic areas (94). There is also some evidence indicating that malaria tolerance could involve neutralizing antibody generation against different malaria toxins, such as Glycosylphosphatidylinositol anchors (95) and haemozoin (96), as their binding decreases the cytokine stimulating and pyrogenic capacity these compounds have (97, 98), without affecting parasite replication. Looking at murine models, disease tolerance can come at the price of weakening the host's ability to control parasite replication (99), in fact, in human cohorts, among children, asymptomatic infection can occur with significant levels of parasitaemia in areas of high transmission (93, 100-102). Overall, dampened cytokine responses seem to protect individuals from symptomatic disease, but at the same time may interfere with prevention of re-infection (103).

1.8 Pathogenesis of severe malaria

What drives the pathogenesis of SM has been one of the most difficult questions that researchers still try to answer since understanding that could lead to the development of new more effective treatments. The distinct but sometimes overlapping syndromes which severe malaria (SM) can manifest are additional facets of its complex nature (10). The major mechanisms that have been proposed to underlie SM pathogenesis are parasite sequestration and obstruction of the microvasculature, vascular endothelial dysfunction and inflammation (71). The unique ability of *P. falciparum* to induce cytoadhesion of infected RBCs to the vascular endothelium is probably the most important piece in the puzzle of severe malaria pathogenesis (72). In order to achieve this the parasite modifies the host RBC surface (adding receptors) so that late stage asexual parasites as well as immature gametocytes can adhere to the host endothelium avoiding splenic clearance (10, 68). Sequestration was initially identified and shown in cases of cerebral malaria as postmortem studies by Marchiafava E and Bignami A. in 1894 revealed microvascular obstruction in the brain (10, 104), and after some years sequestration was shown in the microvasculature of the retina (105). Sequestration occurs in many organs apart from the brain and retinal microvasculature such as, the lungs, subcutaneous fat, and small vessels of the bowel (106).

Another commonly cited mechanism in malaria pathogenesis is the excessive immune response of the host (71, 107, 108). The elevated levels of released cytokines along with other inflammatory mediators may have direct or indirect effects sometimes giving rise to symptoms similar to sepsis (70). The most recent emerging mechanism trying to explain severe malaria pathogenicity is endothelial dysfunction due to vascular endothelium activation (104). Many candidates can be responsible for the activation such as inflammatory cytokines and products released from parasitized RBCs or sequestration. Endothelial dysfunction can be devastating for the host since it can lead to vascular leak and blood –brain barrier breakdown (109), coagulation and perfusion abnormalities (110) and brain swelling (10, 111).

1.8.1 Sequestration and microvascular obstruction

Developing parasites transport *P. falciparum* erythrocyte membrane protein 1 (PfEMP1) to the surface of the RBC, to act as the main ligand for cytoadhesion (112). PfEMP1 is expressed on knobs (protrusions) on the RBC surface, which confer attachment points to the

endothelium (72). PfEMP1 proteins are strain specific and encoded by the highly variable *var* gene family, offering antigenic variation which leads to immune evasion as well as binding to different endothelial receptors (113). Known endothelial surface molecules to which PfEMP1 can bind include: vascular cell adhesion molecule 1 (VACM-1), intracellular adhesion molecule 1 (ICAM-1), endothelial protein C receptor (EPCR), and cluster of differentiation 36 (CD36) (114-120). Sequestration can occur in several organs and along with erythrocytes increased rigidity, is believed to lead to vascular occlusion(121). Microvascular obstruction can be exacerbated by RBC clumping and rosette formation (116, 117, 122), as the infected erythrocytes aggregate with platelets and infected erythrocytes bind uninfected ones (114). Both, clump and rosette formation have been associated with CM (123) and severe disease (8). It was recently shown that PfEMP1 is not the only ligand that parasites use in rosette formation. The family of repetitive interspersed proteins (RIFINs) mediate the infected erythrocytes binding to uninfected erythrocytes, preferring blood group A and forming large rosettes of >10 infected RBCs. This was not seen in cases of blood group O, a common blood group found in malaria endemic countries, in which case infected erythrocytes of blood group O were found to form weak and small rosettes (8, 124). The use of anti –RIFIN antibodies disrupted the rosette formation, confirming their role in severe disease development and their contribution in *P. falciparum* virulence (8).

Sequestration, clumping and rosetting may lead to tissue hypoxia and ischemia due to reduced blood flow in the microvasculature (109), accounting for the pathology of cerebral malaria (114), ALI/ARDS and acidosis (75). In adults with cerebral malaria or other severe manifestation of malaria *in vivo* imaging of the microcirculation as well as fluorescein angiography of the retina performed in paediatric cases of CM revealed occlusion of the vessels and reduced perfusion (76, 125). This direct visualization of retina microvascular obstruction in CM patients helped to identify what is now termed as malaria retinopathy (105, 126). There is often an increase of the intracranial pressure in children, but not so often seen in adult patients (127, 128). Measuring *P. falciparum* histidine rich protein 2 which is used for the estimation of total parasite biomass is another indirect assessment of sequestration, shown to contribute to acute kidney injury (AKI) in severe malaria adult patients (129), and in CM using cerebrospinal fluid (130) or plasma (131).

1.8.2 Endothelial activation and inflammation

There are various functions that a healthy endothelium implements in order to sustain homeostasis, such as release of nitric oxide to regulate blood flow, anti-coagulant properties by inhibiting platelet aggregation and adhesion, prevention of plasma protein extravasation to the tissue, control of the endothelial permeability, and prevention of leukocyte adhesion (132). Adult CM patients, show variable inflammatory responses, astroglial and endothelial activation in the brain, with mild changes in the blood brain barrier (72, 133). In children with retinopathy positive cerebral malaria breakdown of the blood brain barrier is observed especially in areas of sequestration (134). There are differences in the histopathology of the brain during cerebral malaria, among children and adults, with less oedema and fewer inflammatory infiltrates in the adult cases (135). A recent MRI study looking at paediatric cases, revealed that 35% showed some evidence of brain swelling mainly in the fatal cases suggestive of brainstem herniation as the cause of death (136). In another MRI study in India looking at both children and adults, it was shown that 50% of the cases had some evidence of brain swelling along with vascular congestion in the basal nuclei and posterior vasogenic oedema (137). All of them had radiological reversibility and rapid clinical improvement with evidence suggestive of posterior reversible encephalopathy syndrome (72). Under systemic inflammatory conditions such as *P. falciparum* infection, endothelial function may be seriously impaired by endothelial activation (114). Expression of adhesion molecules as ICAM-1 and VCAM-1 on the surface of the endothelium indicates endothelial activation. Based on plasma measurements of the soluble adhesion molecules, systemic endothelial activation was reported for sepsis and *P. falciparum* infected patients (138). In fatal CM cases immunohistochemistry revealed increased ICAM-1 expression in the brain vasculature when compared to non-malaria biopsies (138). Similarly, increased ICAM-1 expression was detected in the endothelial cells from brain of *P. berghei ANKA* infected mice which developed ECM compared to mice which do not develop ECM infected with the non-lethal strain of *P. yoelii* (139). Following these findings Icam-1 deficiency was protective against ECM induced by *P. berghei ANKA* infection (140). Since there is evidence for the adhesion molecules promoting leukocyte and infected erythrocyte binding to the endothelium, and given the association of murine and human CM with leukocyte accumulation in the brain vasculature, endothelial activation seems to play a critical role in CM pathogenesis (114, 141). Apart from endothelial activation, platelets have also been shown in the recent years to be able to modulate severe

malaria pathogenesis. Thrombin, being a common factor among these processes, is now considered as a driver of CM pathology (8). Thrombin engaging with thrombomodulin on an intact endothelial plasma membrane, promotes protein C activation. This is accelerated by EPCR, which after binding protein C presents it, to facilitate optimum activation through thrombin-thrombomodulin complex (8). The generated APC (anticoagulant activity) can also initiate protective cellular responses by trigging a number of cell-signaling pathways upon exposure to pro-apoptotic pro-inflammatory, or toxic insult (8). Parasitized erythrocytes that express PfEMP1 compete with APC and protein C for EPCR, decreasing activation of protein C by the thrombin-thrombomodulin complex. This results in loss of the cytoprotective signalling induced by EPCR-APC, decreasing blood-brain barrier properties, possibly causing vasogenic oedema in cerebral malaria (8).

Another cause of endothelial dysfunction due to *P. falciparum* infection, is the dysregulation of coagulation and the local microvascular lesions (142). Sequestration leads to microvascular obstruction and impaired perfusion, apoptosis associated with endothelial activation, decreased dilatory capacity and a pro-coagulant state (110, 117, 143). Endothelial dysfunction can also be due to reduced nitric oxide bioavailability and synthesis (3, 144, 145) along with increased oxidative stress (146, 147), and increased oxygen consumption (144) which can reduce the deformability of the erythrocytes (148, 149) and impair the control of vascular tone as well as the neurovascular coupling (143, 150).

In severe malaria recovery of the endothelial function is associated with recovery from lactic acidosis and hypoargininemia, suggestive of the potential for an adjunctive treatment such as L-arginine which can improve endothelial function via increasing NO production (151). However, when Yeo and colleagues added L-arginine as adjunctive treatment (first clinical trial of an adjunctive treatment aimed at increasing NO bioavailability in severe malaria), L-arginine did not improve endothelial NO bioavailability or lactate clearance (152). L-arginine bioavailability alters during malaria in pregnancy affecting placental vascular development (153). A quite recent study showed that l-arginine supplementation improved birth outcome in a model or MIP (malaria in pregnancy) (153). This could suggest that l-arginine adjunctive treatment might be more useful in pregnant malaria patients.

Inflammatory cytokines are another factor to consider for endothelial activation. *In vitro*, lymphotoxin a (LTa) and TNF can activate human endothelial cells (154, 155). Similarly, IL-1b, IL-1a and IFN-y play a role in endothelial activation (156). In *P. falciparum* infected cases a marked elevation in the plasma levels of the pro-inflammatory cytokines has been shown, while IL-1b, IL-1a and TNF have been associated with severity of CM (157, 158). Subsequently, cytokines might be one of the mediators in the endothelial activation seen in *P. falciparum* infections (114). In agreement, with the role proposed for endothelial activation in human CM, in murine ECM pathology we see an association with T helper 1 immune response, while LTa, TNF and IFN-y cytokines, along with immune cells, $CD8^+$ and $CD4^+$ T cells with NK cells together are involved in ECM (141, 159-163). On the other hand, despite the association of TNF with CM severity, it was shown that *Tnf-deficiency* did not protect mice from developing ECM, and blocking of TNF with pentoxifylline or anti-TNF antibodies did not prolong survival in human CM (161, 164-167). These findings highlight the complexity of malaria disease and the CM syndrome, indicating that additional mechanisms play a critical role in CM pathogenesis, and suggesting that single cytokines associated with severity of CM do not always translate in beneficial treatment (114).

Endothelial cells have a critical role to play as part of the innate immune response, as they can recognize PAMP's through their pattern recognition receptors such as NLR and TLR. Endothelial cells can secrete pro-inflammatory cytokines, such as IL-6, IL-1b and IL-1a, along with immunomodulatory cytokines, as TGF-b and IL-10, as well as chemokines, RANTES/CCL5, MCP-1 (monocyte chemoattractant protein 1)/CCL2 and IL-8/CXCL8, after stimulation with LPS or pro-inflammatory cytokines *in vitro* (168). Microvascular endothelial cells deriving from adipose tissue of patients with either fatal CM or uncomplicated malaria, gave rise to a different endothelial inflammatory response after *ex vivo* stimulation with TNF (169). The CM derived endothelial cells, expressed significantly higher levels of platelet and parasite receptors, released more pro-inflammatory cytokines, were more prone to apoptosis and produced more endothelial microparticles (169). Based on these results, it was hypothesized that genetic variations controlling inflammatory genes may have a role in the disease course of CM patients (170), similar to what has been shown for sepsis (171). This evidence supports the concept of endothelial cells enhancing the pro-inflammatory microvascular setting under

infection by *P. falciparum*. Interestingly, microvascular endothelial cells from human brain have been shown as able to phagocytose merozoites (*P. falciparum*) *in vitro* (172).

Human endothelial cells, upon co-culture with erythrocytes infected with *P. falciparum*, were reported to express higher levels of ICAM-1 (173, 174), to secrete IL-8/CXCL8, MCP1/CCL2, and MIP-3a/CCL20 (173, 175), and to have higher transcription of IL-6, CCL20, CXCL8, CXCL1, and CXCL2 (176). These *in vitro* observations are suggestive of a potentially direct role for endothelial cells in the immune response malaria infection. Although, the extent to which chemokines deriving from endothelial cells contribute in the leukocyte accumulation process in the brains of CM patients or ECM mice needs to be established, several clinical studies report that numerous chemokines are higher in CSF and serum of CM patients, providing a potential connection between CSF and serum chemokine concentrations and progression from mild to severe disease (114). There has been some evidence to support the role of chemokines in CM from the murine models of ECM, in which it was shown that Cxcl10-, Cxcl9- and Cxcl4-deficiency reduced mortality associated with ECM (177-179). *Cxcl4* deficiency had as a result decreased serum IFN-γ and TNF levels in a *P. berghei ANKA* infection, indicating the possible contribution of CXCL4/PF4 in the establishment of a pro-inflammatory environment, which may further amplify immune responses promoting CM pathogenesis (178). In the *Cxcl10* deficient mice protection from ECM was associated with reduced sequestration of leukocytes in the brains of *P. berghei ANKA* infected mice, while an increased number of $CXCR3^+$ T cells (parasite specific) was identified in spleens of *Cxcl10* deficient mice when compared to wild type, suggestive of CXCL10 as a mediator for the recruitment of $CXCR3^+$ T cells in the brain, contributing in ECM development (114, 179).

Together, there seems to be evidence for activated endothelial cells contributing to local inflammation through the secreted chemokines and cytokines, which in turn recruit leucocytes, such as neutrophils, macrophages, T cells, and monocytes, which accumulate in human and mouse brains during CM and ECM respectively (180, 181). Sequestration, inflammation and endothelial activation all interact, on one hand making it difficult to define the initiating or dominant mechanism, but on the other creating an amplifying cycle between all three (10).

1.8.3 Pathogen load

Pathogen load, and specifically in malaria, parasite load has attracted a lot of attention the last years as it has been recognised as one of the main determinants of severe malaria (71). In malaria, symptoms occur only during the blood stage of the parasite so the most common way of measuring pathogen load and diagnosing the disease has been the microscopic examination of Giemsa stained blood smears for the assessment of parasitaemia (182). However, certain species of *Plasmodium* sequester and avoid sampling, leading to an underestimate of the total parasite biomass when only circulating parasites are taken into account. This underestimation could be the reason why in some cases parasitaemia measured from the circulating parasites does not prove as a valid outcome predictor (71, 182). The concentration of a soluble parasite protein named histidine rich protein 2, found in plasma has been shown as an approximate of the total parasite biomass in the body (71, 183). Since the discovery of this method it has been widely utilized to show parasite biomass as a severity and outcome predictor in children (184-188). In malaria, evaluation of host-parasite interactions in whole blood through transcriptomic analyses can provide a paradigm for understanding the general role of systemic host-pathogen interactions (12). As presented in chapter 3 we showed that ~99% of the human differentially expressed genes in severe malaria were primarily driven by the parasite load.

1.8.4 Lactate

Metabolic acidosis is one of the most important determinants of survival in severe malaria and leads to respiratory distress (189). In most cases this is a lactic acidosis, which can be due to various causes such as decreased clearance by the liver, increased parasite production of lactic acid and most probably due to a combination of factors that lead to reduced delivery of oxygen to the tissues (68, 190). In a study of Gambian children with severe malaria, 46% of which had cerebral malaria and 18% died, blood lactate concentration in the fatal cases was almost double of that of the survivors (7.1 mmol/L vs. 3.6 mmol/L; $P < 0.001$), and found to be correlated with TNF ($r = 0.42$, $n = 79$; $P < 0.0001$) and IL 1-alpha ($r = 0.6$, $n = 34$; $P < 0.0001$), while the glucose concentrations were lower in fatal cases (191). Another study, looking at severe *P. falciparum, P. vivax*, and mixed malaria patients with hyperlactataemia, revealed an association between serum lactate and renal failure, jaundice, thrombocytopenia and anaemia. Waller et al., found hyperlactataemia to be an independent indicator of death in African children with severe malaria (192). Another study, showed that hyperlactataemia is

associated with metabolic acidosis (193), while acidosis is significantly associated with fatal outcome (190). Van Genderen et al., showed that plasma lactate levels at admission were significantly higher in travelers with *P. falciparum* severe malaria compared to those with uncomplicated disease. This suggested that timely determination of plasma lactate on admission could be a useful tool for clinicians who want to estimate disease severity (194). Lactate levels have also been found to be increased in the cerebrospinal fluid of patients with cerebral malaria. There was also a negative correlation revealed between lactate and glucose levels in CSF. All patients recruited in this study, with lactate higher than 6 mmol/l in their CSF, died (195). A study looking at a tribal population of adults in India, with CM due to *P. falciparum* (78%) or due to *P. vivax* (22%), suggested that there is a strong correlation of coma depth and duration, retinal changes (hemorrhage, vessel changes and whitening) and hyperlactataemia with increased mortality, longer hospitalization, neurological consequences and death (196). All of these studies, reveal the need for better understanding of the mechanism underlying hyperlactataemia and also the development of adjunctive treatment that could reverse this fatal imbalance.

1.9 Treatment and protection from severe malaria

For severe malaria, two major drug classes are available for parenteral treatment and these are the cinchona alkaloids (quinine) and the most preferred artemisinin derivatives (artesunate) (197, 198). The use of artemisinins has a key advantage and this is the rapid action they have against all erythrocytic stages of *Plasmodium* (as well as gametocytes) offering a major clinical benefit (197). The WHO recommendation for first line treatment is artesunate administered intravenously or intramuscularly (for at least 24h) until the patient can tolerate oral therapy (199).

Malaria control programs include insecticide-treated bed nets, environmental insecticide spraying, drug treatments and prophylactic measures for travelers. However, there are major problems arising such as mosquito resistance in pyrethroids, multi drug resistance to all the available anti-malarials and lack of effective vaccines (198). In malaria endemic countries, *P. falciparum* resistance has been widely detected to multiple drugs. The drug resistance of parasites comes from mutations of genes encoding important components of the drug targets such as the dihydrofolate reductase (*Pf*dhfr) and dihydropteroate synthase (*Pfdhps*) (198, 200, 201), the gene encoding for *P. falciparum* Kelch 13 (PfKelch13), also shown to be a

major causative artemisinin-resistance marker and predicted to act as a quality control regulator for proteins (202-204), as well as mutation in *pfcytb* (leading to catalytic activity changes) (205), *pfcrt (206)*, and *pfmdr1* (207, 208).

Despite artemisinin being the best available therapy for malaria, mortality rates remain quite high, indicating the need for supportive management in order to reduce this (72). Comatose patients need endotracheal intubation and mechanical ventilation for the protection of the airway (209). Most of pediatric CM cases experience convulsions. Paracetamol to control fever and glucose replacement to correct glucose levels are important. Anticonvulsant therapy as prophylactic is not recommended, as a randomized controlled trial (RCT) where phenobarbital was administered in children with CM, showed that mortality rates increased, probably due to respiratory depression (210). For the management of malaria induced AKI, avoidance of nephrotoxic drugs and fluid management are key. However, fluid management needs to be done with caution as AKI patients are not always hypovolemic and may be at risk for pulmonary oedema development (211, 212).

Many potential adjunctive treatments have been studied through murine models of malaria although none of them proved effective or improved the disease outcome in humans (9). Anti-TNF antibodies (165, 213), steroids (214, 215) and mannitol (216, 217), are not recommended as cerebral malaria treatment since studies proved that they have no benefit and can be potentially harmful. This evidence highlights the critical need for development of adjunctive treatments able to reverse the underlying pathogenesis of severe malaria.

1.10 New discovery approaches

Transcriptomics, the genome-wide analysis of RNA expression, is a common approach to investigate host and pathogen processes in infectious diseases. Bioinformatic and technical advances have permitted progressively thorough analyses of RNA expression and the association with pathogenesis, immunity, fundamental biology, prognosis and diagnosis. Transcriptomic approaches can now be used to study something that previously seemed impossible, the simultaneous RNA expression in both the host and the pathogen, allowing better understanding of the interactions. The development of transcriptomic technologies in the last two decades, motivated a lot of transcriptomic studies in infectious disease and malaria specifically, although many emphasized on the new technology application instead of

addressing important clinical or biological questions. Microarrays were the first commercially available transcriptomic tool, though it was never ideal for host-pathogen interaction studies due to the limited species range covered by the arrays commercially available and the significant restriction of probes which were designed only for predicted or known transcripts. This is why initially, studies using microarrays focused on host side of gene expression, while as pathogen genomes were assembled, analysis of the expression for the pathogen genes became possible. RNA seq in theory, is a much more suitable method for studying host-pathogen interactions, however in practice it is not as straightforward always (78, 218). One of the main challenges is that pathogen RNA may be only a fraction of the total isolated RNA, especially in cases of bacterial infection.

There is increasing interest in applying dual-RNA seq in *in vivo* infections, while deep RNA seq has already shown some progress (219, 220). This has revealed that the gene expression of the pathogen can vary inside the host (220) and this can be driven by the host response, providing further motivation for this type of approach. The use of dual-RNA seq for viral infections, allowed the transcriptomic analysis of both the virus and the host (221), viral load quantification (222), and revealed variation in the levels of viral gene expression (223). In general eukaryotic pathogens have larger genome and contain more RNA, and this could potentially give them a greater ability to shift their gene expression in response to the host. This has been demonstrated, in various examples, as in the gut of mice with a whipworm infection (224), as well as in the blood of malaria patients infected *with P. falciparum* (225). Other discovery based approaches such as Genome-wide association studies (GWAS) have also been used in malaria research looking at range of topics such as multi-drug resistance (226), genetic basis of the *Plasmodium* pathogenicity (227), and genome wide association with severe malaria (228). Proteomics have also been employed extensively for understanding severe malaria pathogenesis (229-234), prevention/vaccine development (235), treatment (236-239), diagnosis/biomarkers (240, 241), and *Plasmodium falciparum* biology (242, 243).

1.11 Transcriptomic approaches to understanding malaria

So far various transcriptomic techniques have been used trying to identify host biomarkers for severe malaria, elucidate severe malaria pathogenesis, understand how the parasite interacts with host, or how they affect each other (Table 9 in the Appendix). Microarrays

(commercial or bespoke) and RNA sequencing have developed through the years and their use has increased, however the use of these approaches has not yet led to substantial changes in the way people understand SM pathogenesis. Although these approaches offer a plethora of data their interpretation to novel and useful information and identification of therapeutic targets seems to be very challenging (78). This is mainly due to the limitations that all of these studies had. One of the limitations applying to most of studies has been the relatively small numbers of subjects (244, 245). Another limitation of these studies was their inability to adjust their results for the different cell types present in the blood, and the different parasite stages (225). The adjustment for different cell types is of great importance since it reduces variability within subject groups due to different cell composition, and it accounts for differences between groups in cell types. The main result from a gene expression analysis in which this adjustment is overlooked may just be due to a difference in cell proportions between groups. Additionally, the circulating forms of *P. falciparum* do not express all the genes that can be expressed throughout the parasite's life cycle, so studies that use blood to examine the transcriptional profile of the parasite without adjusting for the stage may give misleading results. Other limitations of the transcriptomic approaches that have been used so far are the low read depth of RNA sequencing especially for the parasite RNA (225), while for the studies using animal models alone in order to extract information for the host RNA the lack of a single animal model that could reproduce the human features of SM is a weakness (246), (247), (248), (249), (250), (251), (252).

1.12 Key points:

- Even with prompt antimalarial drug administration, many people still die from severe malaria highlighting the need for unravelling pathogenesis and developing adjunctive treatments. Modern discovery approaches such as transcriptomics create new opportunities for insights into the genes, proteins and pathways responsible for malaria pathogenesis and targets for intervention.
- The main pathological features which are associated with SM include high parasite load, parasite sequestration/obstruction of the microvasculature, vascular endothelial dysfunction and inflammation. The mechanisms which control each of these processes and link them to different severe malaria phenotypes still needs to be elucidated.

- Numerous mouse models are employed in malaria research but the models which best represent aspects of human pathophysiology are unclear, limiting the translational potential of findings in these models

Hypothesis: Dual-RNA sequencing of whole blood in malaria can be used to identify host-pathogen interactions associated with severity and protection, and for unbiased comparison of mouse models and human disease.

Aim: In this thesis, I test this hypothesis through biological and mechanistic validation of dual-RNA sequencing results and I identify models for the study of pathogenesis through comparative transcriptomics between human and mouse malaria.

1.13 Objectives of the thesis

1st Objective: Explore dual-RNA sequencing results from Gambian children with *P. falciparum* malaria using pathway analysis tools and select candidates for further biological validation, presented in chapter 3.

2nd Objective: Prioritise and biologically validate putative mechanistic correlates of protection identified by combining RNA seq with mathematical modelling of parasite load dynamics, presented in chapter 4.

3rd Objective: Identify differences and similarities in the host response in severe malaria between humans and mice, at a transcriptomic level, to reveal the most appropriate mouse models for further mechanistic evaluation, presented in chapter 5.

Chapter 2: Methods

In this chapter I discuss all the methodology used throughout this thesis and highlight key methods used by collaborators involved in different parts of the project.

2.1 Ethics

2.1.1 Human subjects

Gambian children under the age of 16 with *P. falciparum* malaria were recruited from three health centres, Brikama Health Centre, The MRC Gate Clinic, and The Jammeh Foundation for Peace Hospital, Serekunda. All of them underwent full clinical examination and were managed in accordance with Gambian government guidelines. The collection of samples was done with approval from the Gambia Government / MRC Laboratories Joint Ethics Committee, and with informed consent from the child's parent or legal guardian. These subjects were recruited as part of a larger longitudinal study aiming to address the immunological, parasitological, clinical, and genetic factors that underlie pathogenesis of severe malaria (253-255). Severe malaria was diagnosed following the World Health Organization criteria: Cerebral Malaria (CM) = a Blantyre coma score < 2 for at least 2 hours in the absence of hypoglycaemia; Hyperlactataemia (HL) = blood lactate > 5mmol/L; both CM and HL (CH). Kidney function tests were not performed, while severe anaemia was very rare in this low transmission setting, making impossible to include any children with severe anaemia (SA) in our dataset.

For the Malawian archived post-mortem human ocular tissue, from children with fatal *P. falciparum* cerebral malaria as well as other infectious diseases, used for immunohistochemistry and immunofluorescence, ethical and scientific approval was first obtained from the guardians of the samples: Professor Terrie E Taylor of Michigan State University, Professor Stephen Gordon of the Malawi Liverpool Wellcome Trust Clinical Research Programme (MLW), and Professor Simon Harding of the University of Liverpool.

2.1.2 Mice

C57BL/6 female pathogen free mice (8-10-weeks old) from Charles River Laboratories were used for all the *in vivo* experiments discussed here. All protocols and procedures were approved by Imperial College Animal Welfare and Ethical Review Board, in accordance with conditions of the project license (70/8919) and personal licences, and following LASA good practice guidelines.

2.2 Mouse Infections

Initially parasites kept in Alsever's solution with 10% glycerol (mixed at 1:2 ratio) in liquid nitrogen were defrosted and accordingly diluted (depending on parasitaemia of the frozen stock) to infect a passage mouse. Then the passage mouse infection was closely monitored until healthy parasites were observed in a blood smear and parasitaemia reached at least 2%. Sterile blood was collected, before parasitaemia reached 5% according to our project licence protocols, by cardiac puncture under non-recovery anaesthetic (isoflurane) and diluted in sterile PBS to achieve desired concentration. For all the *in vivo* experiments (unless otherwise stated) mice were infected with 10^5 parasites by ip (intra-peritoneal) injection. All mice were monitored daily or every other day depending on the severity of the infection. Tail bleeds (micro-sampling) were used to prepare blood smears and/or flow cytometry samples for parasitaemia check and lactate measurement. For lactate measurements "Lactate Pro 2" (HAB direct) device was used with Lactate Pro 2 Test Strips (HAB direct), using just 1-2ul of whole blood collected from the tail vain.

2.2.1 Protocols used for monitoring

General health scoring of the mice including weight, appearance, and behaviour were measured according to the severity of infection following specific protocols (appendix). For parasite passage Protocol 5 (moderate severity) was used to monitor mice every other day. Moderate severity protocol (1) was used to monitor mice every other day for non-lethal infections such as *P. yoelii* 17XNL, and *P. chabaudi* AS. For *P. yoelii* 17XL and *P. berghei* ANKA protocol 2 was used for monitoring mice every day (severe severity). For *P. berghei* ANKA infection the protocol included a neurological assessment called Rapid Murine Coma and Behaviour Scale (RMCBS) (256). RMCBS assessment included gait, motor performance, balance, limb strength, body position, touch escape, pina reflex, toe pinch, aggression and grooming.

2.3 RNA isolation

PAXgene blood tubes were used (for 1ml of whole blood 2.76ml of PAXgene liquid was used) to collect whole blood samples for both human subjects and mice discussed in this study. For the RNA extraction, the PAXgene Blood RNA Kit (Qiangen) was used according to the manufacturers' instructions (257).

2.3.1 Quantification and purity of RNA

After the isolation of the RNA, Nanodrop ND-1000 Spectrophotometer (Labtech) was used to obtain the ratio of absorbance at 260 nm and 280 nm (260/280) which is used to assess the purity of RNA (or DNA). Values of ~2 are generally accepted as pure for RNA. RNA HS Assay and dsDNA HS Assay were also performed using Qubit™ 3.0 Fluorometer (Invitrogen) for the quantification and as a secondary purity control of the RNA as well as potential DNA contamination. In order to consider an RNA sample as pure enough, it had to have less than 10% of DNA contamination.

2.3.2 Integrity of RNA

For the RNA integrity assessment Agilent RNA 6000 Nano Kit (Agilent) was used according to the manufacturers' instructions with Agilent 2100 Bioanalyzer (Agilent). I examined the bioanalyser traces that were obtained for sample integrity and not the RIN values as the double peaks, due to parasite RNA being present, interfere with the calculation of RIN (Figure 5).

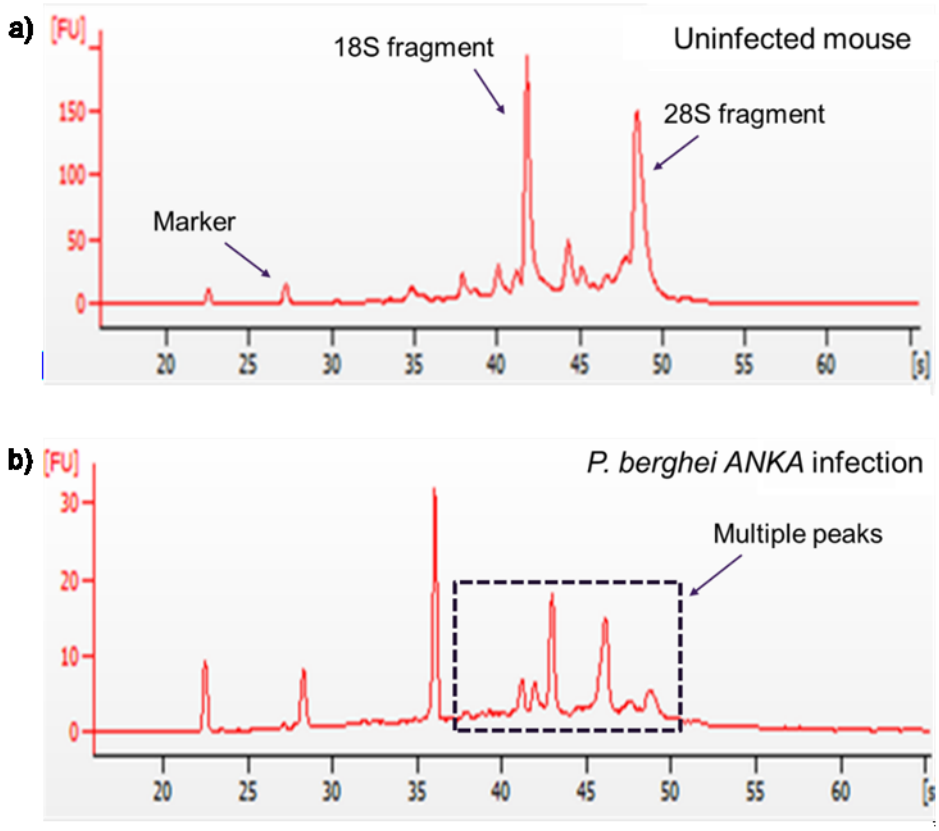

Figure 5: Bioanalyzer traces.

a) Uninfected mouse blood RNA sample showing the expected two peaks of 18S and 28S fragments. b) *P. berghei ANKA* infected mouse blood RNA with multiple peaks due to the presence of two species of RNA in the sample (mouse and parasite) making difficult for the software to calculate a RIN number.

2.4 Dual-RNA sequencing

Exeter University sequencing service was responsible for sequencing and library preparation. Libraries were prepared from 1µg of total RNA with the use of ScriptSeq v2 RNA-seq library preparation kit (Illumina) and the Globin-Zero Gold kit (Epicentre) in order to remove globin mRNA and ribosomal RNA. Prepared strand-specific libraries were sequenced using the 2x100 bp protocol for human and an updated protocol with 2x125bp for mice with an Illumina HiSeq 2500 instrument.

2.4.1 Human

For the human study we obtained per sample medians of 36 million reads, 91% uniquely mapped, 21 million human and 9 million of parasite origin, giving sufficient depth for robust simultaneous host and parasite global gene expression analysis.

2.4.2 Mice

For the mouse study we obtained per sample medians of 44 million reads, 91% uniquely mapped, 8 million mouse and 33 million of parasite origin. Due to the high parasitaemia that some of the malaria mouse models develop we had an overrepresentation of parasite reads after RNA seq. The lower read depth for mouse genes limits our gene detection.

2.5 Gene annotations

Human reference genome (hg38) was obtained from UCSC genome browser (http://genome.ucsc.edu/), mouse reference genome (mm10) was obtained from UCSC genome browser (http://genome.ucsc.edu/) and *Plasmodium falciparum* reference genome (release 24) was obtained from PlasmoDB (http://plasmodb.org/). Human gene annotation was obtained from GENCODE (release 22) (http://gencodegenes.org/releases/), mouse gene annotation was obtained from GENCODE (release M16) (http://gencodegenes.org/releases/) and *P. falciparum* gene annotation from PlasmoDB (release 24) (http://plasmodb.org).

2.6 Differential gene expression analysis

Differential gene expression analysis for the human subjects was performed by Dr Hyun Jae Lee from the Coin Group (bioinformatics collaborators) at University of Queensland. With R package edgeR, raw read counts of each data set were normalised using a trimmed mean of M-values (TMM), which takes into account the library size and the RNA composition of the input data. Deconvolution analysis was performed on RNA-seq data in order to account for inter-individual variation in the proportions of different types of blood leukocyte, and for variation in the distribution of circulating parasites through intraerythrocytic developmental cycle (IDC). The tool that was used was Cell-type COmputational Differential Estimation (CellCODE) (253).

Five key immune cell types were selected from the microarray dataset Immune Response In Silico (IRIS) (258) to create the human reference dataset of cell-type specific signatures: neutrophil, monocyte, CD4 T cell, CD8 T cell, and B cell. For the parasite reference dataset, RNA-seq datasets were obtained for four specific time points in parasite asexual (erythrocytic cycle) and sexual stage (gametocytes stage V). The output of CellCODE is estimation of the relative proportion of each cell type/parasite stage between samples – the surrogate proportion variable (SPV).

A generalised linear model (GLM) approach was employed to perform differential gene expression analysis (DGEA) between disease groups with adjustment for leukocyte and parasite SPVs in comparisons of human and parasite genes respectively. The Benjamini-Hochberg procedure was used for False Discovery Rate (FDR) and genes with FDR less than 0.05 were considered to be differentially expressed. Genes were considered as upregulated or downregulated only when they were differentially expressed after adjustment for respective SPVs. A second analysis was performed including adjustment for plasma PfHRP2 concentration, which is indicative of parasite load in the host, in order to identify genes that could be the cause of pathogenesis and not solely a response to high parasitaemia. Further analyses were performed to identify genes which correlated with quantitative traits (such as blood lactate concentration) again incorporating adjustment for SPVs.

Differential gene expression analysis for the mice was performed by Pablo Soro Barrio from the Department of Paediatrics at Imperial College London. With R package edgeR, raw read counts of each data set were normalised using a trimmed mean of M-values (TMM), which takes into account the library size and the RNA composition of the input data. Deconvolution analysis was performed on RNA-seq data in order to account for inter-individual variation in the proportions of different types of blood leukocyte using FACS (flow cytometry) data fed into edgeR. For this analysis, the proportions of 5 white blood cells (neutrophil, monocyte, CD4 T cell, CD8 T cell, and B cell) were measured, as in humans.

2.7 Pathway analysis

I used Ingenuity Pathway Analysis (Ingenuity) and Metacore (Thomson Reuters) with the resulting lists of differentially expressed or associated genes to perform functional and pathway enrichment analyses, and identify key network nodes. I have also have used the Gene Ontology and metabolic pathway enrichment tools in PlasmoDB to identify parasite pathways of interest. Working with the bioinformatics collaborators to perform and interpret differential co-expression analysis identifying *de novo* clusters of parasite and host genes which show evidence of co-regulation. Identification of candidates for experimental validation was based on strength of evidence for involvement in the disease process, relevance in the model system if known, feasibility of experimental manipulation of the target, and plausibility of therapeutic manipulation in humans (discussed in chapter 3).

2.8 *In vitro* parasite culture

I performed all the *in vitro* parasite culture experiments at the London School of Hygiene and Tropical Medicine. *P. falciparum* 3D7 strain was used in continuous culture for all experiments unless otherwise specified. Asexual blood stage parasites were cultured under standard conditions, briefly human A+ RBCs were used at 1-5% haematocrit, incubated at 37 °C and maintained in growth medium containing RPMI-1640 (without L-glutamine with HEPES) (Sigma) supplemented with 5 g/liter Albumax II (Invitrogen), 147 M hypoxanthine, 2 mM L-glutamine, 10 mM D-glucose in 5% CO_2 and low oxygen (5%) and 90% N_2 (259, 260). Human blood group A RBCs were used provided by the National Blood Service, first washed twice with RPMI by centrifugation, and the upper layer (containing any remaining white blood cells and plasma) was removed each time. After washing the RBCs were kept as 50% haematocrit suspension in culture medium, at 4˚C for no longer than 4 days.

2.8.1 Synchronisation

In order to keep parasites synchronous (most of the parasites to be at the same stage of their life cycle) 5% D-sorbitol (Sigma) was used to obtain almost exclusively ring stage parasites and uninfected RBCs (260). The culture was centrifuged at 800 g for 2 minutes and the pellet was incubated with 5 times its volume sorbitol solution for 5 minutes. The pellet was then washed in warm RPMI and then suspended back in to fresh culture media. In order to separate parasites at schizont stage Percoll gradients or magnetic separation column (MACS, Miltenyi Biotec) were used (261, 262). For the Percoll gradients separation, the pellet of a culture (~1-2ml) was carefully laid over 3ml of warm Percoll and centrifuged at 16.000 x g for 10 minute with no brake. Then the top layer containing the mature stage parasites was collected and washed in warm RPMI before putting back into culture with fresh blood. For magnetic purification of mature stage parasites, the culture at 50% haematocrit was slowly (1 drop/second) passed through the magnetic separation column. The late stage parasites that were now attached to the column so the column was removed from the magnetic holder and complete RPMI was passed through in order to elute the parasites. The eluted parasites were then centrifuged and the number of mature parasites needed was suspended in complete RPMI and fresh RBCs.

2.8.2 Growth assay

For a growth assay parasites were synchronized either at ring or schizont stage and left in culture at 2% haematocrit with a treatment or without for 48 or 72 hours respectively. Samples were always prepared at least in triplicates and starting parasitaemia at 0 hours ~0.5-1% depending on the treatment. Cultures were miniaturized to 96 well plates to reduce the quantities of treatment needed. For this type of assay mainly *P. falciparum* 3D7 parasites were used as well as the strains D10, Dd2, and HB3 (263).

2.8.2.1 Lactate supplementation

For this experiment *P. falciparum* 3D7 parasites were synchronized to ring stage using the methods mentioned above (Percoll & sorbitol) with parasitaemia of 1% at 0h and supplementation with sodium L-lactate (Sigma) at various concentrations (5mM, 10Mm, 30mM) or the equivalent concentrations of NaCl as control. All the different treatments were added in synchronous ring stage cultures at ~1.0% parasitaemia at 0 hours and 2% haematocrit.

2.8.2.2 Cathepsin G and MMP9 supplementation

Cathepsin G (Abcam) or recombinant active MMP9 (Enzo) were added for a 72 hour incubation allowing the parasites two replication cycles. Growth under each condition was calculated after subtracting the average growth in untreated/control samples.

2.8.3 Invasion assay

For an invasion assay parasites were synchronized at schizont stage and left in culture at 2% haematocrit with a treatment for 24 hours. Samples were always prepared at least in triplicates and starting parasitaemia at 0 hours ~0.5-1% depending on the treatment. Cultures were again miniaturized to 96 well plates to reduce the quantities of treatment needed. This type of assay was mainly used to assess whether a treatment affects the invasion of parasites

2.8.3.1 Cathepsin G and MMP9

Cathepsin G and MMP9 were either pre-incubated with the target cells overnight followed by four washes with RPMI to completely remove the treatment, or they were added directly to the culture of schizonts with target erythrocytes for 24 hours. The same protocol was followed for other *P. falciparum* strains (D10, HB3) except Dd2, for which magnetic purification was used to purify schizonts (264).

2.8.4 Blood smears

Blood smears were used to assess parasitaemia in both *in vivo* (tail vain micro-sampling) and *in vitro* experiments. After the preparation of a thin blood smear the smear was fixed with 100% methanol and then 10% Giemsa stain was applied for 10 minutes. Afterwards slides were washed with tap water and then left to dry.

2.9 Flow cytometry

2.9.1 Parasitaemia counting using flow cytometry

To assess parasitaemia, 1µl of sample at 50% hematocrit was stained with Hoechst 33342 (Sigma) which stains DNA and dihydroethidium (Sigma) which stains RNA and DNA in viable cells for 30 minutes in the dark on ice. Then samples were washed twice in PBS and fixed in FACS buffer (400ml PBS + 8mlFBS + 400ul of 10% sodium azide) with 2% paraformaldehyde (PFA) before flow cytometry assessment as previously described (265).

2.9.2 White blood cell proportions count with flow cytometry

In order to account for the different white blood cell counts in infected mice for the *in vivo* experiment and use these data for deconvolution analysis, I stained the leucocytes with different surface marker antibodies. For this staining ~50ul of blood per mouse were used and 2 ml lysis buffer was added for 5 minutes at room temperature. Samples were then centrifuged at 1000g for 5 mins at room temperature and the supernatant was removed. The cells were washed in FACS buffer and centrifuged at 500g for 5 mins at room temperature. The washed cells were mixed with 50ul of antibody cocktail with the surface markers (Table 2). For the initial experiment compensation samples (with anti-CD4 antibodies) were prepared stained with each of the antibodies separately. After staining the samples for 30 minutes in the dark on ice, they were washed in 2ml of FACS buffer and centrifuged at 500g for 5 mins at room temperature and the supernatant was discarded. The cells were then resuspended in 300ul FACS buffer with 2% PFA to fix, and stored in the fridge before the FACS analysis. All the antibodies used for this were purchased from Biolegend. Anti-CD4 antibodies were used for compensation.

Antibody, (catalogue number)	**Compensation control**
Alexa Fluor® 488 anti-mouse/human CD11b Clone M1/70 (101217)	Alexa Fluor® 488 anti-mouse CD4 Clone GK1.5 (100425)
APC anti-mouse Ly-6G Clone 1A8 (127614)	APC anti-mouse CD4 Clone GK1.5 (100411)
PE anti-mouse CD19 Clone 6D5 (115508)	PE anti-mouse CD4 Clone GK1.5 (100407)
Brilliant Violet 421™ anti-mouse CD4 Clone GK1.5 (100443)	* Brilliant Violet 421™ anti-mouse CD4 acts as its own compensation control
Alexa Fluor® 700 anti-mouse CD8a Clone 53-6.7 (100730)	Alexa Fluor® 700 anti-mouse CD4 Clone GK1.5 (100429)
Brilliant Violet 650™ anti-mouse CD3 Clone 17A2 (100229)	Brilliant Violet 650™ anti-mouse CD4 Clone GK1.5 (100545)

Table 2: Antibodies used for defining WBC proportions using FACS.

2.9.3 Instruments and software

Flow cytometry was performed using a BD LSR Fortessa machine at the St. Mary's NHLI FACS core facility after being trained by Dr Yanping Guo (Flow Cytometry Core Facility Manager, St. Mary's Campus). BD FACSDiva software was used to collect the data and analysis was conducted using FlowJo v10 (TreeStar Inc.)

2.9.4 Gating strategy

FSC-A/SSC-A was used to define the RBC or WBC population and exclude debris, while FSC-A/FSC-H was used to define the single cells and exclude the doublets (Figure 6-7). Here, I show figures created using FlowJo to present the gating strategy followed for parasitaemia counting and RBC receptor detection (Fig 6), as well as the gating strategy used for defining WBC proportions in mice (Fig 7).

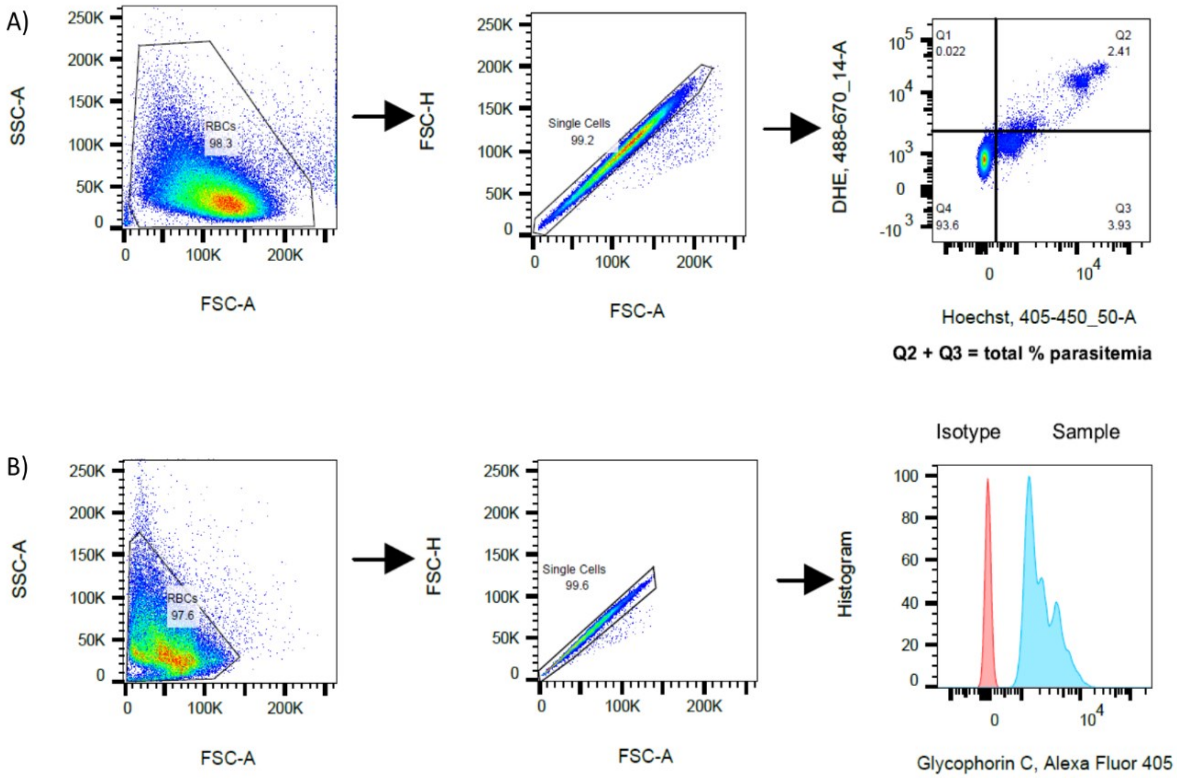

Figure 6: Gating strategy for parasitaemia counting and RBC receptor detection.

Figures created in FlowJo. A) Gating strategy for parasitaemia counting using Hoechst 33342 and dihydroethidium dyes. B) Gating strategy for RBC receptor detection. The initial step for both A & B was defining the RBC population using FSC-A (forward scatter area) and SSC-A (side scatter area) dot plot. Then doublets were excluded with FSC-A and FSC-H (forward scatter hight). A) The final step for parasitaemia measurement was to look at the Hoechst-DHE plot and add a cross which divides the stained from unstained population. Adding quarters 2 and 3 should give the % of total parasitaemia. B) The expression of a receptor can be presented using the histogram plots. Here in pink colour in the isotype control and with light blue is the peak for glycophorin C expression.

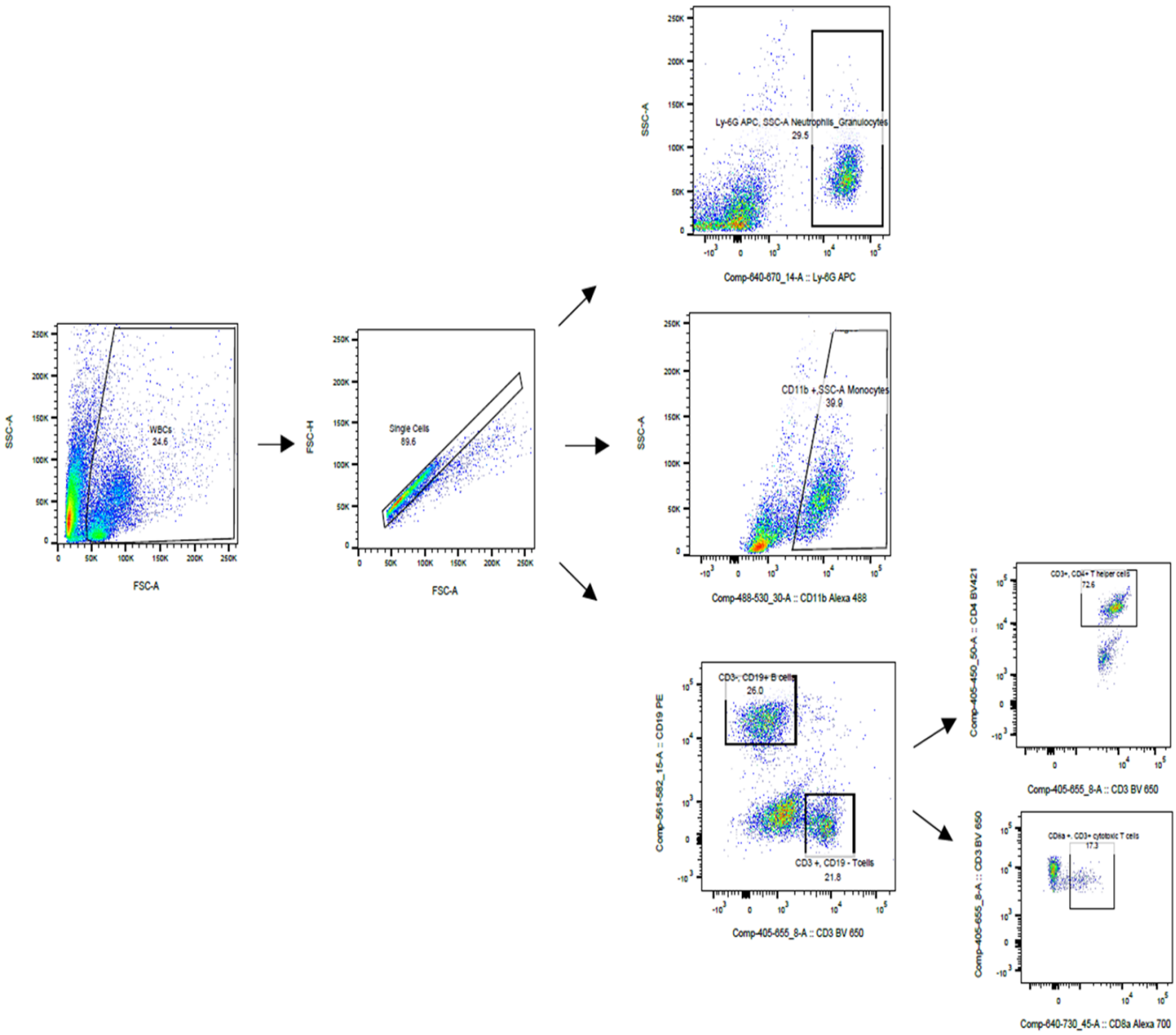

Figure 7: Gating strategy for defining WBC proportions in mouse blood

For defining the white blood cell proportions using FACS, the strategy included gating around the WBC population excluding red blood cells that did not lyse and debris using FSC-A/SSC-A. Then doublets were excluded with FSC-A and FSC-H. Finally, using different combinations of antibodies or antibody/ SSC-A proportions of the populations of interest were defined. For T cells gating CD3 +, CD19- cells were used, for B cells: CD3-, CD19+, for Monocytes: CD11b +, SSC-A, for Neutrophils: Ly-6G+, SSC-A, for T helper cells: CD8a- , CD4+, and for cytotoxic T cells: CD8a+, CD4-.

2.10 Erythrocyte surface receptor expression

The expression of the erythrocyte surface receptors was assessed by median fluorescence intensity after erythrocyte staining with the monoclonal antibodies shown at Table 3. Erythrocytes were initially washed twice before re-suspending at 50% haematocrit, from this 1-2µl was stained in 100µl of antibody mix in FACS buffer (2% fetal bovine serum, 0.01% sodium azide in PBS) for 30 minutes in the dark on ice. Samples were afterwards washed twice in FACS buffer and fixed in 300µl FACS buffer with 2% PFA. The loss of surface receptor was calculated from the difference between the treated and untreated sample median fluorescent intensities after the isotype control antibody fluorescence had been subtracted.

Table 3: ***Antibodies used to assess the erythrocyte receptors surface expression.***

Antibody, Clone	Isotype control
APC Mouse anti-human CD235ab Antibody, Clone HIR2 (Biolegend)	APC Mouse IgG2b, κ (Biolegend)
PE Mouse anti-human CD108 Antibody, Clone MEM-150 (Biolegend)	PE Mouse IgM, κ (Biolegend)
Alexa Fluor® 488 Mouse anti-human CD147 Antibody,Clone HIM6 (Biolegend)	Alexa Fluor® 488 Mouse IgG1, κ (Biolegend)
Alexa Fluor® 405 Mouse anti-human Glycophorin C Antibody (BRIC10) (Novus Biologicals)	Alexa Fluor® 405 Mouse IgG1 (Novus Biologicals)
PE Mouse anti-human CD35 Antibody (CR1), Clone E11(Biolegend)	PE Mouse IgG1 (Biolegend)
FITC Mouse anti-Human CD55 Clone IA10 (RUO) (BD Biosciences)	FITC Mouse IgG2a, κ (BD Biosciences)

2.11 Whole blood stimulation with PMA

Whole blood was collected from 8 healthy adult donors and plated at 25% haematocrit in RPMI. The samples were incubated overnight with the addition or not of 1µM PMA (Sigma). Supernatant was then collected for ELISA experiments, while RBCs were collected for assessment of surface receptor expression after the PMA stimulation.

2.12 ELISA

ELISA (enzyme-linked immunosorbent assay) was one of the most widely used techniques to determine the protein concentration of various samples in different parts of my project (266). Most of the ELISA kits used included pre-coated plates with the primary capture antibody, so the first step was to prepare/dilute the samples and standards following the instructions and according to the detection range of each assay. Each ELISA assay (Table 4) was performed according to the manufacturer's instructions. The last step was to read the absorbance with a plate reader (VersaMax) at 450nm and use SoftMax Pro software, Excel and GraphPad Prism7 (GraphPAD Software Inc.) to analyse the data.

Table 4: ELISA Kits

ELISA Kit (catalogue number)	Company
Human MMP-9 Legend Max (444907)	Biolegend
Defensin Alpha 3, Neutrophil specific (SEE135Hu)	Cloud Clone Corp
PMN Elastase Human ELISA Kit (ab119553)	Abcam
Human MMP8 SimpleStep ELISA Kit (ab219050)	Abcam
G-CSF Human ELISA Kit (ab100524)	Abcam
Human CTSG / Cathepsin G ELISA Kit (Sandwich ELISA) - LS-F11031	LifeSpan Biosciences

2.13 Immunohistochemistry

Immunohistochemistry experiments on human retinal tissue from Malawi described in this thesis were performed at Liverpool University, Institute of Ageing and Chronic Disease under a collaboration with Professor Simon Harding (guardian of the samples) and Dr Chris Moxon. Paraffin sections were deparaffinised in 2 changes of xylene 100% for 5 minutes each and then hydrated in 2 changes of 100% ethanol for 5 minutes each, 90% and 70% ethanol for 1 minute each. Then rinsed in distilled water. For antigen retrieval UNI-TRIEVE (Universal Mild Temperature Retrieval Solution) was used to incubate the slides at 60 ^{o}C. Sections were then rinsed in PBS and then endogenous peroxidase activity was blocked with 3% H_2O_2. Afterwards

slides were rinsed in PBS Tween and blocked with Normal Horse serum for 30 minutes. Serum was removed and sections were incubated with primary antibody at appropriate dilution (1:200) in Normal Horse serum overnight at 4 °C. Sections were rinsed in PBS Tween and then incubated with secondary antibody: Biotinylated Horse Anti-Mouse/Rabbit Ig (Vector) for 30 minutes. Rinsed with PBS Tween 20 and then ABC reagent (Vector) was added for 30 min. DAB was used to visualize the staining for time optimized for each antibody. Sections were finally rinsed in tap water/PBST and counterstained with Mayers Hematoxylin. Afterwards slides were washed in dH_2O, dehydrated in ethanol and cleaned in xylene before mounting (VectaMount Permanent Mounting Medium, Vector).

Antibody, Clone	**Isotype control**
Anti-Neutrophil Elastase antibody (Rabbit) (ab68672)	Abcam
Anti-Histone H3 (citrulline R2 + R8 + R17) (Rabbit) antibody - ChIP Grade (ab5103)	Abcam
Goat Anti-Rabbit IgG H&L (Alexa Fluor® 488) preadsorbed (ab150081)	Abcam
Goat Anti-Mouse IgG H&L (Alexa Fluor® 594) (ab150116)	Abcam
OLFM4 Antibody (Rabbit) NBP2-24535	Novus Biologicals
Anti-MMP8 antibody [EP1252Y] (ab81286)	Abcam
Goat Anti-Mouse IgG H&L (Alexa Fluor® 568) (ab175473)	Abcam
Donkey Anti-Goat IgG H&L (Alexa Fluor® 647) preadsorbed (ab150135)	Abcam
Rabbit IgG, monoclonal [EPR25A] - Isotype Control (ab172730)	Abcam
Neutrophil Elastase Antibody (G-2): sc-55549 (Mouse)	Santa Cruz Biotechnology
DyLight 649 labeled Ulex Europaeus Agglutinin I (UEA I) Cat. No: DL-1068	Vector Laboratories

Fibrinogen Antibody Goat / IgG (PA1-26809)	ThermoFisher

Table 5: Antibodies used for IHC and IF

2.13.1 Immunofluorescence

For immunofluorescence staining, a similar protocol was followed omitting the endogenous peroxidase activity blocking step for the first day of the experiment. After the overnight incubation with primary antibody the fluorescent secondary antibody was added at appropriate concentration (1:400) for ~30minutes in the dark and then the slides were rinsed in PBS Tween 20 for 3x5 min before mounting with a DAPI containing medium (VECTASHIELD Antifade Mounting Medium with DAPI Cat. No: H-1200, Vector) which counterstains the nuclei.

2.14 Microscopy

Inverted Widefield Microscope (WF1-Zeiss) with LED illumination Zeiss Axio Observer and the highly sensitive Hamamatsu Flash 4 camera were used for fluorescent imaging at the FILM facility at South Kensington Campus of Imperial College.

2.14.1 Imaging software

Fiji, which is a free open source package was used for processing the fluorescent images collected with the WF1-Zeiss (267). ICY, is another open access platform for bio-image informatics and was used for 3D visualization of z stack images (268). Huygens software was used for deconvolution of z-stack images through the Imperial College FILM facility.

Slides stained with IHC were digitized (LEICA SCN400, Leica microsystems U.K) by IQPath (UCL Institute of Neurology) and images viewed and processed with Aperio ImageScope software (© 2018 Leica Biosystems Imaging, Inc.).

2.14.2 Evaluation of parasitaemia by microscopy

In the experiments where parasitaemia was assessed by microscopy, thin blood smears were prepared and stained with 10% Giemsa as explained above. The blood smears were then examined at 100x magnification using bright field microscopy. Using a counting grid (Miller) and looking at different fields of the smear, parasites (in the big square) and RBCs (in the small square) were counted. Percentage parasitaemia was then calculated dividing the number of parasites by the number of RBCs counted x 9.

2.14.3 Haemorrhages counting in mouse brain

Haemorrhages are a common feature seen in brains of mice that have developed ECM. Histological analysis was used to measure haemorrhages per unit area by a student blinded to the treatment these mice previously received. For this examination, I collected brains from mice developing ECM after being infected with *P. berghei ANKA* parasites. Brains were fixed overnight in 4%PFA and then sent for paraffin embedding, tissue sectioning and H&E staining at IQpath (UCL Institute of Neurology). Slides were digitized (LEICA SCN400, Leica microsystems U.K) by IQPath and images viewed and processed with Aperio ImageScope software (© 2018 Leica Biosystems Imaging, Inc.).

2.15 Statistics

GraphPad Prism 7 (GraphPad Software, Inc.) was used for the statistics analysis needed for all experiments discussed. Statistical analyses were performed each time depending on the data available for analysis, continuous variables were compared between groups using paired or unpaired Student's t-test (when the data were normally distributed) and the Mann-Whitney-Wilcoxon or Wilcoxon matched pairs tests (when I could not assume normal distribution), ANOVA was used for comparison across multiple groups. All hypothesis tests presented are two-sided unless specifically stated otherwise, with one-sided testing used only when justified by small sample size and a strong prior hypothesis for the direction of effect (269, 270).

P values <0.05 are considered as significant and are either presented by the actual calculated P value or by using asterisks (P values <0.05 are designated with (*), P values <0.01 are designated with (**), P values <0.001 are designated with (***), and P values <0.0001 are designated with (****). For the RNA seq analyses and mathematical model, statistics were undertaken using the R statistical software (271).

Chapter 3: Uncovering pathogenesis mechanisms of severe malaria

In this chapter the bioinformatics analysis for RNA sequencing was performed by Dr Hyun Jae Lee from University of Queensland (Fig 8, 9). RNA sequencing and library preparation was performed at Exeter University Sequencing Service.

Infectious diseases pathogenesis depends on the interaction of the pathogen and the host. Dual RNA sequencing of whole blood from *Plasmodium falciparum* malaria patients, can reveal the interactions between the host and the parasite. Using samples from 46 Gambian children (21 uncomplicated, 25 severe) infected with malaria we performed a dual transcriptome analysis, in an effort to identify the mechanisms that drive severe malaria pathophysiology (270). We integrated these transcriptomic data with detailed clinical information and adjusted our analysis for the differences in the development stage of the parasite, the leukocyte proportions, and total pathogen burden. We reported hundreds of parasite and human genes differentially expressed among severe and uncomplicated malaria, while distinct profiles associated with hyperlactataemia, coma, and thrombocytopenia (270). One of the main findings was the upregulation in expression of neutrophil related genes being consistently associated with all severe malaria phenotypes (270).

In this chapter, I present the results of analyses aiming to provide biological *in vitro* and *in vivo* validation, aiming to examine one host and one parasite mechanism. Findings of this study provide a framework for better understanding the contributions of the host and parasite to severe malaria pathogenesis and support the identification of potential adjunctive therapy targets.

3.1 Introduction

In most of the infectious disease studies looking at pathogenesis the efforts focus on either the host or the pathogen although the interaction between these two determines the outcome. Such interactions can be assessed at a transcriptomic level by dual RNA sequencing (78, 272), even though this has not been extensively applied in human systemic infection

studies. In malaria, the parasite pathogenic stage is restricted to blood where it can interact with the host leukocytes, giving the opportunity for assessment by dual RNA sequencing (11). The blood is also the channel for systemic responses to infection, and gene expression in blood will mirror the inflammatory and metabolic environment to which leukocytes and parasites are exposed.

Plasmodium falciparum malaria is one of the most important infectious diseases affecting humans (11). Most malaria deaths occur in children, in whom three major syndromes are associated with increased risk of death and distinguish severe malaria from uncomplicated malaria: i) hyperlactataemia/acidosis (often manifesting as deep breathing), ii) cerebral malaria (manifesting as coma), and iii) severe anaemia (8, 11, 71, 273). These severe malaria syndromes can occur on their own or in overlapping combinations (71), with the highest mortality seen when hyperlactataemia/acidosis and cerebral malaria coexist (71). Severe malaria is more likely to occur when the parasite load is high (183-185, 188) and various accompanying pathophysiological imbalances (8, 71, 106), mainly arising from vascular endothelial dysfunction, inflammation, and parasite sequestration (10, 71). The interactions between these mechanisms make it challenging to define their individual contributions to specific features of severe malaria disease (10, 27). Looking at rodent models of severe malaria, the major determinant for the severity outcome is the host immune response, and similarly it has been supposed that an excessive host response may also be responsible for some forms of human severe malaria (274, 275). Severity in other infectious diseases such as Ebola, respiratory syncytial virus and bacterial sepsis can be explained through a similar concept (276-278); though, direct evidence is often missing, and the confounding effect of pathogen load on the extent of the host response is rarely quantified. Models of controlled human infection have provided insights into the relationship between early immune responses to infection and pathogen load (279) however this cannot be extended to investigate severe disease. It has already been demonstrated that it is feasible to use dual RNA sequencing for host and parasite in uncomplicated human malaria (225).

Here, the application of dual RNA sequencing was extended to infectious disease pathogenesis by integrating gene expression analysis with detailed laboratory and clinical data that characterize the systemic pathophysiology of severe malaria (270). The analysis was refined, taking into account the major confounders that possibly vary among the different

severity groups. Allowing the characterization of parasite and human differential gene expression as well as the role of parasite load in controlling the host response (270). One of the most important and interesting findings was that ~99% of the human differentially expressed genes in severe malaria was primarily driven by the parasite load, while the gene expression of the parasite was very little associated with parasite load differences (270). In this chapter, I present plasma levels, histological examination and an *in vivo* experiment as part of the host mechanism validation, while for the parasite I present some *in vitro* parasite culture experiments focusing on understanding hyperlactataemia mechanism.

This analysis provides a unique insight in the severity associated host-pathogen interactions revealing new perspectives on the pathogenic mechanisms of severe malaria in humans.

Host

3.2 Dual RNA sequencing on whole blood from Gambian Children with malaria

3.2.1 Subjects

From available RNA 46 samples were selected based on RNA quantity, quality, clinical phenotype of the subject, age and gender, and availability of associated data from other studies (21 uncomplicated, 5 CM, 8 hyperlactataemic, and 12 with a phenotype combining CM and hyperlactataemia) (Table 6).

Table 6: Characteristics of subjects selected for RNA-sequencing

CM, cerebral malaria; CH, cerebral malaria plus hyperlactatemia; HL, hyperlactatemia (CM, CH, and HL are all subgroups of severe malaria); UM, uncomplicated malaria; PfHRP2, P. falciparum histidine rich protein 2; Hb, haemoglobin concentration; WBC, white blood cell count. Data are median (IQR), superscripts indicate the number of subjects with data for each variable if less than the total; P for Kruskall-Wallis test comparing all groups (degrees of freedom = 3) except for sex where P is for Fisher's exact test. Leukocyte population numbers and proportions measured by clinical hematology analyser. Reproduced from "Integrated pathogen load and dual transcriptome analysis of systemic host-pathogen interactions in severe malaria" deposited in BioRxiv after obtaining approval by the senior author, Dr Aubrey Cunnington.

	CM (*n* = 5)	**CH (*n* = 12)**	**HL (*n* = 8)**	**UM (*n* = 21)**	***P***
Age (years)	4.3 (4.2-4.8)	4.9 (3.6-5.7)	5.0 (3.8-8.3)	6.0 (4.0-9.0)	0.24
Male (%)	3 (60%)	5 (42%)	7 (88%)	13 (62%)	0.24
Parasitaemia (%)	8.3 (5.3-9.0)[4]	12.6 (9.4-19.0)	9.6 (1.8-12.2)	5.1 (3.8-7.0)	0.02
Parasites (x10^5 /uL)	2.3 (1.7-3.1)[3]	3.5 (2.7-8.4)[11]	2.8 (0.7-5.0)	2.3 (1.6-3.2)	0.02
Clones	2 (1.5-2.5)[4]	2 (1-2)[9]	1 (1-2)[5]	2 (1-2)[15]	0.68
PfHRP2 (ng/mL)	202 (93-528)[4]	763 (374-1750)	470 (164-2214)	163 (128-227)	0.001
Duration of illness (days)	2.0 (1.7-3.0)	2.0 (2.0-2.5)	2.0 (2.0-3.5)	2.7 (2.0-3.0)	0.57
Hb (g/dL)	9.7 (7.4-10.4)	9.3 (7.8-11.5)[11]	9.1 (7.4-11.0)	10.8 (9.9-12.1)	0.10

WBC ($x10^9$/L)	9.8 (8.2-12.9) [4]	8.8 (6.4-9.4) [11]	15.3 (7.9-16.8) [7]	9.5 (7.7-11.8)	0.30
Platelets ($x10^9$/L)	41 (40-82) [4]	36 (23-65) [11]	59 (33-132)	122 (96-132)	0.04
Lymphocytes ($x10^9$/L)	2.7 (2.1-3.6)[4]	2.9 (2.4-3.6)[11]	3.1 (1.8-5.2)[7]	2.4 (1.4-3.1)[20]	0.53
Lymphocyte (%)	29.8 (20.6-37.3) [4]	37.8 (29.9-49.9)[11]	22.3 (14.7-37.3)[7]	23.9 (16.0-33.5)[20]	0.05
Neutrophils ($x10^9$/L)	6.4 (4.0-8.7)[4]	4.0 (2.9-4.3)[10]	6.5 (5.8-10.4)[7]	7.0 (5.3-7.7)[20]	0.17
Neutrophil (%)	55.1 (49.0-69.6) [4]	48.3 (39.6-56.2) [10]	61.5 (55.6-74.9) [7]	68.0 (59.9-79.6)[20]	0.01
Monocytes ($x10^9$/L)	0.6 (0.6-0.7)[4]	0.6 (0.5-0.9)[10]	0.8 (0.6-1.3)[7]	0.7 (0.4-0.9)[20]	0.53
Monocyte (%)	7.1 (6.0-7.7)[4]	7.8 (6.8-8.6)[10]	6.6 (5.1-7.8) [7]	6.7 (4.8-7.3)[20]	0.38

We excluded all the highly polymorphic regions, such as *rifin, var*, and *stevor*, since reference genome based mapping is not possible. We detected the expression of 3,880 parasite and 12,253 human genes. Systemic infection can alter the proportions of blood leukocytes, and this can dominate differences seen in gene expression and confound the interpetation (279). Another factor which can affect parasite gene expression *in vivo* is the stage of the parasite at the time of sampling, and this is due to the phasic variation in the parasite gene expression (16), and also due to the increase in the total amount of RNA as the parasite matures (280). Accounting for inter-individual differences in parasite stage and the variation in the proportions of blood leucocyte using CellCODE as explained in the methods chapter (Figure 8) allowed a more refined analysis (270).

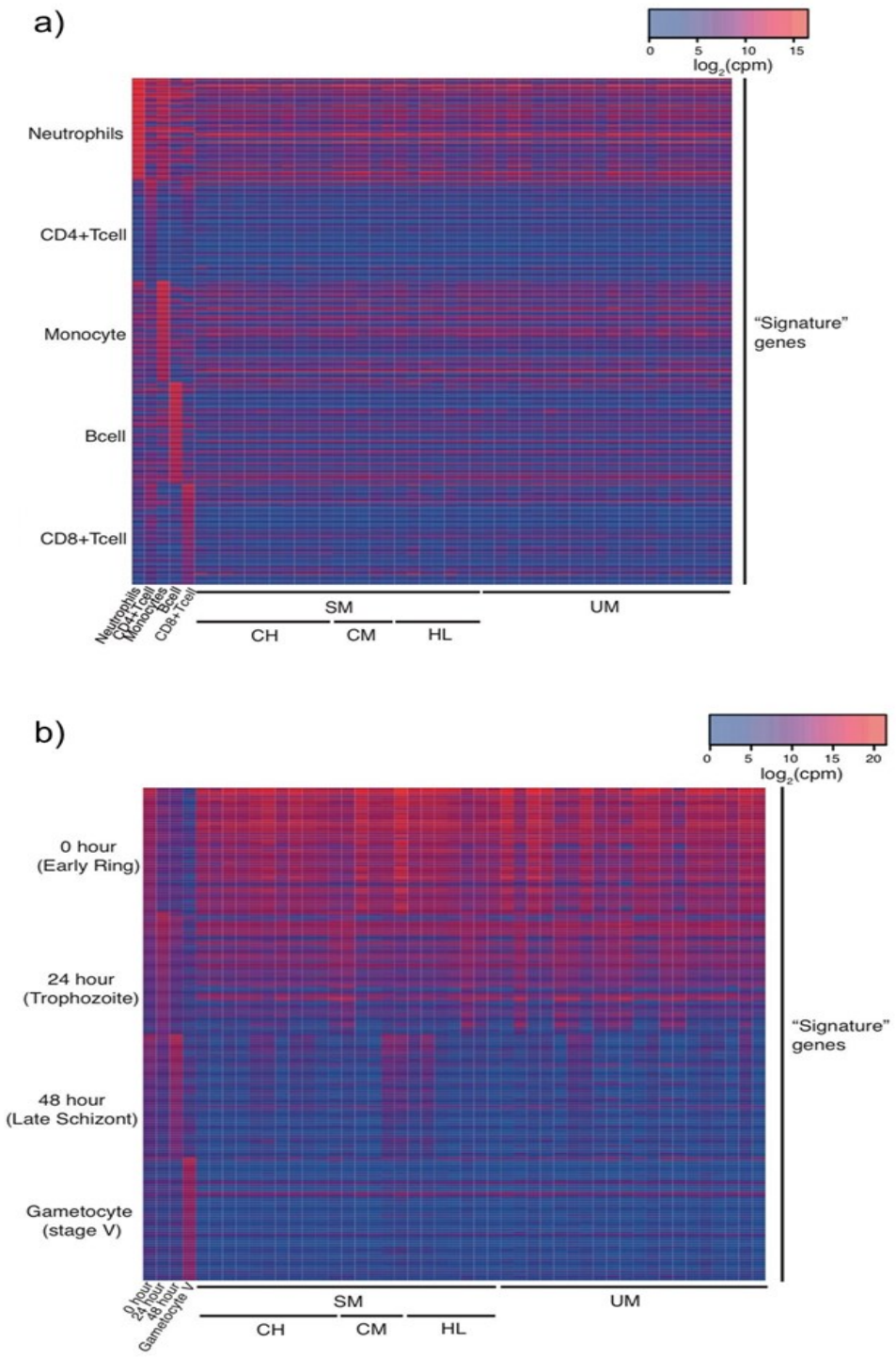

Figure 8: Deconvolution heatmaps.

a) Heatmaps showing counts per million signature gene expression for a) different leukocyte populations, and b) parasite developmental stage, and their relative intensity for each individual subject. Reproduced from: "Integrated pathogen load and dual transcriptome analysis of systemic host-pathogen interactions in severe malaria" deposited in bioRxiv after obtaining approval by the senior author, Dr Aubrey Cunnington.

3.3 Candidate selection

In order for us to decide which of the resulting candidates we should further pursue *in vitro* or *in vivo* we had to set certain criteria. The significance of each candidate according the RNA sequencing data was one of the most important and obvious criteria. Genes were considered as significant when after adjusting for FDR, they were differentially expressed with low p values < 0.05 and highly upregulated or downregulated. However, biological plausibility, the existing knowledge, and tractability of the candidates were equally important.

3.4 Identification of MMP8 as a plausible contributor to SM pathogenesis

Generalised Linear Model (GLM) approach from edgeR was used by our bioinformatics collaborator Dr Hyun Jae Lee (University of Queensland) in order to identify the different transcriptional signatures that the host develops in uncomplicated malaria (UM) versus severe malaria (SM). Differential expression analysis of human genes in severe versus uncomplicated malaria revealed MMP8 as the most significantly different and the most highly expressed in SM relative to UM (Fig 8).

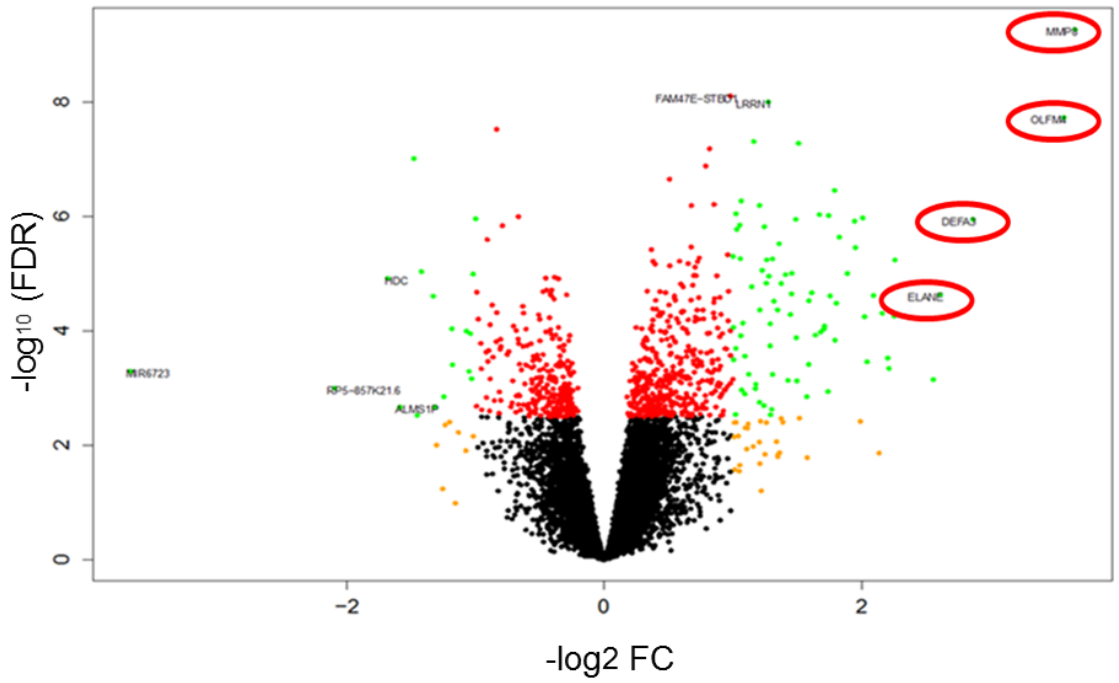

Figure 9: Comparisons of human gene expression between severe and uncomplicated malaria.

Red = significant differential expression after adjustment for FDR; orange logFC>1; green = significant difference and logFC >1. Expression has been adjusted for FDR. Reproduced from: "Integrated pathogen load and dual transcriptome analysis of systemic host-pathogen interactions in severe malaria" deposited in BioRxiv after obtaining approval by the senior author, Dr Aubrey Cunnington.

Serum levels of TIMP-1 and MMP8 are elevated in patients with malaria (281). MMP8 is a metallopeptidase and MMPs are a family of proteolytic enzymes that can be involved in disruption of tight junctions (eg endothelial) modulation of inflammatory response and degradation of sub-endothelial basal lamina (282). MMP8 can cleave collagen in the extracellular matrix of choroid plexus cells (immune sensor of the brain) leading to disruption of the blood-CSF barrier. This can result in brain inflammation, increased cerebrospinal fluid cytokine levels, and downregulation of the glucocorticoid receptor in the brain, suggesting that excessive release of MMP8 could plausibly contribute to severe malaria pathogenesis. MMP8 inhibition protected mice, that were treated in various ways in order to induce SIRS (systemic inflammatory response syndrome), against systemic inflammation (283). Sepsis is a clinically similar condition to malaria, while these acute diseases are in fact syndromes caused by the acute release of cytokines in hyper-immune state patients (284). Another study supportive of MMP8 as a strong candidate proposed that inhibition of MMP8 can be beneficial in cases of experimental sepsis (285) while it is known the fatal sepsis patients also have increased MMP8 serum levels (286).

3.4.1 Validation using Gambian plasma samples protein levels

Looking at the differentially expressed genes (Fig 9) there is a strong neutrophil associated signature with genes such as MMP8, OLFM4, Elastase, and DEFA3 being significantly upregulated in severe malaria cases. We decided to validate these findings measuring the levels of the coding proteins in plasma from Gambian children of the same cohort including GCSF which is the upstream regulator for all these genes. Proteins of interest, were measured in stored Gambian plasma samples collected on the day of clinical presentation using ELISAs according to the manufacturers' instructions: MMP8, human neutrophil elastase (Elastase), GCSF, and defensin A3 (DEFA3) (Fig 10). OLFM4 protein was excluded as it is very sensitive to proteolysis. Even though the gene expression came up as highly upregulated in SM versus UM looking at the RNA seq data, the plasma levels of these proteins did not seem to have such significant differences (apart from DEFA3) between SM and UM cases.

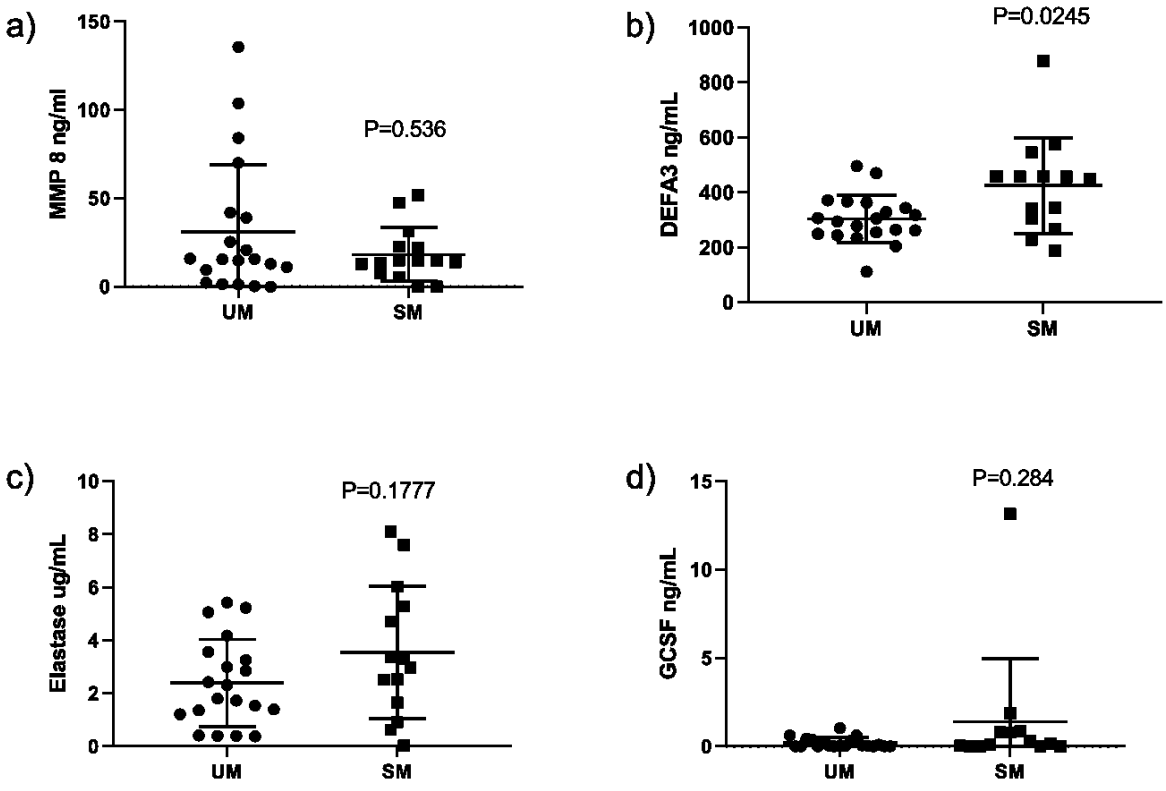

Figure 10: Plasma protein concentrations in Gambian plasma samples.

a) MMP8, b) DEFA3, c) Elastase, d) GCSF. Bars show mean with SD. Statistical analysis done with non-parametric T test (Mann Whitney), N = 34; severe malaria, N = 14; uncomplicated malaria, N = 20

I then decided to test whether parasite material (schizont lysate) could stimulate neutrophil degranulation in healthy donors. Whole blood was collected from 8 healthy donors and stimulated overnight with schizont lysate (or left untreated) and afterwards ELISA was used to assess MMP8 release in the supernatant. As seen in Figure 11 MMP8 concentrations reached levels similar to those observed in plasma of malaria patients. Given that parasite material can trigger degranulation but systemic levels of most of the neutrophil granule proteins were not significantly different between SM and UM, I wondered whether we might find evidence for their localized release adjacent to sites of parasite sequestration in the microvasculature. In this microenvironment the effect of granule protein release may also be particularly damaging to the host tissues.

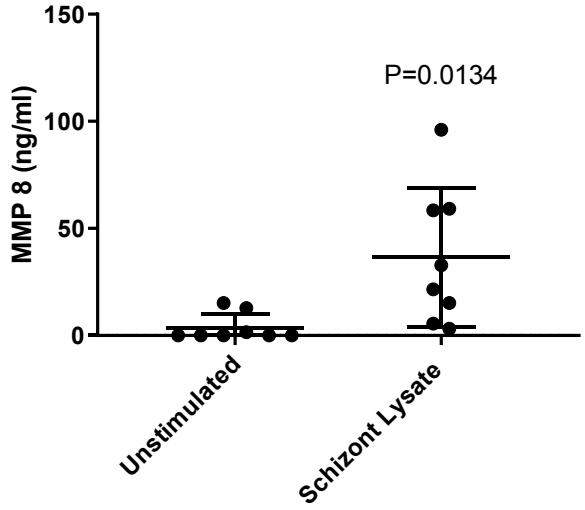

Figure 11: MMP8 release after overnight stimulation with P. falciparum 3D7 schizont lysate from healthy donor whole blood

Bars show mean with SD. Statistical analysis done with Wilcoxon matched pairs test, N=8.

3.4.2 Immunohistochemistry on human retinal tissue

A longstanding collaboration dating back to 1994 between University of Malawi, University of Liverpool (UoL), Michigan State University (MSU), and Liverpool School of Tropical Medicine has been investigating cerebral malaria in children in Malawi. As part of this an autopsy study was performed to gain insights into mechanisms of the disease and causes of death. Autopsy tissue (brain and ocular) is stored in designated archives under the joint guardianship of the Directors of the Blantyre Malaria Project (BMP), Prof Terrie E Taylor of Michigan State University and Prof Stephen Gordon at the Malawi Liverpool Wellcome Trust Clinical Research Programme (MLW). One of the archives is held in UoL under the guardianship of Prof Simon

Harding, located in the designated store in the Institute of Ageing and Chronic Disease at Liverpool. Through our collaboration with Dr Chris Moxon we were able to access these valuable samples. Based on our RNA sequencing results showing MMP8 and OLFM4 as the most upregulated genes in severe malaria cases we decided to use immunohistochemistry and immunofluorescent methods to study these archived post-mortem human ocular tissue from children with fatal *P. falciparum* cerebral malaria of 9 retinopathy positive and 7 retinopathy negative as well as one non-cerebral case, with other infectious disease (Table 7).

Table 7: Clinical diagnosis and classification of subjects whose ocular tissue was used for immunohistochemistry and immunofluorescence experiments.

Class 1= Clinical CM, sequestration only (> 25% VPC, < 50 pg/100v), Class 2= Clinical CM, sequestration + pigment (> 25% VPC, > 50 pg/100v, Class 3=Clinical CM, no sequestration, no supporting pathology, CM3 mimics CM during life so these children are control for being really sick and for premorbid events but in fact there is no sequestration and there is an alternative cause of death – suggesting a different pathogenic process - so they represent an excellent comparator for sequestration driven pathology. Class 7= Non-malarial encephalopathy, infectious. %VPC is "percentage of vessels containing parasites", and it refers to brain capillaries in cross section. pg /100v is the number of extra-erythrocytic pigment globules counted in the process of counting 100 cerebral capillaries in cross section.

Sample	Clinical Diagnosis	CLASS	Ret
1	Clinical CM	1	ret
2	Clinical CM	1	ret
3	Clinical CM	1	ret
4	Clinical CM	1	ret
5	Clinical CM	1	ret
6	Clinical CM + SMA	2	ret
7	Clinical CM	2	ret
8	Clinical CM, severe pneumonia, severe meningoencephalitis	2	ret
9	Clinical CM	2	ret
10	Clinical CM - pneumonia Reye's	3	no ret
11	Clinical CM, likely cause of death is anaemia	3	no ret
12	Clinical CM + SMA, hepatitis	3	no ret
13	Clinical CM; Severe pneumonia	3	no ret
14	Clinical CM, severe pneumonia with spread to meninges	3	no ret
15	Clinical CM, left ventricular failure with pulmonary oedema	3	no ret
16	Clinical CM, fatal pneumonia	3	no ret
17	Salmonella sepsis	7	no ret

Malarial retinopathy is a set of retinal abnormalities unique to severe malaria which is common in children with cerebral malaria. The presence and severity of retinopathy are correlated with length of coma in survivors and risk of death (105). These unusual retinal signs were described in children with CM first by Lewallen et. al. using direct and indirect ophthalmoscopy in Malawi (287). Since then these signs have been further characterized and documented using fundus photographs in Gambian and Kenyan children as well (288-291). There are four main components consisting malaria retinopathy: retinal haemorrhages, vessel changes (105), retinal whitening (290), and papilledema (288), while vessel changes and retinal whitening are specific to malaria abnormalities (105). Embryologically, the retina is part of the central nervous system and has analogous cellular structure as well as blood tissue barrier (105) similar to the brain (125). So we focused at the retinal vasculature as it mirrors changes happening in the brain vasculature (292) (Fig 12). Use of human tissue can reveal changes that happen locally, which can be more important than the systemic ones, and could not otherwise be identified if we used only whole blood RNA seq or protein concentration measurements in plasma. The proposed mechanism is that high sequestered parasite loads (Fig 13) drive local recruitment and/or activation of neutrophils which degranulate, releasing MMP8, OLFM4 and Elastase, and undergo NETosis. In turn these NETs and the released host histones damage the endothelium, causing receptor cleavage and coagulopathy.

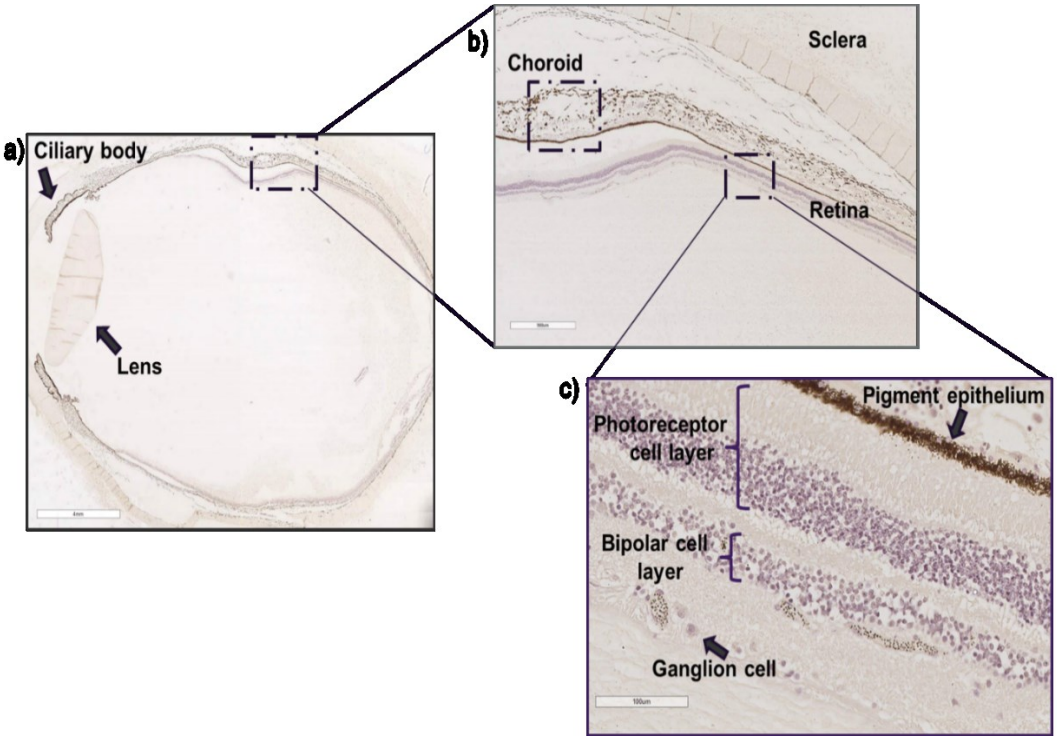

Figure 12: Histology of the whole ocular tissue showing the anatomy (a & b) and cell layers of the retina (c)

The choroid found between the sclera and the retina is the vascular layer of the eye supplying the outer retina (293, 294).

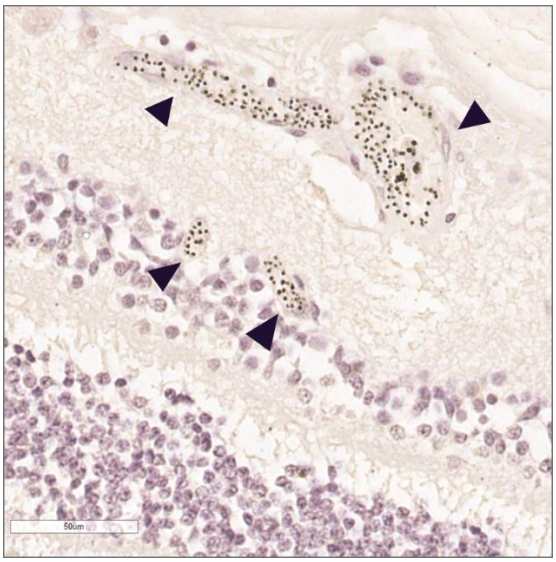

Figure 13: Retinopathy positive case showing extensive sequestration (arrowheads) of parasites on the retinal endothelium. Mature parasites appear as black dots due to the hemozoin pigment accumulated in their food vacuole.

Scale bar 50 µm.

3.4.2.1 Retinal tissue MMP8 & OLFM4 immunohistochemistry

Having access to the whole ocular tissue we focussed and zoomed in on the retinal vasculature. Both MMP8 and OLFM4 stained the retina, with MMP8 staining particularly the endothelium especially in vessels and capillaries with high sequestration and OLFM4 staining the endothelium as well as the ganglion cells (Figure 14). MMP8 is expressed primarily by neutrophils (295), but is also known to be expressed by endothelial cells (296) and macrophages (297) along with other immune related cells. OLFM4 is interestingly expressed by a subset of neutrophils (298) and widely expressed in the gastrointestinal tract epithelial cells (299, 300). OLFM4 has mostly been known for its role in cancer and has not been implicated previously with malaria pathogenesis. Total intensity of positive staining was calculated in ImageScope from 3 CM ret- cases and 7 CM ret+ after adding 10 same size annotation boxes around different parts of the retinal vasculature, randomly for each sample. Interestingly, there were differences within same samples when comparing between vessels with and without sequestration as seen in Figure 15, with the staining appearing more intense around vessels with sequestered parasites.

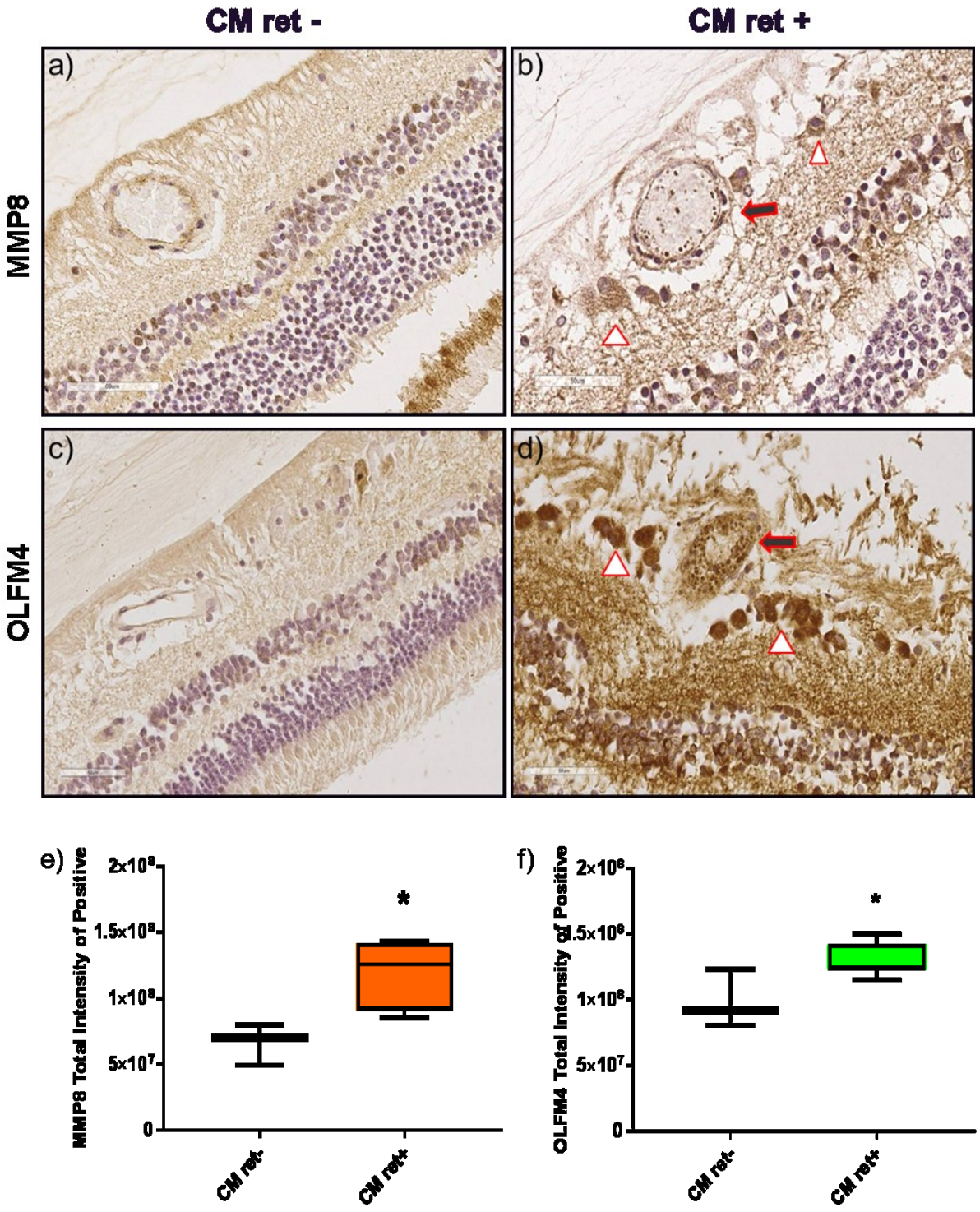

Figure 14: Immunohistochemistry staining with MMP8 (a & b) and OLFM4 (c & d) on cerebral malaria retinopathy negative (CM ret-) or positive (CM ret+) cases.

Scale bars 50µm. Arrows (b & d) show staining of endothelial cells and arrowheads staining of ganglion cells. Total intensity of positive staining measured from 3 CM ret- cases and 7 CM ret+ cases using in Image Scope for e) MMP8 and f) OLFM4. Boxes show statistical analysis done with T test, P=0.0168 (MMP8), P=0.0180 (OLFM4)

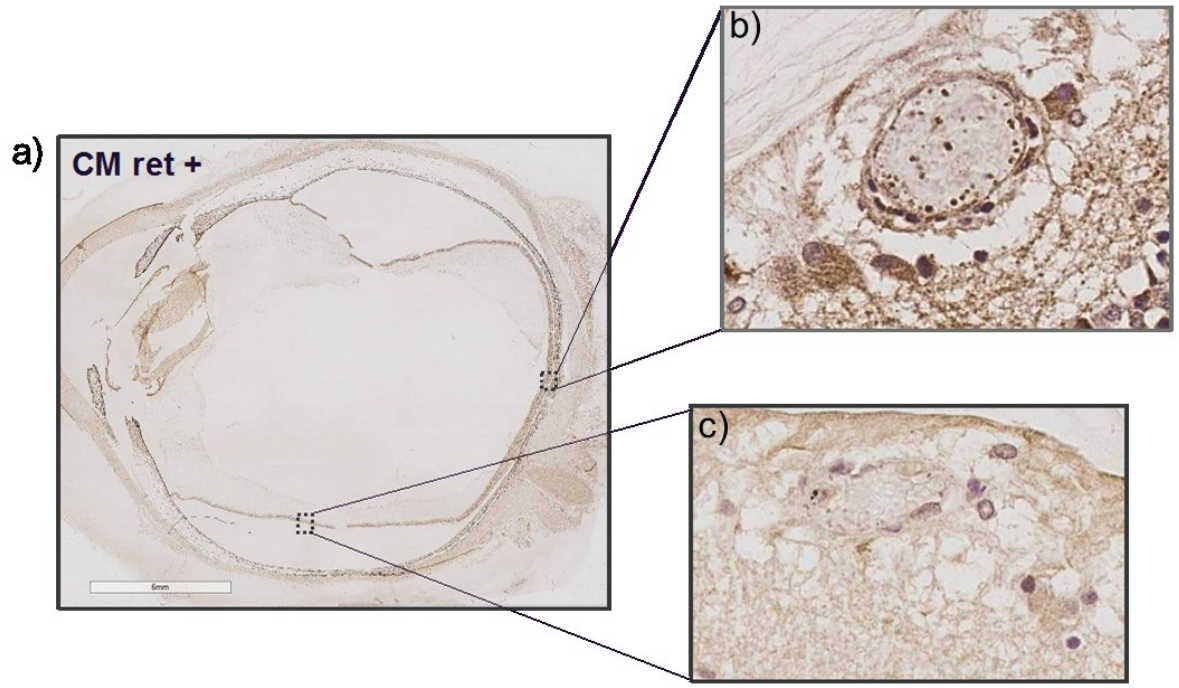

Figure 15: Retinopathy positive sample stained with MMP8.

a) Whole ocular tissue, Scale bar 6mm. b) vessel with moderate sequestration of parasites, c) vessel without sequestered parasites.

3.4.2.2 MMP8 co-localizes with fibrinogen leak

As the initial experiments showed strong staining of the endothelium in CM ret+ cases and specifically capillaries with high sequestration I then decided to further investigate if the expression of MMP8 co-localizes with pathological features of malaria and barrier breakdown. In order to assess this I used immunofluorescence and stained the retinal samples with MMP8 and fibrinogen to detect potential fibrinogen leak co-localizing with MMP8. Fibrinogen is a plasma soluble protein that is broken down to fibrin by thrombin to form clots, plays a role in platelet aggregation and facilitates wound healing (301). Fibrinogen is also a biomarker of inflammation (302), and when elevated, it indicates the presence of inflammation and high risk for cardiovascular disorders (303). Increased levels of FNG have as result changes in blood rheological properties such as platelet thrombogenesis, increases in

plasma viscosity, alterations in vascular reactivity, erythrocyte aggregation and compromises of the endothelial layer integrity (303, 304). In addition to affecting blood viscosity experimental evidence suggests that FNG changes vascular reactivity and damages endothelial cell layer integrity through binding to its endothelial cell membrane receptors and activating signalling mechanisms (303). It has also been shown that when the BBB is compromised in diabetic patients fibrinogen leaks into the retina (305).

What I proposed was that the sequestered parasites lead to increased activation and recruitment of neutrophils which locally release MMP8 and other proteases damaging to the endothelium leading to fibrinogen leak. As seen in Figure 16 MMP8 expression co-localises with vascular leak of FNG. For these experiments, I used 9 CM retinopathy positive cases and 8 retinopathy negative cases including 7 CM and 1 with other infectious disease (Table 7). Whole retinal vasculature was examined under the microscope and images from~10 fields per sample were collected. In the retinopathy negative cases, FNG leak was detected in only one of the cases and just one of the capillaries.

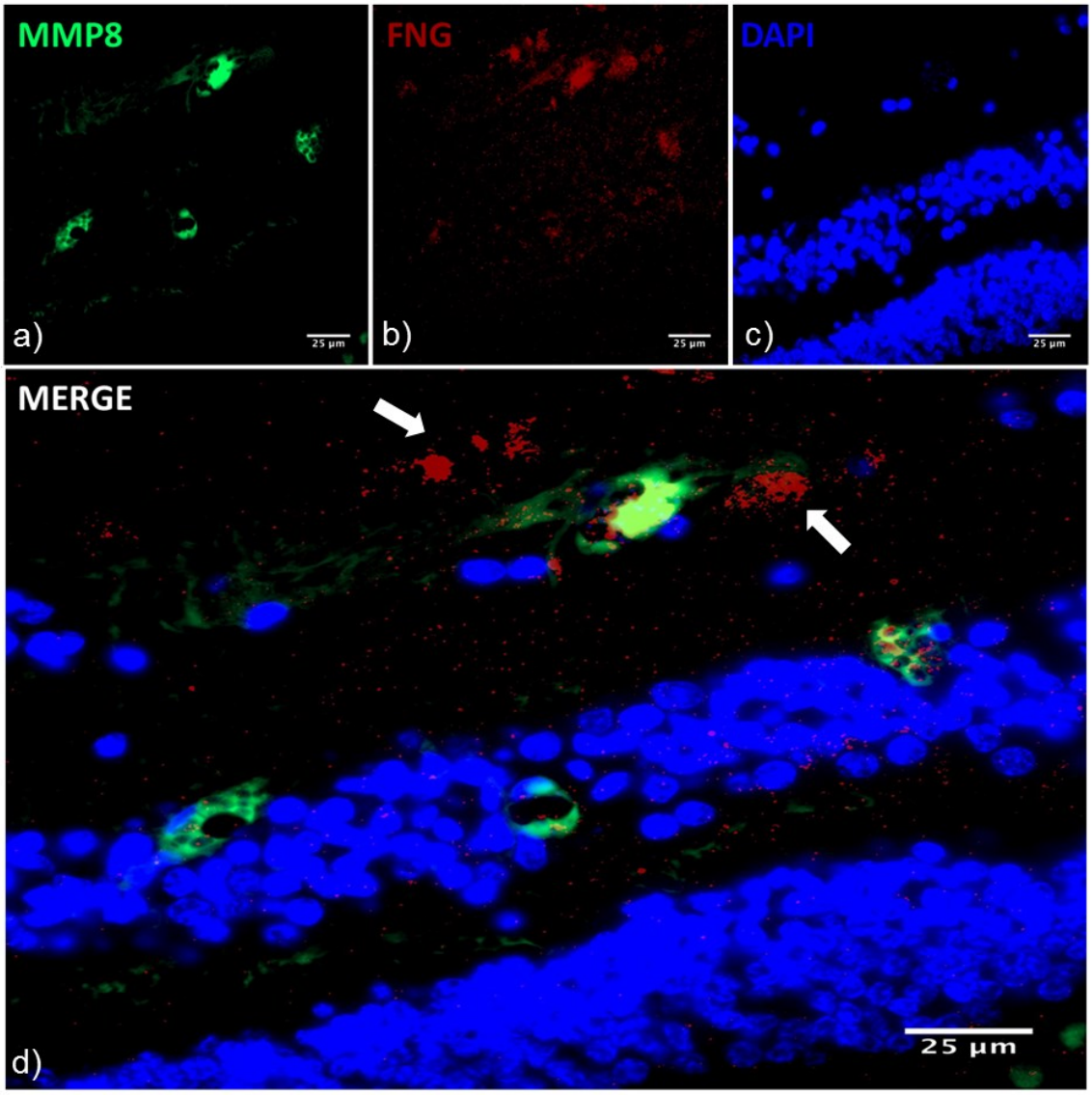

Figure 16: MMP8 co-localises with fibrinogen leak.

a) MMP8 (green) stains the endothelium as well as intravascularly. b) Fibrinogen (red) stains intravascularly in areas of micro-thrombi formation and outside the vessels suggestive of leak and damage of the endothelium. c) DAPI (blue). d) Merge shows co-localization of MMP8 and fibrinogen leak (arrows) suggesting that MMP8 might be responsible for the damage causing the fibrinogen leak. Scale bar at 25µm. This *shows 1 sample representative of the 9 examined with the same condition.*

3.4.3 Netosis

Neutrophils are the most abundant cell type of the human innate immune response system. They have effective antimicrobial enzymes stored in their granules. Their collection of antimicrobials can be damaging to the host tissues so that is why their activity is tightly regulated in three main strategies, degranulation, phagocytosis and neutrophil extracellular trap release (306). NETs are extracellular, large web-like structures composed of granule and cytosolic proteins assembled on a decondensed chromatin scaffold (307). The majority of NET DNA originates from the nucleus, however they are also enriched in mitochondrial DNA (308). The NET structures can trap, neutralize and kill parasites (309), viruses (310), bacteria (307), and fungi (311), while thought to act preventing fungal and bacterial spreading (312, 313). On the other hand, if the process gets dysregulated, NETs can contribute in immune related diseases pathogenesis (306). Stimulation of neutrophils with PMA (phorbol 12-myristate 13-acetate), which triggers reactive oxygen species production and activates protein kinase C leads to NETosis and 24 proteins had been initially identified in the structures released. These proteins included neutrophil elastase (NE or ELANE), myeloperoxidase (MPO), histones, defensins, calprotectin, actin, and cathelicidins (314). Following studies extended this list, suggesting that NETs composition varies with different stimuli however, how the different NET composition impacts on the function needs to be further investigated (306). Primarily NETs get released through NETosis which is a cell death process (315). Neutrophils start this process by arresting their actin dynamics and then depolarize (316). After disassembly of the nuclear envelope, chromatin decondenses in the cytoplasm, mixing with granule and cytoplasmic components (315). Then the plasma membrane gets permeabilized allowing NETs to expand extracellularly (306). There is also an alternative mechanism called non-lytic NETosis though which NETs get rapidly released within minutes of exposure to the stimuli through secretion of granule contents and chromatin, without undergoing lysis and retaining their ability to multitask (317, 318).

Neutrophil extracellular traps have been identified in the lungs and blood of *PbA*-infected DBA/2 mice (model of malaria-associated lung injury), where neutrophil depletion or inhibition of NET formation (before the appearance of symptoms) reduced tissue damage, ALI/ARDS symptoms and increased mouse survival (319).

In human malaria NETs have been observed in blood smears of Nigerian children presenting with uncomplicated malaria, under the age of six (320). It has been hypothesised that the formation of NETs intravascularly is contributing to vasculopathy which drives severe malaria (321). The trigger for the formation of NETs has been attributed to uric acid and hemozoin crystals that get released in circulation during rupture of infected erythrocytes encountering immune system, while uric acid forms MSU crystals in the presence of sodium rich plasma (322, 323). MSU crystals are potent inducers of NETosis in a ROS (reactive oxygen species)-dependent way (323), while hemozoin crystals induce IL-1β production via an inflammasome dependent pathway (324). A recent study, using blood samples and conventional Giemsa microscopy or immunofluorescence, also showed increased levels of circulating NETs in adults with uncomplicated malaria (infected with *P. vivax*, and *malariae* or *falciparum*) compared to controls with no parasites (325).

Neutrophil extracellular trap products such as NE, PR3, and metalloproteinases are known to break down glycocalyx which is a carbohydrate-rich layer of the endothelium, important for the maintenance of the endothelial integrity (326). Loss of glycocalyx is considered key in promoting severe malaria pathogenesis (327). Angiopoietin-induced release of NETs may also contribute to angiopoietin-mediated activation of the endothelium (328) and increase microvascular dysfunction caused by parasite sequestration (329). Moreover, release of NETs may aggravate intravascular thrombosis (330) as well as promote ischemia and decreased tissue perfusion (321).

Neutrophil granule proteins such as elastase are known to promote chromatin decondensation and formation of NETs (331), making the stimulation of NETosis likely in malaria and particularly in severe disease. The strong neutrophil signature standing out from our RNA seq data prompted me to investigate whether NETosis can occur in retinopathy positive malaria cases where the retinal vasculature is packed with sequestered parasites (Figure 13) compared to retinopathy negative cases were no sequestration occurs in the retina.

3.4.3.1 NETosis in cerebral malaria retinopathy

This is the first time that NETs formation is investigated in human tissue from malaria patients and for this I used the retina of 9 CM retinopathy positive versus 8 retinopathy negative (including one non-CM) samples (Table 7). Histones are the main components of NETs and the next most abundant protein is Elastase (314), so for the visualization of NETs I used citrullinated Histone 3, Elastase and DAPI (332) in the initial experiments (Fig 17-19) and then included UEA I (Ulex europaeus lectin I) which is an endothelial marker. For the qualitative results shown here I examined the whole retina tissue for each sample under the microscope so I can have a clear understanding and then imaged ~5 fields at low and ~10 at high magnification for each sample. For some of the samples tilling method was used to image a large part of tissue at the same time.

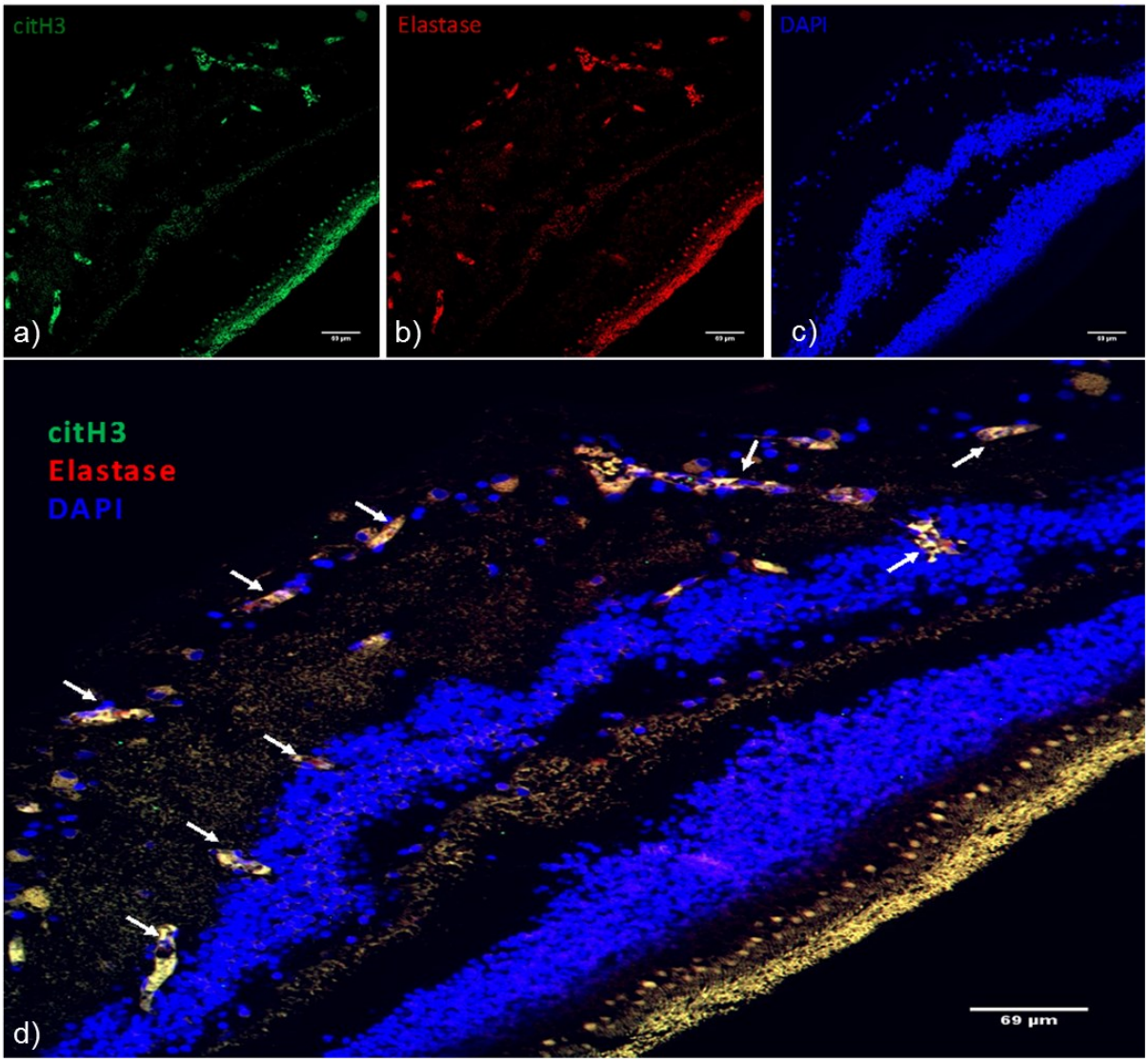

Figure 17: CM retinopathy positive case stained with citrulinated histone H3, Elastase and DAPI.

a) Citrullinated Histone 3 (green), b) Elastase (red), c) DAPI (blue), d) Merge. In this CM ret+ sample evidence of NETosis can be seen in the areas noted with arrows where citrullinated histone H3 and Elastase co-localize suggesting release of NETs inside the retinal capillaries where parasites sequester. Scale bar at 69 µm. This shows 1 sample representative of the 9 examined with the same condition.

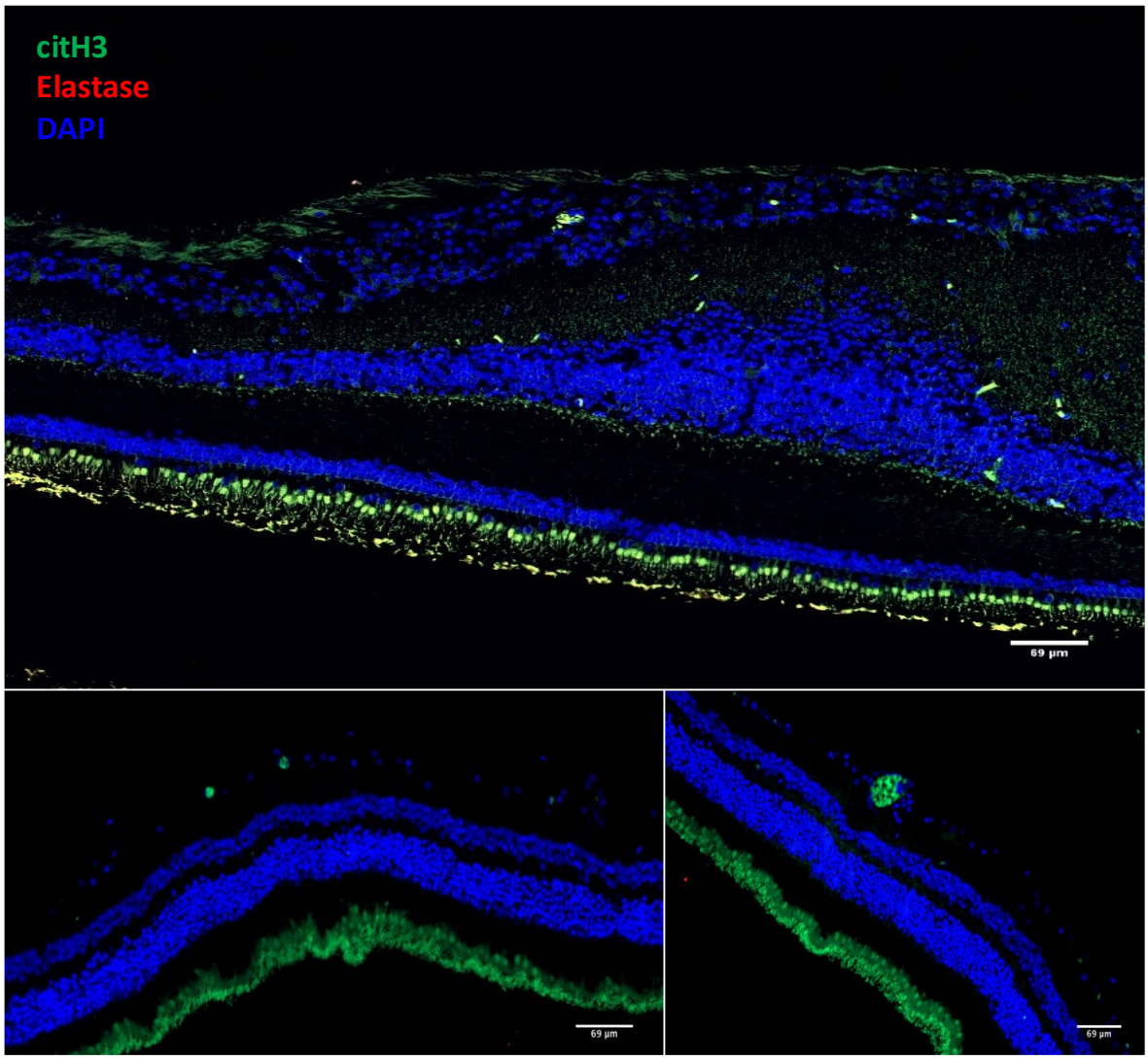

Figure 18: CM retinopathy negative and non-CM case stained with citrulinated histone H3, Elastase and DAPI.

All images show staining after merging all the chanels: Citrullinated Histone 3 (green), Elastase (red) and DAPI (blue). Scale bar at 69µm. This shows 3 different samples representative of the 8 retinopathy negative cases examined .

Most of the retinal capillaries in CM retinopathy cases were packed with sequestered parasites, these were the cases that gave evidence of NETosis for the first time in human tissue samples. These NETs seem to form a glue-like structure inside the retinal capillaries (Fig 19) possibly immobilizing the parasitized erythrocytes around them while at the same time promote pathogenesis through endothelial activation and induction of additional inflammatory response.

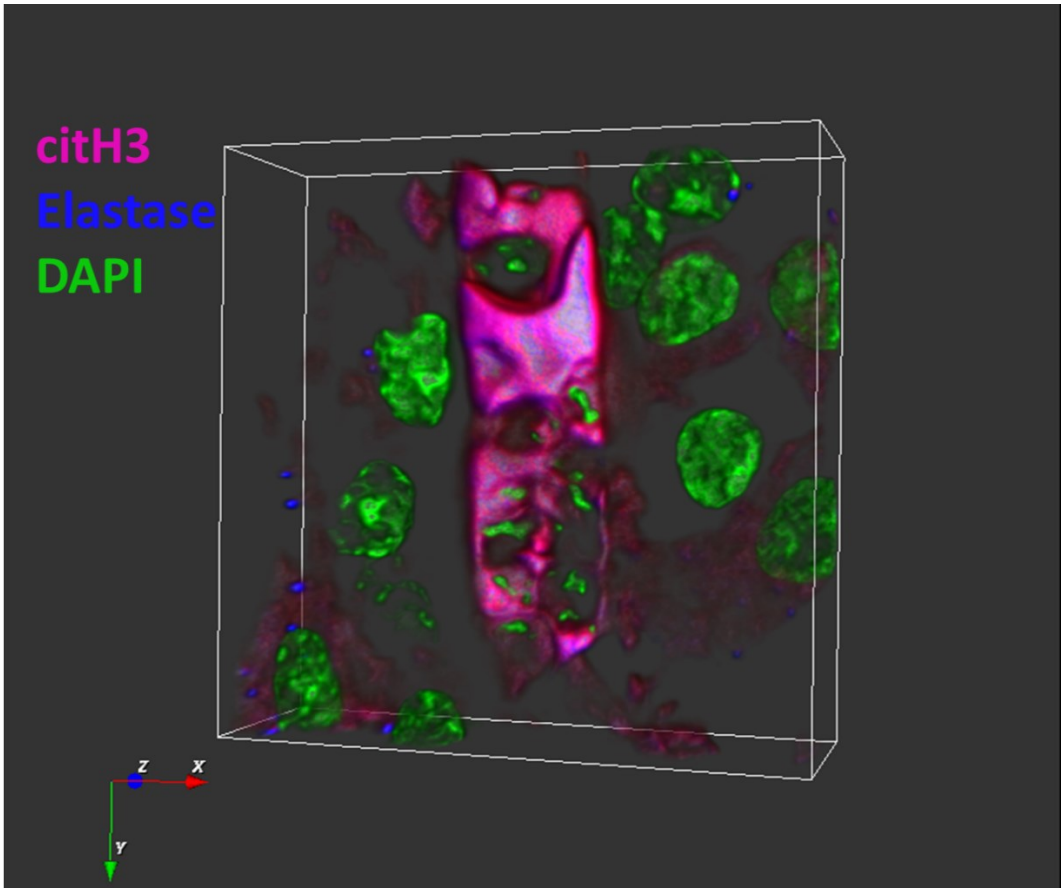

Figure 19: 3D visualization of a CM ret+ capillary stained for NETosis

Image created using z-stack imaging, deconvolution was performed using Huygens software and ICY software was used for the 3D visualisation. Citrullinated Histone 3 shown with magenta colour, Elastase with blue, and DAPI with green. Each side of the square canvas is 40µm.

The addition of UEA I (marker of the endothelium) staining results agreed with the hypothesis of NETs inducing the host endothelium damage. As seen in Figure 20 the retinopathy negative cases showed clear staining of the endothelium while the retinopathy positive case gave no staining or patchy staining of the endothelium. This suggests that there is a damage in the areas of the endothelium where the UEA I lectin should bind, possibly caused though cleavage or breakdown by the neutrophil granule enzymes.

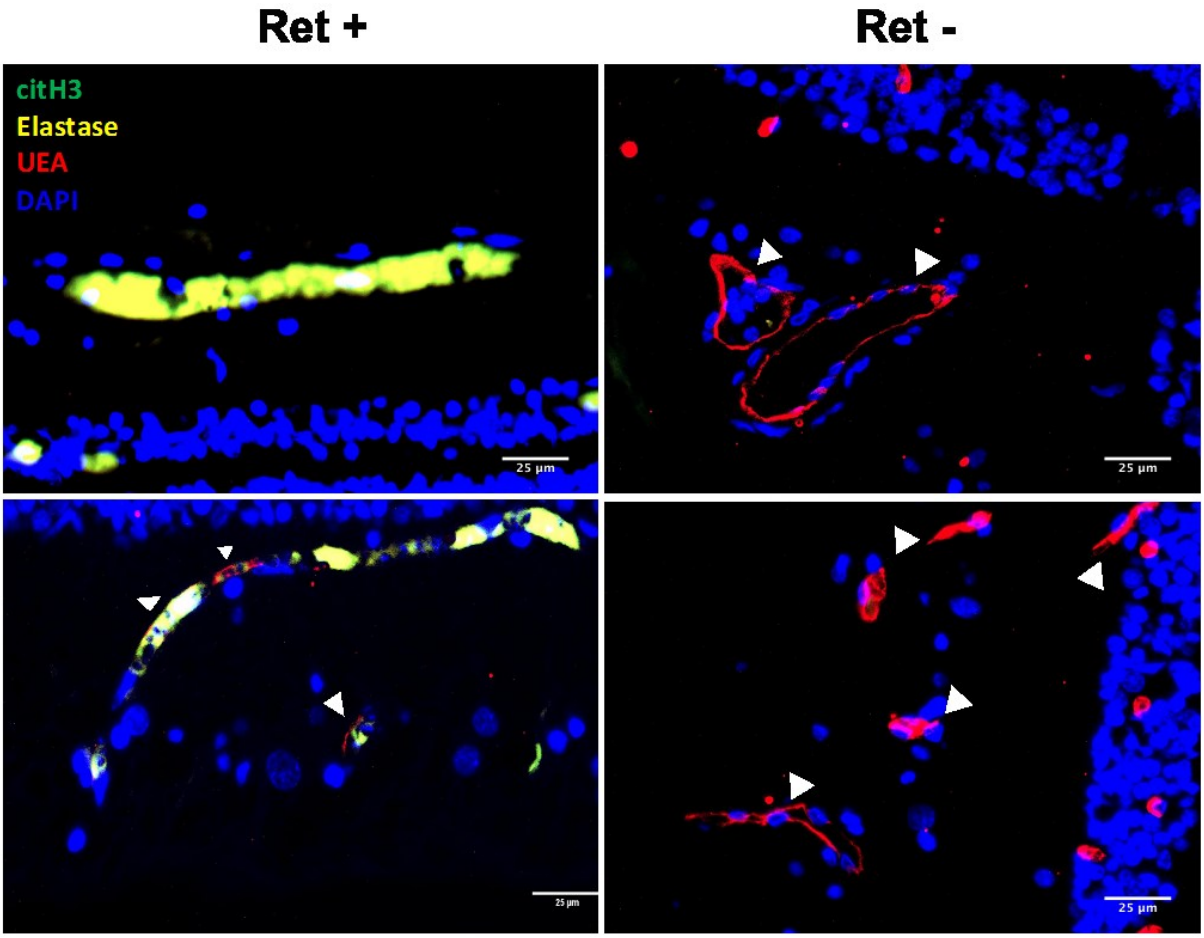

Figure 20: NETosis and UEA I staining in CM ret + versus CM ret - cases.

All images show staining after merging all the chanels: Citrullinated Histone 3 (green), Elastase (yellow), UEA I (red) and DAPI (blue). Arrowheads show UEA I staining the endothelium. Both CM retinopathy positive cases show co-localization of cit H3 and Elastase while the endothelium seems to be damaged as UEA does not stain properly. On the other side the CM retinopathy negative cases show clear staining of the endothelium with no evidence of NETs. Scale bar at 25µm. This shows 2 different CMret+ cases and 2 CM ret-.

One of the limitations when using paraffin embedded sections for immunofluorescent staining is autofluorescence signal, usually from RBC and the tissue due to the fixation method and paraffin. As seen in figures 17 and 18, rods and cones especially, located at the edge of the retina give strong autofluorescence signal which might have been avoided with the use of a commercially available product for reducing autofluorescence background. I am focusing at the changes seen in the vasculature so this does not obstruct our observations however for future experiments I would use background decreasing product if using non-perfused tissue (as these samples) to also avoid RBCs strong autofluorescence. Another issue with these

samples was their fixation for longer periods than normal which may interfere with the antigen retrieval of epitopes.

3.5 Targeting MMP8 *in vivo*

Looking at the volcano plot (Figure 9) MMP8 seemed to be the most promising target for SM pathogenesis, from our RNA sequencing data and along with the existing literature discussed above it became a tractable and plausible candidate for us to further pursue. I decided to do this *in vivo* using one the of the most commonly used malaria mouse models, with *Plasmodium berghei ANKA* parasites which leads to fatal experimental cerebral malaria, and increased mRNA expression levels of MMP8 in the brain (282). I used 8 C57BL/6 female mice infected with 10^6 *P. berghei ANKA* parasites, and treated them with either 200ul of a specific MMP8 Inhibitor I ((3R)-(+)-[2-(4-Methoxybenzenesulfonyl)-1,2,3,4-tetrahydroisoquinoline-3-hydroxamate] (Calbiochem®) at 5mg/kg/day or 200ul of vehicle (PBS with 1% DMSO) starting at day 3 post infection. As seen from Figure 21 treatment with the MMP8 inhibitor did not affect weight loss Fig 21.a, or parasitaemia levels Fig 21.c, but slightly delayed the neurological symptoms (RMCBS score) by a day Fig 21.b. and no significant difference in the mean total haemorrhages count per μm^2 between treatments at the time of death (two-tailed Mann-Whitney test, p=0.6571).

This treatment did not manage to prevent the neurological symptoms or alter overall survival. This could be due to many reasons, from the number of subjects used and the dose of inhibitor not being sufficient to having an effect on another immunological process. MMP8 is known to affect macrophage polarization, and it has been shown that MMP8 deficiency favours M1 macrophage phenotype which induces inflammation, over M2 which dampens excessive inflammatory response (297). MMP8 is possibly needed for the cleavage of fibromodulin which then increases TGF-β1 bioavailability which in turn induces M2 macrophages (297).

Before pursuing further assessment of different dosing volumes and schedules, or trying to use a MMP8-deficient mouse model we had a discussion with Professor Philippe Van den Steen (KU Leuven) who has worked extensively on MMPs, including their roles in malaria. Prof Van den Steen shared with us some unpublished data of his group showing that MMP8 knockout mice infected with *P. berghei ANKA* or *P. berghei NK65* presented the same clinical

symptoms as the wild type, and no change in disease outcome. Could this mean that MMP8 is the outcome and not the cause of pathogenesis in severe malaria? This also stimulated the question of whether I used the correct mouse model to test this in the first place. Thinking about what the appropriate mouse model would be it was concluded that this should be the mouse model closest to human malaria disease first at transcriptomic level and then clinical presentation, prompting the work described in chapter 5.

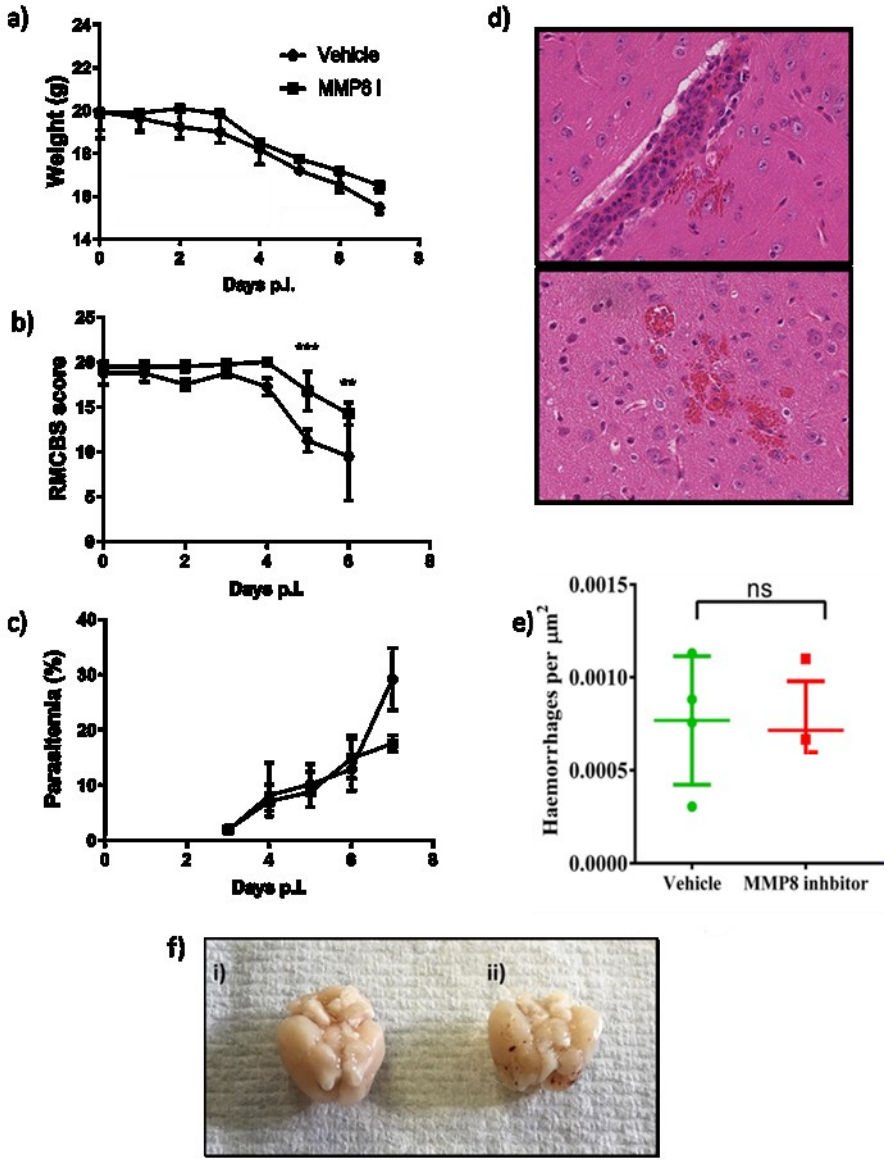

Figure 21: In vivo supplementation with MMP8 inhibitor in mice infected with P. berghei ANKA did not improve survival but delayed the neurological symptoms manifestation.

a) Weight loss monitoring, bars show mean and error with SD. b) RMCBS scoring, bars show mean and error with SD. c) Parasitaemia percentage levels, bars show mean and error with SD. d) Brain sections stained with H & E showing haemorrhages e) Haemorrhages per um^2 measure by a student blinded to the treatment p=0.657, f) i. Brain collected from an uninfected control mouse, ii. Brain collected from P. berghei ANKA infected mouse at day 7 post infection showing obvious haemorrhages.

Parasite

3.6 Sodium L-lactate supplementation *in vitro*

The earliest RNA seq data analysis completed by our collaborator was the parasite gene expression correlation with human blood lactate concentration. This revealed 180 genes significantly associated with lactate after adjustment for parasite stage SPVs and log PfHRP2 concentration (Appendix). One way to identify important pathogenic mechanisms in transcriptional data is to use pathway analyses, which identify whether differentially expressed genes are significantly overrepresented in any particular biological pathway. To try and understand the biological process involved in hyperlactataemia I imported this gene list into the metabolic pathways analysis tool in PlasmoDB. I decided to focus on glycolysis, which is the metabolic pathway of glucose metabolism and lactate production, as this came up as the most enriched pathway (Table 8).

Pathway ID	Pathway Name	Genes in the background with this pathway	Genes in your result with this pathway	Percent of background Genes in your result	Fold enrich ment	Odds ratio	P-value	Benjamini	Bonferroni
ec00010	**Glycolysis / Gluconeogenesis**	**26**	**5**	**19.2**	**7.88**	**9.15**	**6.09e-4**	**7.31e-3**	**7.31e-3**
ec00260	Glycine, serine and threonine metabolism	11	3	27.3	11.17	12.23	3.75e-3	2.20e-2	4.49e-2
ec00564	Glycerophospholipid metabolism	45	5	11.1	4.55	5.21	5.49e-3	2.20e-2	6.59e-2

Table 8: Pathways in which genes associated with lactate are involved (PlasmoDB)

However, these five genes involved in the pathway showed a negative correlation with lactate levels. Therefore, rather than indicating that parasite glycolysis was driving high lactate levels, the results suggested that increasing blood lactate was associated with downregulation of key genes involved in glucose metabolism and aerobic glycolysis (Figure 22). Overall this was suggestive of a negative feedback mechanism – high levels of lactate may decrease parasite glycolysis and parasite growth.

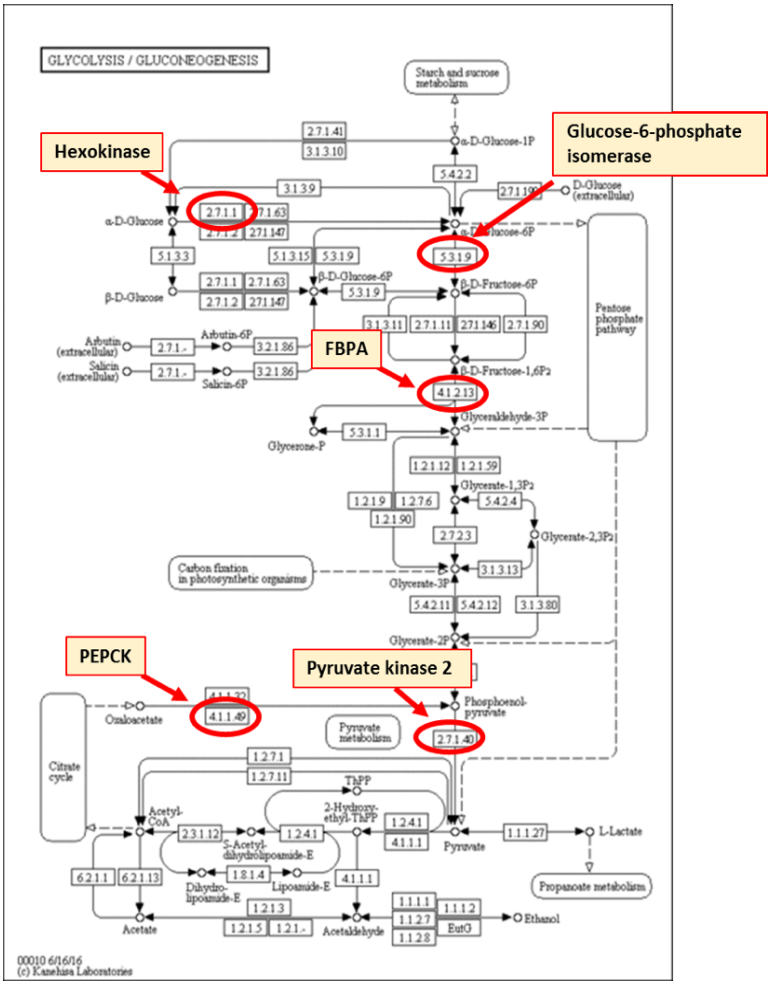

Figure 22: Key genes that belong in the parasite glycolysis pathway which are negatively associated with increased blood lactate.

These genes are hexokinase, pyruvate kinase 2 (PyKII), phosphoenolpyruvate carboxykinase (PEPCK), glucose-6-phosphate isomerase (GPI), fructose-bisphosphate aldolase (FBPA). KEGG pathway ec00010

Although, PlasmoDB has been a very useful tool its use has some limitations, such as the inability of the software to distinguish which genes are expressed during the erythrocytic stage of the parasite (which I am interested in) and gives results that take into account genes expressed in other stages of the parasite's life cycle potentially reducing our ability to detect a significant difference.

Having in mind that hyperlactataemia/acidosis is still one of the least researched syndromes of malaria and the fact that the mechanism behind it being highly debated with no proof of how it develops, I decided to look more closely. Even with the above mentioned limitations of PlasmoDB the result from our RNA seq analysis was encouraging enough along with a

recent paper showing that supplementation of parasites *in vitro* with lactate suppresses their growth and slows down their development (333). This prompted us to investigate whether we could demonstrate the same result and possibly find evidence of a negative feedback mechanism controlling parasite growth.

The control against the sodium L-lactate was the supplementation of parasites with the equivalent concentration of sodium chloride (NaCl) and an untreated parasite culture. When I used 30mM of L-lactate to supplement *in vitro* parasite cultures (3D7 strain), parasitaemia levels were significantly lower in the lactate supplemented culture at 48 hours compared to both NaCl and non-treated control (Fig 23). However, I noticed that when using the more physiological concentrations of lactate (found in hyperlactataemia syndrome) to supplement cultures (5, 10mM) the difference was not very significant compared to the NaCl controls at 48 hours of culture. Therefore, we decided to look at parasitaemia levels after two life cycles of the parasite instead of one like Hikosaka et al did.

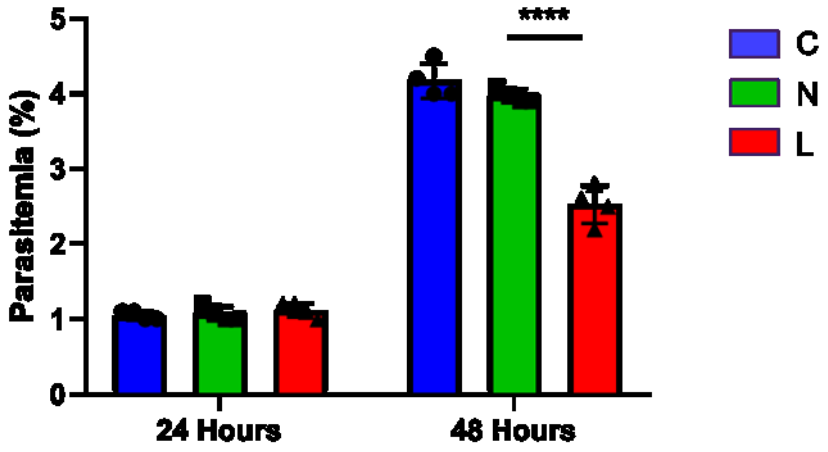

Figure 23: Supplementation of in vitro parasite cultures with sodium L-lactate for 48 hours.

These experiments were performed in a 96 well plate starting with 1.0% parasitaemia at 0 hours, 2% haematocrit. Blood smears were collected at 0, 24, and 48 hours and parasitaemia was counted. N=4, 95% CI C: control parasite culture with no treatment, N: 30mM NaCl, L: 30mM Sodium L-lactate. Representative of three experiments.

Supplementation of cultures with 5, 10, & 30mM sodium L-lactate after 96 hours resulted in a significant decrease of total parasitaemia. As shown in Figure 24 supplementation with lactate even at 5mM (the lower limit for clinical diagnosis of hyperlactataemia in humans) significantly decreased the percentage of parasitaemia after 96 hours of culture (2 parasite life cycles).

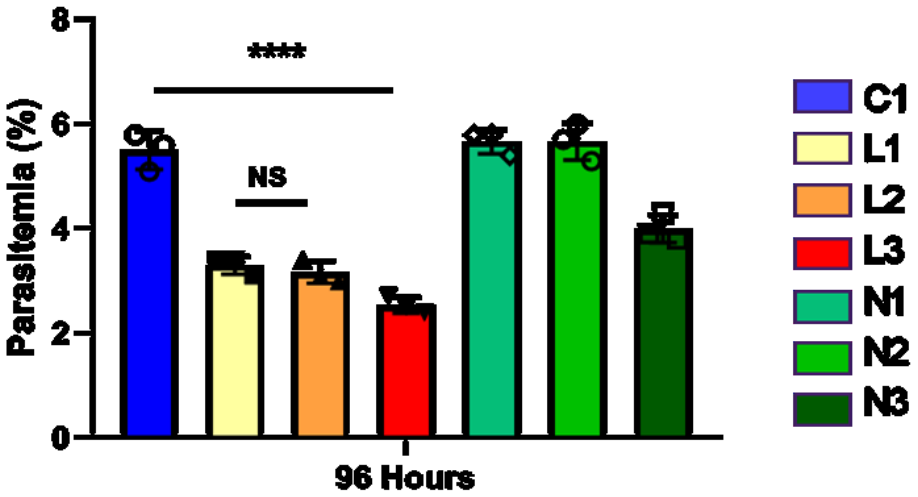

Figure 24: Supplementation of in vitro parasite cultures with sodium L-lactate for 96 hours.

This experiment was performed in a 96 well plate starting with 0.9% parasitaemia at 0 hours, 2% haematocrit. Blood smears were collected at 0 and 96 hours and parasitaemia was counted. N=3, 95% CI C1: control parasite culture with no treatment, L1: 5mM Sodium L-lactate, L2: 10mM Sodium L-lactate, L3: 30mM Sodium L-lactate, N1: 5mM NaCl, N2: 10mM NaCl, N3: 30mM NaCl. Representative of three experiments.

3.7 RNA sequencing of lactate supplemented 3D7 parasite cultures

We tested the effect of hyperlactataemia on parasite gene expression *in vitro,* in order to establish whether parasite gene expression changes seen in glycolysis pathway were the consequence or cause of hyperlactataemia *in vivo*. Before proceeding to RNA extractions and sequencing we confirmed the effect of lactate supplementation in parasitaemia after 48 hours of culture (Figure 25).

P. falciparum 3D7 strain was grown in human A+ erythrocytes at 1-5% haematocrit. Parasites were synchronised at early ring stage through a combination of Percoll & sorbitol treatments and adjusted to 5% parasitaemia immediately prior to supplementation with 15 mM sodium L-lactate (reflecting the maximum concentration seen in our clinical samples) or control medium. For this experiment, I prepared n = 4 lactate-supplemented and n = 5 control untreated cultures. To minimise any possible impact of progression through the normal parasite developmental cycle on gene expression, erythrocytes were pelleted after just 5h incubation, adjusted to 50% haematocrit and transferred to Paxgene tubes (Qiagen). RNA extraction, quality control, RNA sequencing and analysis including deconvolution of parasite

developmental stage, adjustment for SPVs and differential expression analysis were performed as described in the methods, with a 2x125bp sequencing protocol (270).

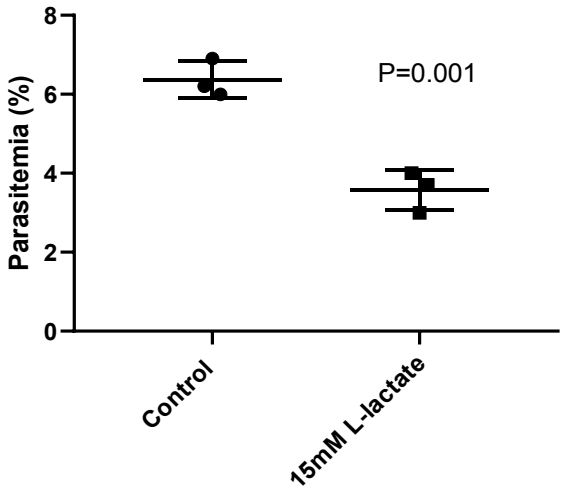

Figure 25: Parasitaemia measurement at 48 hours after supplementation with 15mM L-lactate.

I left 3 samples from the control group and 3 from the L-lactate treated to grow over 48 hours and then assessed parasitaemia by flow cytometry to confirm there was an effect in parasitaemia before sending the samples for RNA sequencing.

Sixty-one genes were identified as differentially expressed between lactate-supplemented (n = 4) and control (n = 5) early ring-stage parasite cultures, mainly enriched in genes associated with transcription and RNA processing (270). The two most highly induced after lactate supplementation genes were PF3D7_0202000 (knob-associated histidine-rich protein) and PF3D7_1016300 (GBP), which were also found as highly expressed in the human phenotype combining hyperlactataemia and cerebral malaria (CH) (270). This is suggestive of lactate as a potential influence on the parasite virulence phenotype, which is consistent with a recent study showing that *Plasmodium* can sense and respond to the metabolic environment of the host (34). This lactate supplementation did not confirm downregulation of glycolysis pathways. This could simply be due to the short treatment time and possibly the need for more than one life cycle of the parasite growing in the lactate supplemented medium before seeing anything similar to what happens *in vivo*. It could also be due to the genetic differences between *in vitro* cultured and *in vivo* growing parasites, as the second ones need a large repertoire of mechanisms allowing them to adjust in a constantly changing host environment.

3.8 Summary

We used dual RNA sequencing to simultaneously detect host and parasite gene expression, as well as their interactions which associate with severity of human *P. falciparum* malaria. Our findings add to the thought of a combined understanding of infectious diseases, suggesting that we should be studying both the host and the pathogen simultaneously when possible. Malarial hyperlactataemia is usually ascribed to anaerobic metabolism due to microvascular obstruction by rigid and adherent parasitized erythrocytes (71, 334). These parasite properties are determined partly by the expression of specific members of the *rif, stevor* and *var* gene families (27), which have been excluded in our analysis due to their extreme polymorphism, preventive of a reference genome-based quantification. Regardless of this limitation we still identified associations between severity and lactate concentration and *in vivo* variation in the expression of other parasite genes known to modify the infected erythrocyte biophysical properties. There might be a genetic basis for some variation in parasite gene expression (335) but our *in vitro* data from lactate supplementation suggest that it may also happen as a response to the host environment (270). Hyperlactataemia is a pathogenic condition negative for both the host and the parasite, as when the host dies the parasite cannot continue infecting other hosts. This suggest that although hyperlactataemia seems to negatively affect the parasite growth, it should not be considered as a mechanism of the host trying to fight the parasite but an adaption of the parasite to the host environment.

The human genes that came up as the most correlated with lactate were immune response-associated, suggesting that inflammation, and possibly its effect on glycolysis, may play a role (336, 337). If lactate production is related with the robustness of the host response, then the shift in parasite gene expression in response to lactate might favour evasion of innate immune cells and sequestration as a parasite survival strategy. A lot of our results agree on a putative role for neutrophils in severe malaria. Using different analytical approaches repetitively identified the association of genes encoding for neutrophil granule proteins (such as MMP8, OLFM4, ELANE, DEFA3) and upstream regulators of granulopoiesis (CEBPA and CSF3) with severe disease outcome (270). Immature neutrophils, which are mobilised from the bone marrow to the circulation in malaria (320, 338), are enriched with granule proteins (339, 340) and there is evidence of neutrophil degranulation occurring in severe malaria (252, 281). Neutrophil granule protein release can be very damaging to host tissues (340), while

increased production and release of these proteins could be underlying many of the pathological features of severe malaria. Neutrophil granule proteins and histones get released into the circulation during NETosis which is the production of neutrophil extracellular traps (NETs) (340, 341), a phenomenon described very briefly until now in malaria (320). The reason for no significant difference in most granule protein levels between UM and SM plasma levels, may be explained by localized release in the microvasculature associated with sequestration, and even though proteins released in these obstructed vessels reach high local concentrations they may not enter the systemic circulation. Here, I have shown that MMP8 and OLFM4 staining in the retina from CM ret+ cases is associated with parasite sequestration, while MMP8 co-localises with fibrinogen leak suggesting that the upregulation in expression of MMP8 might be damaging the endothelium which leads to FNG leak. I have also shown evidence of NETosis for the first time in the retinal vasculature of CM ret + children associated again with sequestration. In the future, I will also examine brain samples from the same Malawian children cohort, to assess these neutrophil related protein expression as well as NETosis.

Findings from this chapter show direct evidence for the involvement of neutrophils in the pathogenesis of severe disease. The common association of neutrophil granule protein genes with all severe malaria manifestations suggests that targeting neutrophil function may be a therapeutic strategy in the future.

It is important to note here that similar neutrophil related signatures have not been reported in whole blood transcriptomics of rodent models examined to date (247, 342), challenging the prospects for experimental validation. Neutrophil depletion has been shown to rescue mice from experimental cerebral malaria (343), and although this is not a viable therapeutic option for humans, pharmacological inhibitors of specific functions of the neutrophils such as NETosis are being evaluated in other diseases (341).

3.9 Conclusion

This chapter shows that dual RNA sequencing can be used to simultaneously detect host and parasite gene expression, which can reveal new targets responsible for severity. Looking at the host side we identified a very strong neutrophil signature being associated with severe disease. This was validated using ELISA to measure plasma levels of the encoding proteins for the neutrophil genes identified, in the same Gambian children cohort. Having access to archived post-mortem human ocular tissue from Malawian children with fatal *P. falciparum* cerebral malaria (retinopathy positive versus retinopathy negative) I used immunohistochemistry and immunofluorescence revealing upregulated expression of MMP8 & OLFM4 in the retinopathy positive cases as well as NETosis formation, associated with parasite sequestration. Examining parasite gene expression associated with host lactate level, glycolysis came up as the most enriched pathway while the parasite genes involved were negatively associated with host lactate indicating that high lactate levels in the host lead to downregulated parasite glycolysis. Supplementation of parasite cultures *in vitro* with lactate showed decreased parasite growth and upregulation in the expression of virulence associated genes [PF3D7_0202000 (knob-associated histidine-rich protein) and PF3D7_1016300 (GBP)].

Chapter 4: Investigation of mechanistic correlates of protection in malaria

In this chapter the mathematical model fitting and analysis was performed by Dr Michael Bretscher from the Malaria Modelling Group at Imperial College (Fig 27); the bioinformatics analysis for RNA-sequencing was performed by Dr Hyun Jae Lee from University of Queensland (Fig 28). RNA sequencing and library preparation was performed at Exeter University Sequencing Centre.

Parasite load is a key determinant of severe malaria and is a consequence of pathogen multiplication rate, number of replication cycles completed and the ability of the host to constrain parasite growth (71, 269). We aimed to develop a new method to identify the host mechanisms which constrain parasite growth.

Using a mathematical model of longitudinal infection dynamics for orientation, we made individualized estimates of parasite multiplication and growth inhibition in Gambian children at presentation with acute malaria and used whole blood RNA-sequencing to identify their correlates. We identified 26 human genes positively correlated with parasite growth inhibition, largely linked together in a network focused around extracellular signal-regulated kinases, which integrate cellular inflammatory and metabolic responses in innate defence. Focussing on two genes which encode secreted products, we identified novel roles for cathepsin G and matrix metallopeptidase 9 (MMP9) as direct effector molecules which inhibit *P. falciparum* growth. Cathepsin G acts on the erythrocyte membrane, cleaving surface receptors required for parasite invasion, whilst MMP9 acts on the parasite (269).

Our findings underline the importance of accounting for the interaction between host and pathogen when seeking to identify correlates of protection, and reveal novel mechanisms controlling parasite growth in humans.

4.1 Introduction

Both parasite and host related factors contribute to the pathogenicity of the severe forms of the disease (4). One of the key determinants of severe disease is high parasite biomass, which is a consequence of pathogen multiplication rate, time and the ability of the host to constraint the pathogen (182). The puzzle of factors that facilitate resistance of the host or favour the parasite's growth still has significant missing parts. Although some of the ones we know include sickle cell trait and other red blood cell polymorphisms (344) from the host side, and *var* genes that affect virulence (cytoadherence - rosetting) (345) from the parasite side.

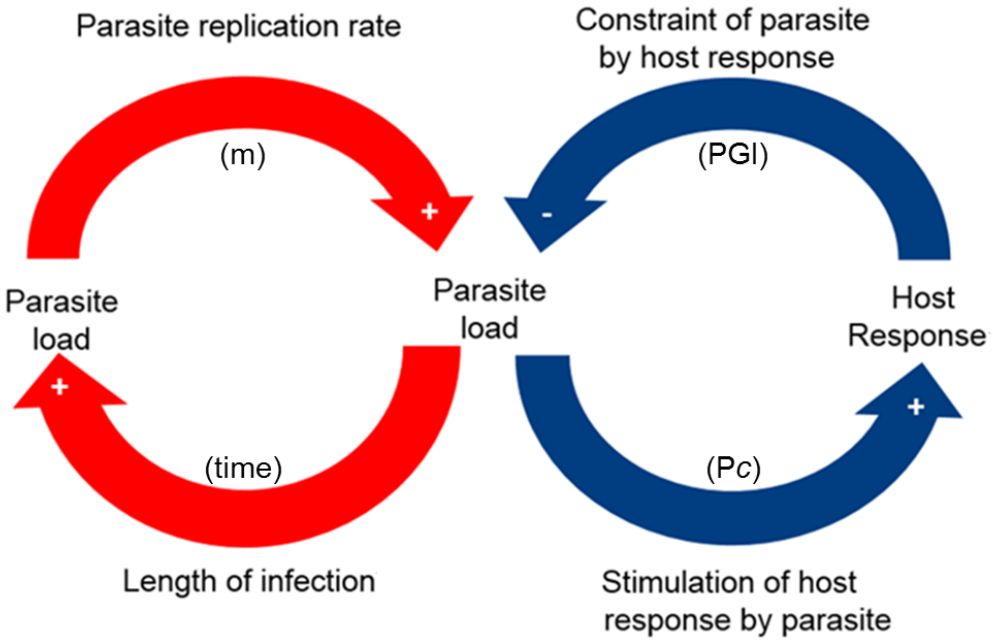

Figure 26: Factors affecting parasite load.

Conceptual model of parasite load determinants. m= multiplication rate, time= number of replication cycles, PGI= parasite growth inhibition, Pc= is the host-specific parasite load threshold at which the host response is strong enough to inhibit 50% of parasite growth in that cycle.

This raises the need for development of new methods that will identify the mechanisms which mediate protection against parasites. Modern discovery approaches such as transcriptomics and proteomics have created new opportunities for insights into the genes, proteins and pathways responsible for the control of parasite load in malaria.

This work is part of validation for a mathematical model of *in vivo* dynamics of host-parasite interactions developed by Dr Aubrey Cunnington and Dr Michael Bretscher who employed a

historical reference dataset of the longitudinal course of untreated malaria and the mathematical model proposed by Klaus Dietz (346) to define relationships between measured and latent variables. These relationships were then fitted to a dataset from Gambian children at the time of acute presentation with malaria and used the measured variables (parasite load, duration of illness and TNF) to make individualised estimates of parasite growth inhibition. Gambian children with malaria constituted the discovery dataset, using whole blood for RNA sequencing after multiple adjustments for leukocyte mix and false discovery rate. The output of the mathematical model was used to estimate the parasite multiplication rate and growth inhibition in each subject at the time of taking the blood sample used for RNA seq, and then the adjusted gene expression was correlated with the estimated parasite growth inhibition.

4.2 Mathematical model and RNA seq combination

We tried to estimate the parasite load dynamics in patients naturally infected with malaria by calibrating a statistical prediction model utilising the outcome of a mechanistic simulation combining information from two datasets. A historical dataset, of 97 patients' longitudinal course of untreated malaria infection (malariatherapy) who were infected with *P. falciparum* in order to be treated for neurosyphilis was used, since detailed records of parasitaemia and fever episodes were meticulously kept from these patients providing with an excellent reference of parasite load change over the course of infection along with measurements of clinical parameters that could affect it. In this dataset (malariatherapy), relationships were defined among latent (assumed as determinants of the change in parasite load) and measured variables, based on the Dietz et al. mathematical model (346). To estimate the likely values of these variables in our patient dataset, of 139 Gambian children with malaria at clinical presentation time, the malariatherapy dataset was employed.

In our model, increasing parasite load dynamics from the malariatherapy dataset can be described using two latent variables (specific for each individual): the within-host parasite multiplication rate (*m*), which is the initial rate of parasite load increase prior to any host response constraint, and the parasite load required to elicit a host response which decreases parasite growth by 50% (*Pc*) (Fig 26-27) (269). When parasite load, *Pc* and *m* have been estimated, an estimate of host response mediated parasite growth inhibition (PGI) can be calculated (269).

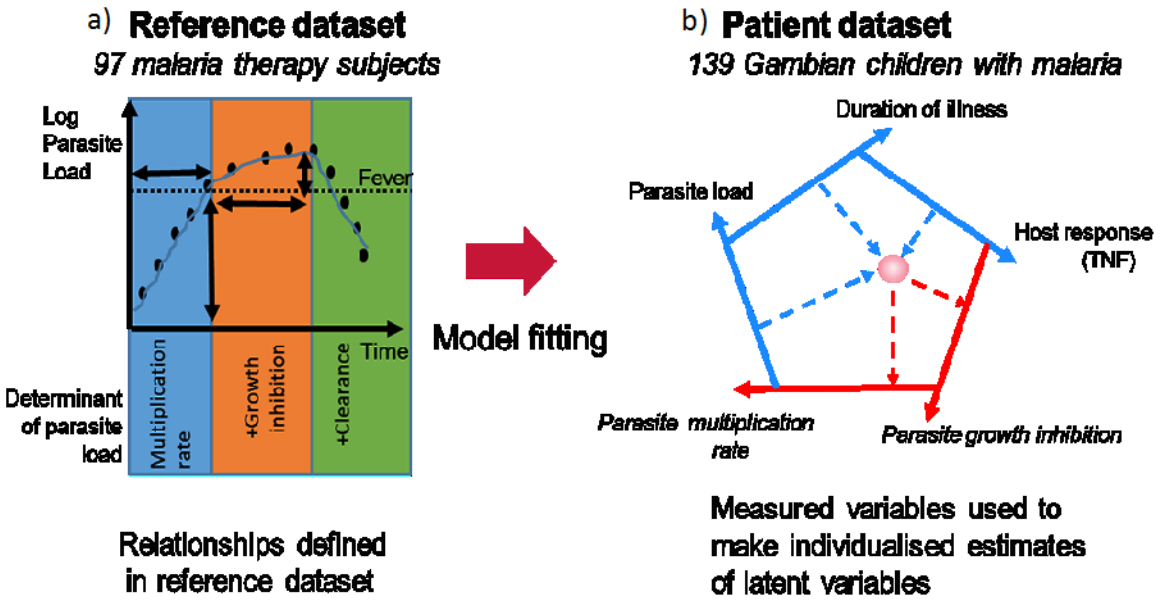

Figure 27: Estimating the host response and parasite load dynamics in malaria

a)Graphic of the relationships between multiplication rate, parasite growth inhibition and parasite load derived from the malariatherapy longitudinal dataset. b)Schematic of the model fiting using the patient dataset of 139 Gambian children. With blue color we show the measured variablesand with red the latent variables.

4.3 Identification of mechanistic correlates of parasite growth inhibition

To define if the mathematical model derived estimates that could be utilised to identify novel protection or susceptibility correlates, human gene expression was analysed using whole blood from 24 subjects at the time of presentation. To account for inter-individual variability in the proportions of white blood cells, a gene-signature deconvolution was performed and the total gene expression was adjusted for cell mixture, as described in previous chapters. 11702 human genes were detected, 51 of which came up as significantly correlated, after adjustment for false discovery rate (Benjamini-Hochberg P<0.05), with the estimated PGI.

The combination of mathematical modelling and RNA sequencing resulted in 26 genes, positively correlated with parasite growth inhibition, which were largely linked together in a network focused around Akt and ERK 1/2 kinases which integrate cellular inflammatory and metabolic responses to control innate defence mechanisms (Fig 28 A) such as phagocytosis, cytokine secretion and degranulation (347, 348). On the other side, 25 genes were negatively correlated with parasite growth inhibition, which were largely linked in a network focussed around type 1 interferon response (Fig 28 B). These findings are consistent with observations

that continuous type 1 interferon signalling can impair control of parasite load in mice (349-353) and possibly in humans (349, 354). CXCL10, the gene with the highest log fold change from the negatively correlated gene list, has been shown to inhibit control of parasite load in mice, while neutralisation and deletion of CXCL10 in mice decreased the parasite load (355).

A)

Gene Name	Log FC	P	FDR
CTSG	10.06	0.000208	0.048
MMP9	5.43	7.19E-05	0.033
SLC7A11	4.79	6.66E-05	0.033
SLC27A2	4.67	4.35E-07	0.003
CA4	4.37	1.01E-05	0.011

B)

Gene Name	Log FC	P	FDR
CXCL10	-9.42	0.000205045	0.048
FAM26F	-7.55	6.03218E-05	0.033
ISG15	-7.42	7.39977E-05	0.033
IFI6	-5.68	0.000107411	0.037
AATBC	-5.22	0.000146525	0.038

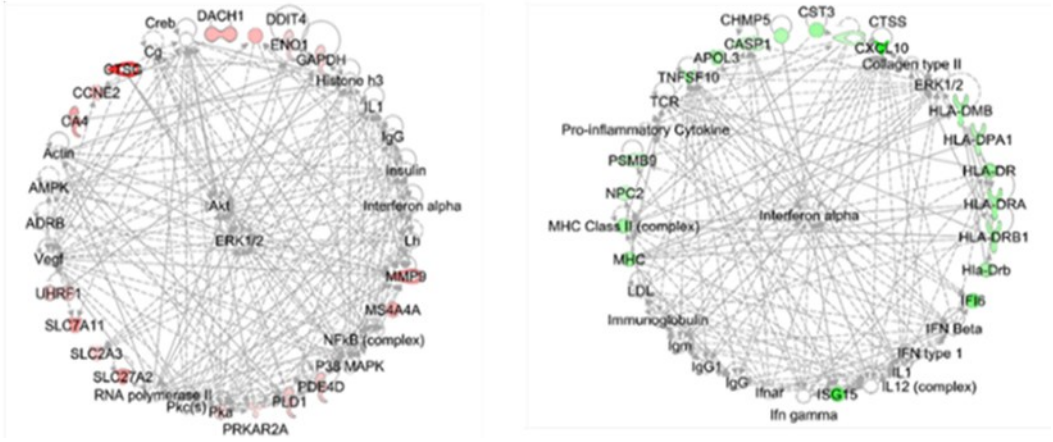

Figure 28: Transcriptional correlates of parasite growth inhibition.

(A) Genes significantly positively and (B) genes significantly negatively correlated with parasite growth inhibition after adjustment for false discovery rate and the primary network derived from the full lists of genes. Only the top 5 genes are shown here.

None of the genes positively correlated with parasite growth inhibition had previously been ascribed a role in host defence in malaria, therefore we sought to validate our predictions by focussing on genes encoding for secreted proteins. Of the 26 genes, two encode secreted proteins: CTSG (cathepsin G) and MMP9 (matrix metallopeptidase 9). Cathepsin G localizes in neutrophil azurophilic granules while MMP9 localises in neutrophil specific and gelatinase granules (339).

4.4 *In vitro* experiment methods

P. falciparum 3D7 strain was used in continuous culture using methods as described previously (Chapter 2) (259, 260). Parasite synchronisation was performed using 5% D-sorbitol to obtain ring stage parasites and Percoll gradients for schizont stage enrichment (260, 261). For growth assays, schizonts were mixed at <1% parasitaemia with uninfected erythrocytes at 2% final haematocrit. Cathepsin G (Abcam) or recombinant active MMP9 (Enzo) were added for 72-hour incubation to allow two replication cycles. Growth under each condition was calculated relative to the average growth in untreated samples. Invasion assays were performed by adding parasites synchronised at the schizont stage to target erythrocytes and incubated for 24 hours. Cathepsin G and MMP9 were either pre-incubated with the target cells overnight followed by four washes with RPMI to completely remove them, or added directly to the culture of schizonts with target erythrocytes for 24 hours. Flow cytometry was performed using a BD LSR Fortessa machine and analysis was conducted using FlowJo v10 (TreeStar Inc.) to assess parasitaemia.

4.5 Growth assays reveal that both Cathepsin G and MMP9 inhibit parasite growth

Treatment with cathepsin G and MMP9 inhibited growth of *P. falciparum* 3D7 strain *in vitro* (Fig 29.A). To explain the mechanisms of action we examined whether these proteases inhibited parasite growth by inhibiting invasion of erythrocytes.

4.6 Invasion assays show that Cathepsin G acts on the RBC

Addition of cathepsin G to schizont cultures produced a dramatic reduction in invasion, and pre-treatment of erythrocytes with cathepsin G before adding them to schizont cultures produced a similar reduction in their invasion (Fig 29.B), indicating that cathepsin G acts predominantly on the erythrocyte (Fig 29.B). Addition of MMP9 to schizont cultures produced a more modest reduction, whilst pre-treatment of erythrocytes did not reduce invasion, implying that MMP9 likely acts against the parasite rather than the erythrocyte surface (Fig 29.B).

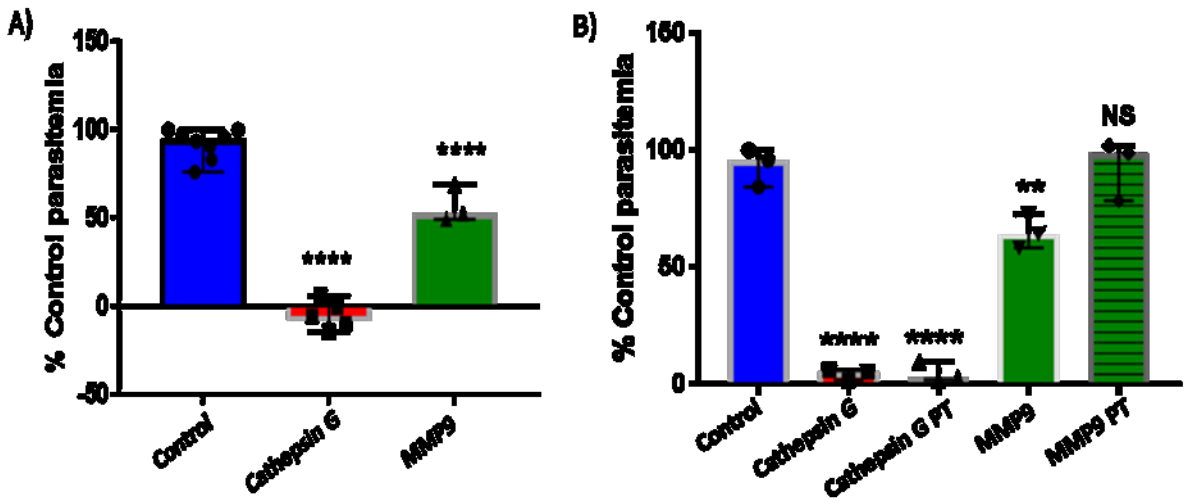

Figure 29: Cathepsin G and MMP9 growth assay (A) and invasion assay (B).

A) Effect of cathepsin G (18 µg/mL) and MMP9 (18 µg/mL) on in vitro growth (assessed after 72 hours) of P. falciparum 3D7 (n=3-5 per condition). B) Effect of cathepsin G and MMP9 on erythrocyte invasion of P. falciparum 3D7 (assessed after 24 hours). Cathepsin G (18 µg/mL) and MMP9 (18µg/mL) were either added directly to a mixture of schizonts and donor red cells, or were pre-incubated with donor red cells before washing and adding to schizonts (PT) (n=3). A & B) Bars show median with 95% CI. Statistical analysis done with Ordinary one way ANOVA, P<0.0001 – (****) 4 asterisks, P=0.0040 - (**). Multiple comparisons with control/untreated culture.

4.7 PMA stimulation of healthy donor whole blood

In order to identify *in vivo* achievable concentrations of cathepsin G and MMP9 we measured their concentrations (CTSG ELISA Kit-Human, Aviva Systems Biology and Legend Max Human MMP9, Biolegend) in whole blood from healthy donors before and after stimulation with 1µM PMA (Sigma) (Fig. 30), although these concentrations may underestimate local concentrations during infection *in vivo* when emergency granulopoiesis may increase the abundance of these granule proteins (356).

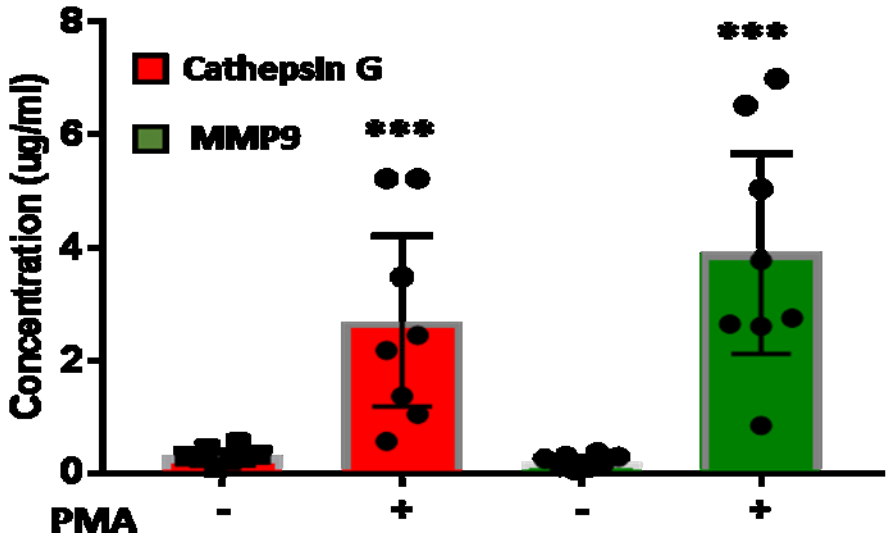

Figure 30: Cathepsin G and MMP9 release following healthy donor whole blood (n=8) stimulation with 1µM PMA.

Bars show mean with 95% CI. Statistical analysis done with paired t test, P=0.0016.

4.8 The effect of cathepsin G is independent of the parasite invasion phenotype

Differences in invasion phenotype, have been studied previously by treating RBCs with enzymes such as neuraminidase (cleaving sialic acid groups from glycoproteins and glycolipids) or trypsin, to examine different culture-adapted *falciparum* isolates ability to invade using different combinations of RBC receptors (357). This variation in phenotype can offer a survival advantage in the parasites able to invade RBCs using any of the available receptors. Most of the *in vitro* parasite culture experiments performed are with a 3D7 strain so we decided to assess the effect of cathepsin G on three additional parasite strains with different invasion phenotypes D10, Dd2, HB3 (358). In order to assess this, we pre-treated erythrocytes with increasing concentrations of cathepsin G and after washing off the

treatment added them in culture with mature schizonts ready to rupture and invade for 24 hours. Parasite invasion was dose-dependently inhibited by cathepsin G pre-treatment of erythrocytes, with similar effects in each of four parasite strains with different invasion phenotypes (359) (Fig. 31).

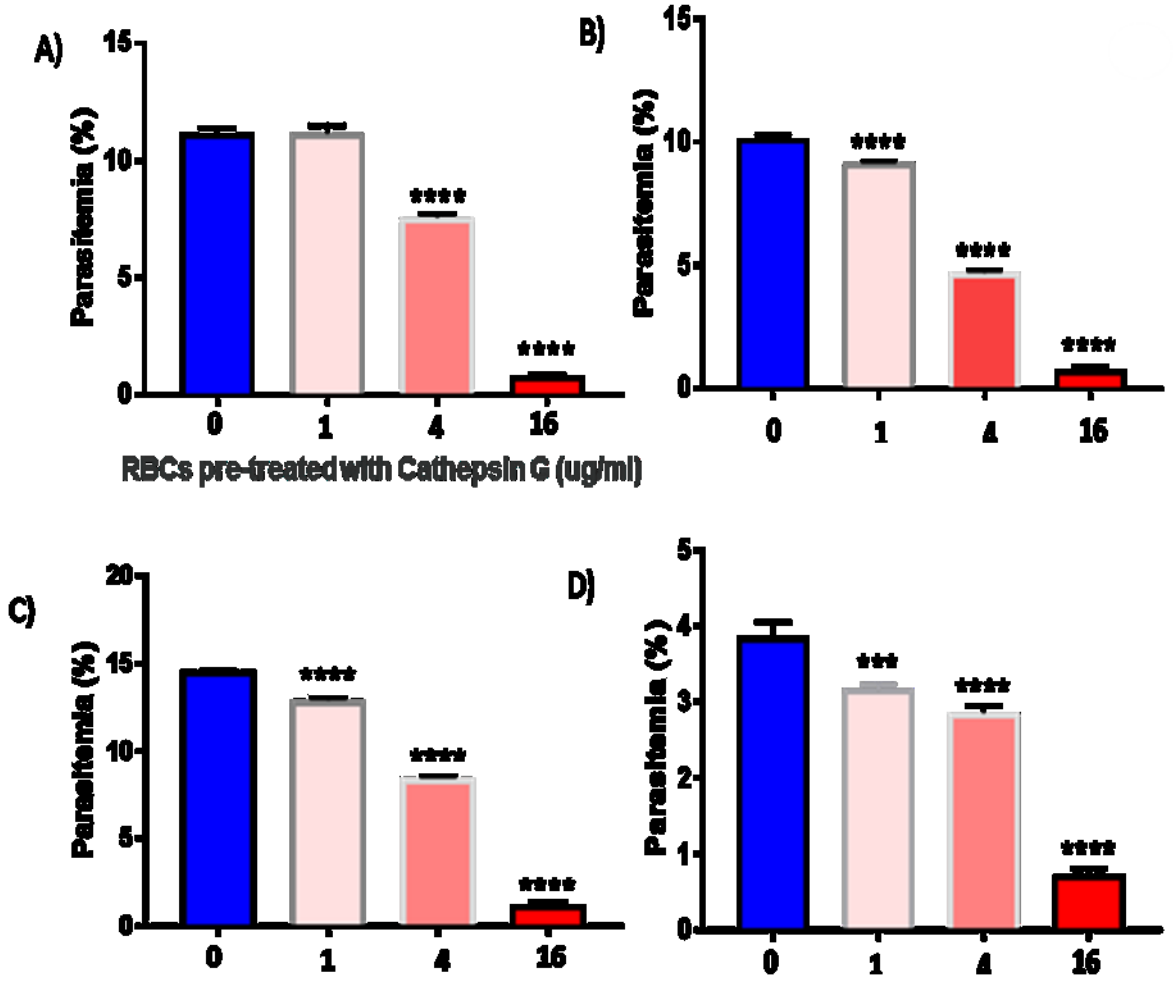

Figure 31: Dose response for invasion inhibition using cathepsin G pre-treated erythrocytes against four parasite strains.

A) 3D7, B) D10, C) Dd2, D) HB3. Bars show mean with range, (n=3, representative of two experiments. Statistical analysis done with Ordinary one way ANOVA, P<0.0001 – (****), P=0.0004 – (***). Multiple comparisons with control/untreated culture.

4.9 Cleavage of RBCs receptors after dose response treatment with cathepsin G

Looking at this quite clear result suggesting that cathepsin G has a broad effect, we investigated whether cathepsin G might cleave a range of RBC surface proteins which are used as invasion receptors by *P. falciparum* (360). Consistent with its broad inhibition of parasite invasion (Fig. 31), cathepsin G dose-dependently cleaved most of the known *P. falciparum* invasion receptors including basigin (CD147), glycophorins A, B, and C (GYPA, B, C), complement receptor 1 (CR1) and semaphorin 7A (CD108), but not DAF receptor (CD55) (Fig 32). MMP9 given as a dose response did not cleave any of these surface receptors (Fig 33). Erythrocyte surface receptor expression was assessed by median fluorescence intensity of erythrocytes labelled with monoclonal antibodies (Biolegend, Novus Biologicals, BD Biosciences). Surface receptor loss was calculated from the difference between the treated and untreated sample median fluorescent intensities after the isotype control antibody fluorescence had been subtracted.

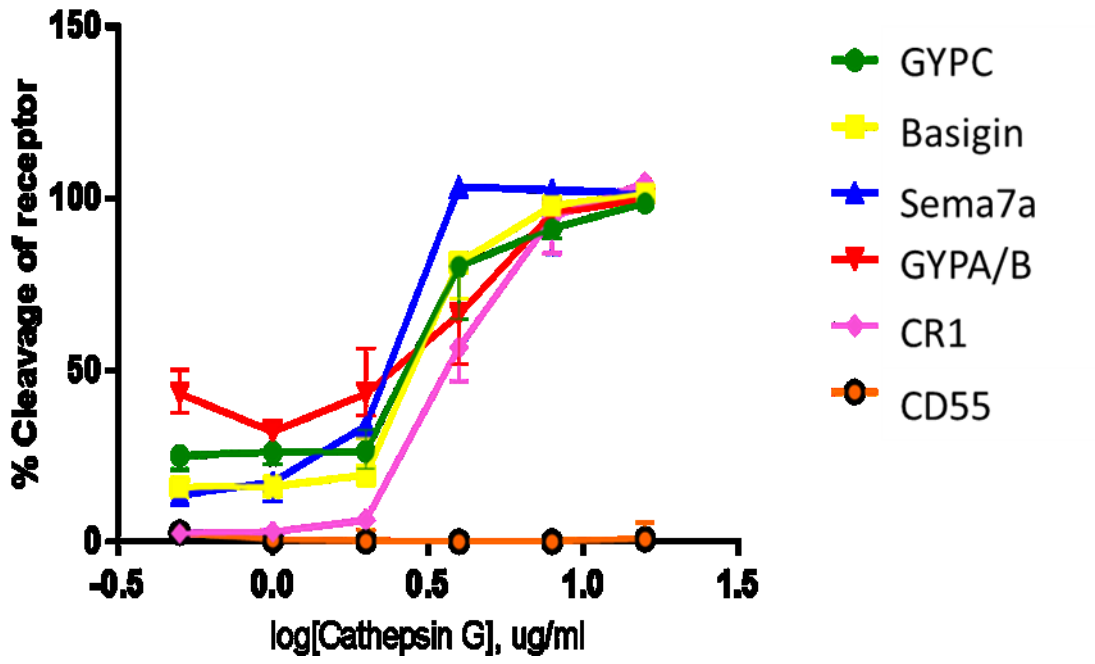

Figure 32: Dose response of cathepsin G for the assessment of erythrocyte surface receptor cleavage.

Points show median and error with 95% CI, n=3, representative of two experiments. Statistical analysis done with Ordinary one way ANOVA showed significant difference in the expression of basigin (CD147), glycophorins A, B, and C (GYPA, B, C), semaphorin 7A (CD108), and complement receptor 1 (CR1,) but no difference in the expression of DAF receptor (CD55).

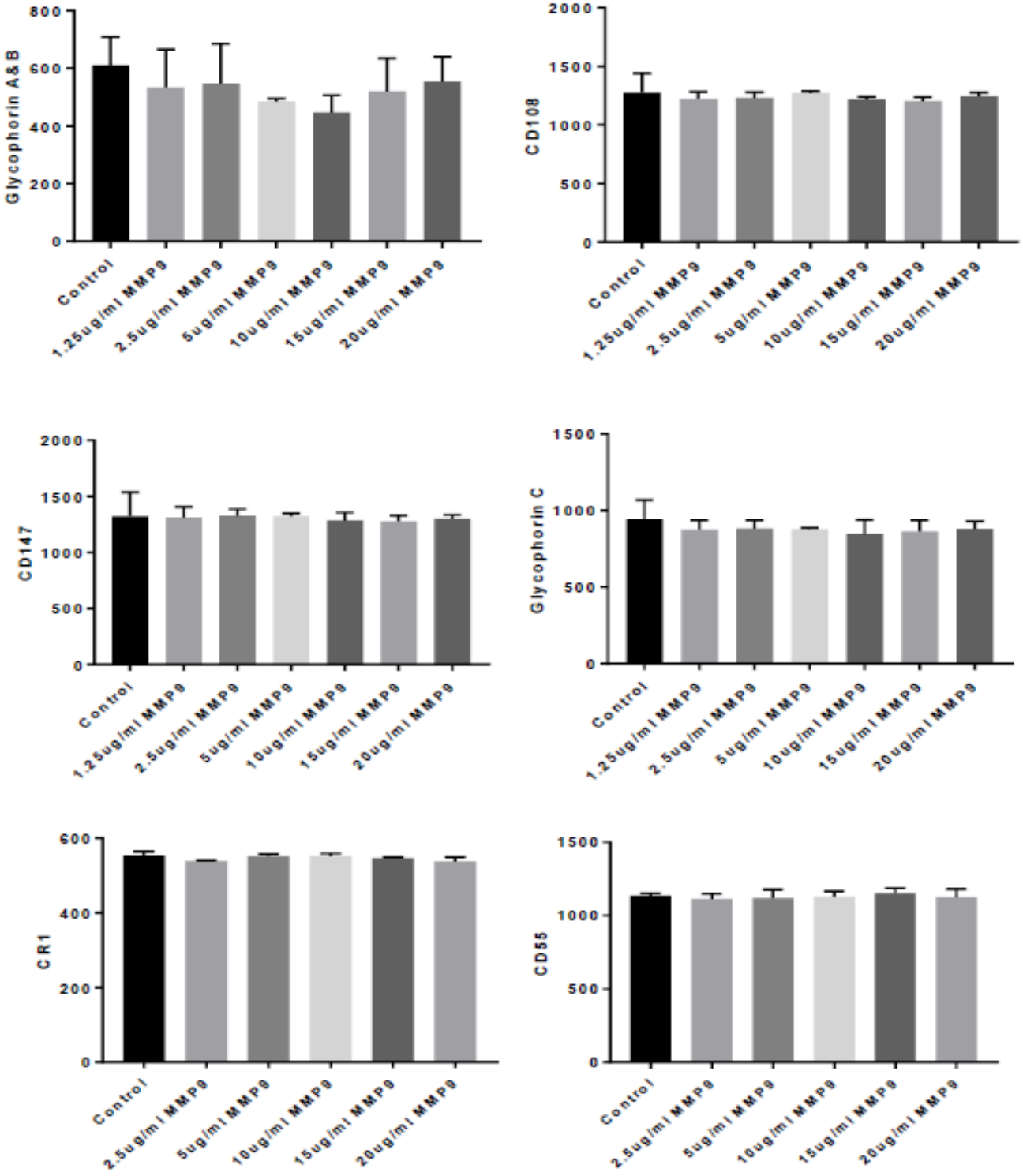

Figure 33: Dose response of MMP9 for the assessment erythrocyte surface receptor cleavage.

Bars show mean with range, n=3, representative of two experiments. Statistical analysis done with Ordinary one way ANOVA showed no significant difference in the expression of basigin (CD147), glycophorins A, B, and C, complement receptor 1 (CR1,) semaphorin 7A (CD108), or DAF receptor (CD55) even with the highest dose of 20ug/ml MMP9.

4.10 RBC receptors get cleaved after PMA stimulation of healthy donor whole blood

PMA (1uM) stimulation of healthy donor whole blood recapitulated the loss of erythrocyte surface glycophorins A and B (GYPA/B), Basigin (CD147) and Semaphorin7a (CD108) in all donors' erythrocytes (Fig. 34), it also decreased Glycophorin C (GYPC) expression in 6 of 8 donors, but did not consistently reduce CR1. CD55 similarly with the erythrocytes treated with cathepsin G results did not show any difference in expression before and after PMA stimulation. The importance of basigin and glycophorins in RBC invasion and genetic susceptibility to severe malaria is well known (44, 59, 361-363), and so it is quite likely that the cleavage of these receptors by cathepsin G could have a protective effect *in vivo*.

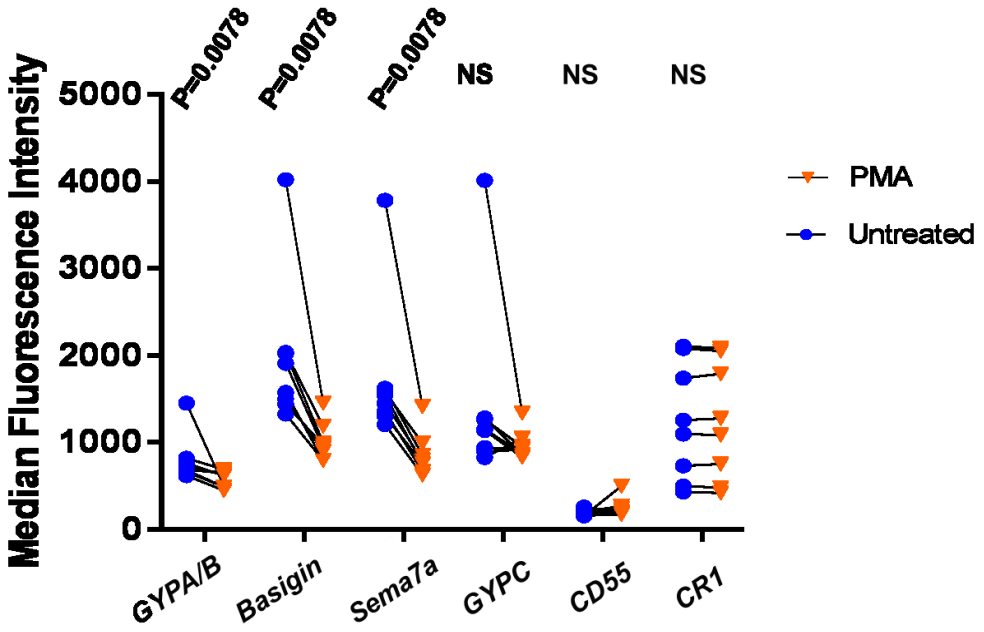

Figure 34: Effect of PMA stimulation of healthy donor whole blood erythrocyte surface receptor expression assessed by fluorescence intensity.

Statistical analysis done with two-tailed, Wilcoxon matched pairs t test. Glycophorin A&B (GYPA/B), Basigin (CD147), and Semaphorin 7a (CD108) showed significantly reduced expression after PMA treatment, while and Glycophorin C (GYPC), DAF receptor (CD55), and complement receptor 1 (CR1) did not have a significant difference in expression (n=8).

4.11 Validation using Gambian samples

ELISAs were performed using plasma from Gambian children of the same cohort that was used in the RNA sequencing analysis. This showed that levels of both cathepsin G and MMP9 rise during malaria infection while cathepsin G came up as significantly higher in the uncomplicated malaria group compared to severe and MMP9 seemed to follow a similar trend without reaching significance (Fig 35).

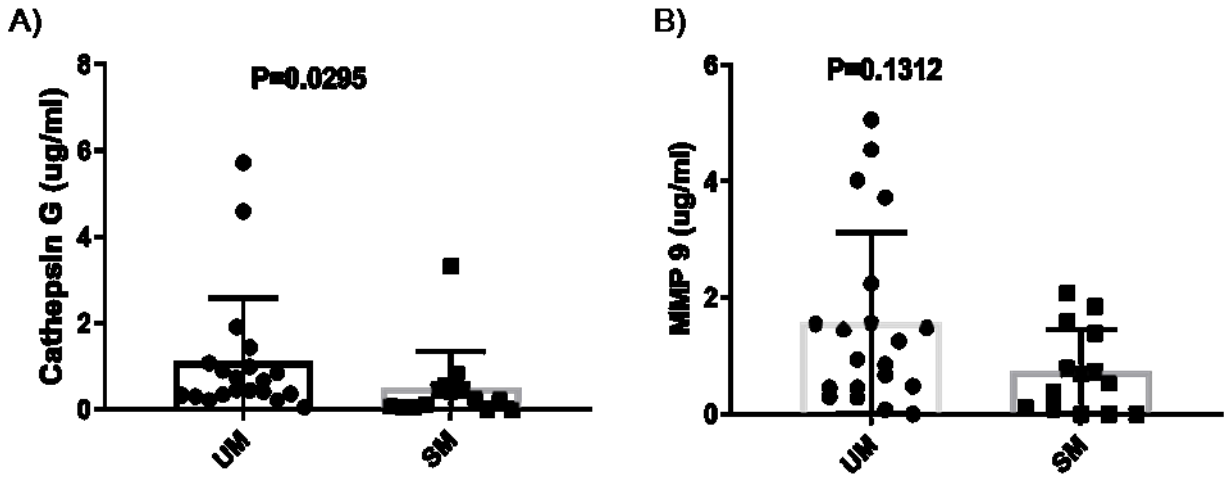

Figure 35: Plasma concentrations of A) Cathepsin G and B) MMP9 using Gambian samples from uncomplicated and severe malaria cases.

A & B) Bars show mean with SD, Statistical analysis done with Mann-Whitney test. (N=34, 20 Uncomplicated Malaria, and 14 Severe Malaria). Cathepsin G was significantly higher in UM cases compared to SM. MMP9 did not reach significance.

For a small number of subjects paired red cell pellet samples from the day of presentation and 28 days later had been stored at -80C. We stained these samples after careful thawing and analysed them using flow cytometry for the expression of glycophorins, Semaphorin7a, and Basigin. Regardless of the limitations from using thawed RBC samples, which very easily lyse , for the percentage of expression of glycophorins A and B (GYPA/B), Basigin (CD147) and Semaphorin7a (CD108) and Glycophorin C (GYPC) we identified a significant increase in the expression of GYPA/B and Basigin (Figure 36) at day 28 compared to the acute phase matching sample. This would be consistent with our hypothesis of a host protective mechanism against the increasing parasite load, which leads to partial cleavage of erythrocyte receptors that reduce parasite invasion rates. This result could have been a lot more significant if we had available fresh samples and if we had convalescent samples after three to four months of recovery from the infection since at 28 days RBCs from day 0 could still be circulating as their life span is approximately 120 days (364).

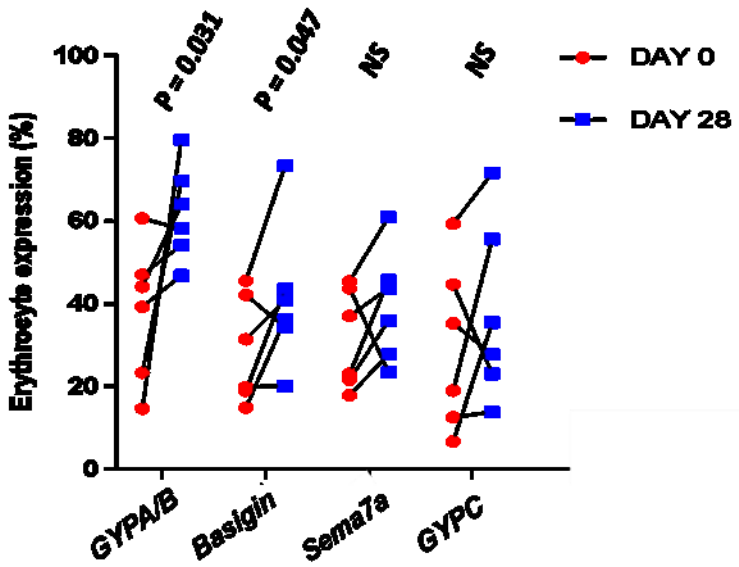

Figure 36: Percentage of erythrocyte receptor expression using erythrocytes from Gambian children

Samples used from (DAY 0) day of presentation (acute), and their matching convalescent sample (DAY 28), to assess the expression of erythrocyte surface receptors by fluorescence intensity. Statistical analysis done with one-sided Wilcoxon matched pairs t test, N=6.

4.12 Summary

This work demonstrates by proof of principle that mechanistic correlates of protection can be identified by combining individualized estimates of parasite growth inhibition derived from a mathematical model with omics approaches to discovery of their biological correlates.

I showed here that Cathepsin G and MMP9 which came up as positively correlated with PGI have indeed a negative effect on parasite growth. Cathepsin G, acts on the surface of the RBC cleaving receptors crucial for parasite invasion and possibly important for parasite sequestration and rosetting, all of which are features of severe malaria. MMP9, acts directly on the parasite inhibiting the growth although we have not yet dissected the exact mechanism of its action.

We used a model-based approach to estimate the host dynamics of pathogen load and its determinants, in human malaria infection, we estimated the relative contributions of host response to parasite load and parasite multiplication measured at one single time-point, and then applied these predictions to identify mechanistic determinants of malaria parasite load.

The main limitation of this model was the inability to propagate uncertainty throughout the sequential stages of the model fitting, prediction of parameter estimates for the individual subjects, and association of these parameter estimates with real variables (269). Another, important limitation was the small size of the RNA seq dataset reducing the chance for finding something significant. In reality we would expect that multiple mechanisms can act in parallel, and though each of them may have a small effect, the overall cumulative effect is stronger.

Nevertheless, our biological validation shows that the relative estimates of PGI and m are accurate enough to be used, providing proof-of -principle validation of the ability to estimate pathogen load dynamics in humans (269). The dynamic nature of host-pathogen interactions and pathogen load are rarely addressed in human infectious diseases studies, although their importance is obvious (182). This happens due to the difficulty of accurately measuring the total body pathogen load while the obvious need to treat individuals with serious infections, does not allow longitudinal observations of host response and changes in pathogen load. Consequently, much of our understanding on human infection interactions comes from comparison of individuals with a single time point observation, even though these individuals may be at quite different stages in the dynamic process of infection (269).This results in quite

a few paradoxical observations as the consistent observation of low levels of platelets or high levels of TNF associated with high parasite load and severe malaria (10, 365), while there is also strong evidence to indicate that platelets and TNF mediate defence against malaria parasites (365-368). These paradoxes can be explained only after considering the dynamic nature of host-parasite interactions, which can initiate a more efficient identification of protective mechanisms.

Our approach could potentially yield additional novel insights into the interactions of the host and the parasite in malaria, which could facilitate discovery of vaccine and new therapeutic targets, improving predictive modelling of their impact on disease (269). Host-directed therapeutics to boost antimalarial treatment could be particularly important for fighting drug resistant parasites. One approach calling for further exploration should be the inhibition of type-1 interferon or C-X-C motif chemokine 10 (CXCL10) signalling with either inhibitory antibodies or small molecules already under development for other indications (369, 370).

Cathepsin G and MMP9 therapeutic potentials of may be counterbalanced by risk of collateral tissue damage, however selective targeting of the important for invasion receptors on the surface of the erythrocyte could prove useful for both treatment and prevention of malaria. Overall, this approach could be applied to other infectious diseases, in which the pathogen load can be accurately measured and no effective treatments currently exist.

4.13 Conclusion

This proof of principle study showed that the combination of mathematical modelling and transcriptomics can reveal correlates of protection in malaria. I validated that cathepsin G and MMP9 which came up as positively correlated with parasite growth inhibition, both inhibit parasite growth. Cathepsin G cleaves surface receptors from the erythrocyte membrane, required for parasite invasion, while MMP9 acts directly on the parasite.

Chapter 5: Transcriptomic comparison of mouse malaria models with the human host

In this chapter the bioinformatics analysis for RNA-sequencing was performed by Pablo Soro Barrio from Imperial College London (Fig 44-46) and Dr Hyun Jae Lee helped with the initial design of the pipeline. RNA sequencing and library preparation was performed by Exeter University Sequencing Centre.

Here I attempt to address differences and similarities among five different commonly used mouse models of malaria as well as assess whether any of these models recapitulates human malaria features at a transcriptomic level. Using five different mouse parasite strains: *P. berghei* ANKA (lethal), *P. berghei* NK65 (lethal), *P. yoelii* 17XL (lethal), *P. yoelii* 17XNL (non-lethal), and *P. chabaudi* AS (non-lethal), I infected C57BL/6 female wild type mice which were monitored closely throughout infection.

I compared early time points (when mice first developed signs of illness) versus late time points (severe malaria) within each infection using RNA sequencing and then tried to find similarities (if any) with our human RNA sequencing dataset to determine which mouse model recapitulates the human malaria transcriptomic features: (mouse severe vs uncomplicated DEGs) vs. (human SM vs UM DEGs).

5.1 Introduction

There are marked differences between mouse and human host in immunity and inflammation in infection (371). However, we still count on insights gained from mouse model experiments to learn more about human immunity and pathogenesis of many human diseases. The suitability of a model is often determined by how well it replicates the "clinical features" or sometimes the histopathological features of human disease, while it is only more recently that people have become interested in transcriptional similarities (12). For immunological studies, the mouse has been the animal of choice for a century (83). It has significantly broadened our understanding of the function and structure of mammalian immune systems and disease mechanisms. Despite evolutionary distance between human and mouse (371) and the high evolutionary pressure on immune systems (372), the principles of the immune systems for these species remain remarkably similar. The main differences include the proportions of lymphoid and myeloid cells in blood, greater repertoire of T and B lymphocytes in human, and heterogeneity in the molecules of adaptive and innate immune signaling (83, 371). The value of the mouse system being used for human disease modeling has been questioned using high throughput genetic technologies. However, comparing between heterologous datasets based on different technology platforms is quite challenging, as these data cannot be combined and evaluated using a simple statistical framework (83). People have started looking at the transcriptional profiles, of seven different (non-stimulated) cell lineages originating from human and mouse during immune development showing similarities in the global gene expression profiles of the two species (373). In contrast, to this Lin et al. pointed out the differences between mouse and human transcriptomes looking at 15 types of tissue (data combined from different projects and publicly available datasets), describing a subset of conserved genes that was driving the species specific expression (374). The first attempts towards understanding the similarity of immune responses to specific stimuli, between human and the corresponding mouse models, by different groups employed whole blood leukocytes (375, 376). The outcome though varied according to the different statistical and biological assumptions these groups used, resulting in contradictory verdicts about the concordance of transcriptional responses among these species (83). Recently, a set of over 5,000 immune system-specific genes was compiled, based on publicly available data from human and mice, facilitating access to concordantly regulated gene modules in immunologically relevant comparisons of various diseases (377). A recent study, trying to

introduce a method that would allow the identification of both concordant and discordant genes between mouse and human, combined gene set enrichment analysis with a novel measure of similarity (83). To validate their approach they looked at concordance and discordance between whole blood from human and mouse models of tuberculosis infection (83). Their analysis revealed prominent differences in gene expression between the highly and low susceptible mouse strains upon infection with TB, they also showed concordant and discordant immune responses in TB infection between human and two mouse strains that have an impact on disease modeling (83). The most recent study adding to the field developed a statistical methodology (FIT; http://www.mouse2man.org) that counts on publicly available gene expression data from both mouse and human to deduce a more informative mapping from a new mouse experiment to the equivalent human condition without the need for prior human data for this condition (378).

There are many different rodent malaria models available, being used for malaria research. Isolated from *Thamnomys* thicket rats in the African Congo, rodent malaria parasites, have provided a unique resource for studying immune response and inflammatory roles in malaria pathology (379). The characteristics of both disease and infection differ between the four species of *Plasmodium* that infect mice (*P. yoelii, P. chabaudi, P. berghei* and *P. vinckei*), and for each species in various strains of mice, with the most common ones being C57BL/6, Balb/c, DBA/2 (379). Using these different strains in combination with the different mouse strains, allows us to examine a range of malaria models as they develop different syndromes (Table 9).

Table 9: Commonly used malaria mouse models.

ALI/ARDS: acute lung injury/ acute respiratory distress syndrome, SMA: severe malarial anaemia, ECM: experimental cerebral malaria.

	Mouse strains		
Parasite strains	**C57BL/6**	**Balb/c**	**DBA/2**
P. yoelii	Lethal (Py17XL) Non-lethal (Py17XNL) (380) ALI/ARDS: Limited lung pathology compared to *P. berghei* infections (381).	Lethal (382) SMA: Anaemia and splenomegaly (383). Hyperparasitaemia. ALI/ARDS: PyXL-infected mice develop interstitial pneumonia and oedema.	Lethal ALI/ARDS: Limited lung pathology compared to *P. berghei* infections.
P. berghei (includes ANKA and NK65 which differ in pathology.)	Lethal ECM: PbANKA is most commonly used model for ECM (384). ALI/ARDS: Infection with PbNK65 results in severe MA-ARDS with a 90% incidence. Most similar to human ALI/ARDS (385). Liver pathology (386)	Lethal ECM resistant (387) SMA: Anaemia with hyperparasitaemia. ALI/ARDS: Pulmonary oedema remains confined.	Lethal ALI/ARDS: PbANKA infection used as a model of ALI/ARDS with 50% incidence (388). Recapitulates human syndrome – pulmonary oedema, and hypoxemia (389).
P. chabaudi	Non-Lethal ALI/ARDS: Limited lung pathology compared *to P. berghei* infections (381). SMA: Resistant to infection. Develop moderate levels of peak parasitaemia, followed by clearance (390).	Non-Lethal SMA: Severe anaemia unrelated to parasitaemia (391). ALI/ARDS: Limited lung pathology after 20 days post infection.	Non-Lethal SMA: Resistant to infection. Develops moderate levels of parasitaemia, before clearance.

One of the most challenging questions for the community of malaria research, resulting in some degree of polarization of viewpoints, has been the validity of *P. berghei ANKA* mouse model being used as equivalent of human cerebral malaria (79). Several groups have provided data supportive of accumulated infected erythrocytes found in various organs, including the brain, while suggesting that high parasite accumulation was associated with ECM susceptibility. The key finding missing, that was essential though was the histological direct evidence of extensive parasitised erythrocyte sequestration packing the brain vessels as seen in human cerebral malaria (79). One of the main differences between human CM and ECM, is the marked accumulation of leukocytes which pack the brain vessels seen in the mice unlike the prominent sequestration of mature schizonts seen in humans (392). ECM is associated with the accumulation of immune cells in the brain, particularly T cells and macrophages/monocytes. Recruitment of CD8+ T cells to the brain late in disease pathogenesis, and production of cytolytic molecules such as perforin and granzyme B, are critical for the development of ECM (393). Even though, these data suggest that ECM model might not be the appropriate one to use for trialing interventions meant to reverse sequestration, it could still be useful for understanding the relationship between inflammation and reversal of vessel blockage in cerebral malaria.

Making the correct choice of animal host combined with the appropriate malaria parasite, to try and mimic as closely as possible the human disease patterns has been essential. The mouse models available can mimic some of the human malaria symptoms however there has not been any study examining closely the similarities and differences between these models and the human host at a transcriptomic level. So how do we know the causal mechanisms in humans without a good model system? I have conducted experiments to compare human and mouse transcriptional responses to malaria infection in whole blood. This is an approach that will facilitate the choice of optimal mouse model for experimental malaria studies.

5.2 Experiment design

C57BL/6 female wild type mice were infected with 10^5 parasites: *P. berghei ANKA* (lethal), *P. berghei NK65* (lethal), *P. yoelii 17XL* (lethal), *P. yoelii 17XNL* (non-lethal), and *P. chabaudi AS* (non-lethal) by ip injection (Fig 37). In total 50 mice were infected, 10 for each different parasite strain, while 10 control uninfected mice where used for weight gain comparisons. Out of the 10 mice in each infection, 5 were culled at an early timepoint when the first symptoms started occurring mimicking uncomplicated malaria and the other 5 mice were culled at the peak of severity symptoms (according to our humane endpoints) mimicking severe malaria. For the RNA seq analysis 6 samples were analyzed from each infection (3 uncomplicated/early timepoint and 3 severe/late timepoint), along with 3 uninfected control. This sample choice was based on the RNA quality and quantity as well as the synchronicity of symptoms developed and parasitaemia levels in each infection. For the comparison with the human host, RNA seq data from our Gambian children cohort (described in chapter 3) were used.

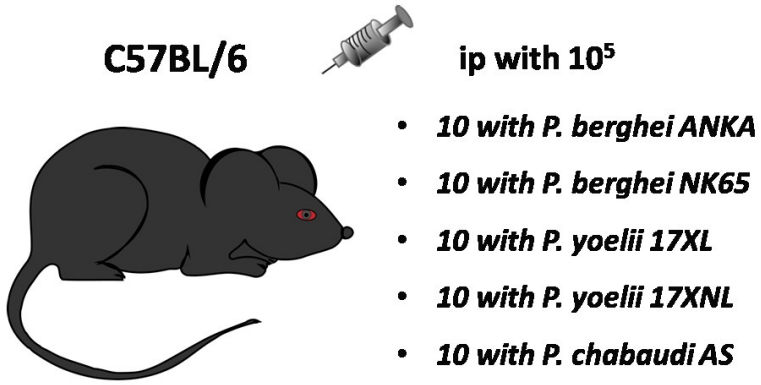

Figure 37: Experimental design for the infections.

C57BL/6 female wild type mice were infected with 10^5 parasites: P. berghei ANKA (lethal), P. berghei NK65 (lethal), P. yoelii 17XL (lethal), P. yoelii 17XNL (non-lethal), and P. chabaudi AS (non-lethal) by intraperitoneal injection. 10 mice were infected with each different parasite strain, from which 5 were culled early in infection, when the first symptoms occurred, and 5 when the maximum severity was reached within the humane endpoints.

5.3 Differences in pathology and severity

P. berghei ANKA (lethal), *P. berghei* NK65 (lethal), *P. yoelii* 17XL (lethal), *P. yoelii* 17XNL (non-lethal), and *P. chabaudi* AS (non-lethal) lead to different severity phenotypes when infecting C57BL/6 wild type mice (Table 9). *P. berghei* ANKA causes experimental cerebral malaria mimicking some of the neurological clinical symptoms seen in human cerebral malaria. This infection is lethal when left untreated at about 5-7 days post infection while neurological

symptoms start appearing around day 4. $CD8^+$ T cells accumulation in the brain of C57BL/6 mice has been considered as the main cause of the ECM neurological symptoms they develop, as depletion of these cells before the onset of symptoms rescues 100% of the mice (394, 395). *P. berghei* NK65 infection of C57BL/6 mice does not lead to ECM and the mice do not develop any neurological symptoms or BBB breakdown (396). However, $CD8^+$ T cells accumulate in the brains of these mice in a similar way as they do in the *P. berghei* ANKA infection, the only difference being the higher amount of parasites accumulating in the brains of *P. berghei* ANKA infected, showing that ECM develops only when both parasites and $CD8^+$ T cells accumulate in the brain (387). *P. berghei* NK65 causes a biphasic lethal infection after about 20 days post infection. This infection causes malaria-associated acute respiratory distress syndrome with pulmonary pathology affecting more than 90% of the infected mice (381).

P. yoelii 17XL is a very severe and lethal infection (397) causing death at 5-7 days post infection reaching extremely high parasitaemia levels. *P. yoelii* 17XNL is a non-lethal self-resolving infection (398) genetically very similar to *Py17XL* with a single mutation which explains virulence (399). It develops moderate symptoms but is characterized by slowly progressive anaemia and reticulocytosis. Transforming growth factor-β is a critical mediator of inflammation induced by malaria in mice (400). *Plasmodium yoelii* infection virulence (in C57BL/6 mice) has been shown to be dependent on TGF-β timing of production and cellular source. The virulence and lethality of *Py17XL* strain has been associated with high levels of circulating TGF-β within 24 h of infection which delayed and diminished IFN-γ and TNF-α response, leading to failed parasite clearance and mortality reaching 100% (400). On the other hand, *Py17XNL* strain which is non-lethal, induces production of TGF-β from 5 days after infection, correlating with parasitaemia resolution, down-regulation of TNF-α, and recovery (400). Eventually mice infected with *P. yoelii 17XNL* manage to overcome this infection clearing parasites quickly after about 2 weeks presumably as an effective humoral (antibody) response is mounted (401). *P. chabaudi* AS (non-lethal) is another very commonly used strain causing relatively mild disease which C57BL/6 mice overcome. During the *P. chabaudi* AS infection mice develop splenomegaly and an exponentially rising parasitaemia up to 30%, which then drops rapidly (402).

5.3.1 Parasitaemia

Parasitaemia was measured every other day using standard Giemsa microscopy as explained in the methods (chapter 2). *P. yoelii 17XL* was the infection with the highest levels of parasitaemia up to 80% just after 5 days post infection. *P. yoelii* 17XNL and *P. chabaudi AS* infections collected at their peak severity, reached up to 10% and up to 29% of parasitaemia respectively (Fig 38), however both would resolve if I kept the mice for longer. *P. berghei ANKA* infection reached up to 13% parasitaemia, while *P. berghei NK65* parasitaemia rise to 33% at the peak of severity.

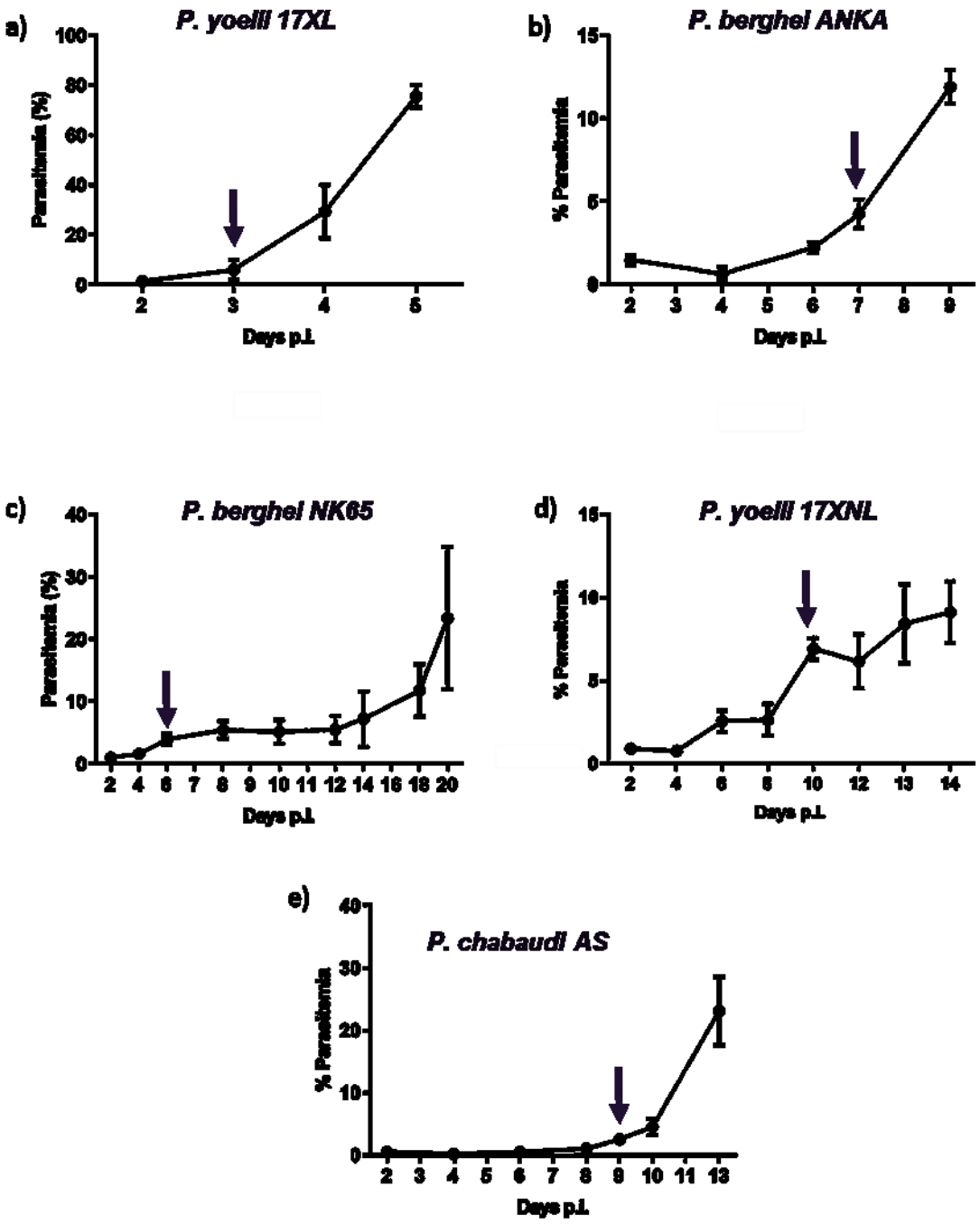

Figure 38: Parasitaemia percentage measured by microscopy.

C57BL/6 female wild type mice with: a) P. yoelii 17XL infection, b) P. berghei ANKA infection, c) P. berghei NK65 infection, d) P. yoelii 17XNL infection, e) P. chabaudi AS infection. Bars show mean with SD. N=6 for each infection with 3 mice harvested early (first symptoms/"uncomplicated malaria") and 3 mice harvested late (peak of severity for each infection). Arrows indicate the day on which the early mice were harvested.

5.3.2 Scoring and severity of infection

According to the severity and predicted outcome of each infection specific protocols were followed monitoring the mice every day or every other day. Severity scores below include weight loss as well apart from the scoring for general appearance and welfare (score sheets in the appendix). Score sheets used take account of both evidence and instructions from our named veterinary surgeon and AWERB.

For parasite passage Protocol 5 (moderate severity) was used as mentioned in the methods chapter. All mice culled at an early timepoint, when the mice just started developing symptoms such as weight loss (uncomplicated malaria), were monitored according to protocol 1 (moderate severity limit), according to this the maximum score before having to euthanise the mice was 2. Those culled at a later timepoint when the mice reached maximum severity were monitored under protocol 2 (severe severity) for the lethal infections *P. yoelii 17XL* and *P. berghei ANKA* (modified version including RMCBS).

Protocol (1) (moderate severity) was used for the non-lethal infections (late timepoints/severe malaria) *P. yoelii 17XNL*, and *P. chabaudi AS*, as well as for the lethal *P. berghei NK65* after modifying the weight loss score as this infection needs more than 14 days to develop maximum severity (the severe severity protocol 2 can be used for maximum of 14 days according to our license). For the severity score presented below (Fig 39) *P. berghei* ANKA infected mice (late timepoint/severe stage) were scored again using protocol 2 (without RMCBS). Severity scores across different infections and protocols are therefore not equivalent.

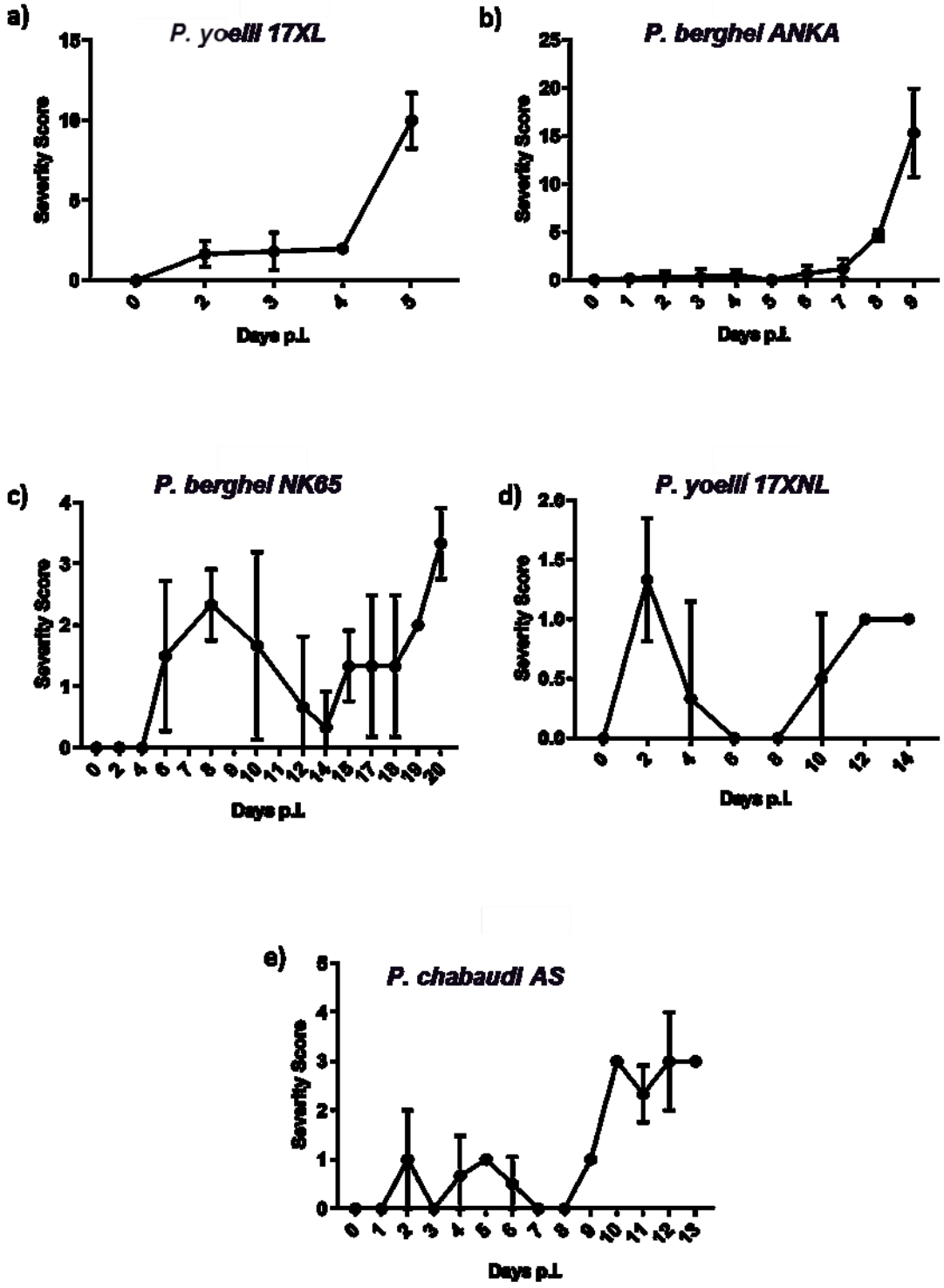

Figure 39: Severity scores.

C57BL/6 female wild type mice with: a) P. yoelii 17XL infection, b) P. berghei ANKA infection, c) P. berghei NK65 infection, d) P. yoelii 17XNL infection, e) P. chabaudi AS infection. Bars show mean with SD. N=6 for each infection with 3 mice harvested early (first symptoms/"uncomplicated malaria") and 3 mice harvested late (peak of severity for each infection).

5.3.3 Weight loss

Weight was measured as part of all monitoring protocols once every day (or every other day depending on the severity) at the same time as instructed by Imperial College Animal Welfare and Ethical Review Board. For experiments lasting for more than 5 days, weights were adjusted for the expected weight gain that would occur in uninfected/control mice. As shown in Figure 40, I calculated the % of weight compared to the baseline weight measured prior to infection. *P. berghei NK65* infection caused a significant loss of weight from day 5 to day 9 post infection as seen before (403). In order to take into account this expected loss of weight and still be able to use protocol 1, I had to adjust the scoring for water and food intake. Weight loss might not always reflect the disease progression but this mainly depends on the different models/infections. This is why it is assessed as part of a larger protocol which examines the animal welfare in many different ways to make sure that humane endpoints are not crossed.

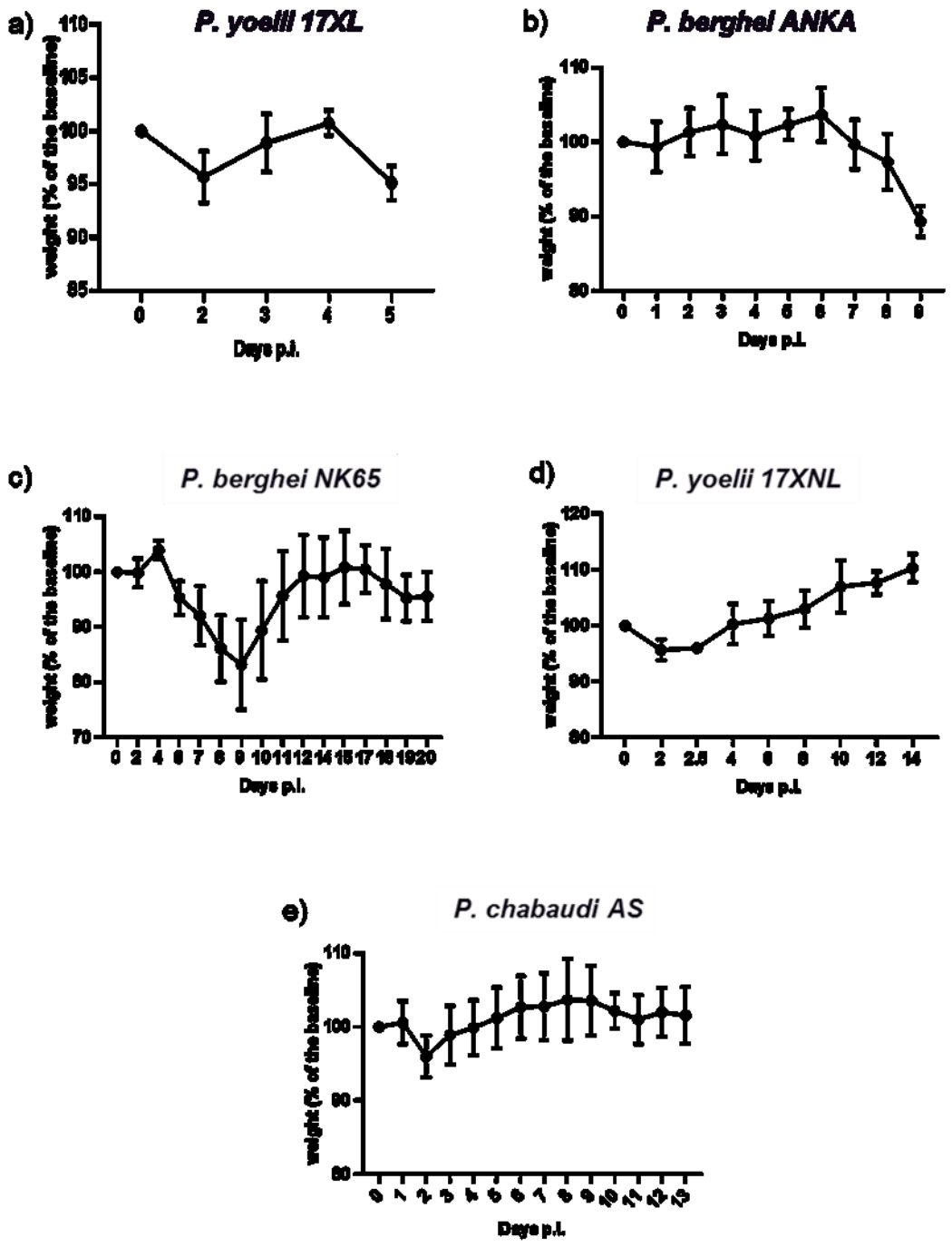

Figure 40: Percentage of weight compared to baseline weight.

C57BL/6 female wild type mice with: a) P. yoelii 17XL infection, b) P. berghei ANKA infection, c) P. berghei NK65 infection, d) P. yoelii 17XNL infection, e) P. chabaudi AS infection. Bars show mean with SD. N=6 for each infection with 3 mice harvested early (first symptoms/"uncomplicated malaria") and 3 mice harvested late (peak of severity for each infection).

5.3.4 Discovery of a new mouse model for hyperlactataemia

Hyperlactataemia is one of the most severe manifestations of severe malaria in human disease while lactate is an independent predictor of death. This suggests the importance of understanding the pathogenesis behind this. During the course of this experiment I decided to measure lactate at two different timepoints within each infection using just 1 µl of tail blood as described in the methods chapter. I report here the discovery of a new malarial hyperlactataemia mouse model which can now be used to further understand pathogenesis leading to this syndrome and also for testing potential treatment. As seen in Figure 41 both *P. yoelii 17XL* and *P. berghei NK65* infected mice developed hyperlactataemia at the peak of severity. The most striking increase in lactate levels is noted during *P. yoelii 17XL* infection which showed the most severe phenotype and the highest parasitaemia levels.

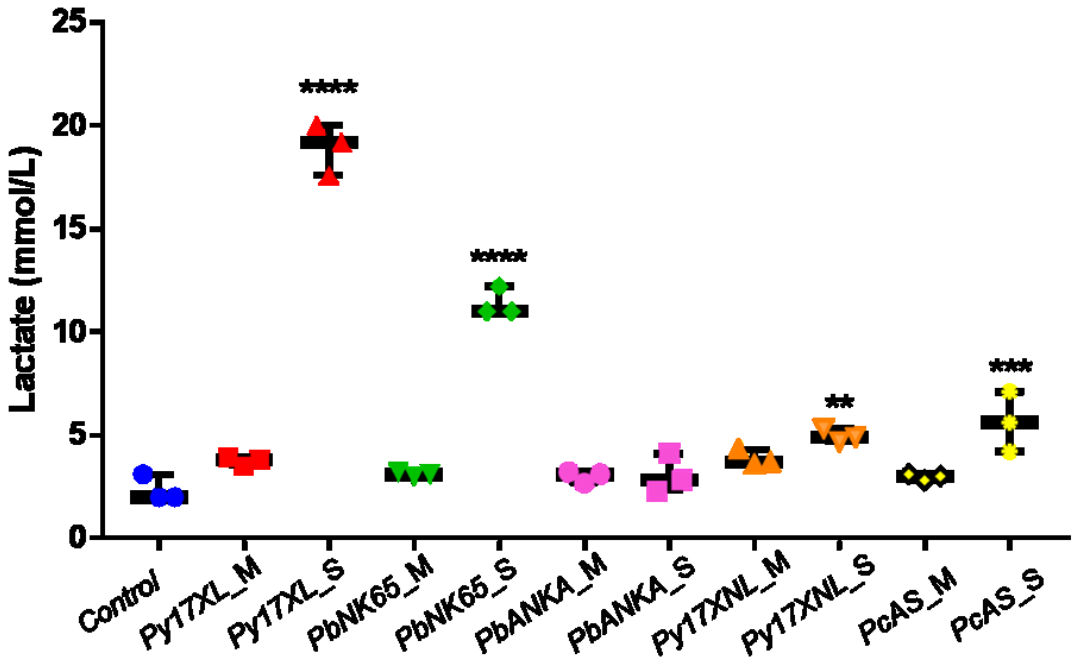

Figure 41: Lactate (mmol/L) measured at the end point for each infection.

C57BL/6 female wild type mice were used. Control (blue) are the uninfected mice used as controls. Py17XL (red), PbNK65 (green), PbANKA (magenta), Py17XNL (orange), PcAS (yellow): lactate measured at the two different timepoints of infection which we then compare at transcriptional level, (M) is the moderate severity or early timepoint, when the very first symptoms start appearing for each group of the infections studied here. (S) is the severe group for each of the infections studied here when the severity and scoring of symptoms according to the protocols followed reached the humane end point. N=3 for each infection timepoint.

5.4 RNA sequencing and data analysis

5.4.1 Deconvolution using flow cytometry data

In order to account for the individual variations in WBC counts found in each mouse we used flow cytometry data. I stained the WBC as explained in methods chapter 2 for cytotoxic T cells, T helper cells, neutrophils, monocytes, and B cells. As seen in Figure 42 there are differences in the proportions of WBCs between the different infections and within each infection (early vs late timepoint). These proportions of WBCs were incorporated in the analysis of DEGs to adjust for any variation.

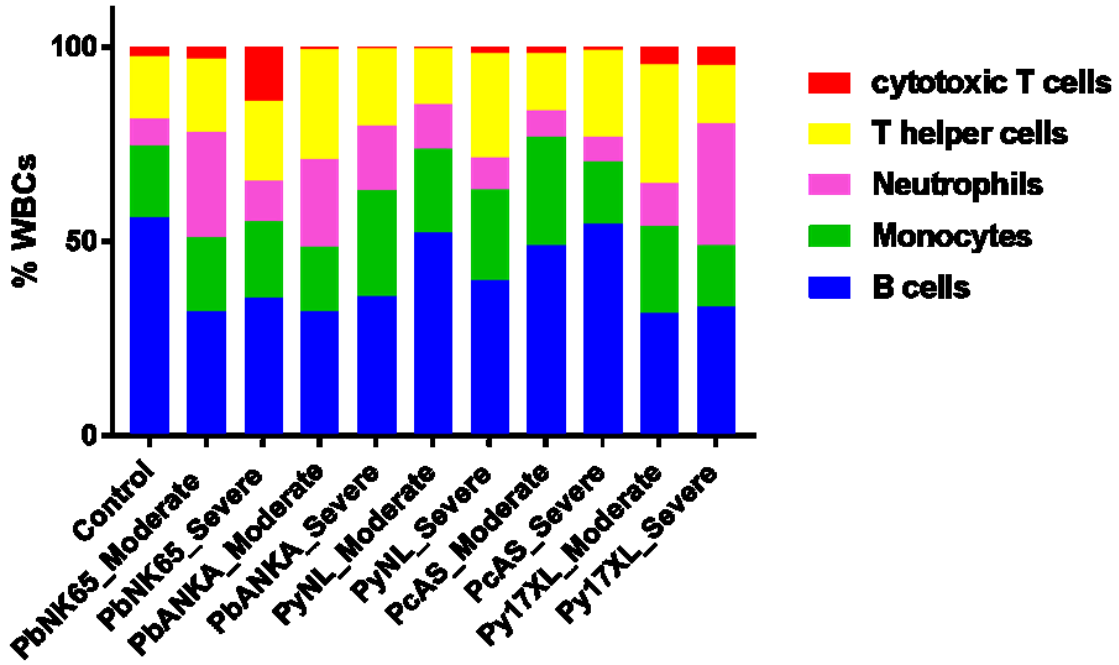

Figure 42: WBC proportions measured in whole blood by flow cytometry in C57BL/6 mice.

5.5 DGEA

5.5.1 Genes associated with high lactate

Comparing the genes positively associated with high lactate in mice (37 identified) and those found in the human host (519 genes identified), 8 came across as orthologs, all of which were neutrophil associated (OLFM4, MMP8, MMP9, S100A8, S100A9, LCN2, LRG1, CD177). I decided then to use IPA comparing the two lists of genes to examine if they have any common upstream regulators which could indicate that a common mechanism might lead to hyperlactataemia seen in both human and mice. The most prominent host genes associated with hyperlactataemia in human and mouse are neutrophil and inflammation-related rather than metabolic, despite the fact that analysis was adjusted for cell-mixture in blood. The top upstream regulators of the genes associated with lactate, were TNF, IL-1B, and IL-6 suggesting that excessive inflammatory response could be accountable for hyperlactataemia in both hosts (Fig 43).

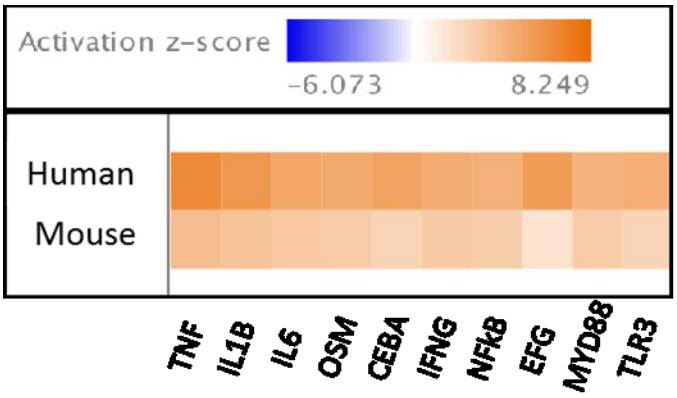

Figure 43: ***Predicted upstream regulators of genes positively associated with lactate concentration in human and mouse blood (edited from Ingenuity Pathway Analysis).***

5.6 Comparison of the mouse with the human host

Using unsupervised clustering based on the top 50 most significantly differentially expressed human genes with mouse orthologs I compared the similarities of differential expression in human hyperlactataemia and human cerebral malaria versus all the mouse models (mouse severe vs uncomplicated DEGs). (Figure 43-44). I first examined the comparison of all mouse models (mouse severe vs uncomplicated DEGs) and the human hyperlactataemia phenotype (CH+HLvsUM). *Py17XL*, the model with the most severe hyperlactataemia, was clustered most closely to the human hyperlactataemia phenotype (Fig 44).

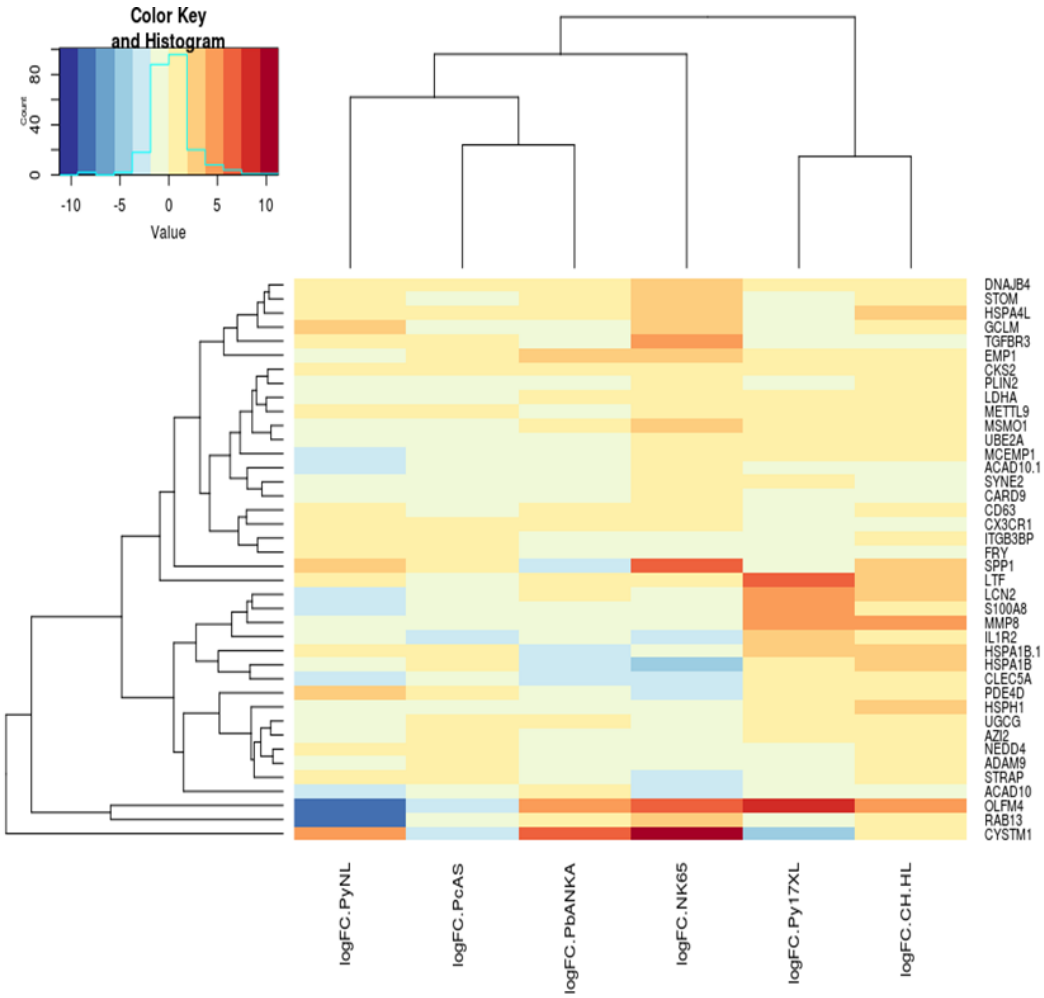

Figure 44: Heatmap of the top human malarial hyperlactataemia phenotype (CH+HL) DE genes with a mouse otholog

Heatmap of the top (lowest FDR) DE genes of CH+HLvsUM human genes, representative of the human hypelactataemia phenotype, versus C57BL/6 mouse orthologs in all severe vs uncomplicated infections (regardless of Pvalue or logFC). 40 genes out of the top 50 examined had a mouse otholog.

The comparison of all mouse models (mouse severe vs uncomplicated DEGs) with the human cerebral malaria phenotype (CH+CMvsUM) DEGs, seen in Figure 45, clustered *P. berghei ANKA* infection (model of ECM) closest to human cerebral malaria at a transcriptomic level. Taking a closer look at this heatmap shows that one of the genes following opposite directions between the *P. berghei ANKA* model and human CM is MMP8 explaining why the *in vivo* inhibition of MMP8 using *P. berghei ANKA* model (presented in chapter 3) did not improve survival or neurological symptoms development.

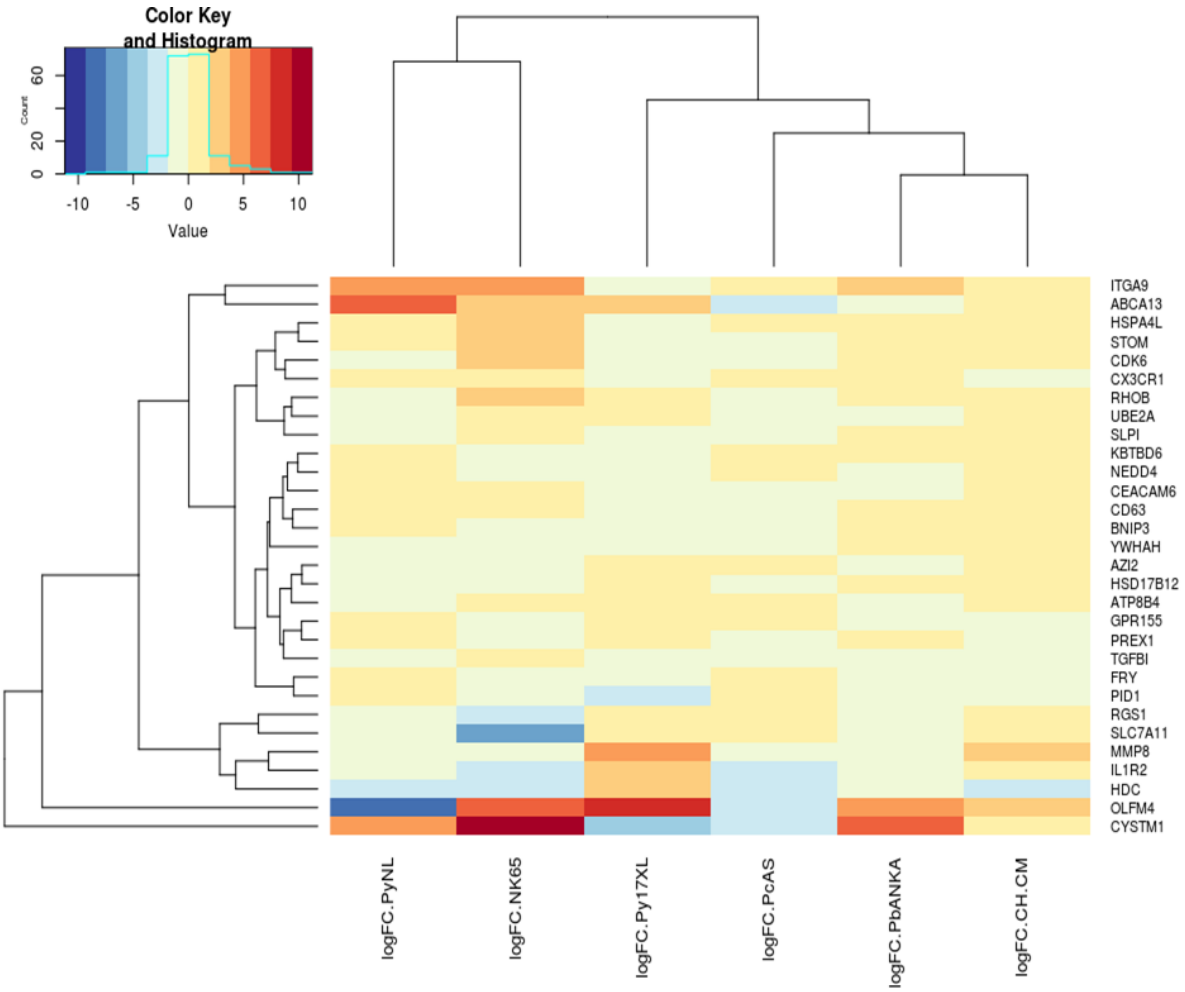

Figure 45: Heatmap of the top human cerebral malaria phenotype (CH+CM) DE genes with a mouse ortholog

Heatmap of the top (lowest FDR) DE genes of CH+CMvsUM human genes, representative of the human cerebral malaria phenotype, versus C57BL/6 mouse orthologs in all severe vs uncomplicated infections (regardless of Pvalue or logFC). 30 genes out of the top 50 examined had a mouse otholog.

5.6.1 Concordance and discordance in gene expression

In the concordant and discordant analysis, human and mouse orthologs were examined. As seen in Figure 46 genes that are orthologs with FDR <0.05 and follow the same direction of differential expression are presented with red colour while genes with FDR<0.05 DE only in human are presented in green, and those DE in mice in yellow. Genes shown in grey colour are orthologs but not differentially expressed in either mouse or human. *Py17XL* infected mice were the mouse model with the highest gene concordance compared to human data, with the 7 concordant genes all neutrophil associated.

Figure 46: Concordant and discordant genes between human hyperlactataemia phenotype (CHHL) and mouse hyperlactataemia phenotype (Py17XL).

FDR<0.05 and DE in C57BL/6 mice (yellow), in human (green), in both mouse and human (red), neither (grey). Total number of genes: 8040, Not DE (grey): 7455, DE in CHHL (green): 563, DE in Py17XL (yellow): 15, DE in both (red): 7

5.7 Summary

Mice are the most cost effective and widely used model for studying human diseases (404, 405). Nevertheless, mice are distant evolutionary and substantially different from humans (371, 406). Disease models can be quite artificial while the usefulness of mice in translational research for human is strongly debated (373, 375). Quite often therapeutic interventions that work in mice fail when used in human clinical trials (407, 408). Thus, developing methods which would improve translational cross-species research are needed (378). In malaria research mouse models are abundantly employed. However, it is still unclear which of these models can represent human pathophysiology aspects, restricting the translational potential from these findings.

Here, I assessed some of the most commonly used mouse models of malaria to examine their relevance with the host at a transcriptomic level. I infected C57BL/6 female wild type mice with: *P. berghei ANKA*, *P. berghei NK65*, *P. yoelii 17XL, P. yoelii 17XNL*, and *P. chabaudi AS* which lead to the development of distinct malaria phenotypes.

During these experiments, I discovered a mouse model of malarial hyperlactataemia reaching up to 20mmol/L lactate. This mouse model which develops hyperparasitaemia (80%) and a very severe phenotype lethal at 5-7 days post infection, seems to be the closest model to the most severe human malaria phenotype which combines cerebral malaria and hyperlactataemia, at a transcriptomic level. The genes identified as concordant between the human host and this mouse model are again emphasizing the importance of neutrophils in malaria pathogenesis, stressing the need for further in depth research needed. With this hyperlactataemia model now in place we will be able to deepen our understanding on hyperlactataemia development and assess potential adjunctive treatments.

Limitations of this experiment include the small number of subjects analysed for each mouse infection and relatively low read depth of the RNA seq for the mouse host. The suboptimal counts for mouse genes received were due to the high parasitaemia levels that some of these mouse models develop. This unfortunately reduces our range of discovery and resulted in short lists of genes detected as differentially expressed. The only way to overcome this obstacle would be to request deeper sequencing of the RNA samples which would though add a lot on the cost.

Future work will involve analysis of the parasite transcriptome in comparison to the parasite transcriptome analysed from our human Gambian children dataset. *P. yoelii 17XL* infection on C57BL/6 mice came up as the closest mouse malaria model to human combined cerebral malaria and hyperlactataemia phenotype at a transcriptomic level, so I will be examining this model at histopathology level as well in comparison to human for other severity features, such as brain micro-haemorrhages and organ damage. We will also assess other commonly used malaria mouse models (different mouse strains including Balb/c, DBA/2 and C57BL/6 infected with different parasite strains) compared to the human host at transcriptional level, increasing the number of mice per infection as well as increasing the depth of RNA seq.

5.8 Conclusion

Using 5 different strains of parasites I infected C57BL/6 mice and examined these commonly used malaria mouse models at a transcriptomic level in comparison with the human host. This comparison at transcriptomic level revealed that the lethal infection with *P. yoelii* 17XL creates the mouse model closest to the most severe malaria human phenotype which combines hyperlactataemia and cerebral malaria. This also led to the discovery of a new mouse model for malarial hyperlactataemia from the infection of C57BL/6 mice with the lethal strain *P. yoelii* 17XL.

Chapter 6: Conclusions-Discussion

In this chapter, I present briefly the conclusions and achievements of my thesis, by bringing together results and conclusions from the previous chapters. I also discuss some limitations and future research routes of this thesis.

6.1 Work achieved in this thesis

In the introduction chapter 1, I discussed the potential of transcriptomics as a discovery based approach which can lead to new insights through revealing the host pathogen interactions leading to pathogenesis. The main features of severe malaria include inflammation, high parasite load, endothelial dysfunction, and parasite sequestration. Although, numerous mouse models are being used as representatives of human malaria to either assist understanding of pathophysiology or to test potential treatment, multiple gaps exist in the translation between the two species.

In chapter 3 I presented our dual RNA sequencing study, emphasising the importance of studying both the host and the pathogen when trying to unravel pathogenesis in infectious diseases. Using dual RNA sequencing we could detect host and parasite gene expression, as well as their interactions which associate with severity of human *P. falciparum* malaria. We revealed that pathogen load is the main determinant of differential gene expression seen in the host, without though affecting parasite gene expression (270). Severe malaria manifestation was strongly associated with a neutrophil signature and hyperlactataemia. Since histology of the human retinal microcirculation offers an exceptional opportunity for the investigation of not only the retinal but also cerebral microvasculature I used immunohistochemistry and immunofluorescence on human retinal tissue to detect whether there is a difference in the expression levels of neutrophil proteins of interest (particularly MMP8 and OLFM4), NETosis formation and their association with the development of coagulopathy among the different severity groups. NETosis formation was visualized by immunofluorescence co-localization of histones (H3) and one of the neutrophil related proteins (ELANE) along with DNA staining (DAPI). I noted NETosis formation in the CM ret +

cases only and that was specifically found in vessels with prominent sequestration and inflammation. The intensity of both MMP8 and OLFM4 staining in the retina was significantly higher in the retina of CM ret+ cases versus CM ret-. MMP8 gave strong signal around vessels with high parasite biomass and sequestration and co-localised with fibrinogen leak found around vessels with sequestration in CM ret+ cases. OLFM4 stained quite intensely the ganglion cells in most of the cases and the endothelium of vessels with high sequestration. Unlike the upregulated gene expression and tissue expression of these neutrophil granule proteins, plasma levels from Gambian children did not show any major differences between SM and UM. This might just indicate that local upregulated expression does not reach systemic circulation. Local release of these neutrophil proteins is damaging to the endothelium and potentially initiates a vicious cycle of endothelial activation inducing further sequestration through cytoadhesion of pRBCs to endothelial surface receptors, and therefore further localisation of parasite products which stimulate the inflammatory response and further neutrophil degranulation and NETosis.

Looking at the parasite gene expression associated with hyperlactataemia I examined what could be the effect of lactate supplementation *in vitro*. This revealed an interesting upregulation of parasite genes associated with its virulence, PF3D7_0202000 (knob-associated histidine-rich protein) and PF3D7_1016300 (GBP), also found as highly expressed in the most severe human phenotype combining hyperlactataemia and cerebral malaria (CH). Neutrophils seem to have a major role in severe malaria pathogenesis so identifying ways to limit their action when they become damaging to the host would be of great importance.

In chapter 4, I presented a combination of mathematical modelling predictions and RNA seq data (Gambian children) which revealed Cathepsin G and MMP9 as positively correlated with parasite growth inhibition. I used *in vitro* methods of parasite culture and identified that both Cathepsin G and MMP9 negatively affect parasite growth. Cathepsin G, does so, by cleaving receptors from the RBC surface important for parasite invasion, rosetting and sequestration. I have not though managed to dissect the mechanism of action for MMP9 which seems to affect the parasite directly. This proof of concept validation suggests that this approach could potentially have an application in other infectious diseases. The findings could lead to new therapeutic interventions including a way of targeting the invasion receptors that cathepsin

G cleaves which could be used for both prevention as well as treatment of malaria (269). This chapter stresses again the importance of parasite load and how useful and novel it may be to be able to predict the factors affecting it, leading the way for developing new therapeutics.

While reviewing the literature (chapter 1) on malaria transcriptomics I identified a gap between mouse models and their translation to human malaria disease. Many studies use mouse models to understand malaria pathophysiology or to test potential treatments without considering the degree of similarity between the two hosts. Unfortunately, numerous treatments have shown promising results when tested in mice while none of them has proven useful for humans. In chapter 5, I assessed some of the most commonly used mouse models of malaria to examine their relevance with the host at a transcriptomic level. I infected C57BL/6 female wild type mice with: *P. berghei ANKA*, *P. berghei NK65*, *P. yoelii 17XL, P. yoelii 17XNL*, and *P. chabaudi AS* which lead to the development of distinct malaria phenotypes. Measuring lactate levels at peak severity I discovered a mouse model of malarial hyperlactataemia. This model according to our RNA seq analysis came up as the closest model to the most severe human malaria phenotype which combines cerebral malaria and hyperlactataemia. The concordant genes between this model and human CH+HL phenotype where neutrophil related suggesting again the crucial role of neutrophils in malaria pathogenesis. This hyperlactataemia model could prove useful in understanding hyperlactataemia pathophysiology as well as for testing potential adjunctive treatments.

6.2 Limitations

Our dual-RNA seq study had a relatively small number of subjects with pure CM phenotype, which limited the power to detect significantly differentially expressed genes. Another limitation is the lack of longitudinal human samples which would be ideal for understanding host response to malaria through the transcriptional changes seen during infection and convalescent period. On the parasite side, as the sample used for this analysis was circulating whole blood we cannot look at transcriptional changes happening in sequestered parasites. Being able to use human retinal samples was a unique opportunity to examine local important changes associated with pathology. These samples however, were collected years ago in Malawi and the fixation methods involved were longer than we would ideally use now, which may have affected the epitope retrieval. The slides I used for both immunohistochemistry and

immunofluorescence were cut ~6 years ago potentially limiting the tissue preservation and quality of staining.

For the mathematical model discovery approach presented in chapter 4 the main limitation was the small number of subjects used for RNA seq analysis part reducing statistical power and ability to detect more significant results. Another limitation of this model was the inability to propagate uncertainty throughout the stages of the model fitting, prediction of parameter estimates for the individual subjects, and association of these parameter estimates with real variables (269).

In chapter 5, where I tried to identify the most relevant to human malaria mouse model, high levels of parasitaemia found in the infected mice decreased the mouse RNA read depth and along with low number of subjects per infection affected the statistical power and allowed detection of a decreased number of genes with high log fold change and probably those most abundantly expressed. For the transcriptomic comparison with the human host, I used mouse samples collected early in each infection (when first symptoms start occurring) compared to samples collected at peak severity in each infection, while in the human dataset we used uncomplicated malaria samples versus severe malaria. These samples are not equivalent as in the mouse infections samples collected at an earlier timepoint of a severe infection might already have differences in gene expression causing the pathology seen later in infection.

6.3 Future directions

The analysis of immunofluorescence microscopy images of retinal samples presented in chapter 3 is largely qualitative, so quantitative examination will be performed by an independent person blinded to the samples clinical background. Brain samples from the same Malawian children cohort will be examined, to assess MMP8 and OLFM4 expression and their association with pathological features (such as BBB breakdown) as well as NETosis. This study clearly demonstrates the strong involvement of neutrophils in malaria pathogenesis, targeting some of their functions, such as NETosis, could be a promising adjunctive treatment which I would like to further examine. The role of neutrophils in malaria has not been extensively explored so this study showing their direct involvement in pathogenesis, suggests that understanding their properties and activity during malaria infection could reveal new

targets. OLFM4 as mentioned before is expressed by a subset of neutrophils whose activity is not completely understood compared to neutrophils that do not express it. Neutrophil heterogeneity needs to be further examined in malaria possibly by single cell RNA sequencing.

The combination of mathematical modelling with RNA seq to discover new targets presented in chapter 4, could have an application to the increasingly popular -omic based approaches such as proteomics and metabolomics. This combination method could apply in other infectious diseases where pathogen load can be measured, to inform for potential contributors to increasing or decreasing pathogen load. Cathepsin G therapeutic potential needs to be further assessed, even if that can only happen by using a molecule that would mimic the receptor cleaving action of cathepsin G avoiding excessive damage that the actual enzyme could cause. The exact mechanism of action for MMP9 is also to be addressed.

High parasitaemia levels achieved in the mouse infections described in chapter 5 did indeed limit our read depth for mouse RNA, on the other hand this gave us great read depth for the parasite. Analysis of the parasite transcriptomes from these mice will be compared to the parasite transcriptomes we have from human Gambian subjects. For our future experiments, we will also consider separating host WBCs from the infected erythrocytes and then do RNA extraction and sequencing as this will allow good read depth for both species. Having in place a model of mouse malarial hyperlactataemia which I found to be the closest to human hyperlactataemia phenotype at transcriptional level, will allow for further exploration of hyperlactataemia syndrome development for both mouse and human. Another plan for future experiments is to increase subjects per group and explore other malaria mouse models compared to human host at transcriptomic level. Collecting mouse tissue (various organs) for transcriptomic comparisons with human tissue transcriptomic data publicly available as well as for histology examination would also increase the impact of these *in vivo* experiments while reducing the use of animals used following one of the 3Rs (Replacement, Reduction and Refinement). Having all these transcriptomic comparisons publicly available will help other researchers to select the model closest to the human phenotype they want to focus. This will offer a refinement in animal use as well as reduction in the amount of animals used for malaria research.

References

1. World Health Organization. World malaria report 2018. November 2018:210.
2. World Health Organization. World Malaria Report. 2017.
3. Miller LH, Ackerman HC, Su XZ, Wellems TE. Malaria biology and disease pathogenesis: insights for new treatments. Nature medicine. 2013;19(2):156-67.
4. Khor CC, Hibberd ML. Revealing the molecular signatures of host-pathogen interactions. Genome Biol. 2011;12(10):229.
5. Olotu A, Fegan G, Wambua J, Nyangweso G, Leach A, Lievens M, et al. Seven-Year Efficacy of RTS,S/AS01 Malaria Vaccine among Young African Children. N Engl J Med. 2016;374(26):2519-29.
6. White MT, Verity R, Griffin JT, Asante KP, Owusu-Agyei S, Greenwood B, et al. Immunogenicity of the RTS,S/AS01 malaria vaccine and implications for duration of vaccine efficacy: secondary analysis of data from a phase 3 randomised controlled trial. Lancet Infect Dis. 2015;15(12):1450-8.
7. Cui L, Mharakurwa S, Ndiaye D, Rathod PK, Rosenthal PJ. Antimalarial Drug Resistance: Literature Review and Activities and Findings of the ICEMR Network. Am J Trop Med Hyg. 2015;93(3 Suppl):57-68.
8. Wassmer SC, Grau GE. Severe malaria: what's new on the pathogenesis front? Int J Parasitol. 2017;47(2-3):145-52.
9. White NJ, Turner GD, Day NP, Dondorp AM. Lethal malaria: Marchiafava and Bignami were right. The Journal of infectious diseases. 2013;208(2):192-8.
10. Cunnington AJ, Riley EM, Walther M. Stuck in a rut? Reconsidering the role of parasite sequestration in severe malaria syndromes. Trends in parasitology. 2013;29(12):585-92.
11. Phillips MA, Burrows JN, Manyando C, van Huijsduijnen RH, Van Voorhis WC, Wells TNC. Malaria. Nat Rev Dis Primers. 2017;3:17050.
12. Lee HJ, Georgiadou A, Otto TD, Levin M, Coin LJ, Conway DJ, et al. Transcriptomic Studies of Malaria: a Paradigm for Investigation of Systemic Host-Pathogen Interactions. Microbiol Mol Biol Rev. 2018;82(2).
13. Gardner MJ, Hall N, Fung E, White O, Berriman M, Hyman RW, et al. Genome sequence of the human malaria parasite Plasmodium falciparum. Nature. 2002;419(6906):498-511.
14. Cowman AF, Healer J, Marapana D, Marsh K. Malaria: Biology and Disease. Cell. 2016;167(3):610-24.
15. Bozdech Z, Llinas M, Pulliam BL, Wong ED, Zhu J, DeRisi JL. The transcriptome of the intraerythrocytic developmental cycle of Plasmodium falciparum. PLoS Biol. 2003;1(1):E5.
16. Otto TD, Wilinski D, Assefa S, Keane TM, Sarry LR, Bohme U, et al. New insights into the blood-stage transcriptome of Plasmodium falciparum using RNA-Seq. Mol Microbiol. 2010;76(1):12-24.
17. Sinha A, Hughes KR, Modrzynska KK, Otto TD, Pfander C, Dickens NJ, et al. A cascade of DNA-binding proteins for sexual commitment and development in Plasmodium. Nature. 2014;507(7491):253-7.
18. Poran A, Notzel C, Aly O, Mencia-Trinchant N, Harris CT, Guzman ML, et al. Single-cell RNA sequencing reveals a signature of sexual commitment in malaria parasites. Nature. 2017;551(7678):95-9.
19. Hoo R, Zhu L, Amaladoss A, Mok S, Natalang O, Lapp SA, et al. Integrated analysis of the Plasmodium species transcriptome. EBioMedicine. 2016;7:255-66.
20. Otto TD, Bohme U, Jackson AP, Hunt M, Franke-Fayard B, Hoeijmakers WA, et al. A comprehensive evaluation of rodent malaria parasite genomes and gene expression. BMC Biol. 2014;12:86.
21. Cunningham D, Lawton J, Jarra W, Preiser P, Langhorne J. The pir multigene family of Plasmodium: antigenic variation and beyond. Mol Biochem Parasitol. 2010;170(2):65-73.

22. del Portillo HA, Fernandez-Becerra C, Bowman S, Oliver K, Preuss M, Sanchez CP, et al. A superfamily of variant genes encoded in the subtelomeric region of Plasmodium vivax. Nature. 2001;410(6830):839-42.
23. Carlton JM, Adams JH, Silva JC, Bidwell SL, Lorenzi H, Caler E, et al. Comparative genomics of the neglected human malaria parasite Plasmodium vivax. Nature. 2008;455(7214):757-63.
24. Pain A, Bohme U, Berry AE, Mungall K, Finn RD, Jackson AP, et al. The genome of the simian and human malaria parasite Plasmodium knowlesi. Nature. 2008;455(7214):799-803.
25. Bohme U, Otto TD, Cotton JA, Steinbiss S, Sanders M, Oyola SO, et al. Complete avian malaria parasite genomes reveal features associated with lineage-specific evolution in birds and mammals. Genome research. 2018;28(4):547-60.
26. Auburn S, Bohme U, Steinbiss S, Trimarsanto H, Hostetler J, Sanders M, et al. A new Plasmodium vivax reference sequence with improved assembly of the subtelomeres reveals an abundance of pir genes. Wellcome Open Res. 2016;1:4.
27. Wahlgren M, Goel S, Akhouri RR. Variant surface antigens of Plasmodium falciparum and their roles in severe malaria. Nat Rev Microbiol. 2017;15(8):479-91.
28. Scherf A, Lopez-Rubio JJ, Riviere L. Antigenic variation in Plasmodium falciparum. Annu Rev Microbiol. 2008;62:445-70.
29. Jiang L, Mu J, Zhang Q, Ni T, Srinivasan P, Rayavara K, et al. PfSETvs methylation of histone H3K36 represses virulence genes in Plasmodium falciparum. Nature. 2013;499(7457):223-7.
30. Yam XY, Preiser PR. Host immune evasion strategies of malaria blood stage parasite. Mol Biosyst. 2017;13(12):2498-508.
31. Kirkman LA, Deitsch KW. Recombination and Diversification of the Variant Antigen Encoding Genes in the Malaria Parasite Plasmodium falciparum. Microbiol Spectr. 2014;2(6).
32. Daily JP, Le Roch KG, Sarr O, Ndiaye D, Lukens A, Zhou Y, et al. In vivo transcriptome of Plasmodium falciparum reveals overexpression of transcripts that encode surface proteins. The Journal of infectious diseases. 2005;191(7):1196-203.
33. Milner DA, Jr., Pochet N, Krupka M, Williams C, Seydel K, Taylor TE, et al. Transcriptional profiling of Plasmodium falciparum parasites from patients with severe malaria identifies distinct low vs. high parasitemic clusters. PLoS One. 2012;7(7):e40739.
34. Mancio-Silva L, Slavic K, Grilo Ruivo MT, Grosso AR, Modrzynska KK, Vera IM, et al. Nutrient sensing modulates malaria parasite virulence. Nature. 2017;547(7662):213-6.
35. Boddey JA, Cowman AF. Plasmodium nesting: remaking the erythrocyte from the inside out. Annu Rev Microbiol. 2013;67:243-69.
36. Cowman AF, Tonkin CJ, Tham WH, Duraisingh MT. The Molecular Basis of Erythrocyte Invasion by Malaria Parasites. Cell Host Microbe. 2017;22(2):232-45.
37. Healer J, Crawford S, Ralph S, McFadden G, Cowman AF. Independent translocation of two micronemal proteins in developing Plasmodium falciparum merozoites. Infection and immunity. 2002;70(10):5751-8.
38. Kremer K, Kamin D, Rittweger E, Wilkes J, Flammer H, Mahler S, et al. An overexpression screen of Toxoplasma gondii Rab-GTPases reveals distinct transport routes to the micronemes. PLoS Pathog. 2013;9(3):e1003213.
39. Yeoh S, O'Donnell RA, Koussis K, Dluzewski AR, Ansell KH, Osborne SA, et al. Subcellular discharge of a serine protease mediates release of invasive malaria parasites from host erythrocytes. Cell. 2007;131(6):1072-83.
40. Dvorak JA, Miller LH, Whitehouse WC, Shiroishi T. Invasion of erythrocytes by malaria merozoites. Science. 1975;187(4178):748-50.
41. Gilson PR, Crabb BS. Morphology and kinetics of the three distinct phases of red blood cell invasion by Plasmodium falciparum merozoites. Int J Parasitol. 2009;39(1):91-6.
42. Dasgupta S, Auth T, Gov NS, Satchwell TJ, Hanssen E, Zuccala ES, et al. Membrane-wrapping contributions to malaria parasite invasion of the human erythrocyte. Biophys J. 2014;107(1):43-54.

43. Zuccala ES, Baum J. Cytoskeletal and membrane remodelling during malaria parasite invasion of the human erythrocyte. Br J Haematol. 2011;154(6):680-9.
44. Sisquella X, Nebl T, Thompson JK, Whitehead L, Malpede BM, Salinas ND, et al. Plasmodium falciparum ligand binding to erythrocytes induce alterations in deformability essential for invasion. Elife. 2017;6.
45. Koch M, Wright KE, Otto O, Herbig M, Salinas ND, Tolia NH, et al. Plasmodium falciparum erythrocyte-binding antigen 175 triggers a biophysical change in the red blood cell that facilitates invasion. Proceedings of the National Academy of Sciences of the United States of America. 2017;114(16):4225-30.
46. Das S, Hertrich N, Perrin AJ, Withers-Martinez C, Collins CR, Jones ML, et al. Processing of Plasmodium falciparum Merozoite Surface Protein MSP1 Activates a Spectrin-Binding Function Enabling Parasite Egress from RBCs. Cell Host Microbe. 2015;18(4):433-44.
47. Miller LH, Hudson D, Haynes JD. Identification of Plasmodium knowlesi erythrocyte binding proteins. Mol Biochem Parasitol. 1988;31(3):217-22.
48. Camus D, Hadley TJ. A Plasmodium falciparum antigen that binds to host erythrocytes and merozoites. Science. 1985;230(4725):553-6.
49. Mayer DC, Cofie J, Jiang L, Hartl DL, Tracy E, Kabat J, et al. Glycophorin B is the erythrocyte receptor of Plasmodium falciparum erythrocyte-binding ligand, EBL-1. Proceedings of the National Academy of Sciences of the United States of America. 2009;106(13):5348-52.
50. Maier AG, Duraisingh MT, Reeder JC, Patel SS, Kazura JW, Zimmerman PA, et al. Plasmodium falciparum erythrocyte invasion through glycophorin C and selection for Gerbich negativity in human populations. Nat Med. 2003;9(1):87-92.
51. Mayer DC, Jiang L, Achur RN, Kakizaki I, Gowda DC, Miller LH. The glycophorin C N-linked glycan is a critical component of the ligand for the Plasmodium falciparum erythrocyte receptor BAEBL. Proceedings of the National Academy of Sciences of the United States of America. 2006;103(7):2358-62.
52. Gilberger TW, Thompson JK, Triglia T, Good RT, Duraisingh MT, Cowman AF. A novel erythrocyte binding antigen-175 paralogue from Plasmodium falciparum defines a new trypsin-resistant receptor on human erythrocytes. J Biol Chem. 2003;278(16):14480-6.
53. Galinski MR, Medina CC, Ingravallo P, Barnwell JW. A reticulocyte-binding protein complex of Plasmodium vivax merozoites. Cell. 1992;69(7):1213-26.
54. Duraisingh MT, Triglia T, Ralph SA, Rayner JC, Barnwell JW, McFadden GI, et al. Phenotypic variation of Plasmodium falciparum merozoite proteins directs receptor targeting for invasion of human erythrocytes. EMBO J. 2003;22(5):1047-57.
55. Rayner JC, Vargas-Serrato E, Huber CS, Galinski MR, Barnwell JW. A Plasmodium falciparum homologue of Plasmodium vivax reticulocyte binding protein (PvRBP1) defines a trypsin-resistant erythrocyte invasion pathway. The Journal of experimental medicine. 2001;194(11):1571-81.
56. Stubbs J, Simpson KM, Triglia T, Plouffe D, Tonkin CJ, Duraisingh MT, et al. Molecular mechanism for switching of P. falciparum invasion pathways into human erythrocytes. Science. 2005;309(5739):1384-7.
57. Triglia T, Duraisingh MT, Good RT, Cowman AF. Reticulocyte-binding protein homologue 1 is required for sialic acid-dependent invasion into human erythrocytes by Plasmodium falciparum. Mol Microbiol. 2005;55(1):162-74.
58. Tham WH, Wilson DW, Lopaticki S, Schmidt CQ, Tetteh-Quarcoo PB, Barlow PN, et al. Complement receptor 1 is the host erythrocyte receptor for Plasmodium falciparum PfRh4 invasion ligand. Proceedings of the National Academy of Sciences of the United States of America. 2010;107(40):17327-32.
59. Crosnier C, Bustamante LY, Bartholdson SJ, Bei AK, Theron M, Uchikawa M, et al. Basigin is a receptor essential for erythrocyte invasion by Plasmodium falciparum. Nature. 2011;480(7378):534-7.

60. Lopaticki S, Maier AG, Thompson J, Wilson DW, Tham WH, Triglia T, et al. Reticulocyte and erythrocyte binding-like proteins function cooperatively in invasion of human erythrocytes by malaria parasites. Infection and immunity. 2011;79(3):1107-17.
61. Volz JC, Yap A, Sisquella X, Thompson JK, Lim NT, Whitehead LW, et al. Essential Role of the PfRh5/PfRipr/CyRPA Complex during Plasmodium falciparum Invasion of Erythrocytes. Cell Host Microbe. 2016;20(1):60-71.
62. Weiss GE, Gilson PR, Taechalertpaisarn T, Tham WH, de Jong NW, Harvey KL, et al. Revealing the sequence and resulting cellular morphology of receptor-ligand interactions during Plasmodium falciparum invasion of erythrocytes. PLoS Pathog. 2015;11(2):e1004670.
63. Egan ES, Jiang RH, Moechtar MA, Barteneva NS, Weekes MP, Nobre LV, et al. Malaria. A forward genetic screen identifies erythrocyte CD55 as essential for Plasmodium falciparum invasion. Science. 2015;348(6235):711-4.
64. Paul AS, Saha S, Engelberg K, Jiang RH, Coleman BI, Kosber AL, et al. Parasite Calcineurin Regulates Host Cell Recognition and Attachment by Apicomplexans. Cell Host Microbe. 2015;18(1):49-60.
65. Kennedy AT, Schmidt CQ, Thompson JK, Weiss GE, Taechalertpaisarn T, Gilson PR, et al. Recruitment of Factor H as a Novel Complement Evasion Strategy for Blood-Stage Plasmodium falciparum Infection. J Immunol. 2016;196(3):1239-48.
66. Boyle MJ, Reiling L, Feng G, Langer C, Osier FH, Aspeling-Jones H, et al. Human antibodies fix complement to inhibit Plasmodium falciparum invasion of erythrocytes and are associated with protection against malaria. Immunity. 2015;42(3):580-90.
67. Schmidt CQ, Kennedy AT, Tham WH. More than just immune evasion: Hijacking complement by Plasmodium falciparum. Mol Immunol. 2015;67(1):71-84.
68. Miller LH, Baruch DI, Marsh K, Doumbo OK. The pathogenic basis of malaria. Nature. 2002;415(6872):673-9.
69. Mawson AR. The pathogenesis of malaria: a new perspective. Pathog Glob Health. 2013;107(3):122-9.
70. Mackintosh CL, Beeson JG, Marsh K. Clinical features and pathogenesis of severe malaria. Trends in parasitology. 2004;20(12):597-603.
71. Cunnington AJ, Walther M, Riley EM. Piecing together the puzzle of severe malaria. Science translational medicine. 2013;5(211):211ps18.
72. Plewes K, Turner GDH, Dondorp AM. Pathophysiology, clinical presentation, and treatment of coma and acute kidney injury complicating falciparum malaria. Curr Opin Infect Dis. 2018;31(1):69-77.
73. Taylor WR, Canon V, White NJ. Pulmonary manifestations of malaria : recognition and management. Treat Respir Med. 2006;5(6):419-28.
74. Mohan A, Sharma SK, Bollineni S. Acute lung injury and acute respiratory distress syndrome in malaria. J Vector Borne Dis. 2008;45(3):179-93.
75. Taylor WRJ, Hanson J, Turner GDH, White NJ, Dondorp AM. Respiratory manifestations of malaria. Chest. 2012;142(2):492-505.
76. Dondorp AM, Lee SJ, Faiz MA, Mishra S, Price R, Tjitra E, et al. The relationship between age and the manifestations of and mortality associated with severe malaria. Clin Infect Dis. 2008;47(2):151-7.
77. von Seidlein L, Olaosebikan R, Hendriksen IC, Lee SJ, Adedoyin OT, Agbenyega T, et al. Predicting the clinical outcome of severe falciparum malaria in african children: findings from a large randomized trial. Clin Infect Dis. 2012;54(8):1080-90.
78. Westermann AJ, Gorski SA, Vogel J. Dual RNA-seq of pathogen and host. Nature reviews Microbiology. 2012;10(9):618-30.
79. Craig AG, Grau GE, Janse C, Kazura JW, Milner D, Barnwell JW, et al. The role of animal models for research on severe malaria. PLoS Pathog. 2012;8(2):e1002401.
80. Strangward P, Haley MJ, Shaw TN, Schwartz JM, Greig R, Mironov A, et al. A quantitative brain map of experimental cerebral malaria pathology. PLoS Pathog. 2017;13(3):e1006267.

81. Zuzarte-Luis V, Mota MM, Vigario AM. Malaria infections: what and how can mice teach us. J Immunol Methods. 2014;410:113-22.
82. Sanders H, Kaaijk P, van den Dobbelsteen GP. Preclinical evaluation of MenB vaccines: prerequisites for clinical development. Expert Rev Vaccines. 2013;12(1):31-42.
83. Domaszewska T, Scheuermann L, Hahnke K, Mollenkopf H, Dorhoi A, Kaufmann SHE, et al. Concordant and discordant gene expression patterns in mouse strains identify best-fit animal model for human tuberculosis. Sci Rep. 2017;7(1):12094.
84. Strugnell RA, Scott TA, Wang N, Yang C, Peres N, Bedoui S, et al. Salmonella vaccines: lessons from the mouse model or bad teaching? Curr Opin Microbiol. 2014;17:99-105.
85. Breschi A, Gingeras TR, Guigo R. Comparative transcriptomics in human and mouse. Nat Rev Genet. 2017;18(7):425-40.
86. Artavanis-Tsakonas K, Tongren JE, Riley EM. The war between the malaria parasite and the immune system: immunity, immunoregulation and immunopathology. Clin Exp Immunol. 2003;133(2):145-52.
87. Valiathan R, Ashman M, Asthana D. Effects of Ageing on the Immune System: Infants to Elderly. Scand J Immunol. 2016;83(4):255-66.
88. Wykes MN, Horne-Debets JM, Leow CY, Karunarathne DS. Malaria drives T cells to exhaustion. Front Microbiol. 2014;5:249.
89. Singh NJ, Schwartz RH. The strength of persistent antigenic stimulation modulates adaptive tolerance in peripheral CD4+ T cells. The Journal of experimental medicine. 2003;198(7):1107-17.
90. Netea MG, Joosten LA, Latz E, Mills KH, Natoli G, Stunnenberg HG, et al. Trained immunity: A program of innate immune memory in health and disease. Science. 2016;352(6284):aaf1098.
91. Saeed S, Quintin J, Kerstens HH, Rao NA, Aghajanirefah A, Matarese F, et al. Epigenetic programming of monocyte-to-macrophage differentiation and trained innate immunity. Science. 2014;345(6204):1251086.
92. Boutlis CS, Yeo TW, Anstey NM. Malaria tolerance--for whom the cell tolls? Trends in parasitology. 2006;22(8):371-7.
93. Ademolue TW, Aniweh Y, Kusi KA, Awandare GA. Patterns of inflammatory responses and parasite tolerance vary with malaria transmission intensity. Malar J. 2017;16(1):145.
94. Moncunill G, Mayor A, Bardaji A, Puyol L, Nhabomba A, Barrios D, et al. Cytokine profiling in immigrants with clinical malaria after extended periods of interrupted exposure to Plasmodium falciparum. PLoS One. 2013;8(8):e73360.
95. Boutlis CS, Gowda DC, Naik RS, Maguire GP, Mgone CS, Bockarie MJ, et al. Antibodies to Plasmodium falciparum glycosylphosphatidylinositols: inverse association with tolerance of parasitemia in Papua New Guinean children and adults. Infection and immunity. 2002;70(9):5052-7.
96. Biswas S, Karmarkar MG, Sharma YD. Antibodies detected against Plasmodium falciparum haemozoin with inhibitory properties to cytokine production. FEMS Microbiol Lett. 2001;194(2):175-9.
97. Bate CA, Taverne J, Bootsma HJ, Mason RC, Skalko N, Gregoriadis G, et al. Antibodies against phosphatidylinositol and inositol monophosphate specifically inhibit tumour necrosis factor induction by malaria exoantigens. Immunology. 1992;76(1):35-41.
98. Bate CA, Kwiatkowski D. Inhibitory immunoglobulin M antibodies to tumor necrosis factor-inducing toxins in patients with malaria. Infection and immunity. 1994;62(8):3086-91.
99. Raberg L, Sim D, Read AF. Disentangling genetic variation for resistance and tolerance to infectious diseases in animals. Science. 2007;318(5851):812-4.
100. Goncalves BP, Fried M, Duffy PE. Parasite burden and severity of malaria in Tanzanian children. N Engl J Med. 2014;371(5):482.
101. Reyburn H, Mbatia R, Drakeley C, Bruce J, Carneiro I, Olomi R, et al. Association of transmission intensity and age with clinical manifestations and case fatality of severe Plasmodium falciparum malaria. JAMA. 2005;293(12):1461-70.

102. Snow RW, Guerra CA, Noor AM, Myint HY, Hay SI. The global distribution of clinical episodes of Plasmodium falciparum malaria. Nature. 2005;434(7030):214-7.
103. Farrington L, Vance H, Rek J, Prahl M, Jagannathan P, Katureebe A, et al. Both inflammatory and regulatory cytokine responses to malaria are blunted with increasing age in highly exposed children. Malar J. 2017;16(1):499.
104. Turner GD, Ly VC, Nguyen TH, Tran TH, Nguyen HP, Bethell D, et al. Systemic endothelial activation occurs in both mild and severe malaria. Correlating dermal microvascular endothelial cell phenotype and soluble cell adhesion molecules with disease severity. The American journal of pathology. 1998;152(6):1477-87.
105. Beare NA, Taylor TE, Harding SP, Lewallen S, Molyneux ME. Malarial retinopathy: a newly established diagnostic sign in severe malaria. Am J Trop Med Hyg. 2006;75(5):790-7.
106. Haldar K, Murphy SC, Milner DA, Taylor TE. Malaria: mechanisms of erythrocytic infection and pathological correlates of severe disease. Annu Rev Pathol. 2007;2:217-49.
107. Clark IA, Rockett KA. The cytokine theory of human cerebral malaria. Parasitol Today. 1994;10(10):410-2.
108. Day NP, Hien TT, Schollaardt T, Loc PP, Chuong LV, Chau TT, et al. The prognostic and pathophysiologic role of pro- and antiinflammatory cytokines in severe malaria. The Journal of infectious diseases. 1999;180(4):1288-97.
109. Medana IM, Turner GD. Human cerebral malaria and the blood-brain barrier. Int J Parasitol. 2006;36(5):555-68.
110. Moxon CA, Heyderman RS, Wassmer SC. Dysregulation of coagulation in cerebral malaria. Mol Biochem Parasitol. 2009;166(2):99-108.
111. Mohanty S, Taylor TE, Kampondeni S, Potchen MJ, Panda P, Majhi M, et al. Magnetic resonance imaging during life: the key to unlock cerebral malaria pathogenesis? Malar J. 2014;13:276.
112. Magowan C, Wollish W, Anderson L, Leech J. Cytoadherence by Plasmodium falciparum-infected erythrocytes is correlated with the expression of a family of variable proteins on infected erythrocytes. The Journal of experimental medicine. 1988;168(4):1307-20.
113. Cooke B, Coppel R, Wahlgren M. Falciparum malaria: sticking up, standing out and out-standing. Parasitol Today. 2000;16(10):416-20.
114. Dunst J, Kamena F, Matuschewski K. Cytokines and Chemokines in Cerebral Malaria Pathogenesis. Front Cell Infect Microbiol. 2017;7:324.
115. Pasloske BL, Howard RJ. Malaria, the red cell, and the endothelium. Annu Rev Med. 1994;45:283-95.
116. Chen Q, Schlichtherle M, Wahlgren M. Molecular aspects of severe malaria. Clinical microbiology reviews. 2000;13(3):439-50.
117. Rowe JA, Claessens A, Corrigan RA, Arman M. Adhesion of Plasmodium falciparum-infected erythrocytes to human cells: molecular mechanisms and therapeutic implications. Expert Rev Mol Med. 2009;11:e16.
118. Smith JD, Rowe JA, Higgins MK, Lavstsen T. Malaria's deadly grip: cytoadhesion of Plasmodium falciparum-infected erythrocytes. Cell Microbiol. 2013;15(12):1976-83.
119. Turner L, Lavstsen T, Berger SS, Wang CW, Petersen JE, Avril M, et al. Severe malaria is associated with parasite binding to endothelial protein C receptor. Nature. 2013;498(7455):502-5.
120. Lennartz F, Adams Y, Bengtsson A, Olsen RW, Turner L, Ndam NT, et al. Structure-Guided Identification of a Family of Dual Receptor-Binding PfEMP1 that Is Associated with Cerebral Malaria. Cell Host Microbe. 2017;21(3):403-14.
121. Dondorp AM, Pongponratn E, White NJ. Reduced microcirculatory flow in severe falciparum malaria: pathophysiology and electron-microscopic pathology. Acta Trop. 2004;89(3):309-17.
122. Adams Y, Kuhnrae P, Higgins MK, Ghumra A, Rowe JA. Rosetting Plasmodium falciparum-infected erythrocytes bind to human brain microvascular endothelial cells in vitro, demonstrating a dual adhesion phenotype mediated by distinct P. falciparum erythrocyte membrane protein 1 domains. Infection and immunity. 2014;82(3):949-59.

123. Wassmer SC, Taylor T, Maclennan CA, Kanjala M, Mukaka M, Molyneux ME, et al. Platelet-induced clumping of Plasmodium falciparum-infected erythrocytes from Malawian patients with cerebral malaria-possible modulation in vivo by thrombocytopenia. The Journal of infectious diseases. 2008;197(1):72-8.
124. Rowe JA, Handel IG, Thera MA, Deans AM, Lyke KE, Kone A, et al. Blood group O protects against severe Plasmodium falciparum malaria through the mechanism of reduced rosetting. Proceedings of the National Academy of Sciences of the United States of America. 2007;104(44):17471-6.
125. Maude RJ, Dondorp AM, Abu Sayeed A, Day NP, White NJ, Beare NA. The eye in cerebral malaria: what can it teach us? Trans R Soc Trop Med Hyg. 2009;103(7):661-4.
126. Maude RJ, Beare NA, Abu Sayeed A, Chang CC, Charunwatthana P, Faiz MA, et al. The spectrum of retinopathy in adults with Plasmodium falciparum malaria. Trans R Soc Trop Med Hyg. 2009;103(7):665-71.
127. Newton CR, Kirkham FJ, Winstanley PA, Pasvol G, Peshu N, Warrell DA, et al. Intracranial pressure in African children with cerebral malaria. Lancet. 1991;337(8741):573-6.
128. Waller D, Crawley J, Nosten F, Chapman D, Krishna S, Craddock C, et al. Intracranial pressure in childhood cerebral malaria. Trans R Soc Trop Med Hyg. 1991;85(3):362-4.
129. Plewes K, Royakkers AA, Hanson J, Hasan MM, Alam S, Ghose A, et al. Correlation of biomarkers for parasite burden and immune activation with acute kidney injury in severe falciparum malaria. Malar J. 2014;13:91.
130. Mikita K, Thakur K, Anstey NM, Piera KA, Pardo CA, Weinberg JB, et al. Quantification of Plasmodium falciparum histidine-rich protein-2 in cerebrospinal spinal fluid from cerebral malaria patients. Am J Trop Med Hyg. 2014;91(3):486-92.
131. Park GS, Opoka RO, Shabani E, Wypyszynski A, Hanisch B, John CC. Plasmodium falciparum Histidine-Rich Protein-2 Plasma Concentrations Are Higher in Retinopathy-Negative Cerebral Malaria Than in Severe Malarial Anemia. Open Forum Infect Dis. 2017;4(3):ofx151.
132. Pober JS, Sessa WC. Evolving functions of endothelial cells in inflammation. Nat Rev Immunol. 2007;7(10):803-15.
133. Davis TM, Suputtamongkol Y, Spencer JL, Ford S, Chienkul N, Schulenburg WE, et al. Measures of capillary permeability in acute falciparum malaria: relation to severity of infection and treatment. Clin Infect Dis. 1992;15(2):256-66.
134. Milner DA, Jr., Whitten RO, Kamiza S, Carr R, Liomba G, Dzamalala C, et al. The systemic pathology of cerebral malaria in African children. Front Cell Infect Microbiol. 2014;4:104.
135. Medana IM, Day NP, Sachanonta N, Mai NT, Dondorp AM, Pongponratn E, et al. Coma in fatal adult human malaria is not caused by cerebral oedema. Malar J. 2011;10:267.
136. Seydel KB, Kampondeni SD, Valim C, Potchen MJ, Milner DA, Muwalo FW, et al. Brain swelling and death in children with cerebral malaria. N Engl J Med. 2015;372(12):1126-37.
137. Mohanty S, Benjamin LA, Majhi M, Panda P, Kampondeni S, Sahu PK, et al. Magnetic Resonance Imaging of Cerebral Malaria Patients Reveals Distinct Pathogenetic Processes in Different Parts of the Brain. mSphere. 2017;2(3).
138. Turner GD, Morrison H, Jones M, Davis TM, Looareesuwan S, Buley ID, et al. An immunohistochemical study of the pathology of fatal malaria. Evidence for widespread endothelial activation and a potential role for intercellular adhesion molecule-1 in cerebral sequestration. The American journal of pathology. 1994;145(5):1057-69.
139. Grau GE, Pointaire P, Piguet PF, Vesin C, Rosen H, Stamenkovic I, et al. Late administration of monoclonal antibody to leukocyte function-antigen 1 abrogates incipient murine cerebral malaria. Eur J Immunol. 1991;21(9):2265-7.
140. Favre N, Da Laperousaz C, Ryffel B, Weiss NA, Imhof BA, Rudin W, et al. Role of ICAM-1 (CD54) in the development of murine cerebral malaria. Microbes Infect. 1999;1(12):961-8.
141. Hunt NH, Grau GE. Cytokines: accelerators and brakes in the pathogenesis of cerebral malaria. Trends Immunol. 2003;24(9):491-9.

142. Combes V, Coltel N, Faille D, Wassmer SC, Grau GE. Cerebral malaria: role of microparticles and platelets in alterations of the blood-brain barrier. Int J Parasitol. 2006;36(5):541-6.
143. MacCormick IJ, Beare NA, Taylor TE, Barrera V, White VA, Hiscott P, et al. Cerebral malaria in children: using the retina to study the brain. Brain. 2014;137(Pt 8):2119-42.
144. Yeo TW, Lampah DA, Kenangalem E, Tjitra E, Weinberg JB, Granger DL, et al. Decreased endothelial nitric oxide bioavailability, impaired microvascular function, and increased tissue oxygen consumption in children with falciparum malaria. The Journal of infectious diseases. 2014;210(10):1627-32.
145. Yeo TW, Lampah DA, Gitawati R, Tjitra E, Kenangalem E, McNeil YR, et al. Impaired nitric oxide bioavailability and L-arginine reversible endothelial dysfunction in adults with falciparum malaria. The Journal of experimental medicine. 2007;204(11):2693-704.
146. Griffiths MJ, Ndungu F, Baird KL, Muller DP, Marsh K, Newton CR. Oxidative stress and erythrocyte damage in Kenyan children with severe Plasmodium falciparum malaria. Br J Haematol. 2001;113(2):486-91.
147. Narsaria N, Mohanty C, Das BK, Mishra SP, Prasad R. Oxidative stress in children with severe malaria. J Trop Pediatr. 2012;58(2):147-50.
148. Dondorp AM, Angus BJ, Hardeman MR, Chotivanich KT, Silamut K, Ruangveerayuth R, et al. Prognostic significance of reduced red blood cell deformability in severe falciparum malaria. Am J Trop Med Hyg. 1997;57(5):507-11.
149. Dondorp AM, Omodeo-Sale F, Chotivanich K, Taramelli D, White NJ. Oxidative stress and rheology in severe malaria. Redox Rep. 2003;8(5):292-4.
150. Faraci FM. Protecting against vascular disease in brain. Am J Physiol Heart Circ Physiol. 2011;300(5):H1566-82.
151. Yeo TW, Lampah DA, Gitawati R, Tjitra E, Kenangalem E, McNeil YR, et al. Recovery of endothelial function in severe falciparum malaria: relationship with improvement in plasma L-arginine and blood lactate concentrations. The Journal of infectious diseases. 2008;198(4):602-8.
152. Yeo TW, Lampah DA, Rooslamiati I, Gitawati R, Tjitra E, Kenangalem E, et al. A randomized pilot study of L-arginine infusion in severe falciparum malaria: preliminary safety, efficacy and pharmacokinetics. PLoS One. 2013;8(7):e69587.
153. McDonald CR, Cahill LS, Gamble JL, Elphinstone R, Gazdzinski LM, Zhong KJY, et al. Malaria in pregnancy alters l-arginine bioavailability and placental vascular development. Science translational medicine. 2018;10(431).
154. Cavender DE, Edelbaum D, Ziff M. Endothelial cell activation induced by tumor necrosis factor and lymphotoxin. The American journal of pathology. 1989;134(3):551-60.
155. Pober JS, Cotran RS. Cytokines and endothelial cell biology. Physiol Rev. 1990;70(2):427-51.
156. Bauer PR, Van Der Heyde HC, Sun G, Specian RD, Granger DN. Regulation of endothelial cell adhesion molecule expression in an experimental model of cerebral malaria. Microcirculation. 2002;9(6):463-70.
157. Prakash D, Fesel C, Jain R, Cazenave PA, Mishra GC, Pied S. Clusters of cytokines determine malaria severity in Plasmodium falciparum-infected patients from endemic areas of Central India. The Journal of infectious diseases. 2006;194(2):198-207.
158. Thuma PE, van Dijk J, Bucala R, Debebe Z, Nekhai S, Kuddo T, et al. Distinct clinical and immunologic profiles in severe malarial anemia and cerebral malaria in Zambia. The Journal of infectious diseases. 2011;203(2):211-9.
159. Yanez DM, Manning DD, Cooley AJ, Weidanz WP, van der Heyde HC. Participation of lymphocyte subpopulations in the pathogenesis of experimental murine cerebral malaria. J Immunol. 1996;157(4):1620-4.
160. Lucas R, Juillard P, Decoster E, Redard M, Burger D, Donati Y, et al. Crucial role of tumor necrosis factor (TNF) receptor 2 and membrane-bound TNF in experimental cerebral malaria. Eur J Immunol. 1997;27(7):1719-25.

161. Engwerda CR, Mynott TL, Sawhney S, De Souza JB, Bickle QD, Kaye PM. Locally up-regulated lymphotoxin alpha, not systemic tumor necrosis factor alpha, is the principle mediator of murine cerebral malaria. The Journal of experimental medicine. 2002;195(10):1371-7.
162. Schofield L, Grau GE. Immunological processes in malaria pathogenesis. Nat Rev Immunol. 2005;5(9):722-35.
163. Langhorne J, Ndungu FM, Sponaas AM, Marsh K. Immunity to malaria: more questions than answers. Nat Immunol. 2008;9(7):725-32.
164. Di Perri G, Di Perri IG, Monteiro GB, Bonora S, Hennig C, Cassatella M, et al. Pentoxifylline as a supportive agent in the treatment of cerebral malaria in children. The Journal of infectious diseases. 1995;171(5):1317-22.
165. van Hensbroek MB, Palmer A, Onyiorah E, Schneider G, Jaffar S, Dolan G, et al. The effect of a monoclonal antibody to tumor necrosis factor on survival from childhood cerebral malaria. The Journal of infectious diseases. 1996;174(5):1091-7.
166. Looareesuwan S, Wilairatana P, Vannaphan S, Wanaratana V, Wenisch C, Aikawa M, et al. Pentoxifylline as an ancillary treatment for severe falciparum malaria in Thailand. Am J Trop Med Hyg. 1998;58(3):348-53.
167. Lell B, Kohler C, Wamola B, Olola CH, Kivaya E, Kokwaro G, et al. Pentoxifylline as an adjunct therapy in children with cerebral malaria. Malar J. 2010;9:368.
168. Mai J, Virtue A, Shen J, Wang H, Yang XF. An evolving new paradigm: endothelial cells--conditional innate immune cells. J Hematol Oncol. 2013;6:61.
169. Wassmer SC, Moxon CA, Taylor T, Grau GE, Molyneux ME, Craig AG. Vascular endothelial cells cultured from patients with cerebral or uncomplicated malaria exhibit differential reactivity to TNF. Cell Microbiol. 2011;13(2):198-209.
170. Wassmer SC, Taylor TE, Rathod PK, Mishra SK, Mohanty S, Arevalo-Herrera M, et al. Investigating the Pathogenesis of Severe Malaria: A Multidisciplinary and Cross-Geographical Approach. Am J Trop Med Hyg. 2015;93(3 Suppl):42-56.
171. Zehnbauer B. Population genetics in critical illness. Critical care medicine. 2005;33(1):242-3.
172. Howland SW, Poh CM, Renia L. Activated Brain Endothelial Cells Cross-Present Malaria Antigen. PLoS Pathog. 2015;11(6):e1004963.
173. Viebig NK, Wulbrand U, Forster R, Andrews KT, Lanzer M, Knolle PA. Direct activation of human endothelial cells by Plasmodium falciparum-infected erythrocytes. Infection and immunity. 2005;73(6):3271-7.
174. Tripathi AK, Sullivan DJ, Stins MF. Plasmodium falciparum-infected erythrocytes increase intercellular adhesion molecule 1 expression on brain endothelium through NF-kappaB. Infection and immunity. 2006;74(6):3262-70.
175. Chakravorty SJ, Carret C, Nash GB, Ivens A, Szestak T, Craig AG. Altered phenotype and gene transcription in endothelial cells, induced by Plasmodium falciparum-infected red blood cells: pathogenic or protective? Int J Parasitol. 2007;37(8-9):975-87.
176. Tripathi AK, Sha W, Shulaev V, Stins MF, Sullivan DJ, Jr. Plasmodium falciparum-infected erythrocytes induce NF-kappaB regulated inflammatory pathways in human cerebral endothelium. Blood. 2009;114(19):4243-52.
177. Campanella GS, Tager AM, El Khoury JK, Thomas SY, Abrazinski TA, Manice LA, et al. Chemokine receptor CXCR3 and its ligands CXCL9 and CXCL10 are required for the development of murine cerebral malaria. Proceedings of the National Academy of Sciences of the United States of America. 2008;105(12):4814-9.
178. Srivastava K, Cockburn IA, Swaim A, Thompson LE, Tripathi A, Fletcher CA, et al. Platelet factor 4 mediates inflammation in experimental cerebral malaria. Cell Host Microbe. 2008;4(2):179-87.
179. Nie CQ, Bernard NJ, Norman MU, Amante FH, Lundie RJ, Crabb BS, et al. IP-10-mediated T cell homing promotes cerebral inflammation over splenic immunity to malaria infection. PLoS Pathog. 2009;5(4):e1000369.

180. Renia L, Howland SW, Claser C, Charlotte Gruner A, Suwanarusk R, Hui Teo T, et al. Cerebral malaria: mysteries at the blood-brain barrier. Virulence. 2012;3(2):193-201.
181. Storm J, Craig AG. Pathogenesis of cerebral malaria--inflammation and cytoadherence. Front Cell Infect Microbiol. 2014;4:100.
182. Cunnington AJ. The importance of pathogen load. PLoS Pathog. 2015;11(1):e1004563.
183. Dondorp AM, Desakorn V, Pongtavornpinyo W, Sahassananda D, Silamut K, Chotivanich K, et al. Estimation of the total parasite biomass in acute falciparum malaria from plasma PfHRP2. PLoS Med. 2005;2(8):e204.
184. Hendriksen IC, Mwanga-Amumpaire J, von Seidlein L, Mtove G, White LJ, Olaosebikan R, et al. Diagnosing severe falciparum malaria in parasitaemic African children: a prospective evaluation of plasma PfHRP2 measurement. PLoS Med. 2012;9(8):e1001297.
185. Hendriksen IC, White LJ, Veenemans J, Mtove G, Woodrow C, Amos B, et al. Defining falciparum-malaria-attributable severe febrile illness in moderate-to-high transmission settings on the basis of plasma PfHRP2 concentration. The Journal of infectious diseases. 2013;207(2):351-61.
186. Rubach MP, Mukemba J, Florence S, John B, Crookston B, Lopansri BK, et al. Plasma Plasmodium falciparum histidine-rich protein-2 concentrations are associated with malaria severity and mortality in Tanzanian children. PLoS One. 2012;7(5):e35985.
187. Seydel KB, Fox LL, Glover SJ, Reeves MJ, Pensulo P, Muiruri A, et al. Plasma concentrations of parasite histidine-rich protein 2 distinguish between retinopathy-positive and retinopathy-negative cerebral malaria in Malawian children. The Journal of infectious diseases. 2012;206(3):309-18.
188. Cunnington AJ, Bretscher MT, Nogaro SI, Riley EM, Walther M. Comparison of parasite sequestration in uncomplicated and severe childhood Plasmodium falciparum malaria. J Infect. 2013;67(3):220-30.
189. English M, Waruiru C, Amukoye E, Murphy S, Crawley J, Mwangi I, et al. Deep breathing in children with severe malaria: indicator of metabolic acidosis and poor outcome. Am J Trop Med Hyg. 1996;55(5):521-4.
190. English M, Sauerwein R, Waruiru C, Mosobo M, Obiero J, Lowe B, et al. Acidosis in severe childhood malaria. QJM. 1997;90(4):263-70.
191. Krishna S, Waller DW, ter Kuile F, Kwiatkowski D, Crawley J, Craddock CF, et al. Lactic acidosis and hypoglycaemia in children with severe malaria: pathophysiological and prognostic significance. Trans R Soc Trop Med Hyg. 1994;88(1):67-73.
192. Waller D, Krishna S, Crawley J, Miller K, Nosten F, Chapman D, et al. Clinical features and outcome of severe malaria in Gambian children. Clin Infect Dis. 1995;21(3):577-87.
193. Day NP, Phu NH, Mai NT, Chau TT, Loc PP, Chuong LV, et al. The pathophysiologic and prognostic significance of acidosis in severe adult malaria. Critical care medicine. 2000;28(6):1833-40.
194. van Genderen PJ, van der Meer IM, Consten J, Petit PL, van Gool T, Overbosch D. Evaluation of plasma lactate as a parameter for disease severity on admission in travelers with Plasmodium falciparum malaria. Journal of travel medicine. 2005;12(5):261-4.
195. White NJ, Warrell DA, Looareesuwan S, Chanthavanich P, Phillips RE, Pongpaew P. Pathophysiological and prognostic significance of cerebrospinal-fluid lactate in cerebral malaria. Lancet. 1985;1(8432):776-8.
196. Chaudhari KS, Uttarwar SP, Tambe NN, Sharma RS, Takalkar AA. Role of Serum Lactate and Malarial Retinopathy in Prognosis and Outcome of Falciparum and Vivax Cerebral Malaria: A Prospective Cohort Study in Adult Assamese Tribes. J Glob Infect Dis. 2016;8(2):61-7.
197. Rosenthal PJ. Artesunate for the treatment of severe falciparum malaria. N Engl J Med. 2008;358(17):1829-36.
198. Wah ST, Hananantachai H, Kerdpin U, Plabplueng C, Prachayasittikul V, Nuchnoi P. Molecular basis of human cerebral malaria development. Trop Med Health. 2016;44:33.
199. World Health Organisation. World Malaria Report 2015. December 2015.
200. Shandilya A, Chacko S, Jayaram B, Ghosh I. A plausible mechanism for the antimalarial activity of artemisinin: A computational approach. Sci Rep. 2013;3:2513.

201. Triglia T, Wang P, Sims PF, Hyde JE, Cowman AF. Allelic exchange at the endogenous genomic locus in Plasmodium falciparum proves the role of dihydropteroate synthase in sulfadoxine-resistant malaria. EMBO J. 1998;17(14):3807-15.
202. Ariey F, Witkowski B, Amaratunga C, Beghain J, Langlois AC, Khim N, et al. A molecular marker of artemisinin-resistant Plasmodium falciparum malaria. Nature. 2014;505(7481):50-5.
203. Ghorbal M, Gorman M, Macpherson CR, Martins RM, Scherf A, Lopez-Rubio JJ. Genome editing in the human malaria parasite Plasmodium falciparum using the CRISPR-Cas9 system. Nat Biotechnol. 2014;32(8):819-21.
204. Straimer J, Gnadig NF, Witkowski B, Amaratunga C, Duru V, Ramadani AP, et al. Drug resistance. K13-propeller mutations confer artemisinin resistance in Plasmodium falciparum clinical isolates. Science. 2015;347(6220):428-31.
205. Gil JP, Nogueira F, Stromberg-Norklit J, Lindberg J, Carrolo M, Casimiro C, et al. Detection of atovaquone and Malarone resistance conferring mutations in Plasmodium falciparum cytochrome b gene (cytb). Mol Cell Probes. 2003;17(2-3):85-9.
206. Madamet M, Briolant S, Amalvict R, Benoit N, Bouchiba H, Cren J, et al. The Plasmodium falciparum chloroquine resistance transporter is associated with the ex vivo P. falciparum African parasite response to pyronaridine. Parasit Vectors. 2016;9:77.
207. Sidhu AB, Uhlemann AC, Valderramos SG, Valderramos JC, Krishna S, Fidock DA. Decreasing pfmdr1 copy number in plasmodium falciparum malaria heightens susceptibility to mefloquine, lumefantrine, halofantrine, quinine, and artemisinin. The Journal of infectious diseases. 2006;194(4):528-35.
208. Sisowath C, Stromberg J, Martensson A, Msellem M, Obondo C, Bjorkman A, et al. In vivo selection of Plasmodium falciparum pfmdr1 86N coding alleles by artemether-lumefantrine (Coartem). The Journal of infectious diseases. 2005;191(6):1014-7.
209. Maude RJ, Hoque G, Hasan MU, Sayeed A, Akter S, Samad R, et al. Timing of enteral feeding in cerebral malaria in resource-poor settings: a randomized trial. PLoS One. 2011;6(11):e27273.
210. Crawley J, Waruiru C, Mithwani S, Mwangi I, Watkins W, Ouma D, et al. Effect of phenobarbital on seizure frequency and mortality in childhood cerebral malaria: a randomised, controlled intervention study. Lancet. 2000;355(9205):701-6.
211. Hanson J, Anstey NM, Bihari D, White NJ, Day NP, Dondorp AM. The fluid management of adults with severe malaria. Crit Care. 2014;18(6):642.
212. Nguyen HP, Hanson J, Bethell D, Nguyen TH, Tran TH, Ly VC, et al. A retrospective analysis of the haemodynamic and metabolic effects of fluid resuscitation in Vietnamese adults with severe falciparum malaria. PLoS One. 2011;6(10):e25523.
213. Kwiatkowski D, Molyneux ME, Stephens S, Curtis N, Klein N, Pointaire P, et al. Anti-TNF therapy inhibits fever in cerebral malaria. Q J Med. 1993;86(2):91-8.
214. Hoffman SL, Rustama D, Punjabi NH, Surampaet B, Sanjaya B, Dimpudus AJ, et al. High-dose dexamethasone in quinine-treated patients with cerebral malaria: a double-blind, placebo-controlled trial. The Journal of infectious diseases. 1988;158(2):325-31.
215. Warrell DA, Looareesuwan S, Warrell MJ, Kasemsarn P, Intaraprasert R, Bunnag D, et al. Dexamethasone proves deleterious in cerebral malaria. A double-blind trial in 100 comatose patients. N Engl J Med. 1982;306(6):313-9.
216. Mohanty S, Mishra SK, Patnaik R, Dutt AK, Pradhan S, Das B, et al. Brain swelling and mannitol therapy in adult cerebral malaria: a randomized trial. Clin Infect Dis. 2011;53(4):349-55.
217. Namutangula B, Ndeezi G, Byarugaba JS, Tumwine JK. Mannitol as adjunct therapy for childhood cerebral malaria in Uganda: a randomized clinical trial. Malar J. 2007;6:138.
218. Westermann AJ, Forstner KU, Amman F, Barquist L, Chao Y, Schulte LN, et al. Dual RNA-seq unveils noncoding RNA functions in host-pathogen interactions. Nature. 2016;529(7587):496-501.
219. Thanert R, Goldmann O, Beineke A, Medina E. Host-inherent variability influences the transcriptional response of Staphylococcus aureus during in vivo infection. Nat Commun. 2017;8:14268.

220. Shenoy AT, Brissac T, Gilley RP, Kumar N, Wang Y, Gonzalez-Juarbe N, et al. Streptococcus pneumoniae in the heart subvert the host response through biofilm-mediated resident macrophage killing. PLoS Pathog. 2017;13(8):e1006582.
221. Wesolowska-Andersen A, Everman JL, Davidson R, Rios C, Herrin R, Eng C, et al. Dual RNA-seq reveals viral infections in asthmatic children without respiratory illness which are associated with changes in the airway transcriptome. Genome Biol. 2017;18(1):12.
222. Park SJ, Kumar M, Kwon HI, Seong RK, Han K, Song JM, et al. Dynamic changes in host gene expression associated with H5N8 avian influenza virus infection in mice. Sci Rep. 2015;5:16512.
223. Abate F, Ambrosio MR, Mundo L, Laginestra MA, Fuligni F, Rossi M, et al. Distinct Viral and Mutational Spectrum of Endemic Burkitt Lymphoma. PLoS Pathog. 2015;11(10):e1005158.
224. Foth BJ, Tsai IJ, Reid AJ, Bancroft AJ, Nichol S, Tracey A, et al. Whipworm genome and dual-species transcriptome analyses provide molecular insights into an intimate host-parasite interaction. Nat Genet. 2014;46(7):693-700.
225. Yamagishi J, Natori A, Tolba ME, Mongan AE, Sugimoto C, Katayama T, et al. Interactive transcriptome analysis of malaria patients and infecting Plasmodium falciparum. Genome research. 2014;24(9):1433-44.
226. Wang Z, Cabrera M, Yang J, Yuan L, Gupta B, Liang X, et al. Genome-wide association analysis identifies genetic loci associated with resistance to multiple antimalarials in Plasmodium falciparum from China-Myanmar border. Sci Rep. 2016;6:33891.
227. Penman B, Buckee C, Gupta S, Nee S. Genome-wide association studies in Plasmodium species. BMC Biol. 2010;8:90.
228. Jallow M, Teo YY, Small KS, Rockett KA, Deloukas P, Clark TG, et al. Genome-wide and fine-resolution association analysis of malaria in West Africa. Nat Genet. 2009;41(6):657-65.
229. Lal K, Prieto JH, Bromley E, Sanderson SJ, Yates JR, 3rd, Wastling JM, et al. Characterisation of Plasmodium invasive organelles; an ookinete microneme proteome. Proteomics. 2009;9(5):1142-51.
230. Fontaine A, Bourdon S, Belghazi M, Pophillat M, Fourquet P, Granjeaud S, et al. Plasmodium falciparum infection-induced changes in erythrocyte membrane proteins. Parasitol Res. 2012;110(2):545-56.
231. Torrentino-Madamet M, Almeras L, Desplans J, Le Priol Y, Belghazi M, Pophillat M, et al. Global response of Plasmodium falciparum to hyperoxia: a combined transcriptomic and proteomic approach. Malar J. 2011;10:4.
232. Moussa EM, Huang H, Thezenas ML, Fischer R, Ramaprasad A, Sisay-Joof F, et al. Proteomic profiling of the plasma of Gambian children with cerebral malaria. Malar J. 2018;17(1):337.
233. Antwi-Baffour S, Adjei JK, Agyemang-Yeboah F, Annani-Akollor M, Kyeremeh R, Asare GA, et al. Proteomic analysis of microparticles isolated from malaria positive blood samples. Proteome Sci. 2016;15:5.
234. Bertin GI, Sabbagh A, Argy N, Salnot V, Ezinmegnon S, Agbota G, et al. Proteomic analysis of Plasmodium falciparum parasites from patients with cerebral and uncomplicated malaria. Sci Rep. 2016;6:26773.
235. Doolan DL, Mu Y, Unal B, Sundaresh S, Hirst S, Valdez C, et al. Profiling humoral immune responses to P. falciparum infection with protein microarrays. Proteomics. 2008;8(22):4680-94.
236. Makanga M, Bray PG, Horrocks P, Ward SA. Towards a proteomic definition of CoArtem action in Plasmodium falciparum malaria. Proteomics. 2005;5(7):1849-58.
237. Le Roch KG, Johnson JR, Ahiboh H, Chung DW, Prudhomme J, Plouffe D, et al. A systematic approach to understand the mechanism of action of the bisthiazolium compound T4 on the human malaria parasite, Plasmodium falciparum. BMC genomics. 2008;9:513.
238. Jensen K, Plichta D, Panagiotou G, Kouskoumvekaki I. Mapping the genome of Plasmodium falciparum on the drug-like chemical space reveals novel anti-malarial targets and potential drug leads. Mol Biosyst. 2012;8(6):1678-85.
239. Briolant S, Almeras L, Belghazi M, Boucomont-Chapeaublanc E, Wurtz N, Fontaine A, et al. Plasmodium falciparum proteome changes in response to doxycycline treatment. Malar J. 2010;9:141.

240. Ye X, Blonder J, Veenstra TD. Targeted proteomics for validation of biomarkers in clinical samples. Brief Funct Genomic Proteomic. 2009;8(2):126-35.
241. Issaq HJ, Xiao Z, Veenstra TD. Serum and plasma proteomics. Chem Rev. 2007;107(8):3601-20.
242. Ramaprasad A, Pain A, Ravasi T. Defining the protein interaction network of human malaria parasite Plasmodium falciparum. Genomics. 2012;99(2):69-75.
243. Florens L, Washburn MP, Raine JD, Anthony RM, Grainger M, Haynes JD, et al. A proteomic view of the Plasmodium falciparum life cycle. Nature. 2002;419(6906):520-6.
244. Sobota RS, Dara A, Manning JE, Niangaly A, Bailey JA, Kone AK, et al. Expression of complement and toll-like receptor pathway genes is associated with malaria severity in Mali: a pilot case control study. Malaria journal. 2016;15:150.
245. Ylostalo J, Randall AC, Myers TA, Metzger M, Krogstad DJ, Cogswell FB. Transcriptome profiles of host gene expression in a monkey model of human malaria. The Journal of infectious diseases. 2005;191(3):400-9.
246. Oakley MS, McCutchan TF, Anantharaman V, Ward JM, Faucette L, Erexson C, et al. Host biomarkers and biological pathways that are associated with the expression of experimental cerebral malaria in mice. Infection and immunity. 2008;76(10):4518-29.
247. Oakley MS, Anantharaman V, Venancio TM, Zheng H, Mahajan B, Majam V, et al. Molecular correlates of experimental cerebral malaria detectable in whole blood. Infection and immunity. 2011;79(3):1244-53.
248. Miu J, Hunt NH, Ball HJ. Predominance of interferon-related responses in the brain during murine malaria, as identified by microarray analysis. Infection and immunity. 2008;76(5):1812-24.
249. Lovegrove FE, Gharib SA, Patel SN, Hawkes CA, Kain KC, Liles WC. Expression microarray analysis implicates apoptosis and interferon-responsive mechanisms in susceptibility to experimental cerebral malaria. The American journal of pathology. 2007;171(6):1894-903.
250. Lovegrove FE, Pena-Castillo L, Mohammad N, Liles WC, Hughes TR, Kain KC. Simultaneous host and parasite expression profiling identifies tissue-specific transcriptional programs associated with susceptibility or resistance to experimental cerebral malaria. BMC genomics. 2006;7:295.
251. Sexton AC, Good RT, Hansen DS, D'Ombrain MC, Buckingham L, Simpson K, et al. Transcriptional profiling reveals suppressed erythropoiesis, up-regulated glycolysis, and interferon-associated responses in murine malaria. The Journal of infectious diseases. 2004;189(7):1245-56.
252. Feintuch CM, Saidi A, Seydel K, Chen G, Goldman-Yassen A, Mita-Mendoza NK, et al. Activated Neutrophils Are Associated with Pediatric Cerebral Malaria Vasculopathy in Malawian Children. mBio. 2016;7(1):e01300-15.
253. Walther M, Jeffries D, Finney OC, Njie M, Ebonyi A, Deininger S, et al. Distinct roles for FOXP3 and FOXP3 CD4 T cells in regulating cellular immunity to uncomplicated and severe Plasmodium falciparum malaria. PLoS Pathog. 2009;5(4):e1000364.
254. Cunnington AJ, Njie M, Correa S, Takem EN, Riley EM, Walther M. Prolonged neutrophil dysfunction after Plasmodium falciparum malaria is related to hemolysis and heme oxygenase-1 induction. J Immunol. 2012;189(11):5336-46.
255. Cunnington AJ, Riley EM, Walther M. Microvascular dysfunction in severe Plasmodium falciparum Malaria. The Journal of infectious diseases. 2013;207(2):369-70.
256. Carroll RW, Wainwright MS, Kim KY, Kidambi T, Gomez ND, Taylor T, et al. A rapid murine coma and behavior scale for quantitative assessment of murine cerebral malaria. PLoS One. 2010;5(10).
257. Meyer A, Paroni F, Gunther K, Dharmadhikari G, Ahrens W, Kelm S, et al. Evaluation of Existing Methods for Human Blood mRNA Isolation and Analysis for Large Studies. PLoS One. 2016;11(8):e0161778.
258. O'Gorman WE, Dooms H, Thorne SH, Kuswanto WF, Simonds EF, Krutzik PO, et al. The initial phase of an immune response functions to activate regulatory T cells. J Immunol. 2009;183(1):332-9.

259. Trager W, Jensen JB. Human malaria parasites in continuous culture. Science. 1976;193(4254):673-5.
260. Maier AG, Rug M. In vitro culturing Plasmodium falciparum erythrocytic stages. Methods Mol Biol. 2013;923:3-15.
261. Dluzewski AR, Ling IT, Rangachari K, Bates PA, Wilson RJ. A simple method for isolating viable mature parasites of Plasmodium falciparum from cultures. Trans R Soc Trop Med Hyg. 1984;78(5):622-4.
262. Paul F, Roath S, Melville D, Warhurst DC, Osisanya JO. Separation of malaria-infected erythrocytes from whole blood: use of a selective high-gradient magnetic separation technique. Lancet. 1981;2(8237):70-1.
263. Murray L, Stewart LB, Tarr SJ, Ahouidi AD, Diakite M, Amambua-Ngwa A, et al. Multiplication rate variation in the human malaria parasite Plasmodium falciparum. Sci Rep. 2017;7(1):6436.
264. Ribaut C, Berry A, Chevalley S, Reybier K, Morlais I, Parzy D, et al. Concentration and purification by magnetic separation of the erythrocytic stages of all human Plasmodium species. Malar J. 2008;7:45.
265. Malleret B, Claser C, Ong AS, Suwanarusk R, Sriprawat K, Howland SW, et al. A rapid and robust tri-color flow cytometry assay for monitoring malaria parasite development. Sci Rep. 2011;1:118.
266. Voller A, Bartlett A, Bidwell DE. Enzyme immunoassays with special reference to ELISA techniques. J Clin Pathol. 1978;31(6):507-20.
267. Schindelin J, Arganda-Carreras I, Frise E, Kaynig V, Longair M, Pietzsch T, et al. Fiji: an open-source platform for biological-image analysis. Nat Methods. 2012;9(7):676-82.
268. de Chaumont F, Dallongeville S, Chenouard N, Herve N, Pop S, Provoost T, et al. Icy: an open bioimage informatics platform for extended reproducible research. Nat Methods. 2012;9(7):690-6.
269. Bretscher MT, Georgiadou A, Lee HJ, Walther M, van Beek AE, Fitriani F, et al. Estimating parasite load dynamics to reveal novel resistance mechanisms to human malaria. bioRxiv. 2018.
270. Lee HJ, Georgiadou A, Walther M, Nwakanma D, Stewart LB, Levin M, et al. Integrated pathogen load and dual transcriptome analysis of systemic host-pathogen interactions in severe malaria. Science translational medicine. 2018;10(447).
271. Team RC. R: A Language and Environment for Statistical Computing. 2014.
272. Westermann AJ, Barquist L, Vogel J. Resolving host-pathogen interactions by dual RNA-seq. PLoS Pathog. 2017;13(2):e1006033.
273. Marsh K, Forster D, Waruiru C, Mwangi I, Winstanley M, Marsh V, et al. Indicators of life-threatening malaria in African children. N Engl J Med. 1995;332(21):1399-404.
274. Higgins SJ, Kain KC, Liles WC. Immunopathogenesis of falciparum malaria: implications for adjunctive therapy in the management of severe and cerebral malaria. Expert Rev Anti Infect Ther. 2011;9(9):803-19.
275. Gazzinelli RT, Kalantari P, Fitzgerald KA, Golenbock DT. Innate sensing of malaria parasites. Nat Rev Immunol. 2014;14(11):744-57.
276. van der Poll T, van de Veerdonk FL, Scicluna BP, Netea MG. The immunopathology of sepsis and potential therapeutic targets. Nat Rev Immunol. 2017;17(7):407-20.
277. Prescott JB, Marzi A, Safronetz D, Robertson SJ, Feldmann H, Best SM. Immunobiology of Ebola and Lassa virus infections. Nat Rev Immunol. 2017;17(3):195-207.
278. Openshaw PJM, Chiu C, Culley FJ, Johansson C. Protective and Harmful Immunity to RSV Infection. Annu Rev Immunol. 2017;35:501-32.
279. Shen-Orr SS, Gaujoux R. Computational deconvolution: extracting cell type-specific information from heterogeneous samples. Curr Opin Immunol. 2013;25(5):571-8.
280. Hoeijmakers WA, Bartfai R, Stunnenberg HG. Transcriptome analysis using RNA-Seq. Methods Mol Biol. 2013;923:221-39.
281. Dietmann A, Helbok R, Lackner P, Issifou S, Lell B, Matsiegui PB, et al. Matrix metalloproteinases and their tissue inhibitors (TIMPs) in Plasmodium falciparum malaria: serum levels

of TIMP-1 are associated with disease severity. The Journal of infectious diseases. 2008;197(11):1614-20.
282. Polimeni M, Prato M. Host matrix metalloproteinases in cerebral malaria: new kids on the block against blood-brain barrier integrity? Fluids and barriers of the CNS. 2014;11(1):1.
283. Vandenbroucke RE, Dejonckheere E, Van Lint P, Demeestere D, Van Wonterghem E, Vanlaere I, et al. Matrix metalloprotease 8-dependent extracellular matrix cleavage at the blood-CSF barrier contributes to lethality during systemic inflammatory diseases. The Journal of neuroscience : the official journal of the Society for Neuroscience. 2012;32(29):9805-16.
284. Clark IA, Alleva LM, Mills AC, Cowden WB. Pathogenesis of malaria and clinically similar conditions. Clinical microbiology reviews. 2004;17(3):509-39, table of contents.
285. Solan PD, Dunsmore KE, Denenberg AG, Odoms K, Zingarelli B, Wong HR. A novel role for matrix metalloproteinase-8 in sepsis. Critical care medicine. 2012;40(2):379-87.
286. Lauhio A, Hastbacka J, Pettila V, Tervahartiala T, Karlsson S, Varpula T, et al. Serum MMP-8, -9 and TIMP-1 in sepsis: high serum levels of MMP-8 and TIMP-1 are associated with fatal outcome in a multicentre, prospective cohort study. Hypothetical impact of tetracyclines. Pharmacological research. 2011;64(6):590-4.
287. Lewallen S, Taylor TE, Molyneux ME, Wills BA, Courtright P. Ocular fundus findings in Malawian children with cerebral malaria. Ophthalmology. 1993;100(6):857-61.
288. Lewallen S, Bakker H, Taylor TE, Wills BA, Courtright P, Molyneux ME. Retinal findings predictive of outcome in cerebral malaria. Trans R Soc Trop Med Hyg. 1996;90(2):144-6.
289. Hero M, Harding SP, Riva CE, Winstanley PA, Peshu N, Marsh K. Photographic and angiographic characterization of the retina of Kenyan children with severe malaria. Arch Ophthalmol. 1997;115(8):997-1003.
290. Lewallen S, Harding SP, Ajewole J, Schulenburg WE, Molyneux ME, Marsh K, et al. A review of the spectrum of clinical ocular fundus findings in P. falciparum malaria in African children with a proposed classification and grading system. Trans R Soc Trop Med Hyg. 1999;93(6):619-22.
291. Beare NA, Southern C, Chalira C, Taylor TE, Molyneux ME, Harding SP. Prognostic significance and course of retinopathy in children with severe malaria. Arch Ophthalmol. 2004;122(8):1141-7.
292. Hawkes M, Elphinstone RE, Conroy AL, Kain KC. Contrasting pediatric and adult cerebral malaria: the role of the endothelial barrier. Virulence. 2013;4(6):543-55.
293. Nickla DL, Wallman J. The multifunctional choroid. Prog Retin Eye Res. 2010;29(2):144-68.
294. Margolis R, Spaide RF. A pilot study of enhanced depth imaging optical coherence tomography of the choroid in normal eyes. Am J Ophthalmol. 2009;147(5):811-5.
295. Owen CA, Campbell EJ. The cell biology of leukocyte-mediated proteolysis. J Leukoc Biol. 1999;65(2):137-50.
296. Hanemaaijer R, Sorsa T, Konttinen YT, Ding Y, Sutinen M, Visser H, et al. Matrix metalloproteinase-8 is expressed in rheumatoid synovial fibroblasts and endothelial cells. Regulation by tumor necrosis factor-alpha and doxycycline. J Biol Chem. 1997;272(50):31504-9.
297. Wen G, Zhang C, Chen Q, Luong le A, Mustafa A, Ye S, et al. A Novel Role of Matrix Metalloproteinase-8 in Macrophage Differentiation and Polarization. J Biol Chem. 2015;290(31):19158-72.
298. Clemmensen SN, Bohr CT, Rorvig S, Glenthoj A, Mora-Jensen H, Cramer EP, et al. Olfactomedin 4 defines a subset of human neutrophils. J Leukoc Biol. 2012;91(3):495-500.
299. van der Flier LG, Haegebarth A, Stange DE, van de Wetering M, Clevers H. OLFM4 is a robust marker for stem cells in human intestine and marks a subset of colorectal cancer cells. Gastroenterology. 2009;137(1):15-7.
300. Zhang X, Huang Q, Yang Z, Li Y, Li CY. GW112, a novel antiapoptotic protein that promotes tumor growth. Cancer Res. 2004;64(7):2474-81.
301. Mosesson MW. Fibrinogen and fibrin structure and functions. J Thromb Haemost. 2005;3(8):1894-904.
302. Ross R. Atherosclerosis--an inflammatory disease. N Engl J Med. 1999;340(2):115-26.

303. Lominadze D, Dean WL, Tyagi SC, Roberts AM. Mechanisms of fibrinogen-induced microvascular dysfunction during cardiovascular disease. Acta Physiol (Oxf). 2010;198(1):1-13.
304. Lowe GD, Lee AJ, Rumley A, Price JF, Fowkes FG. Blood viscosity and risk of cardiovascular events: the Edinburgh Artery Study. Br J Haematol. 1997;96(1):168-73.
305. Murata T, Ishibashi T, Inomata H. Immunohistochemical detection of extravasated fibrinogen (fibrin) in human diabetic retina. Graefes Arch Clin Exp Ophthalmol. 1992;230(5):428-31.
306. Papayannopoulos V. Neutrophil extracellular traps in immunity and disease. Nat Rev Immunol. 2018;18(2):134-47.
307. Brinkmann V, Reichard U, Goosmann C, Fauler B, Uhlemann Y, Weiss DS, et al. Neutrophil extracellular traps kill bacteria. Science. 2004;303(5663):1532-5.
308. Lood C, Blanco LP, Purmalek MM, Carmona-Rivera C, De Ravin SS, Smith CK, et al. Neutrophil extracellular traps enriched in oxidized mitochondrial DNA are interferogenic and contribute to lupus-like disease. Nat Med. 2016;22(2):146-53.
309. Abi Abdallah DS, Lin C, Ball CJ, King MR, Duhamel GE, Denkers EY. Toxoplasma gondii triggers release of human and mouse neutrophil extracellular traps. Infection and immunity. 2012;80(2):768-77.
310. Saitoh T, Komano J, Saitoh Y, Misawa T, Takahama M, Kozaki T, et al. Neutrophil extracellular traps mediate a host defense response to human immunodeficiency virus-1. Cell Host Microbe. 2012;12(1):109-16.
311. Urban CF, Reichard U, Brinkmann V, Zychlinsky A. Neutrophil extracellular traps capture and kill Candida albicans yeast and hyphal forms. Cell Microbiol. 2006;8(4):668-76.
312. Walker MJ, Hollands A, Sanderson-Smith ML, Cole JN, Kirk JK, Henningham A, et al. DNase Sda1 provides selection pressure for a switch to invasive group A streptococcal infection. Nat Med. 2007;13(8):981-5.
313. Branzk N, Lubojemska A, Hardison SE, Wang Q, Gutierrez MG, Brown GD, et al. Neutrophils sense microbe size and selectively release neutrophil extracellular traps in response to large pathogens. Nat Immunol. 2014;15(11):1017-25.
314. Urban CF, Ermert D, Schmid M, Abu-Abed U, Goosmann C, Nacken W, et al. Neutrophil extracellular traps contain calprotectin, a cytosolic protein complex involved in host defense against Candida albicans. PLoS Pathog. 2009;5(10):e1000639.
315. Fuchs TA, Abed U, Goosmann C, Hurwitz R, Schulze I, Wahn V, et al. Novel cell death program leads to neutrophil extracellular traps. J Cell Biol. 2007;176(2):231-41.
316. Metzler KD, Goosmann C, Lubojemska A, Zychlinsky A, Papayannopoulos V. A myeloperoxidase-containing complex regulates neutrophil elastase release and actin dynamics during NETosis. Cell Rep. 2014;8(3):883-96.
317. Pilsczek FH, Salina D, Poon KK, Fahey C, Yipp BG, Sibley CD, et al. A novel mechanism of rapid nuclear neutrophil extracellular trap formation in response to Staphylococcus aureus. J Immunol. 2010;185(12):7413-25.
318. Yipp BG, Petri B, Salina D, Jenne CN, Scott BN, Zbytnuik LD, et al. Infection-induced NETosis is a dynamic process involving neutrophil multitasking in vivo. Nat Med. 2012;18(9):1386-93.
319. Sercundes MK, Ortolan LS, Debone D, Soeiro-Pereira PV, Gomes E, Aitken EH, et al. Targeting Neutrophils to Prevent Malaria-Associated Acute Lung Injury/Acute Respiratory Distress Syndrome in Mice. PLoS Pathog. 2016;12(12):e1006054.
320. Baker VS, Imade GE, Molta NB, Tawde P, Pam SD, Obadofin MO, et al. Cytokine-associated neutrophil extracellular traps and antinuclear antibodies in Plasmodium falciparum infected children under six years of age. Malar J. 2008;7:41.
321. Boeltz S, Munoz LE, Fuchs TA, Herrmann M. Neutrophil Extracellular Traps Open the Pandora's Box in Severe Malaria. Front Immunol. 2017;8:874.
322. Gallego-Delgado J, Ty M, Orengo JM, van de Hoef D, Rodriguez A. A surprising role for uric acid: the inflammatory malaria response. Curr Rheumatol Rep. 2014;16(2):401.

323. Schorn C, Janko C, Krenn V, Zhao Y, Munoz LE, Schett G, et al. Bonding the foe - NETting neutrophils immobilize the pro-inflammatory monosodium urate crystals. Front Immunol. 2012;3:376.
324. Olivier M, Van Den Ham K, Shio MT, Kassa FA, Fougeray S. Malarial pigment hemozoin and the innate inflammatory response. Front Immunol. 2014;5:25.
325. Kho S, Minigo G, Andries B, Leonardo L, Prayoga P, Poespoprodjo JR, et al. Circulating neutrophil extracellular traps and neutrophil activation are increased in proportion to disease severity in human malaria. The Journal of infectious diseases. 2018.
326. Becker BF, Jacob M, Leipert S, Salmon AH, Chappell D. Degradation of the endothelial glycocalyx in clinical settings: searching for the sheddases. Br J Clin Pharmacol. 2015;80(3):389-402.
327. Hempel C, Pasini EM, Kurtzhals JAL. Endothelial Glycocalyx: Shedding Light on Malaria Pathogenesis. Trends Mol Med. 2016;22(6):453-7.
328. Lavoie SS, Dumas E, Vulesevic B, Neagoe PE, White M, Sirois MG. Synthesis of Human Neutrophil Extracellular Traps Contributes to Angiopoietin-Mediated In Vitro Proinflammatory and Proangiogenic Activities. J Immunol. 2018;200(11):3801-13.
329. Yeo TW, Lampah DA, Gitawati R, Tjitra E, Kenangalem E, Piera K, et al. Angiopoietin-2 is associated with decreased endothelial nitric oxide and poor clinical outcome in severe falciparum malaria. Proceedings of the National Academy of Sciences of the United States of America. 2008;105(44):17097-102.
330. Brill A, Fuchs TA, Savchenko AS, Thomas GM, Martinod K, De Meyer SF, et al. Neutrophil extracellular traps promote deep vein thrombosis in mice. J Thromb Haemost. 2012;10(1):136-44.
331. Papayannopoulos V, Metzler KD, Hakkim A, Zychlinsky A. Neutrophil elastase and myeloperoxidase regulate the formation of neutrophil extracellular traps. J Cell Biol. 2010;191(3):677-91.
332. Brinkmann V, Laube B, Abu Abed U, Goosmann C, Zychlinsky A. Neutrophil extracellular traps: how to generate and visualize them. J Vis Exp. 2010(36).
333. Hikosaka K, Hirai M, Komatsuya K, Ono Y, Kita K. Lactate retards the development of erythrocytic stages of the human malaria parasite Plasmodium falciparum. Parasitology international. 2015;64(3):301-3.
334. Ishioka H, Ghose A, Charunwatthana P, Maude R, Plewes K, Kingston H, et al. Sequestration and Red Cell Deformability as Determinants of Hyperlactatemia in Falciparum Malaria. The Journal of infectious diseases. 2016;213(5):788-93.
335. Mackinnon MJ, Li J, Mok S, Kortok MM, Marsh K, Preiser PR, et al. Comparative transcriptional and genomic analysis of Plasmodium falciparum field isolates. PLoS Pathog. 2009;5(10):e1000644.
336. Norata GD, Caligiuri G, Chavakis T, Matarese G, Netea MG, Nicoletti A, et al. The Cellular and Molecular Basis of Translational Immunometabolism. Immunity. 2015;43(3):421-34.
337. O'Neill LA, Pearce EJ. Immunometabolism governs dendritic cell and macrophage function. The Journal of experimental medicine. 2016;213(1):15-23.
338. Berens-Riha N, Kroidl I, Schunk M, Alberer M, Beissner M, Pritsch M, et al. Evidence for significant influence of host immunity on changes in differential blood count during malaria. Malar J. 2014;13:155.
339. Cowland JB, Borregaard N. Granulopoiesis and granules of human neutrophils. Immunol Rev. 2016;273(1):11-28.
340. Amulic B, Cazalet C, Hayes GL, Metzler KD, Zychlinsky A. Neutrophil function: from mechanisms to disease. Annu Rev Immunol. 2012;30:459-89.
341. Jorch SK, Kubes P. An emerging role for neutrophil extracellular traps in noninfectious disease. Nat Med. 2017;23(3):279-87.
342. Idaghdour Y, Quinlan J, Goulet JP, Berghout J, Gbeha E, Bruat V, et al. Evidence for additive and interaction effects of host genotype and infection in malaria. Proceedings of the National Academy of Sciences of the United States of America. 2012;109(42):16786-93.

343. Porcherie A, Mathieu C, Peronet R, Schneider E, Claver J, Commere PH, et al. Critical role of the neutrophil-associated high-affinity receptor for IgE in the pathogenesis of experimental cerebral malaria. The Journal of experimental medicine. 2011;208(11):2225-36.
344. Williams TN. Human red blood cell polymorphisms and malaria. Curr Opin Microbiol. 2006;9(4):388-94.
345. Kaestli M, Cockburn IA, Cortes A, Baea K, Rowe JA, Beck HP. Virulence of malaria is associated with differential expression of Plasmodium falciparum var gene subgroups in a case-control study. The Journal of infectious diseases. 2006;193(11):1567-74.
346. Dietz K, Raddatz G, Molineaux L. Mathematical model of the first wave of Plasmodium falciparum asexual parasitemia in non-immune and vaccinated individuals. Am J Trop Med Hyg. 2006;75(2 Suppl):46-55.
347. Arthur JS, Ley SC. Mitogen-activated protein kinases in innate immunity. Nat Rev Immunol. 2013;13(9):679-92.
348. Manning BD, Toker A. AKT/PKB Signaling: Navigating the Network. Cell. 2017;169(3):381-405.
349. Spaulding E, Fooksman D, Moore JM, Saidi A, Feintuch CM, Reizis B, et al. STING-Licensed Macrophages Prime Type I IFN Production by Plasmacytoid Dendritic Cells in the Bone Marrow during Severe Plasmodium yoelii Malaria. Plos Pathog. 2016;12(10).
350. Zander RA, Guthmiller JJ, Graham AC, Pope RL, Burke BE, Carr DJ, et al. Type I Interferons Induce T Regulatory 1 Responses and Restrict Humoral Immunity during Experimental Malaria. PLoS Pathog. 2016;12(10):e1005945.
351. Haque A, Best SE, Montes de Oca M, James KR, Ammerdorffer A, Edwards CL, et al. Type I IFN signaling in CD8- DCs impairs Th1-dependent malaria immunity. J Clin Invest. 2014;124(6):2483-96.
352. Edwards CL, Best SE, Gun SY, Claser C, James KR, de Oca MM, et al. Spatiotemporal requirements for IRF7 in mediating type I IFN-dependent susceptibility to blood-stage Plasmodium infection. Eur J Immunol. 2015;45(1):130-41.
353. Haque A, Best SE, Ammerdorffer A, Desbarrieres L, de Oca MM, Amante FH, et al. Type I interferons suppress CD4(+) T-cell-dependent parasite control during blood-stage Plasmodium infection. Eur J Immunol. 2011;41(9):2688-98.
354. Montes de Oca M, Kumar R, Rivera FL, Amante FH, Sheel M, Faleiro RJ, et al. Type I Interferons Regulate Immune Responses in Humans with Blood-Stage Plasmodium falciparum Infection. Cell Rep. 2016;17(2):399-412.
355. Ioannidis LJ, Nie CQ, Ly A, Ryg-Cornejo V, Chiu CY, Hansen DS. Monocyte- and Neutrophil-Derived CXCL10 Impairs Efficient Control of Blood-Stage Malaria Infection and Promotes Severe Disease. J Immunol. 2016;196(3):1227-38.
356. Manz MG, Boettcher S. Emergency granulopoiesis. Nat Rev Immunol. 2014;14(5):302-14.
357. Baum J, Pinder M, Conway DJ. Erythrocyte invasion phenotypes of Plasmodium falciparum in The Gambia. Infection and immunity. 2003;71(4):1856-63.
358. Theron M, Hesketh RL, Subramanian S, Rayner JC. An adaptable two-color flow cytometric assay to quantitate the invasion of erythrocytes by Plasmodium falciparum parasites. Cytometry A. 2010;77(11):1067-74.
359. Binks RH, Conway DJ. The major allelic dimorphisms in four Plasmodium falciparum merozoite proteins are not associated with alternative pathways of erythrocyte invasion. Mol Biochem Parasitol. 1999;103(1):123-7.
360. Satchwell TJ. Erythrocyte invasion receptors for Plasmodium falciparum: new and old. Transfus Med. 2016;26(2):77-88.
361. Malaria Genomic Epidemiology N, Band G, Rockett KA, Spencer CC, Kwiatkowski DP. A novel locus of resistance to severe malaria in a region of ancient balancing selection. Nature. 2015;526(7572):253-7.
362. Leffler EM, Band G, Busby GBJ, Kivinen K, Le QS, Clarke GM, et al. Resistance to malaria through structural variation of red blood cell invasion receptors. Science. 2017;356(6343).

363. Pasvol G, Wainscoat JS, Weatherall DJ. Erythrocytes deficiency in glycophorin resist invasion by the malarial parasite Plasmodium falciparum. Nature. 1982;297(5861):64-6.
364. Shemin D, Rittenberg D. The life span of the human red blood cell. J Biol Chem. 1946;166(2):627-36.
365. Kho S, Barber BE, Johar E, Andries B, Poespoprodjo JR, Kenangalem E, et al. Platelets kill circulating parasites of all major Plasmodium species in human malaria. Blood. 2018;132(12):1332-44.
366. Kumaratilake LM, Ferrante A, Rzepczyk CM. Tumor necrosis factor enhances neutrophil-mediated killing of Plasmodium falciparum. Infection and immunity. 1990;58(3):788-93.
367. Kumaratilake LM, Rathjen DA, Mack P, Widmer F, Prasertsiriroj V, Ferrante A. A synthetic tumor necrosis factor-alpha agonist peptide enhances human polymorphonuclear leukocyte-mediated killing of Plasmodium falciparum in vitro and suppresses Plasmodium chabaudi infection in mice. J Clin Invest. 1995;95(5):2315-23.
368. McMorran BJ, Marshall VM, de Graaf C, Drysdale KE, Shabbar M, Smyth GK, et al. Platelets kill intraerythrocytic malarial parasites and mediate survival to infection. Science. 2009;323(5915):797-800.
369. Oon S, Wilson NJ, Wicks I. Targeted therapeutics in SLE: emerging strategies to modulate the interferon pathway. Clin Transl Immunology. 2016;5(5):e79.
370. Pease JE. Designing small molecule CXCR3 antagonists. Expert Opin Drug Discov. 2017;12(2):159-68.
371. Mestas J, Hughes CC. Of mice and not men: differences between mouse and human immunology. J Immunol. 2004;172(5):2731-8.
372. Cagliani R, Sironi M. Pathogen-driven selection in the human genome. Int J Evol Biol. 2013;2013:204240.
373. Shay T, Jojic V, Zuk O, Rothamel K, Puyraimond-Zemmour D, Feng T, et al. Conservation and divergence in the transcriptional programs of the human and mouse immune systems. Proceedings of the National Academy of Sciences of the United States of America. 2013;110(8):2946-51.
374. Lin S, Lin Y, Nery JR, Urich MA, Breschi A, Davis CA, et al. Comparison of the transcriptional landscapes between human and mouse tissues. Proceedings of the National Academy of Sciences of the United States of America. 2014;111(48):17224-9.
375. Seok J, Warren HS, Cuenca AG, Mindrinos MN, Baker HV, Xu W, et al. Genomic responses in mouse models poorly mimic human inflammatory diseases. Proceedings of the National Academy of Sciences of the United States of America. 2013;110(9):3507-12.
376. Takao K, Miyakawa T. Genomic responses in mouse models greatly mimic human inflammatory diseases. Proceedings of the National Academy of Sciences of the United States of America. 2015;112(4):1167-72.
377. Godec J, Tan Y, Liberzon A, Tamayo P, Bhattacharya S, Butte AJ, et al. Compendium of Immune Signatures Identifies Conserved and Species-Specific Biology in Response to Inflammation. Immunity. 2016;44(1):194-206.
378. Normand R, Du W, Briller M, Gaujoux R, Starosvetsky E, Ziv-Kenet A, et al. Found In Translation: a machine learning model for mouse-to-human inference. Nat Methods. 2018;15(12):1067-73.
379. Lamb TJ, Brown DE, Potocnik AJ, Langhorne J. Insights into the immunopathogenesis of malaria using mouse models. Expert Rev Mol Med. 2006;8(6):1-22.
380. Huang BW, Pearman E, Kim CC. Mouse Models of Uncomplicated and Fatal Malaria. Bio Protoc. 2015;5(13).
381. Vandermosten L, Pham TT, Possemiers H, Knoops S, Van Herck E, Deckers J, et al. Experimental malaria-associated acute respiratory distress syndrome is dependent on the parasite-host combination and coincides with normocyte invasion. Malar J. 2018;17(1):102.
382. Swardson-Olver CJ, Dawson TC, Burnett RC, Peiper SC, Maeda N, Avery AC. Plasmodium yoelii uses the murine Duffy antigen receptor for chemokines as a receptor for normocyte invasion and an alternative receptor for reticulocyte invasion. Blood. 2002;99(8):2677-84.

383. Roberts DW, Weidanz WP. Splenomegaly, enhanced phagocytosis, and anemia are thymus-dependent responses to malaria. Infection and immunity. 1978;20(3):728-31.
384. Hunt NH, Grau GE, Engwerda C, Barnum SR, van der Heyde H, Hansen DS, et al. Murine cerebral malaria: the whole story. Trends in parasitology. 2010;26(6):272-4.
385. Van den Steen PE, Geurts N, Deroost K, Van Aelst I, Verhenne S, Heremans H, et al. Immunopathology and dexamethasone therapy in a new model for malaria-associated acute respiratory distress syndrome. Am J Respir Crit Care Med. 2010;181(9):957-68.
386. Gun SY, Claser C, Tan KS, Renia L. Interferons and interferon regulatory factors in malaria. Mediators Inflamm. 2014;2014:243713.
387. Baptista FG, Pamplona A, Pena AC, Mota MM, Pied S, Vigario AM. Accumulation of Plasmodium berghei-infected red blood cells in the brain is crucial for the development of cerebral malaria in mice. Infection and immunity. 2010;78(9):4033-9.
388. Epiphanio S, Campos MG, Pamplona A, Carapau D, Pena AC, Ataide R, et al. VEGF promotes malaria-associated acute lung injury in mice. PLoS Pathog. 2010;6(5):e1000916.
389. De Niz M, Heussler VT. Rodent malaria models: insights into human disease and parasite biology. Curr Opin Microbiol. 2018;46:93-101.
390. Yap GS, Stevenson MM. Blood transfusion alters the course and outcome of Plasmodium chabaudi AS infection in mice. Infection and immunity. 1994;62(9):3761-5.
391. Lamb TJ, Langhorne J. The severity of malarial anaemia in Plasmodium chabaudi infections of BALB/c mice is determined independently of the number of circulating parasites. Malar J. 2008;7:68.
392. Cabrales P, Zanini GM, Meays D, Frangos JA, Carvalho LJ. Murine cerebral malaria is associated with a vasospasm-like microcirculatory dysfunction, and survival upon rescue treatment is markedly increased by nimodipine. The American journal of pathology. 2010;176(3):1306-15.
393. Haque A, Best SE, Unosson K, Amante FH, de Labastida F, Anstey NM, et al. Granzyme B expression by CD8+ T cells is required for the development of experimental cerebral malaria. J Immunol. 2011;186(11):6148-56.
394. Belnoue E, Kayibanda M, Vigario AM, Deschemin JC, van Rooijen N, Viguier M, et al. On the pathogenic role of brain-sequestered alphabeta CD8+ T cells in experimental cerebral malaria. J Immunol. 2002;169(11):6369-75.
395. Hermsen C, van de Wiel T, Mommers E, Sauerwein R, Eling W. Depletion of CD4+ or CD8+ T-cells prevents Plasmodium berghei induced cerebral malaria in end-stage disease. Parasitology. 1997;114 (Pt 1):7-12.
396. Lacerda-Queiroz N, Lima OC, Carneiro CM, Vilela MC, Teixeira AL, Teixeira-Carvalho A, et al. Plasmodium berghei NK65 induces cerebral leukocyte recruitment in vivo: an intravital microscopic study. Acta Trop. 2011;120(1-2):31-9.
397. Walliker D, Sanderson A, Yoeli M, Hargreaves BJ. A genetic investigation of virulence in a rodent malaria parasite. Parasitology. 1976;72(2):183-94.
398. White WI, Evans CB, Taylor DW. Antimalarial antibodies of the immunoglobulin G2a isotype modulate parasitemias in mice infected with Plasmodium yoelii. Infection and immunity. 1991;59(10):3547-54.
399. Otsuki H, Kaneko O, Thongkukiatkul A, Tachibana M, Iriko H, Takeo S, et al. Single amino acid substitution in Plasmodium yoelii erythrocyte ligand determines its localization and controls parasite virulence. Proceedings of the National Academy of Sciences of the United States of America. 2009;106(17):7167-72.
400. Omer FM, de Souza JB, Riley EM. Differential induction of TGF-beta regulates proinflammatory cytokine production and determines the outcome of lethal and nonlethal Plasmodium yoelii infections. J Immunol. 2003;171(10):5430-6.
401. Wijayalath W, Danner R, Kleschenko Y, Majji S, Villasante EF, Richie TL, et al. HLA class II (DR0401) molecules induce Foxp3+ regulatory T cell suppression of B cells in Plasmodium yoelii strain 17XNL malaria. Infection and immunity. 2014;82(1):286-97.

402. Achtman AH, Khan M, MacLennan IC, Langhorne J. Plasmodium chabaudi chabaudi infection in mice induces strong B cell responses and striking but temporary changes in splenic cell distribution. J Immunol. 2003;171(1):317-24.
403. Findlay EG, Greig R, Stumhofer JS, Hafalla JC, de Souza JB, Saris CJ, et al. Essential role for IL-27 receptor signaling in prevention of Th1-mediated immunopathology during malaria infection. J Immunol. 2010;185(4):2482-92.
404. Stuart JM, Segal E, Koller D, Kim SK. A gene-coexpression network for global discovery of conserved genetic modules. Science. 2003;302(5643):249-55.
405. Zheng-Bradley X, Rung J, Parkinson H, Brazma A. Large scale comparison of global gene expression patterns in human and mouse. Genome Biol. 2010;11(12):R124.
406. Liao BY, Zhang J. Null mutations in human and mouse orthologs frequently result in different phenotypes. Proceedings of the National Academy of Sciences of the United States of America. 2008;105(19):6987-92.
407. Bugelski PJ, Martin PL. Concordance of preclinical and clinical pharmacology and toxicology of therapeutic monoclonal antibodies and fusion proteins: cell surface targets. Br J Pharmacol. 2012;166(3):823-46.
408. Hunig T. The storm has cleared: lessons from the CD28 superagonist TGN1412 trial. Nat Rev Immunol. 2012;12(5):317-8.

Appendix

Transcriptomic studies in malaria

Table 10: Selected transcriptomic studies in malaria.

Method (RNA-seq / Microarray)	***Sample/Tissue***	***Subjects***	***Aims***	***Key Findings***	***References***	***Year***
• Microarrays • Affymetrix mouse U74Av2 array, which includes 15,000 probe sets that represent functionally characterized sequences (6000) in the mouse Uni-Gene database plus 6000 EST clusters	*Brain and Spleen*	*C57BL/6 mice infected with P. berghei ANKA strain blood-stage parasites*	*To investigate proximal (biological) processes during development of severe malaria*	*Increased transcription of genes in glycolytic pathway. Suppressed erythropoietic transcription. Considerable transcriptional regulation of chemokines and their receptors. Cytokine genes undetectable. Strong increase of IFN-inducible gene transcripts*	*Transcriptional Profiling Reveals Suppressed Erythropoiesis, Up-Regulated Glycolysis, and Interferon-Associated Responses in Murine Malaria*	*Sexton et al. 2004*
Microarray Data	*Parasites from whole Blood (and in vitro parasites)*	*Human patients with malaria*	*To determine whether it is feasible to study in vivo parasite transcriptome, and also to determine (superficially) the similarities and differences between in vivo and in vitro parasites.*	*Only transcriptome of chromosome 2 was studied. Similar transcriptional profile between in vivo and in vitro. Overexpression of genes encoding surface proteins such as rifins and SERA antigens found in vivo.*	*In vivo transcriptional profiling of Plasmodium falciparum*	*Daily et al. 2004*
• Microarrays • Microarray chips (HG-U133A; Affymetrix) containing 22,215 probes representing 15,003 genes	*Whole Blood*	*Rhesus monkeys (Macaca mulatta) infected with parasite P. cynomologi bastianellii infected with **P vivax***	*Use of human microarrays to analyse gene expression in a rhesus monkey model of human P. vivax malaria (P. cynomolgi in Macaca mulatta)*	*Down-regulation of genes involved in RNA processing during the initial liver phase. Increased number of genes involved in defence response as infection evolved, but not of genes involved in cytoskeleton.*	*Transcriptome Profiles of Host Gene Expression in a Monkey Model of Human Malaria*	*Ylostalo et al. 2005*
Microarray Data	*Parasites from Whole Blood (and also in vitro parasites)*	*Human patients with malaria*	*To investigate similarities and differences of transcriptomes between in vivo and in vitro parasites*	*Strong correlation in gene expression between in vivo and in vitro parasites. Gene expression seem to differ between parasites from an adult and a child. Marked increase in genes encoding surface antigens for in vivo parasites. However, it was acknowledged that it is difficult to accurately determine the expression of var genes.*	*In Vivo Transcriptome of Plasmodium falciparum Reveals Overexpression of Transcripts That Encode Surface Proteins*	*Daily et al. 2005*
• Microarrays • Fluorescent cDNA probes - prepared through direct incorporation of Cy5 and Cy3 and hybridized to the Stanford University cDNA lymphochip microarray	*Whole Blood*	*Human patients (children) with malaria*	*To explore the host response to malaria (broad)*	*Found genes with expression associated with neutrophil counts. Samples could be clustered into patients with acute malaria or convalescent patients. The difference between two groups might be based on neutrophil-related genes. Erythrocyte-related genes increased expression - different from what was found in Sexton et al. Increased expression of genes associated with the interferon response.*	*Genomewide Analysis of the Host Response to Malaria in Kenyan Children*	*Griffiths et al. 2005*

Appendix

• Microarrays • 21,626 mouse probes/ 17,313 malaria sequences • Probe sequences submitted to Agilent Technologies (Palo Alto CA)	Brain, Liver, Spleen, Lung (both host organs and parasite found from organs	C57BL/6 (CM-susceptible) and BALB/c (CM-resistant) mice infected with P. berghei ANKA	To simultaneously examine both sides of the parasite-host interface to identify corresponding PbA and murine organ-specific expression profiles associated with resistance or susceptibility to CM	Showed that both host and pathogen transcriptomes can be examined in a single microarray. Parasites have organ-specific transcriptional profiles. Unique transcriptional profiles for both host and pathogen when susceptible mice compared to resistant mice.	Simultaneous host and parasite expression profiling identifies tissue-specific transcriptional programs associated with susceptibility or resistance to experimental cerebral malaria	Lovegrove et al. 2006
• Microarrays • Mouse Genome 430A 2.0 oligonucleotide microarray (Affymetrix, Santa Clara, CA)	Brain	C57BL/6 and CBA/J (CM-susceptible) and BALB/c and DBA/2 (CM-resistant) mice infected with P. berghei ANKA	To investigates the differences between transcriptomes of infected CM-susceptible and CM-resistant mice.	Showed that the CM-susceptible mice can be transcriptionally distinguished from the CM-resistant mice (31 genes consistently different). Overrepresentation of genes involved in defence and immune responses associated with CM.	Gene-Expression Profiling Discriminates between Cerebral Malaria (CM)-Susceptible Mice and CM-resistant mice	Delahaye et al. 2006
Microarray Data	Brain	C57BL/6 (CM-susceptible) and BALB/c (CM-resistant) mice infected with P. berghei ANKA	To define transcriptional patterns and regulatory pathways that distinguish host brain response to experimental cerebral malaria	CM-susceptible mice had change in transcriptional activity at day 6. Genes involved in immune, inflammatory, and apoptotic pathways increased. Hub genes involved in apoptosis and interferon response found. Promoter sites associated with regulation of interferon-stimulated genes were found	Expression Microarray Analysis Implicates Apoptosis and Interferon-Responsive Mechanism in Susceptibility to Experimental Cerebral Malaria	Lovegrove et al. 2007
Microarray Data	Parasites from Whole Blood	Parasites from 43 patients (Senegal), with a diverse age range 8.3 +_ 6.9 years, parasitaemia 5.5% +_6.2%, haematocrit 32.3+_6.8	To study the transcriptional variation between different P. falciparum strains driven by the host environment (human_in vivo)	Plasmodium parasite exists in the human host in at least three distinct physiological states, apparently related to glycolytic growth, a starvation response and a general (non-nutritional) stress response	Distinct physiological states of Plasmodium falciparum in malaria-infected patients	Daily et al. 2007
• Microarrays • Affymetrix GeneChip Mouse Genome 430 2.0 arrays (~43,000 genes) (Ramaciotti Centre, University of New South Wales)	Brain	CBA/T6 inoculated with PbA (fatal murine CM) or PbK (non-cerebral malaria) parasitized RBCs.	To investigate the response of genetically identical murine hosts to different, but related, parasite strains, PbA and PbK	Certain overlap of DE genes in both PbA and PbK (especially at the late stage for PbK) infected mice. Upregulation seen for IFN signaling pathways and immune response. However, certain critical mediators unique to PbA infection (signaling and transcription, apoptosis, immunomodulation, and antimicrobial activities). First study to compare FMCM with late stages of NCM.	Predominance of Interferon-Related Responses in the Brain during Murine Malaria, as Infected by Microarray Analysis	Miu et al. 2008
• Microarrays • Murine oligonucleotide chip containing 16,600 oligonucleotide probes (Qiagen, Valencia, CA)	Brain	C57BL/6 (ECM moribund - susceptible) and C57BL/6 (ECM nonmoribund), PFP-KO, CD8-KO, BALB/c (resistant) mice	To identify novel host molecules/biomarkers associated with the pathogenesis of ECM	200 genes with altered expression patterns in the brain that are strongly associated with the manifestation of ECM (and a lot of them were previously not found to be associated). Especially p21 and haemoglobin alpha-1.	Host Biomarkers and Biological Pathways That Are Associated with the Expression of Experimental Cerebral Malaria in Mice	Oakley et al. 2008
Microarray Data: Affymetrix PFSANGER arrays / Affymetrix GeneChip Scanner 3000 7G	Parasites from Whole Blood (isolates) cultivated (ex vivo) for 24 - 48 h to mature schizonts	Human patients with mild or severe malaria from Gambia (ex vivo). Along with reanalysis of in vivo data from Daily et al. 2007	To estimate cell cycle progression and commitment to asexual or sexual development lineages in our samples based on microscopy and gene expression patterns	Able to provide accurate estimation of sample age based on the gene expression profile. In cases matched for temporal development (compared samples are of the same age), no difference was found between severe and uncomplicated malaria, but this may have been due to small sample size. But comparing regardless of condition, able to find significantly differentially expressed genes (may reflect genuine variation in the field).	Statistical estimation of cell-cycle progression and lineage commitment in Plasmodium falciparum reveals a homogeneous pattern of transcription in ex vivo culture	Lemieux et al. 2009

Appendix

• Microarrays • Affymetrix U133A 2.0 and Plus 2.0 GeneChips (11-micron technology)	*Human PBMCs*	*Human patients with malaria*	*To determine whether there is a gene expression profile that is predictive of an individual's response to the adjuvanted RTS,S malaria vaccine and to identify the time at which the profile can be discerned before challenge.*	*Gene expression pattern is different between vaccinated and non-vaccinated subjects (all challenged). Certain genes (host inflammatory response, apoptosis, protein cascade kinase) are upregulated when subjects are vaccinated but they come down to normal levels after 72 hours. Subjects were also able to correctly be categorised into 3 different groups based on the gene expression. Proteasome pathway (based on GSEA) upregulated in protected patients.*	*Expression of Genes Associated with Immunoproteasome Processing of Major Histocompatibility Complex Peptides Is Indicative of Protection with Adjuvanted RTS,S Malaria Vaccine.*	*Vahey et al. 2010*
• RNA seq • NSR primers were designed to deplete human cytoplasmic 18S and 28S rRNA and human globin mRNA sequences • Single Illumina (Solexa) GA2 flow cell lane-36-mer sequence tags aligned simultaneously to P. falciparum and Homo sapiens sequences using the BowTie algorithm	*Parasites from Whole Blood (cultured in vitro)*	*Human patients (pregnant women and children) with malaria*	*To determine whether NSR-seq is capable of excluding globin mRNA and rRNA, and subsequently characterise expression profiles of parasites, including lowly expressed transcripts*	*NSR-seq is indeed capable of taking away uninteresting transcripts such as globin mRNA and rRNA, and capable of characterising the expression profiles of parasites from pregnant women and children. The study also identified several genes specific for parasites from pregnant women, as well as genes that can distinguish parasites from children.*	*NSR-seq transcriptional profiling enables identification of a gene signature of Plasmodium falciparum parasites infecting children*	*Vignali et al. 2011*
• Microarrays • Custom-designed-murine oligonucleotide chip - 37,500 probes (Agilent Technologies, Santa Clara, CA)	*Whole Blood*	*C57BL/6 and CBA/CaJ (CM-susceptible) and BALB/c (CM-resistant) mice*	*To identify novel host diagnostic biomarkers for ECM*	*Identified 300 putative diagnostic biomarkers of ECM. Transcriptional profile of whole blood captures the molecular and immunological events associated with the pathogenesis of disease. Study also found that during ECM, erythropoiesis is dysfunctional, thrombocytopenia is evident, and glycosylation of cell surface components may be modified. Susceptible mice have slightly distinct mechanisms of immunopathogenesis compared to resistant mice.*	*Molecular Correlates of Experimental Cerebral Malaria Detectable in Whole Blood*	*Oakley et al. 2011*
• Microarrays • Sentrix BeadChip Arrays, MouseWG-6 v2 (Illumina)	*Splenic (from spleen) CD4+ T-cells*	*C57BL/6 naïve and 4-day infected mice*	*To determine why CD4+ T-cells are ineffective at controlling parasites during PbA (Plasmodium berghei ANKA) infection*	*773 transcriptionally up- or down-regulated in 4 day p.i. mice compared to naïve mice. Type I and II IFN signalling-related genes most overrepresented. (the role of IFN I remains unclear). Protein studies using ELISA showed that IFN-alpha is generated in the spleen during PbA infection and that the CD4+ T-cell transcriptional signature may be shaped by this cytokine.*	*Type I interferons suppress CD4+ T-cell-dependent parasite control during blood-stage Plasmodium infection*	*Haque et al. 2011*
• Microarrays • Affymetrix GeneChip standard 1.0 ST arrays	*Whole Blood*	*Human patients (children) with severe malaria (blood taken when they had severe malaria, and subsequently when they had mild form of malaria)*	*To gain insight into host responses with severe and mild malaria.*	*68 genes identified to be associated with mild malaria and these genes are involved in interferon (IFN) pathway and T cell biology, and further GSEA revealed type I interferon-mediated signaling pathway and T cell activation. However, only 6 genes identified to be associated with severe malaria that includes thymidine kinase 1 which was previously found to be a biomarker for cerebral malaria susceptibility in murine malaria model.*	*Mild Plasmodium falciparum Malaria following an Episode of Severe Malaria Is Associated with Induction of the Interferon Pathway in Malawian Children*	*Krupka et al. 2012*

Appendix

• Microarrays • HumanHT-12 BeadChips (48k probes; Illumina) • Mouse WG-6 v2 BeadChips (Illumina)	*Whole Blood*	*Human patients (children) with malaria and C57BL/6J mice infected with Plasmodium chabaudi AS parasites*	*To uncover the heritable (genetic factors of the host) and infection-response components of host immunity to malaria infection*	*Study found genes associated with malaria that are sensitive to infection, implicate complement system, antigen processing and presentation, and T-cell activation. GWAS revealed SCO1 to be a candidate gene that is associated with malaria, and implicating a binding variation with a noncoding regulatory element.*	*Evidence for additive and interaction effects of host genotype and infection in malaria*	*Idaghdour et al. 2012*
Microarray Data	*Human PBMCs*	*Humans experimentally infected of malaria*	*To gain a better understanding of host immune response patterns associated with P. falciparum infection in humans (specifically TH1 response)*	*Showed upregulation of gene expression for toll-like receptor signalling. Also upregulation of expression of genes involved in TH17 immune response. Also other immune pathways, all in all suggesting that multiple immune pathways may be activated following infection.*	*Human immune responses to Plasmodium falciparum infection: molecular evidence for a suboptimal THαβ and TH17 bias over ideal and effective traditional TH1 immune response*	*Wan-Chung Hu 2013*
Microarray Data: SurePrint in situ synthesis technology (Agilent Technologies France SAS, Les Ulis, France)	*Parasites from Whole Blood (isolates) cultivated (ex vivo) for 24 to 38 h to obtain late trophozoites*	*54 children with P. falciparum infection from Cameroon & Benin: 18 CM, 18 acute uncomplicated malaria (UM), and 18 asymptomatic malaria (AM)*	*To identify potential virulence factors associated with severe clinical manifestations*	*Showed upregulation of genes involved in pathogenesis, adhesion to host cell, and erythrocyte aggregation when parasites from CM compared to parasites from asymptomatic patients. No significant difference seen between CM and UM*	*Differences in Gene Transcription Pattern of Plasmodium falciparum in Children with Cerebral Malaria and Asymptomatic Carriers*	*Almelli et al. 2014*
Microarray Data P. falciparum 244K gene expression array_Agilent platform_probes having 60-mer oligonucleotides representing the 3D7 transcript sequences (PlasmoDB version 5.3) , NCBI EST sequences of P. falciparum and apicoplast sequences of P. falciparum and P. vivax	*Density gradient based separation (Histopaque 1077, Sigma Aldrich, USA) of PBMCs from the RBC's. RNA extracted from the RBC fraction.*	*11 P. falciparum infected patients with uncomplicated (n = 2) or complicated malaria (n = 9) (mixed ages)*	*To determine whether NATs play a critical role in gene regulation*	*Majority of NATs show positive correlation with the expression of sense transcripts. However, 96 genes showed a change in ration between parasites from complicated and uncomplicated malaria. They map to genes involved in a variety of metabolic/biochemical pathways. Also found previously unidentified NATs.*	*Natural antisense transcripts in Plasmodium falciparum isolates from patients with complicated malaria*	*A.K. Subudhi et al. 2014*
RNA seq, TruSeq RNA-seq kit (Illumina), 36-bp single-end seq (Illumina GAIIx platform)	*Whole Blood (containing parasites)*	*116 Indonesian Pf patients, ages 0-40 years, 61 male-55 female.*	*To understand the molecular mechanisms of parasitism in vivo.*	*Parasite transcriptome well represented from data sequenced through dual RNA-seq. Identified human and parasite genes correlated with various clinical data (genes involved in innate immunity correlated with severity of the disease). Found groups of human genes strongly correlated with parasite genes (transcription regulatory factors).*	*Interactive transcriptome analysis of malaria patients and infecting Plasmodium falciparum*	*Yamagishi et al. 2014*

Appendix

Microarray Data	*Density gradient based separation (Histopaque 1077, Sigma Aldrich, USA) of PBMCs from the RBC's. RNA extracted from the RBC fraction.*	*Parasites from 12 P. falciparum infected patients (adults_mixed ages) exhibiting uncomplicated (n = 5) or complicated malaria (n = 7)*	*To investigate the in vivo parasite transcriptome to identify differences in gene expression between uncomplicated and complicated malaria*	*Genes relating to most of the metabolic pathways did not differ in expression profile between uncomplicated and complicated. Upregulation of variant surface antigens like the var B and C groups and upregulation of DC13 containing var A, members of the rifin and stevor, and some members of the exportome in P. falciparum isolates from adult patients showing complicated disease manifested as hepatic and renal dysfunction.*	*Plasmodium falciparum complicated malaria: Modulation and connectivity between exportome and variant surface antigen gene families.*	*A.K. Subudhi et al. 2015*
RNA-seq Data	*Whole Blood*	*Human patients with malaria (malaria-experienced with symptoms, malaria-experienced without symptoms, malaria-naïve with symptoms)*	*To identify molecular predictors and mechanisms of malaria disease to understand how Plasmodium falciparum malaria is controlled.*	*A graded activation of pathways of downstream of pro-inflammatory cytokines, with the highest activation in malaria-naïve Dutch individuals and significantly reduced activation in malaria-experienced Malians. Newly febrile and asymptomatic infections in Malians were statistically indistinguishable except for genes activated by pro-inflammatory cytokines.*	*Transcriptomic evidence for modulation of host inflammatory responses during febrile Plasmodium falciparum malaria*	*Tran et al. 2016*
• Microarrays *• Affymetrix Human Genome U133 Plus 2.0 GeneChip*	*Whole Blood*	*Human patients with malaria (uncomplicated and complicated), at the time of acute disease presentation, 1 week after presentation, treatment initiation, and in the subsequent dry season*	*To identify molecular markers of severe malaria*	*Complement and toll-like receptor differentially expressed (higher expression in severe malaria).*	*Expression of complement and toll-like receptor pathway genes is associated with malaria severity in Mali: a pilot case control study*	*Sobota et al. 2016*
• Microarrays *• Affymetrix GeneChip standard 1.0 ST arrays*	*Whole Blood*	*Human patients (children) with malaria (divided into presence and absence of retinopathy - strongly associated with cerebral malaria)*	*To identify host factors that facilitate iRBC cerebral sequestration*	*Neutrophil transcripts most highly upregulated in Ret+CM patients. Several neutrophil proteins elevated in Ret+CM patients, and neutrophil chemotaxis was impaired.*	*Activated Neutrophils Are Associated with Paediatric Cerebral Malaria Vasculopathy in Malawian Children*	*Feintuch et al. 2016*
Microarry data	*Whole Blood (parasites isolated and cultured)*	*BALB/c mice mice infected with P. berghei ANKA, P. chabaudi AS,P. yoelii.*	*To measure transcriptional changes of the evolutionary conserved syntenic orthologs during the intraerythrocytic developmental cycle across six Plasmodium species*	*For genes that are relatively conserved across species, constant expression can be observed, however, for genes that are species-specific, largely variable in expression. Modelling of the evolutionary relationship based on changes in transcriptional profile reveal a phylogeny pattern of the Plasmodium species that strictly follows its mammalian hosts.*	*Integrated analysis of the Plasmodium species transcriptome*	*R. Hoo et al. 2016*
Microarray data	*Whole blood (isolates)*	*Human patients with malaria*	*To determine the feasibility of studying the transcriptome of field isolates with limited genome sequence information using custom-made array.*	*It is indeed feasible to study the field isolates with limited genome sequence information, with large percentage of genes detected and probes targeting the same genes show perfect correlation. Variant surface antigen transcripts were also detected using the probes.*	*A cross strain Plasmodium falciparum microarray optimized for the transcriptome analysis of Plasmodium falciparum patient derived isolates*	*A.K. Subudhi et al. 2016*

Appendix

Microarray Data	*Spleen*	*BALB/c and BALB.B6-Cmv1 mice infected with P. berghei ANKA.*	*To analyse the impact of the NKC genotype in the development of severe malarial pathogenesis and the nature of various immune responses to infection.*	*Found that NKC regulates several immunopathological responses to malaria, including cerebral pathology, pulmonary oedema, and severe anaemia. NKC genotype was also found to influence parasite-specific antibody responses as well as the TH1/TH2 balance.*	*The Natural Killer Complex Regulates Severe Malarial Pathogenesis and Influences Acquired Immune Responses to Plasmodium berghei ANKA*	*Hansen et al. 2005*
Microarray Data	*Parasites from Whole Blood (isolated and cultured)*	*Human patients with malaria*	*To identify and characterise transcriptional variation among Plasmodium falciparum field isolates as well as laboratory isolates*	*Found that genes coding for parasite protein export into the red cell cytosol and onto its surface, and genes coding for sexual stage proteins involved in parasite transmission are upregulated in field isolates compared to laboratory isolates*	*Comparative transcriptional and genomic analysis of Plasmodium falciparum isolates*	*Mackinnon et al. 2009*
Microarray Data	*Parasites from Placenta and Peripheral Blood*	*Human patients with malaria (pregnant women and children)*	*To characterise the placenta binding phenotype of clinical parasites and to identify novel antigens that are expressed by parasites causing infections.*	*Transcription of six genes was substantially higher in both placental parasites and peripheral parasites from pregnant women, and each gene encodes a protein with a putative export sequence and/or transmembrane domain (var gene, and five genes with unknown functions).*	*Six Genes Are Preferentially Transcribed by the Circulating and Sequestered Forms of Plasmodium falciparum Parasites That Infect Pregnant Women*	*Francis et al. 2007*
Microarray Data Illumina BeadArray Single Color platform (Illumina.Single.Color.MouseRef -8)	*Whole blood*	*P. chabaudi chabaudi AJ. days 0–25 for surviving mice, days 0, 8, 10, 14, and 25 for control mice, days 8 and 11 d post infection for non-survivors*	*Mapping disease space in survivors and non-survivors*	*Dying mice trace a large arc in red blood cells (RBCs) by reticulocyte space as compared to surviving mice.*	*Tracking Resilience to Infections by Mapping Disease Space*	*Torres et al. 2016*
RNA-Seq; Illumina HiSeq2000, with 100-bp paired-end reads	*Whole blood, leukocyte depletion*	*P. c. chabaudi AS in B/6 mice*	*Determine how mosquito passage alters virulence of malaria parasites*	*Mosquito passage attenuates virulence compared to serial blood passage, and is associated with enhanced expression of exported proteins*	*Vector transmission regulates immune control of Plasmodium virulence*	*Spence, P. J. et al. 2013*
Illumina MOUSE WG-6 V2.0 Beadarrays	*Flow-sorted microglia from brain*	*P berghei ANKA*	*To compare gene expression profile of microglia isolated from uninfected mice and from mice infected with PbA at different time points after infection*	*Early proliferative response, followed by upregulation of type 1 interferon responsive genes*	*Transcriptomic profiling of microglia reveals signatures of cell activation and immune response, during experimental cerebral Transcriptomic profiling of microglia reveals signatures of cell activation and immune response, during experimental cerebral*	*Capuccini et al. 2016*
Microarray Data (Affymetrix U74Av2 GeneChips) 8305 mice genes	*Spleen*	*Female BALB/c mice infected with P. yoelli infected erythrocytes (17XNL and 17XL strains)*	*To identify host biomarkers that differentiate lethal and non-lethal blood stage malaria infections*	*Identified genes that correlated with the intensity of infection: metabolic perturbations, erythropoiesis, B-cell immune responses, and other immune responses*	*Genome-wide expression profiling in malaria infection reveals transcriptional changes associated with lethal and nonlethal outcomes*	*Schaecher et al. (2005)*
Microarray Data (Atlas TM 1.0; CLONTECH) 588 mice genes	*Brain collected at time points (2,4,6,8 post-infections)*	*Female Swiss Webster (SW) mice infected with P. yoelli infected erythrocytes (17XL strain)*	*To gain insight into the immunopathogenesis of malaria*	*Chemokine RANTES was upregulated at peak parasitaemia and stayed high through the infection, and upregulation of RANTES protein and plasma RANTES also observed.*	*Plasmodium yoelii 17XL infection up-regulates RANTES, CCR1, CCR3 and CCR5 expression, and induces ultrastructural changes in the cerebellum.*	*Sarfo et al. (2005)*

Appendix

Microarray Data (Affrymetrix GeneChip Mouse Expression 430A 2.0)	*Spleen (specifically, dendritic cells CD11c+ from spleen)*	*BALB/c mice infected with P. yoelli infected erythrocytes (17XNL strain)*	*To shed light into the different observations on DCs responses to Plasmodium parasites*	*Genes involved in cell cycle, glycolysis, purine metabolism, defense responses regulated in DCs of infected mice. Also found differential expression of various cytokine genes*	*Transcriptome profile of dendritic cells during malaria: cAMP regulation of IL-6.*	*Carapau et al. (2007)*
Microarray Data (Affymetrix Human Genome U133 Plus 2.0 GeneChip)	*Placenta (specifically, placenta villi)*	*Human (Tanzanian women aged 18-45)*	*To understand the host response to malaria in the malaria-positive tissue in humans*	*The first genome-wide analysis of human host response to sequestered parasites. Identified B-cell related genes to be most upregulated (B-cell chemoattractant and B cell-activating factor). IG L and H chain transcription also found to be upregulated. Heterogeneity in B-cell types observed in placenta. High upregulation of genes for the Fc binding proteins also observed.*	*Genome-wide expression analysis of placental malaria reveals features of lymphoid neogenesis during chronic infection.*	*Muehlenbachs et al. (2007)*
Microarray (custom combination of pre-existing arrays)	*Mouse whole brain*	*BALB/c (CM-Resistant strain), C57BL/6J and CBA/J (CM susceptible strains)*	*identify genes whose expression differ between CM-R and CM-S mice before the time of CM onset to identify early events that may participate in malaria pathogenesis*	*mouse CM is characterized by the deregulation of both immune response and glucose metabolism*	*Gene expression analysis reveals early changes in several molecular pathways in cerebral malaria-susceptible mice versus cerebral malaria-resistant mice.*	*Delahaye et al. (2007)*
Microarray Data (with oligonucleotides from Malaria Oligo set)	*Parasites from the placenta and 3D7 parasites from culture*	*Human (Pregnant and non-pregnant women, both with infection) (children with asymptomatic infection - only for validation).*	*To identify genes associated with placental tropism in placental malaria*	*In comparison with 3D7 culture gene expression, upregulation of genes located in subtelomeric regions and genes for exported proteins observed. One such gene, PFI1785w was suggested to be contributing to PAM pathogenesis besides VAR2CSA.*	*Plasmodium falciparum transcriptome analysis reveals pregnancy malaria associated gene expression.*	*Tuikue Ndam et al. (2008)*
MicroarrayL GE Healthcare Codelink Uniset Rat array	*Spleen*	*CM-Susceptible young rats (4wks old) vs uninfected age-matched rats; infected young rats vs infected adult rats at the same time post infection infected with PbANKA*	*Identify mechanisms underlying the impaired responses of young infected rats that lead to their susceptibility to CM*	*Small subset of genes differed between adult and juvenile rats in spleen at D13pi; evidence presented that two of these downregulated genes, p2y6r, and cd24 play a causal role*	*Gene profiling analysis reveals the contribution of CD24 and P2Y6R to the susceptibility of young rats to Plasmodium berghei infection.*	*Pierrot et al. (2011)*
Microarray Data	*Harvested PBMCs*	*Human (14 healthy patients infected with P. falciparum before and 3-5 weeks after mefloquine treatment)*	*To investigate the role of TLR-independent DNA sensors in type 1 interferon production during malaria*	*(Transcriptomic study not the main) Found interferon stimulated gens to be upregulated after P. falciparum infection.*	*Innate immune recognition of an AT-rich stem-loop DNA motif in the Plasmodium falciparum genome.*	*Sharma et al. (2011)*
Microarray Data (novel array with 169 format, 2.2 million probes in total, 11 probes per transcript) (contains probes for P. falciparum, P. berghei, P. yoelli, spanning protein-coding genes, non-coding genes, and var genes)	*Parasites from the peripheral blood*	*Human (children with CM and either positive or negative for retinopathy)*	*To determine whether there is specific biology related to severe malaria*	*Found to distinct physiological states that showed significant association with parasitaemia level. When compared to patients with mild disease and P. falciparum life-cycle expression profiles, unique biology of patients with severe malaria was revealed, with upregulation of Hrd1, a member of endoplasmic reticulum-associated protein degradation system*	*Transcriptional profiling of Plasmodium falciparum parasites from patients with severe malaria identifies distinct low vs. high parasitemic clusters.*	*Milner et al. (2012)*

Appendix

Plasmodium yoelii DNA microarrays	*Parasites from peripheral blood*	*Male BALB/c mice infected with P. yoelli infected erythrocytes (17XNL strain)*	*To establish the stability of parasite gene expression between different mice, over time and under immune pressure*	*Gene expression relatively stable between mice, variation during the course of non-lethal infection; translation machinery upregulated during ascending phase of parasitaemia; no difference between B-cell deficient and normal mice; no major effect of immunisation;*	*Remarkable stability in patterns of blood-stage gene expression during episodes of non-lethal Plasmodium yoelii malaria.*	*Cerenetich-Ott et al. (2012)*
Illumina MouseWG-6 v2.0 microarrays	*Brain*	*C57BL/6J (B6) and BXH2 mice (hypomorhpic mutation in IRF8; ECM resistant) either prior to or during P berghei ANKA ECM infection*	*To determine why BXH2 mice are resistant to ECM*	*1. Resistance to ECM-associated neuroinflammation in BXH2 is linked to reduced Irf8-dependent inflammatory and innate immune responses, with a strong involvement of the myeloid compartment; 2. Inflammatory pathways associated with ECM in B6 mice*	*Irf8-Regulated Genomic Responses Drive Pathological Inflammation during Cerebral Malaria.*	*Berghout et al. (2013)*
Mircoarray: Illumina MouseRef-8 v2.0 whole-genome expression BeadChip	*Spleen*	*Mice infected with P yoelii N67 (non-lethal), N67C (lethal) or injected with PBS, Day 4 post infection*	*To determine the reason why the almost isogenic parasites N67 and N67C have very different outcomes*	*Increased early Type 1 IFN associated genes in the non-lethal infection, increased early neutrophil chemoaxis associated genes in the lethal form. Biological validation to show that an early burst of type 1 interferon (D2) mediated by MAVS and RNAPolIII leads to better control of parasitaemia*	*Strain-specific innate immune signaling pathways determine malaria parasitaemia dynamics and host mortality.*	*Wu et al. (2014)*
RNA-seq	*Purified synchronised parasites from different rodent malaria infections*	*Parasites (isolated from mice)*	*To establish a comprehensive gene expression database for these parasites and to enhance genome assembly and annotation*	*Creation of a reference resource*	*A comprehensive evaluation of rodent malaria parasite genomes and gene expression.*	*Otto et al. (2014)*
Microarray: Illumina Mouse-Ref8 v2	*Spleen*	*Mice infected with P yoelii N67 (non-lethal), N67C (lethal) or daughters of cross between N67/N67C*	*To identify host genes/gene clusters with quantitative linkage to parasite gene polymorphisms. To identify from this, regulators of type 1 interferon signalling*	*Multiple parasite genes linked to host gene clusters, inferred function of host genes with unknown function from their clustering with other host genes*	*Genome-wide Analysis of Host-Plasmodium yoelii Interactions Reveals Regulators of the Type I Interferon Response.*	*Wu et al. (2015)*
RNA-Seq, Illumina 50bp PE	*Brain*	*WT, USP15-mutant, or TRIM25-/- mice infected with PbA*	*To determine the mechanism by which USP-15 mutation protects from PbA CM*	*USP15 is a novel regulator of type 1 IFN responses in neuroinflammation, and this type 1 interferon production in brain contributes to immunopathology of ECM*	*USP15 regulates type I interferon response and is required for pathogenesis of neuroinflammation.*	*Torre et al. (2017)*
Micorarray: strand-specific 244 K microarray that contains probes for both sense and antisense transcripts	*Blood*	*Adults with uncomplicated (9) and severe malaria (2)*	*To characterise antisense transcripts in clinical parasite isolates*	*Antisense transcripts were identified*	*An in vivo transcriptome data set of natural antisense transcripts from Plasmodium falciparum clinical isolates.*	*Subudhi et al. (2014)*
Affymetrix U133A GeneChips	*Blood*	*22 adult American volunteers experimentally challenged with P. falciparum; 15 Cameroonian adults with clinical features of malaria; 22 malaria-naïve uninfected American adults*	*To uncover transcriptional events associated with malaria infection in pre-symptomatic and symptomatic disease*	*Differences between early pre-symptomatic infection and natural infection involved genes that regulate the induction of apoptosis through mitogen-activated protein (MAP) kinases and signaling pathways through IL-1β*	*Common and Divergent Immune Response Signaling Pathways Discovered in Peripheral Blood Mononuclear Cell Gene Expression Patterns in Presymptomatic and Clinically Apparent Malaria.*	*Ockenhouse et al. (2006)*

MMP8 Immunohistochemistry

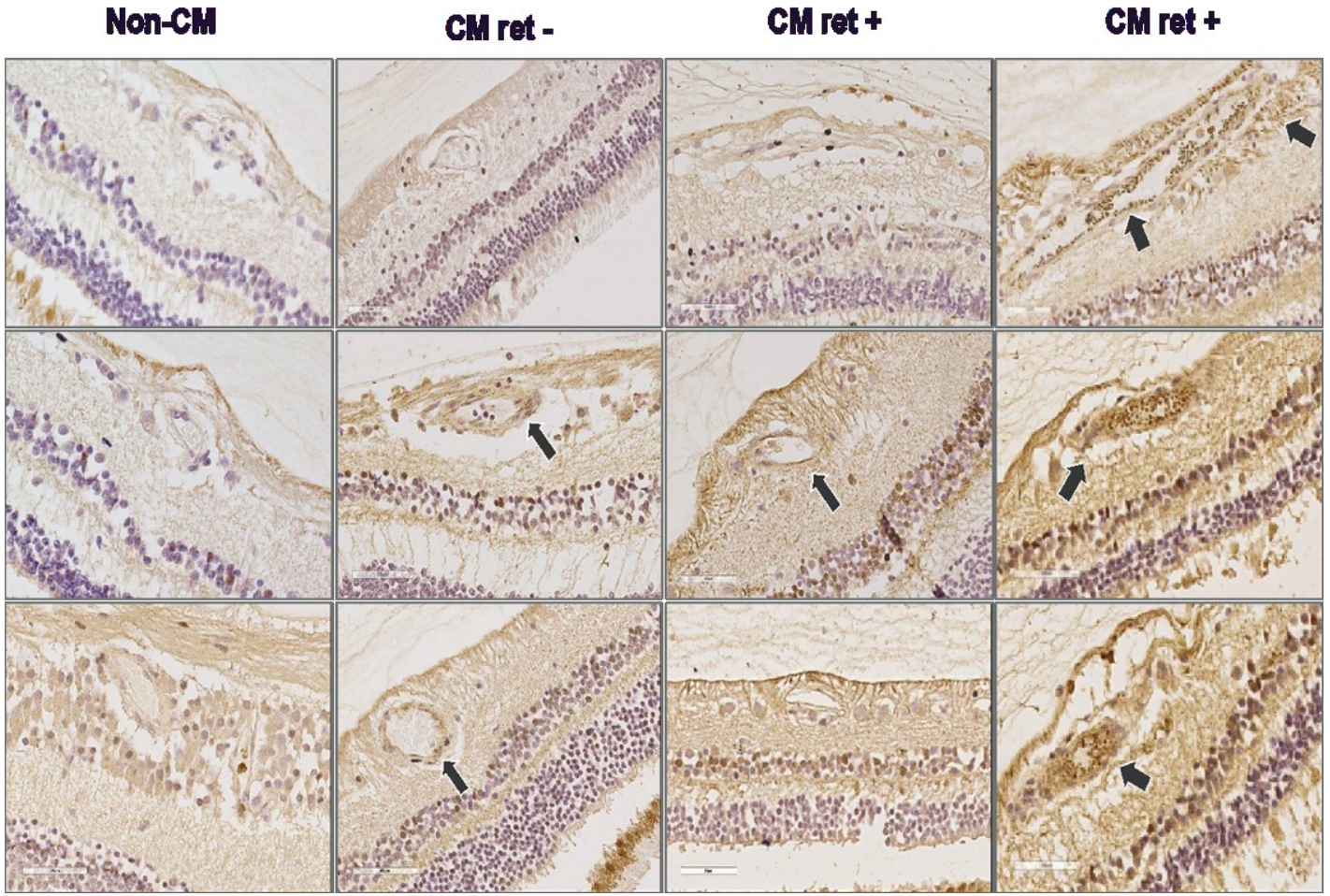

Figure 47: Comparison of MMP8 staining of the retinal vasculature among non-CM, CMret-, CMret+ (vessels without sequestration) and CMret+ (vessels with sequestered parasites).

Protocols used for animal work

Moderate severity limit- Parasite passage

SCORE SHEET FOR SCORING ENDPOINTS IN RODENTS
FOR USE WITH PROTOCOL 5 ONLY (Pathogen Maintenance) – MODERATE SEVERITY LIMIT

PPL details number and Group: PPL 70/8919, Systemic Host Pathogen Interactions And Disease, A. Cunnington

Date: **Time**: **PIL Number:** IB14C4009 **Name of person scoring**: Athina Georgiadou

Name of Supervisor/Chief Investigator: (PPL or Supervisor): Dr Aubrey Cunnington

Indicators	Scoring of independent variables:	Animal Number and Score					
Date							
General Health Eating	drinking and eating well change in eating or drinking habit reduction in skin elasticity not eating/drinking, severely dehydrated						
Locomotion	walking normally limping, stiffness laboured , ataxia severely restricted mobility, paralysis of any limb						
Behaviour:	normal away from littermates aggressive or huddled in corner						

	severe distress, seizures						
Appearance	0. Normal 1. ruffled fur 2. animal appears depressed , hunched, reluctant to move 3. animal appears severely depressed, severe respiratory distress						
Weight loss*	normal 5 – 10% 10-19% (or body condition score <2) >20%						
Total Score							

Contact Telephone Number: **After Hours:**

For Total Scores

0 = normal: continue to monitor according to protocol ******* ***A score of 3 in any one category: euthanase / Schedule 1 kill***

1-2 = mild changes: should be monitored at least once daily

>2 = euthanase

* Assessment of Weight: Weight should be measured once daily, at the same time every day
For experiments lasting up to 5 days, weight loss is calculated relative to the body weight immediately prior to start of the infection (or procedure if uninfected)
For experiments lasting more than 5 days, this calculation must include adjustment for the expected weight gain that would occur in normal mice – calculated from the average weight gain of healthy control mice of the same age and gender as the experimental animals.
Body condition score is determined according to the method of Ullman-Culleré and Foltz, 1999

Signature of person scoring:……..

Appendix

Moderate severity limit

SCORE SHEET FOR SCORING ENDPOINTS IN RODENTS
FOR USE WITH PROTOCOL 1 ONLY (Pathogen Maintenance) – MODERATE SEVERITY LIMIT

PPL details number and Group: PPL 70/8919, Systemic Host Pathogen Interactions And Disease, A. Cunnington

Date: **Time**: **PIL Number:** IB14C4009 **Name of person scoring**: Athina Georgiadou

Name of Supervisor/Chief Investigator: (PPL or Supervisor): Dr Aubrey Cunnington

Contact Telephone Number: **After Hours:**

Indicators	Scoring of independent variables:	Animal Number and Score					
Date							
General Health Eating	drinking and eating well change in eating or drinking habit reduction in skin elasticity not eating/drinking, severely dehydrated						
Locomotion	walking normally limping, stiffness laboured , ataxia severely restricted mobility, paralysis of any limb						
Behaviour: 	normal away from littermates						

Appendix

	aggressive or huddled in corner severe distress, seizures						
Appearance	0. Normal 1. ruffled fur 2. animal appears depressed , hunched, reluctant to move 3. animal appears severely depressed, severe respiratory distress						
Weight loss*	normal 5 – 10% 10-19% (or body condition score <2) >20%						
Total Score							

For Total Scores

0 = normal: continue to monitor according to protocol ******* ***A score of 3 in any one category: euthanase / Schedule 1 kill***

1-2 = mild changes: should be monitored at least once daily

>2 = euthanase

* Assessment of Weight: Weight should be measured at the same time every other day. For experiments lasting up to 5 days, weight loss is calculated relative to the body weight immediately prior to start of the infection (or procedure if uninfected). For experiments lasting more than 5 days, this calculation must include adjustment for the expected weight gain that would occur in normal mice – calculated from the average weight gain of healthy control mice of the same age and gender as the experimental animals. Body condition score is determined according to the method of Ullman-Culleré and Foltz, 1999

Signature of person scoring:……..

1. Morton, D.B. (1997). A scheme for the recognition and assessment of adverseeffects. In:Animal Alternatives, Welfare and Ethics. (Eds. LFM vanZutphen and M. Balls). ElsevierScience, Amsterdam. pp. 235-241.

2. Morton, D.B. (1998). The use of score sheets in the implementation of humaneend points.Proceedings of the Joint ANZCCART / NAEAC Conference on EthicalApproaches to Animalbased Science (Eds. D. Mellor, M. Fisher and G.Sutherland), ANZCCART, Adelaide andWellington. pp: 75-82.

Appendix

Severe severity limit

EXAMPLE SCORE SHEET FOR SCORING ENDPOINTS IN RODENTS
FOR USE WITH PROTOCOL 2 ONLY (*Determinants of severe malaria*) – SEVERE SEVERITY LIMIT

PPL details number and Group: PPL 70/8919, Systemic Host Pathogen Interactions And Disease, A. Cunnington

Date: **Time**: **PIL Number:** IB14C4009 **Name of person scoring**: Athina Georgiadou

Name of Supervisor/Chief Investigator: (PPL or Supervisor): Dr Aubrey Cunnington **Contact Telephone Number:** **After Hours:**

Indicators	Scoring of independent variables:	Animal Number and Score				
Date						
Appearance	0 Normal					
	1 General lack of grooming					
	2 Coat staring, ocular and/or nasal discharges					
	3 Piloerection, hunched up					
	Baseline weight					
	Baseline lactate					
	Baseline glucose					
Food and water intake	0 Normal					
	1 Uncertain: body weight* < 5% reduced					
	2 Reduced intake: body weight* 5-15% reduced or body condition score <2					
	3 No food or water intake					
Natural behaviour	0 Normal					
	1 Minor changes					
	2 Less mobile and alert, isolated					
	3 Vocalisation, self-mutilation, restless or still					
Experimental Cerebral malaria	10 Ataxia					
	Seizures or generalised paralysis Euthanise					
Provoked behaviour	0 Normal					
	1 Minor depression or exaggerated response					
	2 Moderate change in expected behaviour					
	3 Reacts violently or very weak and precomatose					
Score	If you have scored a 3 more than once, score an extra point for each 3 (2-4)					

Appendix

	Total (0-26)					

0-3 = Normal.
4-8 = Monitor carefully, consider supportive care if appropriate.
9-13 = Suffering, provide relief, observe at least twice daily regularly. Seek advice from NACWO and/or NVS.
14-15 = Monitor every 4 hours. Provide support as directed by NACWO and/or NVS
16+ = Euthanise animal

* Assessment of Weight: Weight should be measured at least once daily, at the same time every day
For experiments lasting up to 5 days, weight loss is calculated relative to the body weight immediately prior to start of the infection (or procedure if uninfected)
For experiments lasting more than 5 days, this calculation must include adjustment for the expected weight gain that would occur in normal mice – calculated from the average weight gain of healthy control mice of the same age and gender as the experimental animals.
Body condition score is determined according to the method of Ullman-Culleré and Foltz, 1999

Reference:

Practical use of distress scoring systems in the application of humane endpoints. M.H Lloyd & S.E. Wolfensohn

Appendix

Severe severity limit- Rapid Murine Coma and Behaviour Scale

SCORE SHEET FOR SCORING ENDPOINTS IN RODENTS
FOR USE WITH PROTOCOL 2 ONLY (*Determinants of severe malaria*) – SEVERE SEVERITY LIMIT

PPL details number and Group: PPL 70/8919, Systemic Host Pathogen Interactions And Disease, A. Cunnington

Date: **Time**: **PIL Number:** IB14C4009 **Name of person scoring**: Athina Georgiadou

Name of Supervisor/Chief Investigator: (PPL or Supervisor): Dr Aubrey Cunnington **Contact Telephone Number:**

Indicators	Scoring of independent variables:	Animal Number and Score				
Date						
	Baseline weight (g)					
	Blood lactate (mmol/L, if measured)					
	Blood glucose (mmol/L, if measured)					
Body weight and condition	10 Normal (baseline +/- 0.2g)					
	9 Body weight* < 5% reduced					
	7 Body weight* 5-10% reduced					
	4 Body weight* 10-20% reduced or body condition score <2					
	0 Body weight* > 20% reduced					
Rapid Murine Coma and Behaviour Scale	Gait (0-2) (none; ataxic; normal)					
	Balance (0-2) (no body extension; extends front feet on wall; entire body lift)					
	Motor performance (0-2) (none; 2–3 corners explored in 90 seconds; explores 4 corners in 90 seconds)					
	Body position (0-2) (on side; hunched; full extension)					
	Limb strength (0-2) (hypotonic, no grasp; weak pull-back[front paw grasp only]; strong pull-back [active pull away, jerk away])					
	Touch escape (0-2) (none; unilateral; instant and bilateral [in 3 attempts])					
	Pinna reflex (0-2)					

	(none; unilateral; instant and bilateral [in 3 attempts])					
	Toe pinch (0-2) (none; unilateral; instant and bilateral [in 3 attempts])					
	Aggression (0-2) (none; bite attempt with tail bleed; bite attempt prior to tail bleed [in 5 seconds])					
	Grooming (0-2) (ruffled, with swaths of hair out of place; dusty/piloerection; normal/clean with sheen)					
	RMCBS Total Score (0-20)					
	Total (0-30)					

28-30 = Normal.
24-27 = Monitor at least daily, consider supportive care if appropriate.
17-23 = Suffering, provide relief, observe at least twice daily regularly. Seek advice from NACWO and/or NVS.
12-16 = Monitor every 4 hours. Provide support as directed by NACWO and/or NVS
<12 = Euthanise animal

* Assessment of Weight: Weight should be measured at least once daily, at the same time every day
For experiments lasting up to 5 days, weight loss is calculated relative to the body weight immediately prior to start of the infection (or procedure if uninfected)
For experiments lasting more than 5 days, this calculation must include adjustment for the expected weight gain that would occur in normal mice – calculated from the average weight gain of healthy control mice of the same age and gender as the experimental animals.
Body condition score is determined according to the method of Ullman-Culleré and Foltz, 1999

References:

1. Practical use of distress scoring systems in the application of humane endpoints. M.H Lloyd & S.E. Wolfensohn
2. Carroll RW, Wainwright MS, Kim K-Y, Kidambi T, Go´mez ND, et al. (2010) A Rapid Murine Coma and Behavior Scale for Quantitative Assessment of
Murine Cerebral Malaria. PLoS ONE 5(10): e13124. doi:10.1371/journal.pone.0013124

Parasite genes associated with high lactate

Table 11: Parasite genes associated with host lactate.

LogFC: log Fold Change, logCPM: log counts per million, LR: likelihood ratio FDR: false discovery rate.

Gene	logFC	logCPM	LR	PValue	FDR
PF3D7_1017500	-0.19494	8.141955	9.417974	0.002149	0.068408
PF3D7_1444800	-0.15014	10.92894	8.496571	0.003558	0.090369
PF3D7_0702200	-0.14308	8.440385	15.20432	9.65E-05	0.016203
PF3D7_0424600	-0.14161	12.83015	11.64044	0.000645	0.038966
PF3D7_1143900	-0.13571	4.520061	8.345122	0.003867	0.093108
PF3D7_1205400	-0.13326	5.731411	8.34702	0.003863	0.093108
PF3D7_0902300	-0.13274	8.662607	9.172754	0.002456	0.073076
PF3D7_1302300	-0.13136	6.398397	16.95025	3.84E-05	0.012491
PF3D7_1432000	-0.12455	1.682856	8.515942	0.00352	0.090369
PF3D7_1105600	-0.12447	11.28582	15.24538	9.44E-05	0.016203
PF3D7_1471100	-0.12314	11.52215	16.6074	4.60E-05	0.012491
PF3D7_1007000	-0.12239	4.354201	9.559735	0.001989	0.065766
PF3D7_1115400	-0.12115	9.572239	14.77247	0.000121	0.017746
PF3D7_0711100	-0.11805	6.837561	14.42273	0.000146	0.019375
PF3D7_1013000	-0.11676	3.103123	9.827376	0.001719	0.062191
PF3D7_1114200	-0.11533	9.392282	11.36421	0.000749	0.040688
PF3D7_0936700	-0.11335	8.107404	12.40417	0.000428	0.030717
PF3D7_0424500	-0.11082	10.16602	13.38129	0.000254	0.02555
PF3D7_0105000	-0.10936	5.343698	10.95852	0.000932	0.046031
PF3D7_1221900	-0.10916	9.823651	10.59113	0.001136	0.051459
PF3D7_0621700	-0.10811	3.046579	9.138851	0.002502	0.073076
PF3D7_0210800	-0.10697	7.353318	11.06295	0.000881	0.04501
PF3D7_1345100	-0.10573	7.882772	13.48229	0.000241	0.02555
PF3D7_0523000	-0.10375	13.06495	12.37106	0.000436	0.030717
PF3D7_0814500	-0.10282	9.306563	9.0333	0.002651	0.075258
PF3D7_1116800	-0.1021	12.38952	9.787242	0.001757	0.062191
PF3D7_0304900	-0.10066	5.658884	11.46973	0.000707	0.040688
PF3D7_1343700	-0.09941	10.71738	12.52726	0.000401	0.030717
PF3D7_0818500	-0.0987	8.957502	10.70908	0.001066	0.049457
PF3D7_1213900	-0.0967	10.75209	11.81406	0.000588	0.03727
PF3D7_1104100	-0.09647	6.894929	9.293385	0.0023	0.070667
PF3D7_1321800	-0.0948	8.384576	10.82612	0.001001	0.047959
PF3D7_1129100	-0.09354	12.22959	10.54303	0.001166	0.052194
PF3D7_1404800	-0.09303	12.20867	10.34394	0.001299	0.054905
PF3D7_1404900	-0.09271	10.10144	8.140842	0.004328	0.098931
PF3D7_0831500	-0.08941	9.365943	9.32128	0.002265	0.070626
PF3D7_1355700	-0.08876	8.663444	13.38918	0.000253	0.02555
PF3D7_1347700	-0.08784	10.32369	12.50072	0.000407	0.030717

PF3D7_1364200	-0.08752	9.184887	11.22945	0.000805	0.043135
PF3D7_1218500	-0.08653	11.10889	10.19666	0.001407	0.056761
PF3D7_1226300	-0.08501	10.65154	9.677963	0.001865	0.06278
PF3D7_0909700	-0.08364	9.659467	8.927389	0.002809	0.078003
PF3D7_0917800	-0.08236	5.672458	9.900399	0.001652	0.062191
PF3D7_0805400	-0.08164	4.495207	8.210687	0.004164	0.097913
PF3D7_0304200	-0.08159	8.816123	17.7379	2.54E-05	0.010716
PF3D7_0804900	-0.08144	7.354665	13.32184	0.000262	0.02555
PF3D7_1463000	-0.08061	5.841217	9.826299	0.00172	0.062191
PF3D7_0204700	-0.08052	9.744405	8.624167	0.003317	0.086708
PF3D7_1336700	-0.07928	9.43099	8.379436	0.003795	0.092537
PF3D7_0302000	-0.07714	7.768261	9.13527	0.002507	0.073076
PF3D7_0818200	-0.07568	11.45539	9.723886	0.001819	0.06278
PF3D7_1208100	-0.07496	9.569179	13.26343	0.000271	0.02555
PF3D7_1248500	-0.07455	10.03148	8.186094	0.004221	0.097913
PF3D7_1203900	-0.07378	8.912885	8.385888	0.003781	0.092537
PF3D7_1336000	-0.07218	7.694301	15.09518	0.000102	0.016203
PF3D7_0624000	-0.07158	10.05577	11.02553	0.000899	0.04501
PF3D7_0706000	-0.07114	9.558091	8.463487	0.003623	0.090395
PF3D7_1116700	-0.0708	11.38134	8.060026	0.004525	0.098931
PF3D7_1113100	-0.07034	9.192436	11.46924	0.000708	0.040688
PF3D7_1454500	-0.07007	6.402893	8.422029	0.003707	0.091568
PF3D7_1458000	-0.06859	9.446166	10.18151	0.001419	0.056761
PF3D7_1359000	-0.06829	9.410374	9.290411	0.002304	0.070667
PF3D7_0807300	-0.06764	7.92956	8.481778	0.003587	0.090369
PF3D7_0713400	-0.06761	8.730001	8.082726	0.004469	0.098931
PF3D7_0627800	-0.06759	9.49598	11.0243	0.000899	0.04501
PF3D7_0524000	-0.06688	12.21629	9.724335	0.001818	0.06278
PF3D7_0625400	-0.06681	8.047857	7.984435	0.004718	0.099966
PF3D7_1454200	-0.06656	7.190164	9.817322	0.001729	0.062191
PF3D7_1367400	-0.06591	7.662915	8.098597	0.00443	0.098931
PF3D7_1134200	-0.06492	8.4788	9.793992	0.001751	0.062191
PF3D7_1120400	-0.06416	8.661152	8.618369	0.003328	0.086708
PF3D7_1460100	-0.06366	7.939877	8.803475	0.003007	0.079979
PF3D7_1218200	-0.06026	9.173139	7.979781	0.00473	0.099966
PF3D7_1445600	-0.05798	8.996924	8.521969	0.003509	0.090369
PF3D7_1315900	-0.05771	9.215436	9.633405	0.001911	0.063757
PF3D7_1137300	-0.05625	8.502714	9.186082	0.002439	0.073076
PF3D7_0301600	-0.05442	10.60191	8.18625	0.004221	0.097913
PF3D7_0617100	-0.05111	9.018752	8.814588	0.002988	0.079979
PF3D7_0106700	0.058717	7.630401	8.078304	0.00448	0.098931
PF3D7_0713900	0.063515	8.831597	10.48695	0.001202	0.053177
PF3D7_0103300	0.064293	6.446539	8.742639	0.003109	0.082117

PF3D7_1323900	0.065323	5.482104	9.10535	0.002549	0.073447
PF3D7_1030600	0.06634	6.995498	8.481951	0.003587	0.090369
PF3D7_1457900	0.067386	7.252244	9.778465	0.001766	0.062191
PF3D7_0526900	0.067483	6.195304	9.394844	0.002176	0.068408
PF3D7_1129400	0.069555	7.858595	8.985678	0.002721	0.076557
PF3D7_1367100	0.07046	6.230219	10.75622	0.001039	0.048808
PF3D7_0919800	0.072531	6.898114	8.060275	0.004525	0.098931
PF3D7_1202600	0.074203	7.644408	8.827716	0.002967	0.079979
PF3D7_0719300	0.074449	6.622342	10.68263	0.001081	0.049565
PF3D7_0726300	0.074735	6.538184	8.045668	0.004561	0.099149
PF3D7_0716000	0.076263	6.778958	15.76257	7.18E-05	0.014377
PF3D7_1023200	0.077129	6.129347	11.7036	0.000624	0.038856
PF3D7_0616900	0.078172	5.676815	11.20021	0.000818	0.043211
PF3D7_0708500	0.079074	6.364576	10.16353	0.001432	0.056761
PF3D7_1327200	0.079221	5.547586	9.171892	0.002458	0.073076
PF3D7_1417600	0.080189	8.668452	9.399454	0.002171	0.068408
PF3D7_1464000	0.081247	6.294099	13.25597	0.000272	0.02555
PF3D7_1034000	0.081913	6.037651	12.61588	0.000382	0.030717
PF3D7_1020400	0.08213	6.348512	10.37782	0.001275	0.054821
PF3D7_0930600	0.082438	4.964202	8.858734	0.002917	0.079495
PF3D7_1316800	0.083967	5.918208	12.27593	0.000459	0.031735
PF3D7_0507700	0.086303	5.077189	9.685224	0.001858	0.06278
PF3D7_1249300	0.086656	6.885432	17.19919	3.37E-05	0.012491
PF3D7_0935200	0.08849	6.669433	21.16834	4.21E-06	0.002667
PF3D7_0717400	0.089102	6.097806	16.14052	5.88E-05	0.013625
PF3D7_0618200	0.089823	6.732571	10.81172	0.001009	0.047959
PF3D7_1116300	0.089895	5.164168	8.45733	0.003636	0.090395
PF3D7_1448300	0.090022	7.181425	13.97212	0.000186	0.023527
PF3D7_1250700	0.09113	5.319609	8.330613	0.003898	0.093264
PF3D7_0311100	0.091837	4.35172	12.22971	0.00047	0.03195
PF3D7_1244700	0.092288	5.709649	14.40125	0.000148	0.019375
PF3D7_0110100	0.092292	6.107486	9.973488	0.001588	0.061252
PF3D7_1243100	0.092897	4.960541	8.136291	0.004339	0.098931
PF3D7_0204300	0.093353	6.73738	12.52034	0.000403	0.030717
PF3D7_1020500	0.09358	3.054993	9.089712	0.002571	0.073521
PF3D7_1250600	0.093651	7.568713	22.11583	2.57E-06	0.00213
PF3D7_0723900	0.09399	5.754147	7.992128	0.004698	0.099966
PF3D7_0319500	0.095459	5.284467	12.6192	0.000382	0.030717
PF3D7_1133700	0.096189	8.776918	15.13104	0.0001	0.016203
PF3D7_0208400	0.096754	6.615975	10.10939	0.001475	0.057851
PF3D7_0721000	0.097033	6.217277	9.168182	0.002463	0.073076
PF3D7_1333800	0.09739	5.091205	9.544517	0.002005	0.065766
PF3D7_1441900	0.097963	3.803281	13.24675	0.000273	0.02555

PF3D7_0823100	0.098133	6.185674	11.3983	0.000735	0.040688
PF3D7_1136300	0.099206	8.278159	11.48733	0.000701	0.040688
PF3D7_1228800	0.100646	6.915706	8.250937	0.004073	0.096838
PF3D7_0104500	0.100818	4.422507	9.12851	0.002517	0.073076
PF3D7_0801700	0.100933	5.087594	8.130037	0.004354	0.098931
PF3D7_0521000	0.101916	5.404069	8.120543	0.004377	0.098931
PF3D7_1355900	0.103107	6.117096	11.91264	0.000558	0.036057
PF3D7_0933900	0.103508	6.895923	23.68757	1.13E-06	0.001437
PF3D7_0827800	0.104174	5.96615	9.421607	0.002144	0.068408
PF3D7_0817500	0.106139	7.343101	13.11706	0.000293	0.026503
PF3D7_1015400	0.108678	1.45466	8.013138	0.004644	0.099966
PF3D7_0829300	0.112367	4.453171	12.46235	0.000415	0.030717
PF3D7_0104600	0.112759	3.880338	13.4287	0.000248	0.02555
PF3D7_1214600	0.114833	3.701817	10.43832	0.001234	0.053968
PF3D7_1407000	0.115689	1.910165	9.798505	0.001747	0.062191
PF3D7_0404300	0.116629	4.478183	14.64856	0.00013	0.01825
PF3D7_0610200	0.119545	5.209616	16.62082	4.56E-05	0.012491
PF3D7_1346400	0.119764	8.788284	16.07484	6.09E-05	0.013625
PF3D7_1366400	0.121006	5.772725	11.14146	0.000844	0.043991
PF3D7_1122800	0.122648	6.214481	15.63747	7.67E-05	0.014592
PF3D7_1406000	0.124244	4.061653	14.7876	0.00012	0.017746
PF3D7_0515300	0.125761	5.95208	12.72746	0.00036	0.030717
PF3D7_0206100	0.125782	5.281672	9.966537	0.001594	0.061252
PF3D7_0922800	0.126446	6.496296	9.684393	0.001858	0.06278
PF3D7_1235500	0.127816	4.430654	8.974962	0.002737	0.076557
PF3D7_1228900	0.128125	5.421372	10.89828	0.000963	0.046942
PF3D7_0506900	0.129474	3.362199	8.869336	0.0029	0.079495
PF3D7_0608100	0.135698	4.91096	10.28186	0.001343	0.056159
PF3D7_0932100	0.135778	5.913966	11.67544	0.000633	0.038856
PF3D7_1324000	0.13641	6.108538	10.36736	0.001283	0.054821
PF3D7_0527200	0.136968	4.730057	18.69998	1.53E-05	0.007274
PF3D7_1012000	0.138053	5.68614	11.36698	0.000748	0.040688
PF3D7_0317800	0.138878	4.141137	8.853235	0.002926	0.079495
PF3D7_0729900	0.14101	3.982421	8.200851	0.004187	0.097913
PF3D7_1465600	0.141889	1.780194	9.434976	0.002129	0.068408
PF3D7_0727000	0.142587	3.424491	9.874646	0.001676	0.062191
PF3D7_1430300	0.145493	8.438118	11.41572	0.000728	0.040688
PF3D7_0904100	0.146822	5.457912	21.94937	2.80E-06	0.00213
PF3D7_0522400	0.150451	5.425438	10.22277	0.001387	0.05674
PF3D7_1202300	0.155987	4.08174	11.90697	0.000559	0.036057
PF3D7_1314200	0.157807	3.811614	8.097881	0.004432	0.098931
PF3D7_1119100	0.159802	4.357914	16.6598	4.47E-05	0.012491
PF3D7_0724600	0.160444	3.83825	12.77389	0.000351	0.030717

PF3D7_1474400	0.162392	2.24002	15.797	7.05E-05	0.014377
PF3D7_1417300	0.166269	3.096889	13.37249	0.000255	0.02555
PF3D7_0816300	0.166434	2.318938	7.992962	0.004696	0.099966
PF3D7_1465800	0.170342	3.398056	16.19837	5.70E-05	0.013625
PF3D7_1427200	0.174468	3.294266	13.43097	0.000248	0.02555
PF3D7_1442600	0.175632	3.098868	19.26324	1.14E-05	0.006188
PF3D7_0411900	0.183287	3.633547	12.56709	0.000393	0.030717
PF3D7_0201900	0.187898	7.566878	27.43153	1.63E-07	0.00031
PF3D7_1121800	0.192236	2.289757	13.23081	0.000275	0.02555
PF3D7_0905300	0.192264	4.463924	12.03389	0.000522	0.034865
PF3D7_0308700	0.208725	2.645754	10.24739	0.001369	0.056596
PF3D7_0202000	0.282944	12.49462	12.42091	0.000425	0.030717
PF3D7_1016300	0.546972	9.08698	29.88499	4.58E-08	0.000174